ERRATA

P 83 line 12: "CO_2" for "CO2"
P 84 line 11: "-80ºC" for "-80"
P 150 line 4: "$2x10^4$ " for "2x104"
P 160 line 18: " 6.9B" for "9B"
P 183 line 8: " to form" for " to from"

RESPONSE TO COMMENTS BY EXAMINERS

Comment by Dr H. L. Leo: The thesis title is 'development of miniaturized bioreactor for stem cell culture', however the last two chapters deal mainly with hydrogel scaffold. Strictly speaking, scaffold cannot be considered bioreactor, and in this particular study, miniaturized. I suggest the candidate make changes to the thesis title to reflect a better representation of whatever covered in this thesis work

Candidate: The main aim of the research study is to examine the behaviour of stem cells in different miniaturized bioreactor systems (PDMS micro-bioreactor, liquid marble bioreactor and hydrogel scaffold). In our study, the hydrogel was developed as a biomaterial to construct a bioreactor bed, and the title could be considered as appropriate. Therefore, we have left the original thesis title unchanged.

Comment by Dr H. L. Leo: Chapter discussed the work on surface functionalization of PDMS based micro-bioreactor, and the reviewer do not see how this work is linked with the subsequent chapters on liquid marble, hydrogel etc.. Also, the work on this PDMS bioreactor is not continued in the following chapters, or compared with the LM method. How exactly did the PDMS works contribute to the understanding of subsequent LM and hydrogel works?

Candidate: The aim of this thesis was to study the behaviour of stem cells including proliferation and differentiation in three different miniaturized bioreactor systems. To achieve this goal, we considered three different small-scale bioreactors including a PDMS microchannel bioreactor, and liquid marble and micro-porous hydrogel bioreactors. In Chapter 3, a PDMS microchannel was considered as a micro-bioreactor bed (micro-environment) for improvement of stem cell adhesion and proliferation. The next Chapters (4,5,6 and 7) provide two novel EB formation methods as a critical step for in vitro differentiation in ESCs at small-scale. Therefore, there is a reasonable link between the thesis chapters. In the thesis abstract, there is a comprehensive explanation on the research aims.

Comment by Dr H. L. Leo: The candidate may need to furnish more info on the physical dimension of the PDMS bioreactor, for example, the length and width of the microchannel, the volume of culture medium etc.

Candidate: The details about the dimensions of PDMS microchannel were already presented in the section "Fabrication of PDMS microchannel" in the published paper entitled "Surface-functionalization of PDMS for potential Micro-bioreactor and embryonic stem cell culture applications. The presented information clearly indicated that the volume of the culture medium is equal to the volume of microchannel, which is sufficient for the length and width of the microchannel, the volume of culture medium. Hence, we avoid to repeating these information.

Comment by Dr H. L. Leo: A good control for this PDMS bioreactor would be the 96 well plate. But this is not present in the study.

Candidate: Since all experiments were conducted in 6 well-plates, we also used 6 well-plates TC culture dish as a control for all experiments for consistency (some results have been presented in Figure 8 of Chapter 3)

Comment by Dr H. L. Leo: It is not clear from the thesis; a. How stable are the PTFE material used? What is the thermal decomposition property of PTFE?

Candidate: PTFE is a very stable polymer due to the strength of C–F bonds and shielding by the very electronegative fluorine atoms. Thermal decomposition process starts between 750K and 800K. The principal product of decomposition is the monomer, CF_4, with small amounts of hydrogen fluoride and hexafluoropropene. Thermal decomposition is initiated by random-chain scission, followed by depolymerization. Termination is by disproportionation. It is possible that the actual product of decomposition is CF_2, which immediately forms in the gas phase. (Thermal Decomposition of Polymers, by Craig L. Beyler and Marcelo M. Hirschler)

Comment by Dr H. L. Leo: b. What is the O_2 and CO_2 diffusivity of the PTFE shell?

Candidate: Permeability of PTFE to Oxygen is $x10^{-13}$ cm^3. cm cm^{-2} s^{-1} Pa^{-1} and to Carbon Dioxide is $x10^{-13}$ cm^3. cm cm^{-2} s^{-1} Pa^{-1}

Comment by Dr H. L. Leo: c. What is the typical thickness and diameter of the PTFE shell and the size (diameter) of the EBs within these shells?

Candidate: The thickness of the liquid marble shell is around the size of powder particles (in our studies was 30µm) . The diameter of EBs varies based on different parameters such as powder particle size, volume of liquid marble and cell seeding density, which have comprehensively been presented in Chapter 5.

Comment by Dr H. L. Leo: d. A 3D cell mass of more than 150 microns will affect the oxygen diffusion within the cell core. On average, how many EBs form within a single LM?

Candidate: Tian et al. (2010) showed that the hydrophobic shell of a liquid marble prevents direct contact of the liquid core of the marble with any condensed phases (i.e. solid or liquid) outside the marble, but allows gas and vapour to diffuse across the shell. This property of a liquid marble naturally enables it to discriminately absorb or emit gaseous and vaporous compounds across its shell while denying contact or transport of liquids. The PTFE particles on the shell are not chemically bonded but are closely packed, so there are micro-gaps where gas can pass through. Liquid marbles therefore can be used to form micro-gas reactors for gas detection application when loaded with an indicator solution. Furthermore, Nguyen et al. (2010) showed that the thickness of the liquid marble wall is not uniform since the liquid marble wall is composed of a combination of mono- and multi-layers of particles. Particles, which are approximately larger than 50µm, form the monolayers, while the finer particles form multi-layers in the powder shell. Therefore, the liquid marble wall covers a large range of thicknesses, varying from an average of 43–114µm with a standard error of the mean ranging from 2.6 to 18.5µm. Since we used 30µm powder particle size, the thickness of the shell was not be a barrier for gas diffusion. The number of EBs formed inside LM is dependent on the initial number of cells which has been presented in Figure A-1 appendix 5.3.

Comment by Dr H. L. Leo: e. How do you retrieve the EBs within the LM after several days of culture?

Candidate: the method to retrieve EBs from LM has been presented in Chapter 2, experimental procedure in details.

Comment by Dr H. L. Leo: Also not clear from the thesis was a. What is average size and size range of the EBs formed under LM technique? Similarly, what is average size and size range of the EBs formed under LS technique?

Candidate: The average diameter of EBs depends on different parameters such as powder particle size, volume of liquid marble and initial cell seeding density. The effects of these parameters on efficiency of the formed EBs inside LM and LS at different time points have comprehensively been compared and presented in the published RSC advances journal paper (Chapter 5).

Comment by Dr H. L. Leo: It was mentioned in the thesis that 20,000 cells is the ideal number for each LM. Why is that so? Any physical reason for this?

Candidate: The cell seeding density inside liquid marbles plays an important role in the yield and uniformity of the formed EBs. A liquid marble provides a confined space in which cells are free to interact effectively with one another, while having minimal contact with the powder particles. Moreover, EB formation depends on the accidental impact of ES cells with one another. It suggests that a higher density of cells will provide a higher chance of impact, resulting a higher number of EBs. Our quantitative and qualitative studies showed that the best number of viable EBs was obtained with 20,000 cells. (Appendix 5.3)

Comment by Dr H. L. Leo: In cross-linking process of hydrogel, how consistence is the pore size across the entire cellulosic construct?

Candidate: I have used the hydrogel synthesized by Seiw et al. (Recently published in Journal of materials and chemistry B, 2013, Preparation of a soft and interconnected macroporous hydroxypropyl cellulose methacrylate scaffold for adipose tissue engineering). They have demonstrated that (Figure 3E,F which shows the SEM and pore size distribution graph for HPC-MA-20 wt%) the pore size after cross-linking and lyophilisation, is fairly consistent across the hydrogel.

Comment by Dr H. L. Leo: What is the physical size of the scaffold used in culturing? b. Does the cells aggregate more in certain parts of the constructs, for example, the centre region may have more viable cells compare to the peripheral ones. Did the candidate perform a cross sectional staining looking at the cell viability across the construct?

Candidate: The porous gel had pore diameter of ranging from 30 to 300μm with median pore diameter of approximately (42.4μm) and controlled porosity of (~96 ± 0.9%) as measured by mercury porosimetry, which is believed to be suitable for inducing cell aggregation into EB. The viability of cells in the whole gel was performed quantitatively and presented in Chapter 7 which shows higher viable cells inside hydrogel compared to those formed in LS method. We also did SEM cross-sectional imaging (Figure7.8), which also confirmed the formation of significant numbers of uniform EBs inside hydrogel. All these results confirmed the potential of hydrogel to induce EB formation, which could eventually differentiate towards cardiogenic lineage.

Comment by Dr L Liu: What are the possible causes of black particle to appear in Fig. 2F (Page 140, chapter 5)? Although the scale bar is missing in this figure, the estimated particle size and morphology are similar to PTFE powders as revealed in Figure 2. (Page 132) of Chapter 4. The candidate is welcome to make a small comment on this concern.

Candidate: It is worth mentioning that by retrieving EBs from the LM, some particles will attach to the surface of the micropipette tip and this is the reason for appearance some black particles in some images you can see some particles as well. The scale bar is 100 μm.

Comment by Dr L Liu: Is it possible to compare the quality of EBs formed in liquid marble and hydrogel?

Candidate: The purpose of Chapter 7 was to compare the efficiency of EB formation via hydrogel method with one of the commonest EB formation techniques named (Liquid suspension, LS). I have done some quantitative and qualitative comparison between hydrogel and LM in terms of cell viability, expression of three germ layer markers, immunostaining, real time PCR. The comparison between Hydrogel method and LM was not in the scope of this study.

Development of Miniaturized Bioreactors for Stem Cell Culture

By

Fatemeh (Mariam) Sarvi

A thesis submitted for the degree of

Doctor of Philosophy

Monash University

Faculty of Engineering

Department of Mechanical and Aerospace

Division of Biological Engineering

May 2014

Main Supervisor:

Professor Kerry Hourigan

Associate Supervisors:

Dr. Peggy Chan

Professor Mark Thompson

PART A: General Declaration

Monash University
Declaration for thesis based or partially based on conjointly published or unpublished work
General Declaration

In accordance with Monash University Doctorate Regulation 17.2 Doctor of Philosophy and Research Master's regulations the following declarations are made:
I hereby declare that this thesis contains no material which has been accepted for the award of any other degree or diploma at any university or equivalent institution and that, to the best of my knowledge and belief, this thesis contains no material previously published or written by another person, except where due reference is made in the text of the thesis.
This thesis includes four original papers published in peer reviewed journals and two unpublished publications. The core theme of the thesis is "Development of miniaturized bioreactors for stem cell culture". The ideas, development and writing up of all the papers in the thesis were the principal responsibility of myself, the candidate, working within the Mechanical and Aerospace Engineering Department/Biological Engineering Division under the supervision of Prof. Kerry Hourigan, Dr. Peggy Chan and Prof. Mark Thompson.
[The inclusion of co-authors reflects the fact that the work came from active collaboration between researchers and acknowledges input into team-based research.]
In the case of chapter3,4,5,6 and 7and Appendix 7.3 my contribution to the work involved the following:
[If this is a laboratory-based discipline, a paragraph outlining the assistance given during the experiments, the nature of the experiments and an attribution to the contributors could follow.]

Thesis chapter	Publication title	Publication status*	Nature and extent of candidate's contribution
3	Surface-functionalization of PDMS for potential Micro-bioreactor and embryonic stem cell culture applications	Published	80%
4	Tumor inside a Pear Drop	Published	15%
5	A novel technique for formation of Embryoid Bodies inside liquid marbles	Published	50%
6	Cardiogenesis of Embryonic Stem Cells with Liquid Marble Micro-bioreactor	Submitted	50%
7	Porous Hydroxypropyl cellulose hydrogel for Embryoid Body Engineering	Draft	85%
Appendix 7.3	Thermoresponsive Cellulosic Hydrogel with Cell-Releasing Behavior	Published	45%

[* For example, 'published'/ 'in press'/ 'accepted'/ 'returned for revision']
I have / have not (circle that which applies) renumbered sections of submitted or published papers in order to generate a consistent presentation within the thesis.

Signed: ……
Date: ……

Table of Contents

List of Tables

List of Figures

List of Abbreviations

TE	Tissue engineering
ECM	Extracellular matrix
ESCs	Embryonic stem cells
HSCs	Hematopoietic stem cells
ICM	Inner cell mass
hESCs	Human embryonic stem cells
IVF	In vitro fertilization
MEFs	Murine embryonic fibroblasts
DMEM	Dulbecco's modified Eagle medium
BIO	6-bromoindirubin-3´-oxime
TERT	Telomerase reverse transcriptase
LIF	Leukemia Inhibitory Factor
MHC	Myosin heavy chain
GMP	Good manufacturing practice
RCC	Rotary cell culture
2D	Two dimensional
3D	Three dimensional
EBs	Embryoid bodies
RWV	Rotating wall vessel
HARV	High aspect ratio vessel
STLV	Slow turning lateral vessel
PEG	Poly(ethylene glycol)
PMMA	Poly(methyl methacrylate)
PS	Polysterene
LBL	Layer-by-layer
LMW	Low molecular weight
APTES	Aminopropyltriethoxysilane
APTMS	Aminopropyltrimethoxysilane
MPTMS	Mercaptopropyltrimethoxy silane
PEI	polyethyleneimine
CMD	Carboxymethyl -1,3-dextran
CMC	Carboxymethyl cellulose
FDA	Food and Drug Administration
BSA	Bovine serum albumin
RGD	Arginine–glycine–aspartate
FD-POSS	Fuorinated decyl polyhedral oligomeric silsesquioxane
OTFE	Oligomerictetrafluoroethylene
DMSO	Dimethyl sulfoxide
ESEM	Environmental scanning electron microscopy
MMA	Methylmethacrylate
Fmoc-FF	Fuorenylmethoxycarbonyl-diphenylalanine
PVDF	Polyvinylidene fluoride
PU	Poly(urethane)
PAAm	Poly(acrylic amide)
PAA	Poly(acrylic acid)
PVA	Poly(vinyl alcohol)
GAGs	Glycosaminoglycans
HA	Hydroxyapatite
EHT	Engineered heart tissues
PLL	PolyL-lysine
HPC	Hydroxypropylcellulose

HPMC	Hydroxypropylmethyl cellulose
LCST	Lower critical solution temperature
UCST	Upper critical solution temperature
PDEAAm	Poly(N,N-diethylacrylamide)
PVCL	Poly(N-vinlycaprolactam)
PDMAEMA	Poly[2-(dimethylamino)ethyl methacrylate)]
PNIPAAm	Poly(N-isopropylacrylamide)
MC	Methylcellulose
HPMC	Hydroxypropyl methylcellulose
FTIR	Fourier transform infrared
FACS	Fluorescence-activated cell sorting technique
cTnI	Cardiac troponin I
EDC	Carbodiimide hydrochloride
BCA	Bicinchoninic acid
SDS	Sodium dodecyl sulphate
FTIR	Fourier Transform Infrared spectroscopy
NEAA	Non-essential amino acids
FBS	Fetal bovine serum
RT-PCR	Reverse transcription polymerase chain reaction
DTT	Dithioreitol
cDNA	Complementaryn DNA
MTS	Multicellular tumour spheroids
CSD	Cell seeding density
LMS	Liquid marble size
LM	Liquid marble
LS	Liquid suspension
MLC2v	Myosin light chain-2v
MLC2a	Myosin light chain 2a
GFP	Green fluorescent protein
PBS	Phosphate buffered saline
Oct4-GFP	GFP transgene under control of the Oct4 promoter

Dedicated to

Alireza *for His Endless Love and Patience*

And

My beloved Parents

Abstract

Embryonic stem cells (ESCs) are pluripotent cells capable of indefinite self renewal *in vitro* while maintaining the ability to differentiate into cell types of all three germ layers. ESCs are outstanding options of *in vitro* cell models for regenerative medicine, functional genomics, human developmental biology and drug discovery study. Stem cell research is among the most promising fields of biotechnology, and which provides the potential of developing novel approaches to repair or replace damaged tissues and cells. The present day, exponentially growing effort of stem cell research emphasizes a major need for convergence of more efficient and appropriate laboratory technologies to sustain the growth, proliferation and differentiation potential of stem cells.

Although so far, a variety of conventional bioreactors with different configurations (such as spinner flasks, rotary, perfusion bioreactor, etc.) have been designed and adapted for stem cell expansion and differentiation, bioreactors can be disadvantageous in bench-top research because they need large space, consume huge amount of reagents and need more time to operate and maintain (sterilizing, cleaning, assembling, and disassembling of the bioreactor components). The requirements for costly equipment and generating shear stress due to the fluid flow, and the lack of physical similarity between microenvironments of bioreactor and actual cell microenvironment, make using bioreactors undesirable.

In tissue engineering, micro-scale technology is an approach that combines micro-techniques with materials science and surface engineering, and results in a profound exploration of the microenvironment where cells are embedded. These technologies are able to address some of the limitations imposed by conventional tissue engineering methods. Indeed, developing successful novel small-scale technologies for *in vitro* cultivation of different types of cells can assist in increasing our knowledge on conditions that control stem cell growth and differentiation and organ development. In fact, small scale bioreactors are miniaturized versions of conventional bioreactors, where high-throughput cell based assays can be carried out at low cost compared with their macro-scale counter-parts.

The first aim of this thesis was to develop a disposable miniaturized bioreactor through a novel and inexpensive method for effective stem cell proliferation. To this end, an effective surface functionalization method was developed for enhancing the biocompatibility of a PDMS surface that is protein resistant while facilitating cell proliferation (expansion) and maintaining the pluripotency potential of cells. The micro-bioreactor was fabricated in the form of a fixed bed bioreactor with a microchannel reactor bed. The microchannel was functionalized to enable cell adhesion and resistance to protein adsorption. The functionalized surface was found to be biocompatible with cancer and embryonic stem cells (ESCs), and while facilitating cell proliferation.

Differentiation of ESCs into a variety of cell types is an important characteristic of these types of cells, which is commonly achieved *in vitro* by spontaneously self-assembling in low adhesion culture conditions into 3D cell aggregates called embryoid bodies (EBs). Formation of EBs that simulates many of the characteristics of early embryonic development is considered as a vital step to induce differentiation of stem cells. Formation of three dimensional configurations of ESCs as EBs provides possibilities to mechanistically study early differentiation events of pluripotent cells. In fact, EB formation is of paramount importance for *in vitro* investigation of the embryonic development and differentiation of both the mouse and human ES cells.

The second aim of this thesis was to introduce a novel concept of a miniaturized bioreactor made of liquid marble (LM). A novel application of liquid marbles for formation of embryoid bodies (EBs) was then presented. This study showed that the confined internal space of liquid marble, along with the porous and non-adhesive property of the highly hydrophobic liquid marble shell, can facilitate the formation of uniform EBs inside the liquid marbles. The efficiency of liquid marble-born-EBs compared to the liquid suspension (LS) technique as the chosen control method in terms of cell viability and EB uniformity revealed that cells in liquid marble are more viable than those in suspension. Measuring EB size distribution as an indicator of uniformity also confirmed that EBs obtained by the LM are morphologically more uniform and of a narrower size distribution compared to those formed in LS. The feasibility of using liquid marble bioreactors for cardiomyocyte differentiation of mouse ES (mES) cells after formation of EBs inside the liquid marble was further investigated. The results demonstrated that ES cells can differentiate into myocyte cells through the liquid marble as a facile, cost effective, and straightforward method. We proposed for the first time that liquid marbles greatly contribute to ES cardiac differentiation, which provides a new technology platform for ES biology and genetic studies.

It is worth mentioning that although the majority of our knowledge in modern biology has been provided by classical two dimensional (2D) cell culture techniques, the most common negative aspects of these systems is deficiency of support from extra-cellular matrix, which represents an important role for cell growth and development. It is now well accepted that cells reside, proliferate, and differentiate in complex 3D microenvironments. The concept of using three dimensional (3D) biodegradable scaffolds as alternatives for extracellular matrix (ECM), which more closely reform cells' native structure, is an interesting area of study in current tissue engineering. Because of their unique function, stem cells need to reside in the specialized, 3D microenvironment that surrounds them in native tissues.

The third section of this thesis (chapter 5) focuses on the investigating of the feasibility of forming embryoid bodies using a novel hydrogel as bioreactor embedding material. This hydrogel is porous and biodegradable and is prepared by modifying hydroxypropylcellulose (HPC), with bio-functional methacrylates (MA). Observation of EB formation inside hydrogel implied that the stem cells

attached and penetrated to the pores, and proliferated well, while forming uniform EBs. Uniformity of EBs formed inside hydrogel, compared with those formed via liquid suspension (LS) method, as one of the most widely used EB formation techniques. It was observed that porous hydrogel allows the formation of more homogeneous EBs. It was found that cells inside hydrogel-born EBs are more viable compared to those formed in LS method. Expression of germ markers via quantitative PCR and immunostaining confirmed that the hydrogel-born EBs had expressed 3 germ layers with further *in vitro* differentiation potential. These EBs were allowed to differentiate further in hydrogel, where positive immunostaining of different cardiac markers and observation of beating EBs showed the potential of EBs to further differentiate into cardiac cells lineage.

In summary, this thesis first presents a novel, facile and cost effective method via surface bio-functionalization of PDMS bioreactor for better stem cell adhesion and proliferation, and later introduces two novel methods to prepare bioreactor material, namely liquid marble and porous hydrogel (HPC-MA) for formation of embryoid bodies, which is considered as a critical step for *in vitro* differentiation in ESCs.

Acknowledgments

I would like to thank my supervisors, Prof. Kerry Hourigan and Prof. Mark Thompson for their guidance, time and help with all aspects of the practical and written work undertaken during PhD. Their encouragement and belief in my abilities contributed greatly to the success of this study.

I would like to express my sincere gratitude to Dr. Peggy Chan as a mentor and friend for all her guidance and support throughout my Ph.D. study. She was always available to discuss issues related to my research and generously shared her knowledge and experience.

I am extremely grateful to Prof. Paul Verma for giving me the opportunity of collaboration with his friendly group and for his generous support and guidance.

I am thankful to all who have provided technical, intellectual, and moral support throughout the development, production and writing of this thesis. Completion of the projects would not have been possible without the collaboration/assistance of Ms. Kanika Jain, Dr. Tina Arbatan, Ms. Karla Contreras, Professor Wei Shen, Dr. Siew Pei Hoo, Mr. Mohammad Barati and Mr. Amir Taheri.

I cannot express how I am deeply and forever indebted to my parents Goli Darzi and Mohammadali Sarvi for their unconditional love and encouragement. My warmest and special thanks also go to my lovely brothers Amir and Ali who have always been there for me. You are always my best friends. Sahar Farhadi thank you so much for your moral support and for being like my sister I have never had.

Last but definitely not least, I would like to give my most hearties thanks to my loving husband Alireza Valizadeh for being with me through the good times and the bad times, for his continued moral support and patience. You are my endless source of happiness.

Chapter 1: Literature Review

1.1 An introduction to cell and tissue engineering

Tissue engineering (TE) is a newly emerging biomedical technology that aims to design, create, or replace tissues and organs using combinations of cells, biomaterials or biologically active molecules[1]. Tissue engineering is a highly interdisciplinary area, which amalgamates the principles of the life sciences and medicine with those of engineering toward the development of biologic substitutes that can restore and maintain normal functions. By doing so, TE strategies promise to revolutionize current therapies, and significantly improve the quality of lives of millions of patients. The aim of TE is to develop novel and effective *in vitro* biological methods and technologies that help the better understanding of the normal function of tissues, as well as functions similar to those found *in vivo* [2].

To begin, this discipline was born in 1933 when mouse tumour cells were wrapped in polymer membrane, and implanted into a pig's abdominal cavity[3]. In the late 1970s and 1980s, sheets of collagen or collagen–glycosaminoglycan composites were used as two-dimensional systems for culturing cells and to generate anew skin [4, 5]. The next important progress in tissue engineering was generating three-dimensional structures composed of synthetic polymers for hosting larger number of cells [6]. It was about 20 years ago when Langer and Vacanti published a seminal article describing how biological and engineering principles are utilized to bring cells, biomolecules and scaffolding together to repair or grow new tissues [7]. At the time, the concept of creation of tissues in the laboratory seemed impossible; however, some landmark studies such as the growth of a human shaped ear on the back of a mouse opened a new way of thinking towards the generating of new technologies and constructs capable of mimicking the structure of native tissue and organs [8]. Despite the significant interests and advances that have been reported [9-11], clinical advances have moved much slower than expected and there are several difficulties associated with current implantation practice. The number of organs available for transplantation is far exceeded by the number of patients needing such procedures; many tissues are not stored in banks, so supply problems exist and there is always a possibility of organ and tissue rejection.

One of the important elements to the success of tissue engineering is expanding and generating appropriate numbers of cells that can perform the required biological functions, and maintain the normal phenotype. For instance, some cell functions such as producing the extracellular matrix in the correct organization, secreting cytokines and other signalling molecules, as well as interacting with neighbouring cells/tissues, are some of the essential parts of a normal cell's performances that need to be accomplished. Repairing and/or replacing the damaged tissue as a fundamental principle in TE in

some cases could be possible using the relevant cells as a starting material from the same patient, such as knee repair with, e.g., autologous chondrocytes (primary cells). The type of cells used for tissue engineering could be provided from different cell sources.

For the use of cells in tissue engineering, sufficient numbers of cells are seeded onto a synthesized substrate with the appropriate biomaterial. In fact, in tissue engineering, biomaterials act as artificial extracellular matrix (ECM) to replicate the biological and mechanical function of native ECM.

Therefore, in order to generate constructs capable of accurately mimicking/replacing structures as defined and organized as complex tissues and organs, other critical elements should be carefully considered, including biomaterial substrate.

Biomaterial technology, which is increasing in complexity and becoming smarter, plays an important role, as a mechanical support for cells, in the creation of the cell environment, in which appropriate regulation of cell behaviour (e.g., adhesion, proliferation, migration, and differentiation) can occur. In addition, biomaterials act as temporary mechanical support for tissue to grow and for cells to undergo spatial tissue reorganization.

Another major concern of TE is the ability to miniaturize and parallelize cell-based assays. In TE, miniaturized technology is a new field of study that can be applied to fabricate biomimetic scaffold and novel bioreactors with the ability to perform high-throughput experiments [12]. The control of cell-microenvironment interactions, including cell-cell, cell-extracellular matrix, and cell-soluble factor interactions, is being facilitated using small-scale technologies [13]. For this purpose, much effort has been devoted to the areas of micro- and nanotechnologies, both in terms of production methods and in analysis tools (Figure1.1).

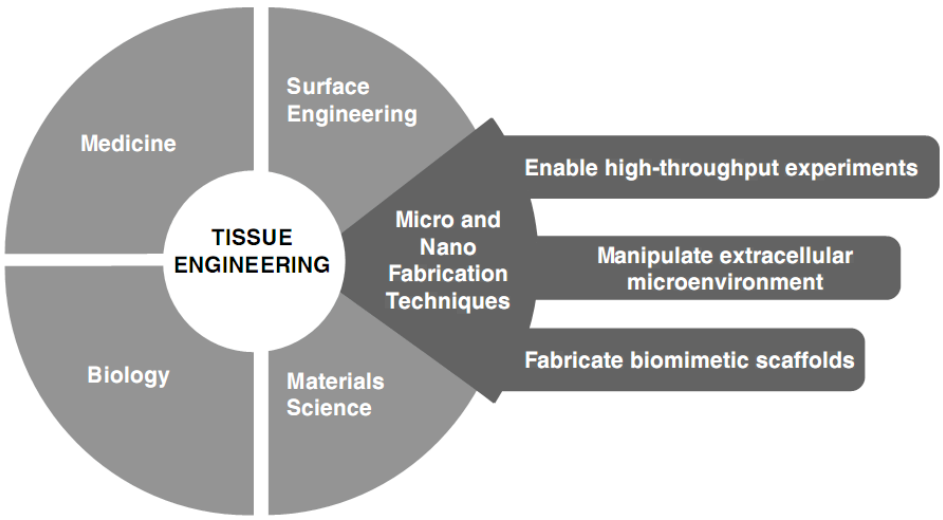

Figure (1.1): Schematic diagram of involvement of different areas of knowledge in tissue engineering with different inputs field[14]

For successful regeneration therapy of tissues and organs, it is indispensable to apply novel small-scale culture systems (such as mini and micro-bioreactors) with combination of materials science and surface engineering, to obtain a deeper understanding of cells' micro-environment, and to support cellular adhesion, proliferation and differentiation.

1.2 Sources of cells for tissue engineering strategies

1.2.1 Primary cells

Construction of an engineered tissue *in vitro*, which resembles the native tissue, usually requires the use of cells to populate matrices. The primary achievements in this area have originated from the employment of primary cells, extracted from the patients, and applied along with scaffolds to produce tissue for re-implantation.

Primary cells are mature cells specific to tissue type that are harvested from explants material and removed by surgical procedures. However, these types of cells are the most desired ones, as a result of immunological compatibility, and they are differentiated cells and post-mitotic. Furthermore, the tendency of some cell types to de-differentiate during *ex vivo* cultivation and expression of an inappropriate phenotype (e.g., articular chondrocytes in culture often produce fibrocartilage as opposed to hyaline cartilage) limited their applications. Although primary cells, especially autologous cells (same species), are still used in tissue engineering, yields and proliferation rates tend to be low, and for some phenotypes, like spinal cord neurons, harvesting from a patient or donor is not an option. These types of cell sources had significant disadvantages, including low yield and the probability of gene alterations associated with aging. These limitations have motivated studies to find and develop alternative cell sources for tissue engineering strategies, and stem cells are already providing solutions to some of the problems encountered using primary cells released from explanted tissues. Embryonic stem cells have shown great promise for providing the functional tissues needed to address the shortfall of tissue and organs in medicine [15, 16]. In recent years, the potential of stem cell research for tissue engineering-based therapies and regenerative medicine clinical applications have become well established. Table 1.1 illustrates some of the common types of cells used in TE, which vary from autologous or allogenic to differentiated to stem or progenitor origin depending on the site where the seeding is required [17].

Table(1.1): Cells that have been used for tissue engineering and cell therapy [17]

Cell type	Human cell source, donor immunogenicity	Ex vivo manipulation and immunogenicity	Clinical experience
Embryonic stem and progenitor cells	Embryonic tissue; tight ethical regulation, allogeneic, presumably with low immunogenicity	High expansion and differentiation capacity; potentially immunogenic culture supplements	Only preclinical studies, (potential teratoma formation); require xeno-/ pathogen-free culture supplements
Induced pluripotent stem cells	Autologous tissue biopsy (e.g., skin, fat, or muscle), require reprogramming	Limited expansion, but high differentiation capacity; epigenetic memory?	Only experimental and preclinical studies (potential teratoma formation)
Fetal, umbilical cord, and placenta-derived stem and progenitor cells	Aborted fetal tissue (e.g., fetal liver or marrow, umbilical cord, amniotic fluid, and placental tissue)	High expansion capacity but unknown long-term risk of maligtransformation; response to allogens?	Mostly preclinical studies; umbilical cord blood cells for cartilage
Adult stem and progenitor cells	Bone marrow aspiration, peripheral blood, adipose, and other adult tissues; usually autologous, but also allogeneic sources	Low to moderate risk of de-differentiation and unknown long-term risk of malignant transformation; potential immunological issues	Pulmonary valve and trachea (autologous EPCs/MSCs); acute GvHD (allogeneic MSCs)
Lineage-committed and differentiated adult tissue cells	Commonly tissue biopsy, but also peripheral blood; selection of cell types, autologous vs. allogeneic donor?	Limited expansion capacity; no immunogenicity expected but immune-response to allogens	Trachea; bladder; cartilage

Although there are several classes of stem cells with their own benefits, limitations, and challenges in bioprocess development (including embryonic and adult stem cells, and more recently induced stem cells), the two most broadly used in TE will be described in the following subsections.

1.2.2 Stem cells

Stem cells are pluripotent cells defined by two unique properties: first, the capacity of self-renewing even after a long period of time; and second, the ability to generate differentiated cells under certain physiological or experimental conditions. In contrast to muscle, blood or nerve cells, stem cells have the capability of replicating themselves many times. These types of cells proliferate for many months in the laboratory and can yield millions of cells. If the resulting cells continue to be unspecialized, like the parent stem cells, the cells are said to be capable of long-term self-renewal. Stem cells can be found in several organs in human such as in the inner cell mass of the early embryo, in some tissues of the fetus, the umbilical cord, placenta, and in several other adult organs.

The remarkable potential of stem cells was recognized after isolation of pluripotential stem cells from early embryos and growing them in the laboratory in the late 90s [18, 19]. One of the fundamental properties of stem cells is that they are not specialized; they can give rise to specialized cells, including heart, muscle, blood or nerve cells, but they do not have any specific tissue structure with specific function.

Differentiation of stem cells is a process in which unspecialized stem cells give rise to specialized cells through several stages. The degree of differentiation of stem cells to various other tissue types varies with the different types of stem cells, and this phenomenon is referred to as plasticity. In this regard, stem cells are classified according to their differentiation capacity into totipotent, pluripotent, multipotent and unipotent stem cells (Figure 1.2).

Totipotent stem cells, which are recognized as the master cells, have the capability of differentiating into all specialized cell types in the body. These cells have the capability of forming a completely new embryo that can develop into a new organism. A fertilised egg is totipotent. None of the stem cells used in research appear to have this capacity.

Stem cells that can differentiate into all of the cell types within the body, such as embryonic stem cells (ESCs), are called pluripotent stem cells. These cells are highly versatile cells and can give rise to all specialized cells except those needed to develop a fetus. Pluripotent stem cells have the capacity to differentiate into the three somatic germs layers compromising mesoderm (muscle, bone, etc.), ectoderm (neurons, skin, etc.) and endoderm (hepatocytes, pancreatic beta cells, etc.).

Multipotent stem cells can generate multiple types of differentiated cells, but are limited to the particular tissue, organ or physiological system of origin. Adult stem cells such as hematopoietic stem cell are the example of multipotent cells that can produce many types of blood cells but cannot differentiate to a brain cell. And finally, unipotent stem cells are the stem cells that can only differentiate into one cell type.

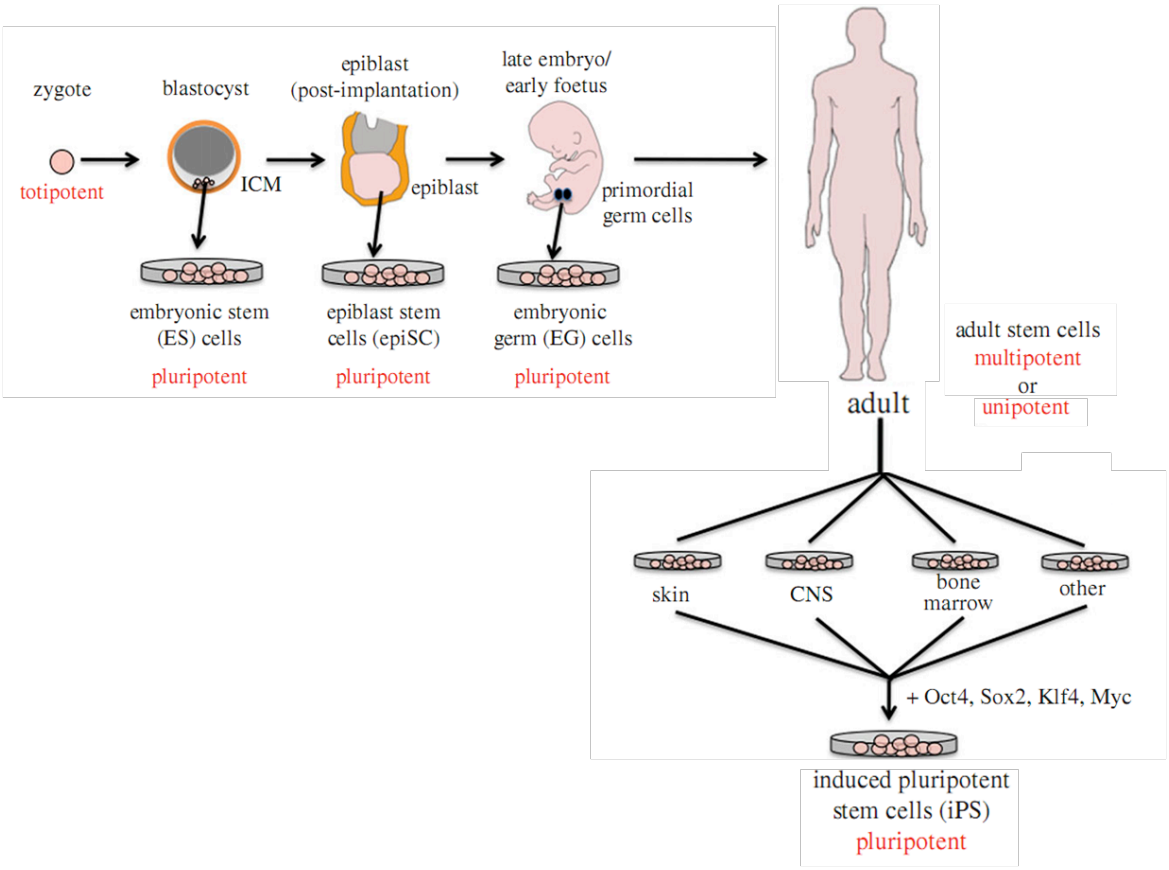

Figure (1.2): Origin of stem cells. Pluripotent stem cells differentiate into many cell types. Only the morula cells are totipotent, able to become all tissues and a placenta. In some cases, a tissue contains only one differentiated lineage and the stem cells that maintain the lineage are described as unipotent. CNS, central nervous system; ICM, inner cell mass [20]

The above-mentioned unique properties of the stem cells have generated more interest among public and professionals. This is because the better understanding of their unique properties may provide deep insights into the biology of cells as well as better knowledge toward treatment of a variety of illnesses, and offers useful application in cell therapies, drug discoveries and tissue engineering [21-23]. Moreover, stem cells play a vital and essential role in the human body, by specifying the starting material for organs and tissues as well as by their continuous maintenance, growth, and renewal throughout ontogeny [24]. With the ability to generate a multitude of tissue types, stem cells have recently been considered as a primary cell source for tissue engineering in which the focus is on developing alternative therapies for degenerative diseases and injuries by regenerating the damaged tissue and restoring their function within the affected individual.

To date, the majority of research has been carried out on two main groups of human and animal stem cells, including non-embryonic (adult or somatic) stem cells, and embryonic stem cells (ESCs).

1.2.2.1 Adult stem cells

Adult stem cell, or postnatal somatic stem cell, populations were identified nearly 50 years ago when it was shown that cells in bone marrow stroma and blood could rescue patients suffering from bone marrow failures [25]. Adult stem cells are undifferentiated types of cells, located among differentiated organs and tissues (Figure 1.3). These types of cells are known to be located in various adult tissue niches throughout the body, including bone marrow, skin, brain, liver, muscle, nervous tissues as well as in the circulation [26].

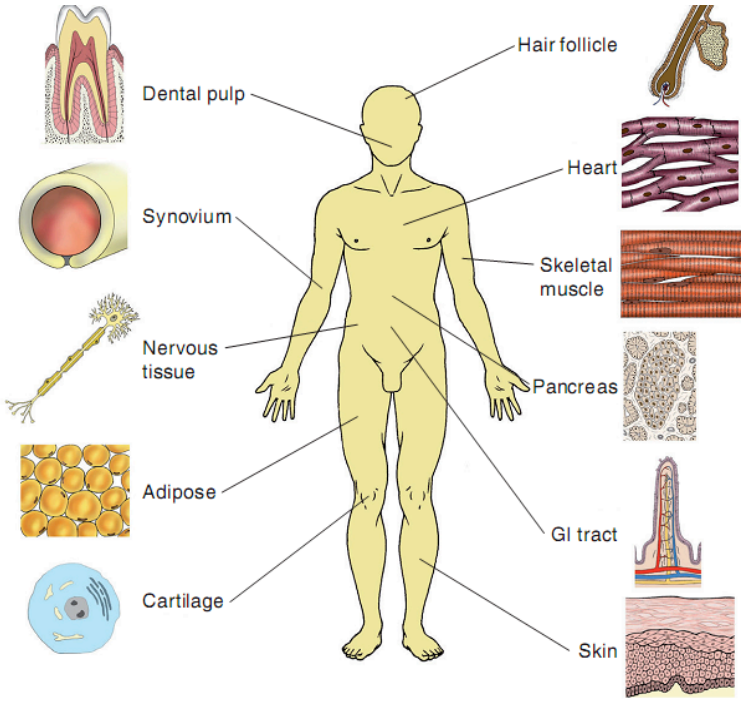

Figure (1.3): Location of human adult stem cells in some of the human tissues [27]

Initially, it was thought that adult stem cells are located only in the tissues in which they form. It was surprising that some components of blood could be capable of developing an entirely different embryonic origin. For example, the generating of muscle tissue and the development of neuron-like cells formed from stem cells in the bone marrow that was mentioned in some investigations, increased researchers' expectation about the capability of hematopoietic stem cell (HSCs) to give rise to multiple cell types from all three germ layers [28-30].

The study reported by Krause et al. in 2001 showed that a single HSC, transplanted into an irradiated mouse, generated not only blood components (from the mesoderm layer of the embryo), but also epithelial cells in the lungs, gut (endoderm layer) and skin (ectoderm layer)[31].

Adult stem cells have the ability to give rise to the cells of tissues in which they have been found. For example, skin stem cells generate new skin cells to replenish old or damaged ones. Although adult stem cells are capable of self-renewal, their ability to differentiate is more limited in comparison with embryonic stem cells (ESCs). In addition, in spite of ES cells' ability to give rise to multiple lineages, adult stem cells are not pluripotent and are also less versatile than ESCs.

The potential of adult stem cells are more limited similar, to primary mature cells. The practical usefulness of adult stem cells in tissue engineering is limited due to difficulties in accessibility, low number of cells (which is roughly 1 stem cell per 100,000 bone marrow cells), restricted differentiation potential, and poor growth. Typically, the small numbers of adult stem cells in tissues make them difficult to find and isolate. Adult stem cells usually stay dormant (non-dividing) unless there is a requirement for repairing injured organs and lost tissues. Although it is believed that adult stem cells are promising sources in cell-based therapies for various diseases and injuries (having been considered to be a safer option for clinical applications than ESC because they have not been shown to form teratomas), isolating and expanding their number *in vitro* has been found to be challenging.

1.2.2.2 Embryonic stem cells (ESCs)

The majority of existing strategies for tissue engineering depend upon a sample of autologous cells coming from the diseased organ of the host. However, for many patients, generating enough normal cells through the tissue biopsy cannot be achievable. Furthermore, in some cases, primary autologous human cells cannot be expanded from a particular organ, such as the pancreas. In these situations, embryonic stem cells are considered as alternative sources of cells from which the desired tissue can be derived. ESCs provide fundamental tools for increasing the understanding of normal development and disease, for cell therapy applications and for treating incurable and damaging disorders, including spinal cord injury, neurological disease, blindness, and type 1diabetes [32].

Embryonic stem cells, with unlimited self-renewal and differentiation potential, represent a major type of pluripotent population that are derived directly from the inner cell mass (ICM) of pre-implantation embryos after the formation of the blastocyst and grown in the laboratory [33, 34]. Formation of blastocyst begins by fertilization of an ovum by a sperm, and results in a zygote, the earliest embryonic stage. 30 hours after fertilization, the zygote begins to divide. By the 16-cell stage, the compacted embryo is termed a morula. The morula cells begin to specialize by day 3 (E3.0) in the mouse and days 5 to 6 in human development after fertilization, and form a hollow sphere of cells, called a blastocyst [35] as illustrated in Figure 1.4.

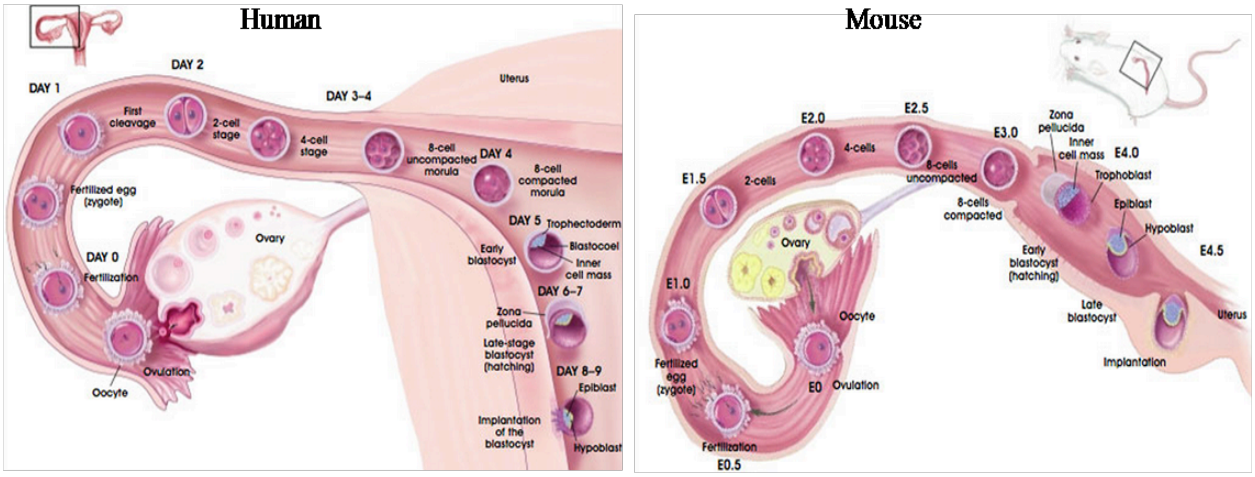

Figure (1.4): Development of the Pre-implantation blastocyst in Human and Mouse [36]

The outer layer of the blasotocyst, called the trophoblast, differentiates into the placenta and other tissues supporting fetus growth, while the inner cell mass develops to a fetus [33]. Derived from ICM, these populations of cells are pluripotent and have the potential to proliferate *in vitro* and to maintain their undifferentiated state continuously while keeping the normal karyotype [33, 34, 37]. In addition to displaying these unique properties, ESCs have the ability to differentiate into all three somatic germ layers (mesoderm, ectoderm and endoderm) under well defined conditions *in vitro,* including cells of the hematopoietic [38, 39], endothelial [40], cardiac [41, 42], and neuronal [43] tissues. Embryonic stem cells have many advantages over somatic stem cells. They offer greater pluripotency and indefinite growth in culture [44, 45]. They also provide a stable population of cells rather than a rare cell among other cell types, having been isolated from a relatively homogeneous population of cells within the ICM. Figure (1.4) illustrates the differentiation potential of ESCs. ESCs first were derived from mice and then from other species, including non-human primates and human [18, 46]. Two main classes of ESCs are described in the following sections.

1.2.2.2.1 Human embryonic stem cells (hESCs)

The derivation of the first human embryonic stem cell (hESC) lines in 1998 by Thomson and colleagues provided a tremendous boost to tissue engineering and to stem cell biology [18]. By definition, ESCs have a remarkable ability to self-renew continuously under appropriate culture conditions, which means they are capable of producing more multipotent cells like themselves, as well as being able to differentiate into cells representative of all three embryonic germ layers. Because of these properties, the derivation of hESCs marked the beginning of a new area of research, for not only basic biology, but also for regenerative medicine and drug discovery.

Human ESCs show several distinct differences from murine ESCs, such as having a slower proliferation rate (~24h doubling time) and showing a flatter morphological form. Human ESCs, in contrast to mESCs, are typically derived from embryos discarded from *in vitro* fertilization (IVF) procedures. They are also generally easier to dissociate into single cells than their murine counterparts [47]. Human ESCs can proliferate for more than 2 years while showing stable and normal complement of chromosomes. However, there is always need for careful monitoring of the aging ESC lines to evaluate the presence of any genetic changes that may occur over time. Most hESC lines have been obtained using murine embryonic fibroblasts (MEFs) as feeder cells, and grown in media composed of defined Dulbecco's modified Eagle medium (DMEM) and serum replacement components that are not entirely free of animal ingredients. Although the feeder cells are inactivated, i.e., they are not dividing and expanding, they still produce growth factors that sustain the ESCs. Furthermore, separating the trophectoderm cells from the ICM via immune-surgery techniques is performed using antibodies raised in animal species. Such *in vitro* culturing of hESCs increases the potential risk of contamination of hESC lines by animal-derived ingredients and the risk of cross-species pathogen transfer, which potentially limits the useful therapeutic applications of hESCs for regenerative medicine. For example, Martin et al. reported that both hESCs and derived embryoid bodies metabolically incorporate substantial amounts of Neu5Gc under standard conditions, which was caused by the murine feeder layer and medium [48].

One of the main concerns in tissue engineering is the need to grow human ESCs without any contamination by animal cells or proteins; this problem was highlighted by a report in January 2005 that showed the expression of a nonhuman protein by human ESC lines grown on animal feeder layers [48]. So far, different methodologies, such as addition of basic fibroblast growth factor to the culture medium [47, 49], growth on matrigel or laminin in feeder cell-conditioned medium [50] or in the presence of GSK-3specific inhibitors such as 6-bromoindirubin-3′-oxime (BIO)[51], and growth on fibroblasts derived from human ESCs, have been applied to get rid of animal feeders cells. However, it is worth noting that none of these methods is totally able to remove animal products, and therefore the problem still remains.

Research involving human ESCs is at the centre of the ethical debate about stem cell use and potential in regenerative medicine. Different cultures and religious groups have their own ethical stance on the use of human ESC. For example, in the UK, human ESC lines can only be derived legally under licence from the Human Fertilization and Embryology Authority, and the lines must be placed in the Medical Research Council's Stem Cell Bank. Since hESCs derived from embryos obtained from IVF procedures is not autologous, the possibility of patient's immune rejection is increased, which limits the clinical applications of hESCs.

1.2.2.2.2 Mouse embryonic stem cells (mESCs) and their role as model of study

The derivation of hESC lines has followed developments in the study of mESCs, which were first established as cell lines in 1981. Mouse development begins with a single-cell zygote, and results in a fairly complex structure, the blastocyst, with three distinct cell lineages. In mESCs, self-renewal is characterized by proliferation and high telomerase activity. It is believed that the mechanisms that play the key role in maintaining mESCs pluripotent status, and their indefinite growing without resulting in genetic anomalies, rely on the transcription factors that are involved in regulating pluripotency. For example, it was shown that telomere shortening could be prevented by KLF4 as the pluripotency transcription factor that can control telomerase reverse transcriptase (TERT) expression in mESCs [52]. The key important motivation of using non-human organism as a model for human disorders is to identify fundamental pathogenic mechanisms that provide opportunities for novel therapeutic targets as well as evaluate the efficiency and safety of new drugs. As a result of physiological, anatomical and genomic similarities between mouse and human, mice have historically been the most frequent model for study of human diseases [53].

Advantages of using mice are the relatively low costs, known age, known genetic background, easy handling, and housing. The initial isolation of murine ESC lines gave developmental biologists a major tool as it provided a simple model system to study the processes of early embryonic development and cellular differentiation. However, it also paved the way for tissue engineering applications if similar totipotent cells could be extracted from human blastocysts.

Mice have been widely used as a model in biological study; this is because mice and humans share approximately 99% of their genes.

It follows that mice and human have very common inherited diseases such as heart, cancer, glaucoma, anaemia, hypertension, obesity, asthma and neurological disorders. Physiological differences exist between mice and humans; the mouse's physiology provides an excellent tool for understanding embryonic development, for understanding diseases, and to discover new treatments. Although there are still other kinds of mammalians that share these diseases, the mouse still is the best model because it is small, can be maintained cost-effectively, and has a short gestation period. Significantly, over the past 100 years, there has been an immerse success in gathering a valuable amount of information resources and experimental approaches for mouse genetics that have been systematically acquired. Indeed, better understanding of the genetic, molecular and cellular basis of human diseases and normal biological processes can be provided by using these type of resources and tools [54]. Due to the fact that mESCs represent the pluripotent stem cells that are naturally present in the early embryo as well as the product of an *in vitro* culture system, without a doubt, they can be thought of as the model to study early mammalian development and for their use in clinical applications. The capacity to differentiate into a broad range of cell types, and the ability to form embryoid bodies

containing differentiated derivatives of endoderm, mesoderm and ectoderm, are the most significant characteristics of mESCs that can be applied in a wide range of experimental settings with various stringencies. *In vivo* pluripotency of mESCs is evidenced by the formation of teratomas after being transplanted in immune-deficient mice that contain tissues originating from all three germ layers. The further potential of mESCs to contribute to all tissues of the adult organism, including germ cells, was confirmed by germ line transmission through the generation of chimaeras by cell aggregation with eight-cell embryos or cell injection into blastocysts [55]. This approach has been used for the past three decades to generate transgenic mice for functional genomics studies.

The progress that has been made for inducing the *in vitro* differentiation of human ESCs into insulin-producing cells with the possible usefulness in treating diabetes was described by Ron McKay; however, he also mentioned studies that have already been carried out with analogous mouse cells transplanted into mice that have diabetes, and that partial restoration of insulin regulation was observed [56].

The successful transplantation of mouse ESCs into rodents having Parkinson's disease symptoms have demonstrated the partial relief of these symptoms [57]. Similarly, studies suggest that mESCs can be transplanted into animals that have spinal-cord injuries and can partially restore neural function [58]. Although hESC lines have not been studied for as long as mESCs, several key differences have already emerged. For example, mESCs have been shown to maintained their pluripotent state in the presence of the cytokine Leukemia Inhibitory Factor (LIF), whereas LIF does not maintain hESCs in the pluripotent state [18].

The population doubling time of hESCs is about 24h, which is longer than that of mESCs (12 h), and this could reflect the longer gestational period in humans compared with mice. If *in vitro* culturing of ESCs resulted in producing a desired cell type, the cells can be tested for their potential to repopulate and to repair damaged or degenerating tissues. Using specific lineages that come from ESC *in vitro* culturing is promising, suggesting that ESC-based cell replacement therapy might be applicable to treating human degenerative diseases associated with a loss or diminished pool of a particular cell type. Despite the differences existing between hESCs and mESCs, mouse studies still are prerequisite to clinical and human applications of ESCs [59]. In theory, although a wide range of human disorders could be treated using hESCs, the proof of fundamental concepts has largely derived from the use of mouse ES cells.

Overall, investigation of stem cell properties could be facilitated using systems of mESCs, due to their ease of culture and rapid growth rate. They can be readily differentiated into multiple cell types, providing closely related progeny that have lost their stem cell potential. Besides, plenty of specific factors that affect their self-renewal have been identified. They are also able to grow clonally, allowing many biological questions to be asked at the single cell level. The ease of testing their

pluripotency using blastocyst injection and the experimental accessibility to their tissue of origin provide rigorous assays of their stem cell activity.

1.3 Application of ESCs

Regenerative medicine, tissue engineering, and bioengineering are new ways of cell therapy, which aim to generate and expand specific cells through different cell and tissue methodologies, in order to replace important differentiated functions lost or altered in various disease states. Indeed, successful progress and development in cell-based therapies depends on the question of cell sourcing. Due to the fundamental attributes of ESCs, these types of cells have gained considerable interest from the biopharmaceutical sector for their use in drug discovery and development and cell replacement therapy. The key event that opened new possibilities in the studies of developmental biology, as well as gene functioning on the level of the whole organism, was after the isolation and identification of embryonic stem cells from mouse by Evans and Kaufman [33, 34]. Through isolation of ESCs from first primates and then from human blastocysts, these cells emerged as promising sources for regenerative medicine and tissue engineering research [18, 46]. The promise of the numerous preclinical animal studies and ongoing ESCs-based research have indicated that the differentiated derivatives of ESCs can provide functional replacements for diseased tissues, such as for Parkinson's disease or spinal cord injury [60, 61].

Although both adult and ESCs can provide starting materials to the development of regenerative medicine, ESCs have the advantages of multipotency and ready use in the laboratory. ESCs exhibit many properties whose improved understanding could assist researchers in modifying adult stem cells to achieve better growth in culture and greater capacity for controlled differentiation. ESCs have great potential in the area of tissue transplantation, drug screening, and cell therapy because of their unique potentials, such as unlimited proliferation potential and pluripotency.

Utilizing ESCs in cell and organ transplantation has led to established treatments for a wide range of diseases. ESCs are used in the development of the cell based Alzheimer's disease screening assay as well as in compound identification and optimization [62]. Production of liver like cells, derived from bone marrow and embryonic stem cells, is an alternative strategy to liver transplantation, which is the only successful treatment modality for end-stage liver failure [63].

Different experiments provided a clear indication that mESCs can serve as a valuable source of specific neuronal and glial cells for transplantation [64, 65]. Differentiating ESCs into functional islet-like cells with the potential to rescue experimentally induced diabetes in mouse models has been reported [66]. ESCs were also differentiated into pancreatic endoderm capable of generating mature pancreatic cell types that function *in vivo* [67]. Both adult stem cells and ESCs have been investigated

for their potential to differentiate into the appropriate cells for repairing damaged bones, cartilages, and tendons [68, 69]. For instance, mouse ESCs were employed as a screening system to identify elements that are both required and sufficient for cartilage and bone formation [70, 71]. In fact, utilizing ESCs as model of cartilage and bone development study can lead researchers to improve protocols for more successful application of ESCs in cartilage and bone tissue engineering. Furthermore, the particular lineages differentiated from ESCs have been used for the early stage evaluation of drug adsorption, metabolism and toxicity [72]. Established mouse ESCs were used for investigation of mutagenic, cytotoxic and embryotoxic effects for developing toxicology [73]. Today, cardiovascular diseases remain the number one cause of death throughout the world. Another important potential of ESCs is the ability to differentiate into cardiac lineages, thus representing a promising source for cardiac regenerative therapy because of the self-renewal capacity. ESCs also provide a novel and applicable source for generation of infinite quantities of cardiomyocytes for myocardial repair, as it is not practical and ethical to test the potential of fetal cardiomyocytes in clinical trials [74].

Differentiation of ESCs into functionally active cardiomyocytes is another important potential of these cells. The unique electrical, mechanical and biological characteristics of cardiomyocytes make them an ideal cell type for implantation to replace diseased or necrotic heart tissue. ESC derived cardiomyocytes display pacemaker-, atrial- and ventricular-like characteristics and spontaneously beating cluster behaviour, which is considered as one of the most impressive phenotypes developed *in vitro* [75, 76].

Field et al. (1996) reported the generation of relatively pure cultures of cardiomyocytes from differentiating mES cells for the first time. They showed that genetically selected mouse ES cardiomyocytes could form viable grafts when injected into the uninjured myocardium [77]. It was found that at each stage of lineage differentiation, specific tissue and lineage genes are developed in a controlled manner. ES cell-derived cardiomyocytes express cardiac molecular markers found in developing cardiomyocytes. For example, it is reported that mesodermal genes such as Brachyury and BMP4 are some of the initially expressed genes during cardiogenesis. The next stage is the expression of genes encoding cardiac transcription factors such as Nkx2.5, followed by structural cardiac proteins such as α and β cardiac myosin heavy chain (MHC), and finally the terminal stage genes such as ANF and myosin light chain-2v (MLC2v) [78]. Currently, implementing pluripotent stem cells (embryonic stem cells or hESCs) for generating heart and vascular endothelial cells is an interesting expanding area with potential application in cell therapy and as a platform for drug discovery and toxicity. The development of engineered products could be accelerated by combination of the available engineering efforts and myocardial infarct scar remodelling, which has the potential clinical applications of stem cells. A reproducible spontaneous cardiomyocyte differentiating system from human ESCs has been described by Kehat et al. [79].

In 2004, Kehat et al. reported the first human ES cardiomyocyte transplantation into the uninjured swine myocardium [80]. The landmark study is the first to document the potential clinical utility of regenerating damaged heart muscle by injecting hESC–derived cardiomyocytes directly into the site of the infarct [81]. To date, ESCs indubitably undergo the most efficient cardiogenesis[82] and are still the most natural and relevant source of cardiomyocytes for use as *in vitro* models of cardiac function and dysfunction, as well as in cell replacement therapy applications. Although the application of ESCs on experimental models of heart disease indicates an initial success to repair and improve myocardial function, a long term monitoring of the incidence of arrhythmias and teratomas in animals transplanted with ES cardiomyocytes preparations is still necessary [74]. ESCs have the potential to be driven down specific-lineage pathways to replenish damaged tissues and, as with adult stem cells, to be used for cell replacement therapy of monocellular degenerative diseases [83]. The versatility of ES cells to form any cell in the body is the normal developmental fate for these cells and makes them the most desirable for generating cells as therapeutics.

1.4 Technologies developed for stem cell culturing

It has been a long-standing challenge for scientists to find effective therapies for numerous numbers of incurable degenerative diseases such as Parkinson's disease and Type I diabetes. In addition to cell therapy applications, stem cell-based technology platforms have drawn great interest in medical applications, and in particular, in the development of novel strategies in tissue engineering, drug screening and *in vitro* toxicology [84, 85].

The present day, exponentially growing effort of stem cell research emphasizes a major need for convergence of more efficient and appropriate laboratory technologies to sustain the growth and proliferation potential of stem cells. This demand for stem cells requires, on the first approach, the implementation of scalable and affordable culture systems for the production of populations of undifferentiated cells without compromising their stem cell characteristics (self-renewal ability and differentiation potential).

However, for successful translation of stem cell-based therapeutics to the clinic, numerous challenges including gaining precise control over stem cell expansion, proliferation and differentiation still remain. For instance, in some cases, the actual number of stem cells with the potential to be transplanted to replace or repair damaged cells is still very low [86].Since stem cells are the desired products, good manufacturing practices (GMP) and safety need to be considered for further related applications. Indeed, different *in vitro* engineering strategies could be successfully applied for better understanding of the cellular mechanism such as stem cell proliferation and differentiation [87]. Generating a tissue, as a multistep process, starts with the isolation of cells through biopsy, followed

by an *in vitro* expansion of cells using appropriate bioreactor or scaffold design (the generation and maturation of a 3D construct), and finally the use of the construct as a test system or graft [88]. Based on the principle of TE, today there has been growing interest in developing the appropriate cell culturing environments *in vitro* using biomechanically active simulation systems, known as bioreactors, to functionally better mimic the behaviour of tissues *in vitro* [89, 90]. Bioreactors have been widely used in research laboratories and industries in large-scale cell culturing to facilitate mass/gas transport, environment monitoring and control, as well as the ability to support high cell densities.

Although there is no optimal and universal system for stem cell culture, the development of bioreactors throughout the last decades has advanced the technology considerably. There is, however, a large range of designs available, which include fluidized bed, packed bed, airlift and disposable wave bioreactors, stirred cultures vessels, rotary cell culture (RCC) systems and perfusion bioreactor. The three last have been the main bioreactors explored in this field and their applications in stem cell research are described in detail in the following sections (1.4.1).

Providing stem cells with a proper physical environment is an essential stage to enhance and regulate their proliferation and differentiation for cell-based tissue regeneration. The demand for using stem cells in tissue engineering/regenerative medicine in the first place requires the proper interaction and integration with tissue and cells through incorporation of appropriate physical and cellular signals [91]. Stem cell characteristics, such as proper differentiation and maintenance of the pluripotency, are regulated not only by the stem cells themselves but also by the micro-environment surrounding cells [92, 93].

In this regard, tissue engineering provides new means to gain critical insight about the behaviour of stem cells, by facilitating the control over the stem cell environment, both chemically and physically. Biomaterial-based TE is another emerging therapeutic approach in which synthetic or natural materials are employed to fabricate microfluidic or micro-bioreactors devices, with efficient small-scale systems mainly used for the optimization of culture conditions for cell growth and differentiation. This concept of biomaterial-based tissue engineering was originally introduced by Langer and Vacanti[7]. It has been demonstrated that the adhesion of cells is a prerequisite for a multitude of cellular functions such as movement, growth, differentiation, as well as in many physiological and patho physiological processes, such as cell development of organism, wound healing, inflammation but also cancer and metastasis [94]. Therefore, control of cell adhesion on biomaterials for implant materials and colonization of tissue engineering biomaterials is a crucial task. Although the contemporary materials used in a variety of biomedical applications have excellent physical and chemical properties, their clinical usage can be restricted by undesired side effects, due to uncontrolled adsorption of proteins and subsequent conformational changes. Therefore, because of intimate contact between the material surfaces and the biological environment, the outermost parts of

the material surfaces need to be modified in a size-scale of a few nano- up to micrometres. In this respect, it has been found that one of the effective approaches for developing a material for biomedical application is to modify and optimize the biocompatibility of the materials physically or chemically [95, 96]. In fact, surface modification aims to create closer *in vivo* local environment that enables cells to promote their proliferation and differentiation. Synthetic biomaterials have been used to create microenvironments that mimic natural extracellular matrix, with the particular aim of directing stem cell differentiation and morphogenesis of the target tissue [97, 98].

Some of the applications of surface modification are with a combination of microscale technologies [13, 99]. It has been shown that small-scale microfluidic devices, or micro-bioreactors, are effectively used for the optimization of culture conditions for cell growth and differentiation, while also providing the precise control over the cell microenvironment [88, 100]. Micropatterning is an important technology that allows for the tailoring of the cell microenvironment through controlled surface chemistry and topography. It has become well established that techniques such as photolithography and soft lithography are able to produce substrates with micro-scale features having defined shapes and positions that control cell shape and function, and create highly structured culture microenvironments [101-104]. Surface modification strategies will be discussed in more detail in section (1.4.1.2).

As mentioned previously, although a majority of our knowledge in modern biology came from the classical two dimensional (2D) cell culture methods, it is now well accepted that cells reside, proliferate and differentiate inside the body within complex three dimensional (3D) microenvironments. In fact, culturing cells in 3D culture systems instead of 2D monolayer culture fundamentally increases their performance and helps to better exploit their potential. Biomaterial-based scaffolds have been one of the most important tools in providing a 3D environment to cells, both in culture and inside the body.

A higher degree of efficiency, robustness, consistency and more predictive cultures could be achieved by engineering 3D microstructures. Varieties of microstructures self-aggregated spheroids (3D cell aggregates), microcarriers and more complex scaffolds based on natural, non-animal polymers such as gels and sponges, like alginate and cellulose microfibers or synthetic materials, have today been established [105-108].

The use of three-dimensional scaffolds with proper degradability, biocompatibility, hydrophobicity, bioactivity, porosity, pore size, and mechanical stability is another successful approach of great interest to biomaterial scientists for many years. Indeed, hydrogels have received special attention as required materials for regenerative medicine, for tissue scaffolds or as therapeutic delivery systems. Due to the innate structural and compositional similarities between hydrogels and the extra cellular matrix, hydrogels are considered as the most widely adopted materials for extensive 3D framework cell cultures, for cellular proliferation and survival [109, 110].

Due to advances in the field of tissue engineering, the need for engineering novel scaffold structures and reproducible fabrication techniques has become of paramount importance and requires to be met. Hydrogel characteristics and applications will be discussed in section (1.6.2).

Taken together, improving the biocompatibility and surface properties of existing biomaterials, and mimicking appropriate stem cell microenvironments and niches using biopolymers (biomaterials), can assist the improvement in proliferation and differentiation of cells and maintain their biological functions. Furthermore, there is still the need for bioengineering efficient and affordable culture systems both in 2D and 3D form without compromising their stem cell characteristics (self-renewal ability and differentiation potential), which promote our understanding of the microenvironment where cells are embedded.

1.4.1 Conventional bioreactors for ESCs culturing

In order to use stem cells successfully as an attractive source for cell therapies and tissue engineering, the clinical efficiency of a tissue-engineered product needs to be accompanied by developing some novel technologies that allow the systematic production of cells in a robust and cost-effective way. One such technology is the bioreactor system, which can be defined as an industrial form of the contained reaction vessel with defined controlled conditions for specific culture outcomes [111]. Ideally, a bioreactor should provide an *in vitro* environment for rapid and organized tissue development, beginning with isolated cells and in many cases, three-dimensional scaffolds. So far, a variety of bioreactor configurations have been designed and adapted for stem cell expansion and differentiation. A bioreactor configuration could be varied as a basic petri dish or as a complicated automatically controlled three-dimensional bio-chamber.

Traditionally, stem cells are cultured on flat two-dimensional (2D) surfaces, which support their growth [112]. The static system is the simplest type of bioreactor, which is usually suitable for maintenance and proliferation of adherent cells on a monolayer. In addition to low-cost and disposability, static cultures provide sterile handling procedure and ease of use, making them the ideal choice for research screening purposes [113]. However, their usefulness is limited when large quantities are required, as well as their inability for online monitoring, which makes these systems inadequate for bio-manufacturing and clinical applications (Figure 1.5). On the other hand, however, although static culture systems are easy to use, they are suitable only for studies of molecular factors and cannot provide physical regulatory factors. In addition, working with static culture requires changing medium constantly. Furthermore, it is known that static cultures may cause non-homogeneous distribution of cells and nutrients and does not allow mimicking the flow stresses that are present *in vivo*.

Although conventional 2D culture systems (i.e., Petri dishes, culture flasks) have been widely used in

both basic biology and tissue engineering studies, 2D culture systems have been shown constantly to be inadequate in resembling the *in vivo* developmental microenvironment. Meanwhile, it is indisputable that cell spatial arrangement and directional cues have strong effects on the cell differentiation and tissue development *in vivo*. It has been recognized that for obtaining a wider understanding of basic cell and tissue function within its native microenvironment, 3D culture model systems are vital [114].

Thus, introducing another dimension is an essential requirement of large-scale production rather than a by-product of the ‘‘scaling-up’’ process. The alternative to static growth is to use dynamic culture systems where homogeneous concentrations of nutrients, toxins, and other components could be achieved through mixing and thereby removing the problems associated with gradients and stabilizing the culture environment.

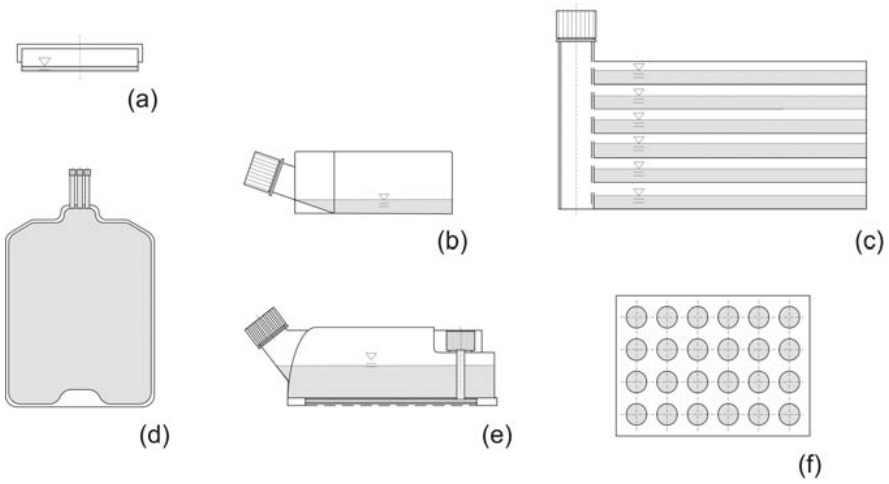

Figure (1.5): Basic schematic of static cell culture bioreactors: (a) Petri dish, (b) T-flask, (c) Multitray cell culture system, (d) Culture bag, (e) Static membrane flask bioreactor (celline), (f) Multiwell plate [115]

In the past years, bioreactors have turn out to be crucial tools to initiate, maintain and direct cell cultures and tissue development in a three-dimensional (3D), physico-chemically defined, tightly controlled, and aseptic environment [114]. Successful stem cell therapies require large-scale generation of stem cells based on robust and reproducible culture conditions. Therefore, a requirement for large quantities of stem cells *in vitro* as well as improving their quality for medical and commercial applications will be highlighted. Bioreactors have shown their capability to provide robust and defined conditions for ESC expansion and embryoid body (EB) formation as well as differentiation. Furthermore, scaling up and designing each type of tissue construct (e.g., skin, bone, blood vessel, and cartilage) should be considered individually [88, 116]. Thus, we should take into

account that it is less likely for a single bioreactor design to generally be used for all cell and tissue culture operations. Tissue-specific bioreactors should be designed in accordance with comprehensive understanding of biological and engineering aspects. The fact is that using bioreactors can address some limitations of static culture, including the lack of mixing and the need for frequent medium replacement rates [117]. During the last few years, a huge number of different bioreactor concepts have been developed. There are several bioreactor designs, which can be broadly grouped into *stirred, rotating* and *perfusion reactors*. In the following paragraphs, brief descriptions of different types of bioreactors, which are commonly used for cell research purposes, are presented.

Stirred (spinner) vessels are the most commonly bioreactor configurations for culturing yeast, bacterial and mammalian cells for commercial purposes (Figure 1.6). Spinner flasks, when compared to other bioreactor technologies, provide more attractive benefits mainly because of their scalable configuration, simple design, a uniform culture condition provided by stirring, and ease of continuous measuring and controlling culture environment factors, such as nutrient and cytokine concentration, pH and dissolved oxygen (pO_2) [118, 119].

Figure (1.6): Photograph of Stirred bioreactor designs [120]

Many research groups have utilized different types of stirrer bioreactors for expansion and differentiation of various ES cells. As mentioned previously, mouse ESCs are commonly used animal models in stem cell and developmental biology. In this regard, Cormier at al. presented a bioreactor process for the large-scale expansion of undifferentiated murine ESCs to get better expansion compared with static culture [121]. Zur Nieden et al. showed that murine ESCs could be maintained undifferentiated as aggregates in suspension culture for at least 28 days while retaining embryonic body formation potential and expressing ESC surface markers [122]. Kehoe et al. also applied suspension aggregate systems successfully to mouse ESC culture [123]. Mouse ESCs expanded in

suspension aggregates in spinner flasks have been shown to be able to differentiate into cardiomyocytes, in a single process without an intermediate dissociation step [124]. The formation of an embryoid body (EB) from ESCs is necessary for their expansion and traditionally achieved in static cultures, but several groups have shown that mESCs can be directly formed in stirred bioreactors with paddle-type impellers or a rotator cell culture system by enzymatic dissociation [125, 126]. Several types of tissue-specific stem cells have been successfully cultured as aggregates in stirred reactors [127, 128]. For example, differentiation of mouse ESCs to osteoblasts in spinner flasks and static culture condition has been compared by Alfred et al. [129]. Niebruegge et al. [130] combined micropatterning-based ESCs aggregate control and physicochemical (oxygen) control using stirred bioreactors, and reported two-step bio process for the generation of human pluripotent cell-derived mesoderm and cardiac cells in a stirred suspension system. Spinner flasks provide a better alternative for cultivation of cartilage and cardiac constructs to those cultivated under static conditions, as a result of providing a well-mixed environment around the cells and minimize the stagnant cell layer at the construct surface [131, 132].

Spinner flasks, however, may not be optimal because of the hydrodynamic shear stress that is created by the agitation and/or aeration[133]. Damaging cells due to mixing is an important challenge that needs be considered in designing suspension cultures, especially when working with mammalian cells, which are very shear sensitive and have delicate membranes. Impellers need to be designed carefully in stirred suspension bioreactors to avoid high shear stress that can damage the cells [134]. A low mixing rate of paddle-impeller results in cell clumping, leading to lower mass transport to the cells, while excessive shear stress due to high rates of paddle-impeller stirring could damage the cells. Consequently, having an optimal fluid flow for suitable shear stress is critical. However, due to diverse sensitivities and necessities, different cell types respond differently in terms of the shear stress, which is an important parameter for the design of bioreactors [122, 135]. It is important to consider that different types of cells have distinct optimal shear stress and oxygen requirement. For example, for mammary epithelial cells, the optimal shear stress was 0.21 Pa; however, mESCs preferred an optimal shear stress of 0.61 Pa and clumped together at a shear stress of 0.45 Pa [121, 136]. In addition, the minimal volume required to set up a cell culture experiment is very high (approximately 50 mL), demanding higher starting cell numbers, increasing the costs associated to optimization studies and compromising the use of stirred tank bioreactors for high-throughput applications. Agglomeration of the EBs is another concern in suspension culture and encapsulation of the cells in agarose beads has been proposed as a solution to minimize this problem [137, 138].

Using different microcarriers such as collagen coated dextran beads, glass microcarriers, and macroporous gelatin-based beads in spinner flasks are alternative options [124, 139, 140]. However, microcarrier cultivation has the disadvantage of requiring dissociation of the cells from the carriers once the cells reach confluency, which leads to cell loss due to low seeding efficiencies and the

fragility of cells.

Although shear stress is essential in modulating the mechanical properties of tissue constructs, high shear stress results in the formation of undesired capsules surrounding the tissues [141], hence various bioreactors featured with low shear stress have been developed. The most commonly used bioreactor that exploits the benefits of low shear stress is the rotating wall vessel (RWV) wherein the cells are grown in a microgravity environment; the RWV is another approach for controlling EB agglomeration enabled 3D cell cultivation under medium mixing with a minimal shear stress. This technology, developed by NASA, is composed of a rotating 3D chamber in which cells remain suspended in near free-fall, simulating microgravity conditions [142]. Although a variety of different names are given to this type of bioreactor, such as the rotating wall perfused vessel, the high aspect ratio vessel (HARV) and the slow turning lateral vessel (STLV), the generic configuration is based on the horizontal rotating vessel (Figure 1.7) [141, 143].

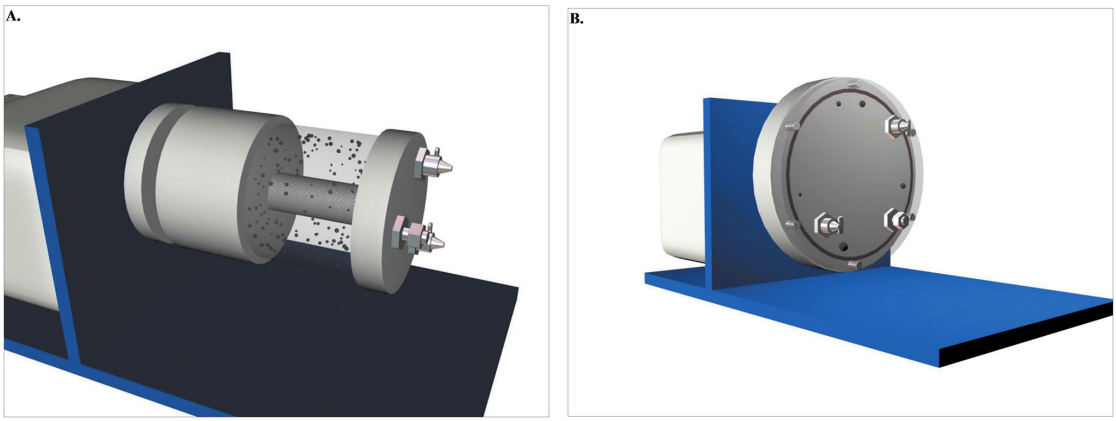

Figure (1.7): Diagram of the rotating bioreactors, Slow turning lateral vessel STLV (A), High aspect ratio vessel HARV (B) [143]

These bioreactors are horizontally rotating, which is characterized by low fluid shear stress. In RWVs, the ratio of membrane area to volume of media is high, which results in an efficient gas exchange [144]. E et al. showed the possibility of cardiomyocyte differentiation in mESCs using a rotary cell culture system [145].

Gerecht-Nir et al. showed that cultivation of embryonic stem cells within a rotating bioreactor increased the cell proliferation rate and maintained cell viability. In addition, EBs formed smaller in size with no necrotic centres in an STLV while forming massive agglomeration in an HARV. They investigated the dynamic generation of EBs in an efficient mixing low shear rotating bioreactors and reported that with the mild mixing, a large number of small EBs will form [143]. Cultivation of cardiac cell constructs in an RWV, in which laminar flow patterns exist, demonstrated improvement in expression of cardiac muscle-specific markers and in acellularity compared to constructs cultured

in mixed or static flasks [131]. Liu et al. reported that hematopoietic stem cells (HSCs) and progenitors could be expanded in an RWV bioreactor with more folding expansion and in a shorter period than other types of bioreactors [146]. RWV bioreactors have also been used in many other tissue culture applications including rat neural stem cells, neural progenitors [147], human endothelial cell [148], human prostate cancer cells [149], and 3D bone constructs [150]. Osteoblasts and rat bone marrow stromal cells were seeded on bioactive glass, bioceramic, and composite microspheres to examine 3D bone cell growth on microcarriers [151], bovine chondrocytes were seeded onto polyglycolide to examine growth under variable metabolic parameters[152], and human osteoblast-like cells (SaOS-2 line) were seeded onto poly(lactide-co- glycolide) to examine mineralized tissue formation [153].

Although the boundary layer around the cell surface decreases efficiently in RWV bioreactors, inefficient mass transfer into the core of the cell constructs is one of the limitations. The main disadvantages of RWVs are the limited control of aggregate size and of the nutrient/gas concentrations throughout the vessel. This may result in the formation of necrotic centres, leading to cell death inside the aggregates, and uncontrolled microenvironments, caused by the concentration gradients resulting from mass transfer limitations.

Bioreactors can also be operated in the form of a perfusion system. *In vivo,* the process of delivery of nutrients via capillaries into a tissue is called perfusion; however, in *ex vivo*, perfusion is described as transferring culture medium directly through a porous cell-seeded matrix (Figure1.8).

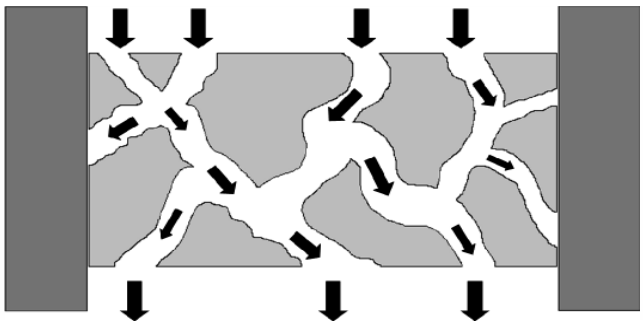

Figure (1.8): Perfusion system. Medium perfuse through macroporous matrix and dissolved oxygen transport is via both convection and diffusion, thus increasing the oxygen balance [154]

The perfusion bioreactor system was developed to improve cell seeding efficiency onto the porous scaffolds by perfusing cell suspensions through 3-dimensional (3D) scaffolds with remarkably uniform cell distribution and high-efficiency [155]. Perfusion bioreactors were successfully tested on both mouse and human ES cells and showed a higher yield than static culture flasks. The use of

perfusion bioreactors has been reported [156] for the expansion of mouse ESC lines on a petri dish with a gas-permeable base. They showed that the cell densities obtained from a perfusion system were 64-fold greater compared to the petri dish controls over 6 days. Several researchers showed that the perfusion culture supports higher hMSC density within the 3D scaffolds, and MSC expansion was accomplished without loss of multi-lineage differentiation potential [157-160]. A variety of perfusion reactors have been used for animal culture cells that required the high amount of medium at very low shear stress. Dvir and et al. showed that cell viability improved by medium perfusion and enabled the functional assembly of cardiomyocytes into cardiac tissue, as a consequence of better oxygen transportation by convection and diffusion rather than oxygen diffusion alone within the static-cultivated cells [161]. Perfusion bioreactors with a frequent feeding system showed positive effects on the expansion of MSCs, ESCs, mammary epithelial stem cells, and proliferation of human bone marrow cells while retaining stem cell potential [136, 158, 160, 162-164]. The perfusion system in Zhao's research [157] provided a more uniform distribution of hMSCs within 3D scaffolds. Perfusion or frequent feeding also enhances culture performance by replacing depleted nutrients and/or removing inhibitory metabolic by products. Indeed, this system provides homogeneous culture conditions, inhibits waste accumulation, and improves process reproducibility.

Gerlach et al. (2003) used a four-compartment capillary membrane technology for EB formation and spontaneous differentiation. They showed that the perfusion system more closely resembles that of mouse fetal tissue development compared to those cultured in petri dish as control [165]. Using a perfusion bioreactor for differentiation of mESCs led to a very low percentage of necrotic areas compared to mouse EBs formed in static condition [165, 166]. Recently, Stachelscheid et al. (2012) introduced a 3D perfusion bioreactor system that allows *in vivo*-like tissue formation by hESCs. They showed that the perfusion bioreactor is capable of formation of 3D tumour structure (teratoma) containing tissue-like structures containing derivatives of all three germ layers [167]. They suggested that this type of bioreactor could be utilized more effectively for formation of embryoid body in ESCs since the physiological situation of the cells within the organism could be estimated more closely[167].

On the other hand, medium flow through the perfusion system removes detached cells, preventing the non-even distribution of cell mass in the constructs [168]. A perfusion fluid flow system is categorized as a bioreactor generating shear force. Pumping media through the scaffold within the bioreactor generates shear force that is influenced by different factors such as flow rate, port size, and scaffold pore shape [169, 170].

The potential for large scale culture in a perfusion bioreactor is still limited by the fact that partial harvesting is very difficult and the continuous removal of secreted factors could have unfavourable effects on cells in terms of yield and phenotype [156, 162]. In addition, relatively low-throughput nature of these systems is another major limitation of perfusion cultures that is mainly due to the

space limitations, as perfusion bioreactors require relatively large amounts of space to operate in a controlled environment [171].

Although several advanced studies have considered culturing specific populations of stem cells, like mesenchymal stem cells, hematopoitic stem cells, neural stem cells or pluripotent stem cells in different types of conventional bioreactors [100, 172-174], a number of fundamental challenges limit the therapeutic applications of traditional tissue engineering.

In fact, although culturing cells in a bioreactor can provide perfusion of medium, control medium composition [116, 161] and therefore support generating high densities of cells such as ESCs and EBs [143, 162], the operating volumes of bioreactors are larger than those of well plates, which is a serious limitation in studies involving the use of expensive media components. Bioreactors can be disadvantageous in benchtop research because they need large space, consume huge amount of reagents and need more time to operate and maintain (sterilizing, cleaning, assembling, and disassembling of the bioreactor components). Bioreactors also have complicated operating processes.

The requirements for costly equipment and generating shear stress due to fluid flow, and the lack of physical similarity between microenvironments of bioreactor and actual cell microenvironment, make using bioreactors undesirable. Furthermore, in conventional cell culture formats, such as dishes and macro-scale bioreactors, it is quite difficult to attain the delivery of a sufficient amount of nutrients and removal of waste throughout the cultured tissue. This is attributed to the difficulty in designing and fabricating large complex bioreactors wherein the cells are fed by a spatially homogeneous distribution of the fluid flow.

It is obvious that there is still a need for additional efforts to tackle the existing challenges in using traditional bioreactors and to develop novel kinds of devices, scaffolds, and technologies that potentially allow the obtaining of a better control over the cellular positioning, organization, and interactions under good manufacturing practices (GMP) conditions.

In response to these challenges, miniaturised devices (micro- and nano-) have led to the advent of a new generation of bioreactors aimed at mimicking *in vitro* the native microenvironment of tissues. Despite the various conducted studies so far, micro-bioreactors represent relatively new directions in TE, and there is still plenty of room for new developments in human 3D models to study the underlying mechanisms in cellular microenvironments. Micro-scale approaches can potentially overcome some of the limitations of conventional culturing systems.

1.4.2 Micro-scale culture system for ESCs culturing

In tissue engineering, micro-scale technology is an approach that combines micro-techniques with materials science and surface engineering, and results in a profound exploration of the microenvironment in which cells are embedded. These technologies are able to address some of the limitations imposed by conventional tissue engineering methods. The culture conditions for stem cell growth and differentiation could be optimized by providing the precise control over the cell microenvironment using small-scaled or micro-bioreactor systems [88, 100]. Indeed, controlling different interactions between cell and the microenvironment including cell-cell, cell-extracellular matrix (ECM), and cell-soluble factor could be facilitated using micro-scale technologies. Nowadays, the importance of mimicking certain *in vitro* parameters, which are present in the native environment of cells and tissues, has been demonstrated.

Developing an engineered bio-mimetic three-dimensional system, which could closely mimic the stem cell environment, and promote their proliferation or differentiation, is a highly recommended strategy. Therefore, besides the basics of TE strategies, it is of utmost importance to provide efficient constructs with the appropriate microenvironment that will encourage effective organization among the elements of a TE strategy.

Small-scale bioreactors (also known as biochips or cell-chips) offer one of those technologies that expand our ability to have better control of material transportation and material manipulation at the micro-scale. Small scale systems are particularly advantageous for biological and medical applications; these advantages include the ability to create bio-mimetic structures that mimic the *in vivo* cellular microenvironment [175], allow experimental parallelization under well-controlled conditions, reduce reagent consumption, and require shorter sample analysis time [176]. Micro-bioreactors are the miniaturized versions of conventional bioreactors where high-throughput cell-based assays can be carried out at low cost compared with their macro-scale counter-parts. In fact, the essential preferences of the small size of micro- bioreactors include the lower consumption of power, portability and reduced space requirements. Consequently, these elements cause small-scale devices to be cheaper to deal with and to be easier to manipulate small populations of cells and to study their behaviour in greater detail. In the case of working with hazardous biological materials, small volumes are also advantageous, especially for minimizing waste materials [177].These technologies accelerate the optimization of the biological process for further clinical applications.

Indeed, small-scale bioreactors have shown to be promising substitutes for conventional bioreactors, not merely as culturing systems but as devices for studying the mechanisms occurring in the tissue microenvironment. This applicability allows the better design of materials and/or culturing systems.

To be able to maintain the self-replicating ability and pluripotency of stem cells, the micro-bioreactor should more closely mimic the *in vivo* microenvironment of stem cells. In this regard, the materials

using for constructing the micro-bioreactors should be carefully chosen to prevent stimuli such as growth factors, while needing to be biocompatible, as well as being surface functionalized to provide cell adhesion sites because pluripotent stem cells are anchorage dependent [178]. Micro-scale bioreactor systems are progressively starting to find wide selection range of applications in various fields such as drug discovery, high-throughput bioprocessing, single cell analysis, stem cell research, and genetic analysis [179].

For instance, micro-bioreactor arrays that contain independent micro-bioreactors perfused with culture medium have been fabricated via soft lithography [180]. These systems have been used for adherent or encapsulated cells (including C2C12 cell line, primary rat cardiac myocytes and human embryonic stem cells (hESCs)) with different levels of hydrodynamic shear and with automated image analysis of the expression of cell differentiation markers [181]. In addition, these devices can also be used to study design parameters, mass transport phenomena and shear stress using numerical simulations [182], providing efficient means to analyse multiple parameters and parameter interactions. Chin et al. [183] reported a microfluidic bioreactor array for high throughput monitoring of stem cell proliferation. Lee et al. [184] reported a novel three dimensional direct printing technique to construct hydrogel scaffolds containing fluidic microchannels for tissue engineering.

A microfluidic device has been developed and utilized to examine the effect of different range of flow rates on ESC cells growth and proliferation [180]. Park et al. [185] used a microfluidic device to culture progenitors derived from ESC for eight days under continuous cytokine gradients and showed that the device was capable of sustaining the differentiation of neural progenitors. Another study showed the capability of a microchannel bioreactor for the long term coculturing of undifferentiated colonies of embryonic stem cells on foreskin fibroblast [182]. A combination of a microfluidic platform with an array of micro-bioreactors was used to control cellular environments and study the factors that regulate the differentiation of human embryonic stem cells [175]. Encapsulated ESCs in alginate beads were used in a perfused microfluidic chip for formation of EBs and differentiation [186]. Moeller et al. [187] developed a microfabricated platform of poly(ethylene glycol) (PEG) microwell arrays for optimisation of EBs formation in ESCs. A multi-layer, microfluidic array platform containing concave microwells and flat cell culture chambers was developed to culture embryonic stem cells and regulate uniform-sized embryoid body (EB) formation [188]. Given these examples, it is clear that microbioreactors are increasingly opening up new opportunities, especially in the area of cell biology. Indeed, developing successful novel small-scale technologies for *in vitro* cultivation of different types of cells can assist in increasing our knowledge of conditions that control stem cell growth and differentiation and organ development [189, 190].

In biological processes, biocompatibility is the leading requirement of any material substrate applied in the construction of functional devices. Because of the inert nature of most of the biomaterials used

in small-scale devices, they must undergo surface modification prior to cell attachment to promote adhesion and to prevent adsorption of proteins on the surfaces [179].

A detailed explanation of some of the common methods that have been used for improving the performance of the micro fluidic devices are presented in the following section, and a new and effective approach for improving the bio-compatibility of microfluidic surfaces that facilitates stem cell adhesion and proliferation will be proposed.

1.4.2.1 Surface modification of micro-scale devices

ES cells are anticipated to serve as unlimited cell sources for cell transplantation therapy. In the early days of stem cell research, and even to date, the use of mouse feeder cells has been required to maintain pluripotency. Although, common techniques such as adding some soluble biochemical and biological factors, such as LIF, cytokines and growth-differentiation factors in the growth medium, have been identified as essential cues for successful ES cell culture [191], these factors are not always sufficient for controlling ESC behaviour.

Stem cell characteristics, such as proper differentiation and maintenance of pluripotency, are regulated not only by the stem cells themselves but also by the microenvironment in which they reside. To safely transfer stem cells into the clinic, there is a need to develop defined and xeno-free culture conditions. This means that substrates (feeder layers) and culture media containing (animal) serum need to be replaced by defined culture substrates and by a chemically defined media. Throughout the last decades, various alternative options have been recognized as feeders to support ESCs self-renewal in monolayer, thereby limiting cross-species contamination. Indeed, a defined culture free of animal components and feeder layer would be an ideal culture method for ESC-based cell and tissue therapy [191-193]. As an essential and a prerequisite step, adhesion of cells to a proper substrate, plays a vital role in many physiological processes such as development of organism, wound healing as well as cellular functions including movement, growth, differentiation and survival [94]. For development of a micro-bioreactor for stem cell expansion, the micro-bioreactor needs to mimic the *in vivo* microenvironment of stem cells in order to retain the self-replicating ability and pluripotency of stem cells. Artificial stem cell niches from the synthetic approaches have been shown to have a great potential to create suitable *in vitro* biological 2D and three-dimensional artificial systems for pluripotent stem cell growth and their conversion to specific cell types of interest [194-196].

Considering the interactions between the receptors on the surface of ES cell membranes with solid surfaces is one of the recent approaches to improve the efficiency for controlling the ES cell fate. In fact, by fixing different signals on a surface of biomaterials that are in intimate contact with their targets on the cell membrane, the interactions of biologically active components with cells would be

stronger mainly because when the signalling components are dispersed in a bulk liquid (medium), they are less likely to encounter their targets.

An important parameter that needs to be considered in the construction of a micro-bioreactor to avoid stimuli such as growth factors is biocompatibility of the surface that could be achieved through functionalization to provide cell adhesion sites, since pluripotent stem cells are anchorage dependent [178]. A micro-bioreactor surface should be engineered to assist cell growth, while being able to resist the adsorption of undesired analyte molecules such as protein and DNA[197].

Although biomaterials assist the regulation of stem cells, due to the inert nature of most commercial polymers, functionalization of their surfaces is a prerequisite before the attachment of any bioactive molecules [198]. A study done by Altankov et al. showed that there is a link between cell adhesion and the presence and conformation of specific attachment proteins on material surfaces [199]. The molecular composition of material surfaces dictates the response of the biological systems in terms of protein adsorption, cell adhesion, and subsequent events. The properties of micro-bioreactor surfaces have a strong influence on cell analysis. Therefore, it is crucial to control adhesion of cells on biomaterials and to improve the biocompatibility of materials, which can be achieved by modification of materials surfaces. On the other hand, since the ultimate goal for the development of miniaturized bioreactor is to create integrated systems, capable of performing various functions on a single device, this goal can be achieved by microfabrication techniques. A variety of structures could be formed by different microfabrication methods that are properly matched to the physical dimensions of most cells organisation [179].

In the past couple of decades, different strategies have been employed to apply two-and three dimensional micro- and nano-featured devices to tissue engineering [200-203]. One such technique is soft lithography, pioneered by Whitesides and colleagues [13], which is a relatively facile and inexpensive method with widespread applications in micropatterning and cell culture devices [99, 177]. In the following section, we provide an overview about common techniques used for modification of cell culture surfaces, which are broadly categorized into physical and chemical techniques.

1.4.2.1.1 Modifying Polydimethylsiloxane (PDMS) surfaces

In order to cultivate various types of mammalian cells in microfluidic devices, the first step is to fabricate a substrate channel at the micrometre scale, which could be from a variety of materials, including polymer materials, silicon and glass. Although glass-made microfluidic devices have been used mostly in the past decades, some of the properties could limit its application in microfluidic devices. Using glass for microfabrication devices is not accessible for all researchers as it needs clean room facilities for photolithography and corrosive etching solution, which make these techniques

relatively expensive [204, 205]. In addition, the thermal bonding technique, which is often used in the fabrication of glass microchips, is time-consuming and often irreproducible. On the other hand, although glass is cheaper and transparent, its amorphous structure makes it difficult to etch vertical walls [206, 207]. Brittleness and materials invariability are other limitations of silicon and glass materials. Furthermore, it is usually difficult to etch deep channels on glass surfaces, which makes it troublesome to fabricate directly interfaces for interaction with macroscopic auxiliary equipment. Therefore, the need for better packing adds cost and complexity.

The above-mentioned disadvantages related to glass microfluidic devices have led scientists to investigate alternative materials for microchip fabrication and to shift to microdevices made entirely from polymeric materials. In fact, polymer based microfluidic devices are rapidly becoming more popular than glass or silicon-based systems in clinical diagnosis and pharmaceutical research [208, 209]. Polymeric materials with almost infinite variability have generated significant interest particularly for production of microfluidic devices due to their superior biocompatibility, greater flexibility, reduced cost, and ease of processing. Light weight as well as durability are important elements that make them easy to handle. In addition, since polymeric materials have different moduli, they can meet the need of rough environments that require tough materials or low modulus for the construction of, for example, on-chip pumps. Polymer technology has been an important element for realizing and defining of the so-called Lab-on-a-Chip concept.

Biomaterials, which assist regulation of stem cells, are of great importance to explore the unique therapeutic potential of stem cells. It has been demonstrated that the interaction between cells and substratum is one of the important parameters in biological phenomena. A variety of polymers have been employed for microchip electrophoresis, including poly (dimethylsiloxane) (PDMS), poly(methyl methacrylate) (PMMA), polysterene (PS) and polytetrafluoroethylene (PTFE) which have high impact on lab on chip systems due to their low cost, wider range of chemical reactivity and easier fabrication, as a clean room is not required [210].

Polydimethylsiloxane (PDMS) is a popular material that has been widely used for microfluidic device construction, especially for biological applications due to its attractive properties [211, 212]. This silicon-based elastomer material is biocompatible, optically transparent at wavelengths greater than 280 nm, highly flexible, thermally stable, and can be readily sealed to many other materials through van der Waals contacts with the surface. Furthermore, the low Young's modulus and durability of PDMS are suitable for various microfluidic applications [213-215]. The gas permeability of PDMS provides better diffusion of dissolved gases such as O_2 through its membrane and extraction by reactions carried out in chambers separated from cell culture by PDMS [216, 217].

PDMS has been used for fabrication of different devices as a cell growth surface, which makes it important to ensure that cells can readily attach [217-219]. For example, endothelial cells were successfully cultured as an attempt of vascular system reconstruction [220]. Leclerc et al.

demonstrated that PDMS could also be used to culture liver cells [221]. Another study by Leclerc showed the successful culturing of hepatocyte cells on microfabricated PDMS in a bioreactor composed of multiple layers of PDMS [222]. There are different types of cells that so far have been successfully cultured on PDMS substrate [223-226].

Considering that developing and producing each and every device requires substantial resources, current attempts are trying to decrease optimization time by means of using rapid prototyping techniques, where device geometries are rapidly assessed. A number of techniques have been employed for fabrication of polymeric micro-devices. The microfabrication process applies these techniques in a sequential manner to produce the desired structure[227].

Photolithography is one of the widely used techniques for fabricating microstructures in the semiconductor and, subsequently, the microelectromechanical systems (MEMS) sectors. This is a technique that is highly developed and well studied since the 1980s in cell and protein patterning [228, 229]. Throughout photolithography, micrometre-sized features on the photo mask will be transferred to photoresists coated on top of the substrate, utilizing the photochemical reaction in the exposed region of photoresists. Etching is the final step that transfers the pattern on the photoresist to the substrate via either plasma etching or wet etching using chemical solutions such as HF, KOH. Although photolithography has been extensively used for fine structures, expensive equipment requirements and the need for clean rooms for manufacturing make this technique inconvenient for biologists. Furthermore, using solvent in the developing process may denature biomaterials, which is a deterrent to the use of this technique [99, 230].

To address some of the problems associated with the photolithography technique, *soft lithography* was developed for creating chemical structures on surfaces for controlling cell-substrate interactions.

This technique is one of the most commonly used approaches for cell culture studies and was developed by Xia and Whitesides [231]. This approach makes it possible to rapidly design and fabricate microfluidic devices compared to traditional micromachining techniques. This method is low cost and can be used for the creation of highly complex microstructures with diverse functionalities [232, 233]. Soft lithography techniques are based on the replica molding of microstructures in elastomer and most typically PDMS [13]. Compared with other microfabrication methods, the soft lithography (Figure 1.9) technique is preferred for many biological applications, due to the fact that PDMS is biocompatible, transparent, inexpensive, permeable to gases, and amenable to surface modification. It is one of the commonly used patterning techniques in which instead of etching the silicon, a polymer such as PDMS is used to cast against the photoresist (usually SU-8) mold [231, 234]. Different techniques are applied in soft lithography, including replica molding, micro-contact printing, micro-transfer molding, micromolding in capillaries, and solvent assisted micro-molding [235]. The patterned PDMS can be directly used as a substrate with relief structures as stamp, mold or mask for cell culture or as a stencil to pattern the inoculation of cells onto other

substrates. This method is one of the most commonly used approaches for cell culture studies [175, 236].

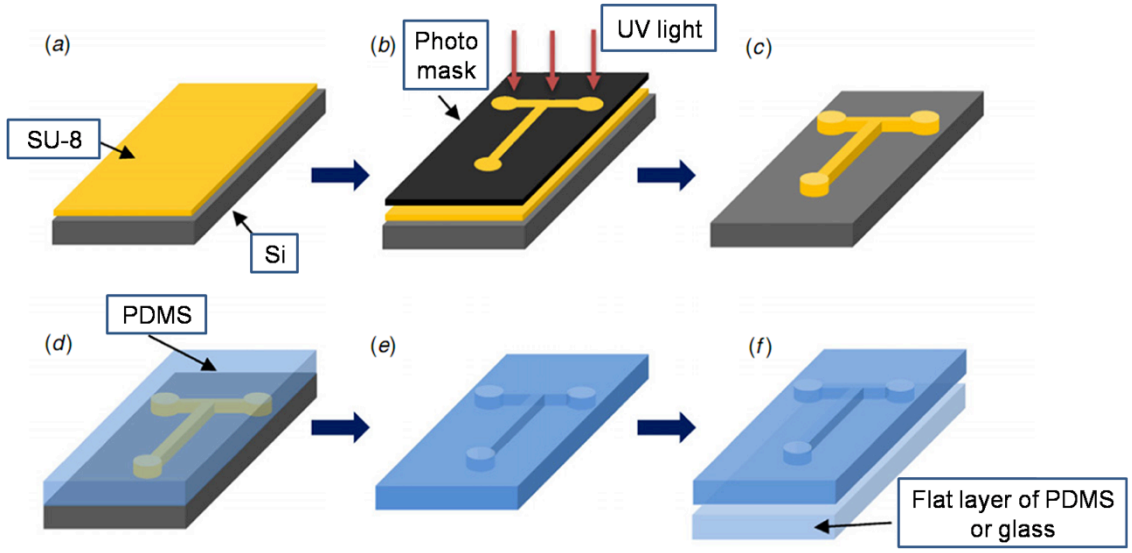

Figure (1.9): A schematic diagram showing the fabrication steps of a PDMS microchannel using soft lithography: (*a–c*) mold fabrication and (*d–f*) replication/bonding processes[237]

As mentioned above, PDMS is one of the organic polymers that are widely used to build constructs within the rapidly developing field of medical implants and biomedical devices and cell-based studies. These properties lead to PDMS being heavily exploited in micro-technology applications in different areas, including the production of active and passive medical implantation devices that have direct contact to human tissues [238], artificial lungs [239], technology applications such as microfluidics and lab-on-chip devices [215, 240], and pharmaceutical applications including porous PDMS membranes to control the release of drug in dermal patches and tablet coatings [241, 242].

Despite its numerous advantages, the major drawbacks of PDMS, especially from a biomedical perspective, are the poor wetting and heterogeneous surface charge of the surface, which hinders the immobilization of biomaterials and causes it to be chemically inert. The hydrophobic surface of PDMS in an unmodified condition results in poor cell attachment and introduces toxicity to some cell types [243]. Moreover, hydrophobicity of the surface leads to surface bio-fouling where deposition and growth of microorganism occur on the polymer surface through the adsorption of small molecules [244], such as fluorescent dyes [245], organic solvents [246], and proteins [247]. The problem will arise when there is any contact between protein-containing solution with the PDMS surface in microfluidic applications. This contact causes nonspecific protein adsorption as a result of the inconsistency of protein composition or the loss of target or biologically important proteins.

The interplay of electrostatic interactions and alteration of the surface and protein structure on the hydrophobic surfaces governs the protein adsorption.

Although electrostatic interaction is not a main powerful interaction for protein adsorption on the surface, it influences the kinetics of the adsorption process as it acts over longer distances. Attached proteins optimize their structural arrangement on the surface to have the maximum number of contact points. The close contact between the protein and the surface often is needed for the hydrophobic interaction between the two components, which may be optimized by structural rearrangements in the protein [248].

Changes in the conformation of extracellular matrix (ECM) molecules and reduction in the accessibility of integrin attachment sites for various cell types are another limitation caused by the hydrophobicity of PDMS surfaces. These changes can affect cell adhesion, proliferation, and differentiation [249-251]. Cell growth and function were found to be strongly related to the surface energy (wettability) of materials [199, 252], which have been outlined in Figure 1.10. The existence of amino or carboxylic groups that represent the charged functional groups has been determined to promote cell attachment, growth, and function while polar groups like methyl may lessen cellular activity [251].

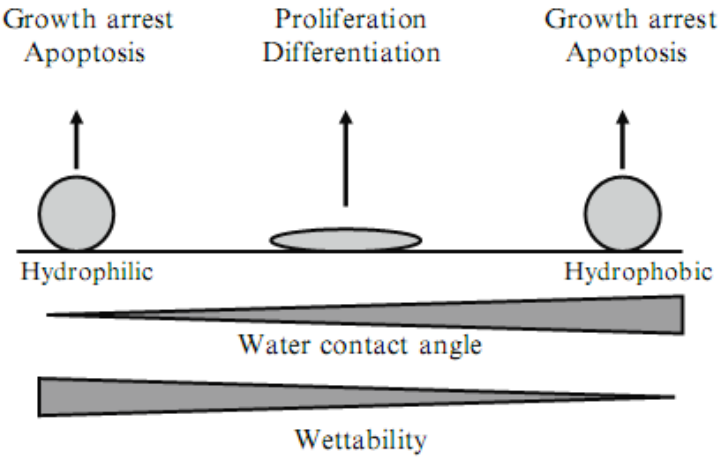

Figure (1.10): Simplified view on dependence of cell adhesion on interfacial forces characterized by water contact angle measurements [253]

The unreactive nature of PDMS is due to its $[-OSi(CH_3)_2-]_n$ backbone (Figure1.11) [254, 255]. Surface coverage by the methyl groups (-CH3) makes it difficult to deal with aqueous solutions [254] and causes inefficient distribution of protein or cell solutions on the surface [256]. Absorption of hydrophobic molecules (biomolecules) on the surface of PDMS could also disrupt the microfluidic devices. The systems are also susceptible to media drying due to the permeability of PDMS to water vapour [257]. The hydrophilic surface with a large degree of mobility is the only surface that prevents

protein adsorption on the surface. The mobility of hydrophilic chains is decreased when proteins come close to the polymer layer; therefore, it opposes the interaction. Hydrophilic polymers are often based on poly-ethylene-oxide PEO (-CH2CH2O-), also called polyethylene glycol (PEG), and polysaccharides such as dextran. It is commonly believed that hydrophilic surfaces have levels of protein adsorption lower than those of hydrophobic surfaces. Studies have shown that while proteins may readily attach to hydrophobic surfaces, most adherent cells have improved attachment and proliferation on hydrophilic surfaces [96, 258].

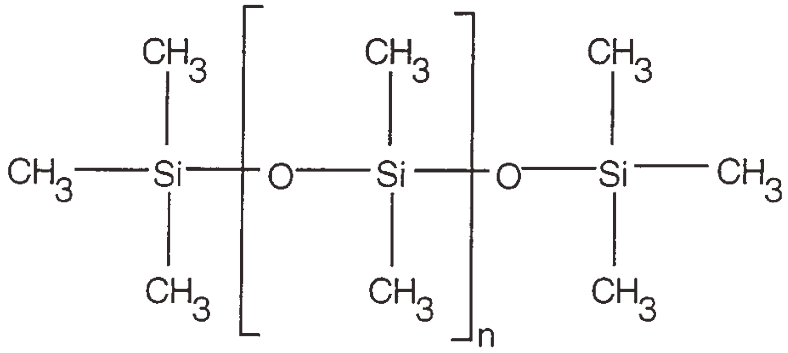

Figure (1.11): Schematic diagram of Molecular structure of polydimethylsiloxane (PDMS)

Native PDMS surface is not suitable for stem cell cultivation; when using a PDMS based micro-bioreactor, the PDMS surface should be functionalized to prevent protein adsorption, to avoid contamination, and to minimize loss of precious samples that are of micro/nano volume [259]. It is vital to modify the PDMS surface suitable for adhesion of target cells, as well as the surface being bio-inert to prevent protein fouling [113]. The modification of material surfaces can be used as a tool to optimize the biocompatibility of materials. Surface property engineering of PDMS is the most crucial step in cell-material interactions. This limitation can be turned to advantage by modifying or selectively immobilizing different molecules.

There are several engineering approaches that have been described for surface modification of PDMS-based microfluidic devices, aiming at a precise control of cell adhesion and spreading. Some processes are based on a direct binding of the biologically active molecules that change the lubricity of the surface [260] and some other processes provide the material with the capacity to give a selective answer to a specific target analyte by binding antibodies or enzymes [261, 262]. Surface modifications of PDMS could be divided into two categories: *physical* or *chemical* techniques. *Physical* treatments are the most common type of surface modification, which focuses on the chemistry of the surface to impart the properties required. In physical modification, there is a hydrophobic interaction (between the hydrophobic PDMS surface and the hydrophobic terminal, amphiphilic molecules, or copolymers) or electrostatic interactions.

Presently, there are many different coating polymer options to be employed for physical adsorption onto the microchannel surface via hydrophobic or electrostatic interactions such as surfactants, amphiphilic copolymers, and charged polymers such as polyelectrolytes, polysaccharides and polypeptides [263]. Electrostatic interaction, van der Waals force, hydrogen bonding, hydrophobic interaction are some of the important interactions associated to the physical technique. Physical techniques usually do not need complicated and expensive facilities and often require simple methods. Nevertheless, physical modification poses some drawbacks, such as limited stability due to the weak interaction force between substrate and immobilized molecules, which limit its practicality. Physical surface modification commonly includes surface coating or entrapment [95], vapour deposition [264] and surface self assembly [265] methods.

The layer-by-layer (LBL) technique is another physical electrostatic deposition method based on alternating adsorption of oppositely charged polymers, including linear polycations and polyanions [266]. Although this technique has been reported in many studies as an inexpensive and easy method to implement and successfully applied for microchannel modification [208, 267], all these LBL procedures involved the manual injection and removal of solutions both for layer formation and the washing steps, which made the whole process very time consuming. In addition, surface functionality and stability are dependent on many factors such as polyelectrolyte ionic strength and concentration, type of solvent, temperature and pH of the solution, particularly for weak polyelectrolytes, which limit the widespread use of LBL coatings [268]. Recently, Park et al. introduced a new and simple modification method to enhance stem cell adhesion by immersing PDMS substrates in boiling deionized water, which creates OH functional groups on the surface [269].

The most common techniques for physical modification of substrates include O_2 plasma treatment [270], corona discharge and ultraviolet-ozone oxidation [271, 272]. These methods alter the surface property of PDMS through functional group implantation. The type of functional groups created can be -COH, -COOH, -CO or -C-O-C [272].

Conventional plasma treatment is simple, straightforward, and does not require multiple step modification. Modification of PDMS surface with oxygen plasma has become a popular tool in the microfluidic application for increasing hydrophilicity and for permanent bonding of PDMS [273]. O_2 plasma treatment provides a rapid operation that improves the hydrophilicity of PDMS surface by generating a hydroxyl (-OH) layer on it. Studies showed that plasma treatment of silicone changes the surface into a silica-like state, which has a low surface roughness and ranges between 10 and 100nm in thickness on the surface [274-276]. Mahlstedt et al. successfully grew hESCs on a surface of the oxygen plasma etched tissue culture polystyrene (PE-TCPS) in conditioned medium to improve the culture surface for maintenance of hESC pluripotency [277], and showed that the untreated TC culture substrate cannot support hESC culture.

Despite the simplicity, there are some disadvantages being noticed on physically treated PDMS. After plasma treatment, if PDMS is left at ambient conditions, hydrophobic recovery occurs over a period of time. Surface modification based on O_2 plasma treatment is temporary and not reliable as hydrophobic recovery occurs. O_2 plasma treated PDMS suffers a relatively short lifetime, i.e., one hour [256, 278, 279], and loses the functionalized effect. The hydrophobic recovery occurs as a result of reorientation of polar groups from a surface to bulk or bulk to surface, diffusion of the un-polymerized buried chain (low molecular weight LMW) from the bulk PDMS to the thermodynamically unstable surface, condensation of surface hydroxyl groups, and migration of *in situ* created LMW species during discharge to surface [254, 280-282]. These LMW chains can possibly be uncross-linked linear PDMS chains or even residual cross-linking agents. Therefore, the fast hydrophobic recovery of O_2 plasma treated PDMS does not assure the production of a permanent hydrophilic surface. Studies have been done on the elimination of LMW species to retain the hydrophilicity for a greater time by thermal aging, i.e., curing the PDMS mixture over extended time [283].

Generally, direct modification on a PDMS surface has caused physical damage as well as altered the bulk properties to a certain extent. Treating PDMS films at a plasma power beyond 150W and longer time interval will cause a change in the film colour and decrease the transparency as a silica-like layer is formed [279]. Wang et al. showed that plasma treatment alone resulted in an insignificant increase in Caco-2 cells adhesion on 10:1 PDMS while pre-incubation with CGM significantly increased cell attachment to an extent similar to that observed on cell culture treated PS surfaces [284]. An ideal surface modification should be able to achieve the best performance in tailoring the surface properties as well as maintaining the existing beneficial characteristics of PDMS for microfluidic devices application. The hydroxyl groups made available through O_2 plasma treatment only modify PDMS surface to be hydrophilic but do not necessarily promote cell adhesion and support cell growth. Physical treatments usually required sophisticated equipment or dedicated instrumentation, hence are cost consuming and demanding of specific technical skills.

Despite the disadvantages discussed earlier, O_2 plasma treatment still appears to be the choice of pre-treatment step before coating PDMS films. The functional groups produced are able to conjugate with the chemical employed to coat the surface. Although modification of the PDMS surfaces via physical methods are simple and quick, thermal and mechanical instabilities of these surfaces due to their weak interactions with the bottom substrate is problematic [247].

Long-term stability of modified PDMS surface and its reproducibility are important issues for specific applications of PDMS devices. Kinetics of protein adsorption and folding, which influence cellular activities, are highly affected by the chemical properties of substrates (e.g., hydrophobicity). Since physically adsorbed coatings are unstable and need periodic reapplication, the coating should be more stable to avoid any loss of molecules due to external factors.

The later stage of surface modification promotes chemical treatment or a combination of both physical and chemical treatment. Chemical modification can be done through surface grafting since various functional compounds can be utilized to modify surface properties of biomaterials. In fact, polymers with different functional side or end groups can be easily grafted onto substrata via covalent binding [285]. The use of high-energy sources is commonly an intermediate step in covalent modification.

Covalent polymer coating is an effective modification approach that gives more stable and stronger substrate for cell culturing [247]. As a result of the advanced mechanical and chemical robustness as well as a high level of synthetic flexibility towards the introduction of a variety of functional groups, covalent modification has the key benefits over other surface modification methods (e.g., self assemble monolayer and physical adsorption) [286]. Distinctive methods have been developed and performed to impart surface properties on PDMS films. Each method has its pros and cons and a balance should be made between the two. Modification without pre-treatment step offers a simple and direct way to tailor the surface properties of PDMS, such as direct coating and grafting polymerization. However, pre-treatment by oxygen plasma treatment does confer to PDMS films higher stability and enhance further coating. Coated surfaces may have problems of folded or denatured molecules and inadequate surface coverage. Surface modification eliminates the need to redesign the bulk material for targeted surface performance.

Silanization is classified as a polymer coating method that is an effective chemical approach for covalent attachment of polymers through silane chemistry and for preparing surface anchoring layers on the surface of substrates [287]. In the silanization method, polymers with the functionalized end groups or with block copolymers are covalently tethered onto the reactive anchoring layer on the surface (e.g., functional groups introduced by self assembly monolayer). The attachment of alkylsilanes, through the formation of Si-O-Si bonds between the silanol groups existing on the oxidized silicon surface and the hydrolyzed organosilane molecules, is the most common way of silicon surface functionalization [288, 289]. Different silane solutions could provide different functional groups, to which the biomolecules can be covalently attached [290]. The presence of NH_2 and COOH end groups on the surface has been shown to be favourable in biological applications to support well-expressed focal adhesions with the formation of pronounced actin stress fibres [197, 253]. A common silanized reagent used to improve the hydrophilicity of PDMS surface is 3-aminopropyltriethoxysilane (APTES) [256, 291].

To this end, Seguin et al. have developed a method to coat PDMS with 3-aminopropyltrimethoxysilane (APTMS) or 3-mercaptopropyltrimethoxy silane (MPTMS). First, they coated an Ar plasma-oxidized PDMS surface with an aluminium film in order to maintain a hydrophilic surface [292]. Silanization of PDMS surfaces after being O_2 plasma-pretreated with four different hydrophobic and hydrophilic aminonaphthol silanes showed that the WCAs of surfaces

modified with two hydrophilic solutions decreased from 109° for native PDMS to 83° and 79°, respectively, while WCA values for the two surfaces modified with hydrophobic ones increased from 109 to 116° and 122°, respectively [293]. Zhang et al. modified the surface of plasma-pretreated PDMS with two silane solutions (3-glycidoxypropyltrimethoxysilane and 3-chloropropyltrichlorosilane) followed by NH_2-PEG and alkyne-PEG grafting.

They showed both surfaces became more hydrophilic compared to native PDMS with increase in the stability of wettability [294]. Tebbe et al. showed that surface silanization of both TiO powder and titanium sheets substrates with N-(3-trimethoxysilylpropyl) diethylenetriamine coupling reaction maintained the biological activity of Heparin in its highest level. In addition, the activity of heparin was found to be the highest for the covalent attachment with N-(3-trimethoxysilylpropyl) diethylenetriamine due to the long chain of this spacer molecule, which gives the highest mobility to the drug [295].

An organic polyethyleneimine (PEI) polymer consists of a high density of amino groups with the potential to get protonated. PEI coated surfaces have been successfully used to enhance the neurons in primary cell cultures [296]. Different types of cell lines have been effectively attached and differentiated to neural cells on a modified version of PEI containing hydrophobic groups. PEI also prevented cell loses during multiple washing steps [297].

Trimethoxysilylpropyl (polyethyleneimine) is an alternative and effective organosilane for micro-bioreactor surface aminization. Yue et al. showed that trimethoxysilylpropyl (polyethyleneimine) is more efficient to aminize PDMS surfaces compared with APTMS and N-(3-trimethoxysilylpropyl) diethylenetriamine [298], due to the presence of multiple amines per molecule.

Regardless of a one-step or multistep modification, a modified surface should possess the following properties; high stability, long durability, and good uniformity. Silanization is usually coupled with O_2 plasma treatment to enhance the conjugation between silane solution and PDMS surface. Wipff et al. [291] showed that the covalent attachment of ECM on the surface of PDMS after oxygen plasma treatment and silinization is more stable and resistant to stretch, compared with ECM protein absorption to untreated PDMS and to electrostatic LBL functionalized PDMS. They showed that the attachment, spreading, and proliferation of cells improved nearly 2-fold, 2.5 and 1.2 fold, respectively.

The amino derivative surface, a surface that has been activated by silanization, can then be coated with polymers that have carboxylated end groups through carbodiimide (EDC/NHS) chemistry. It was proven that antibodies do covalently bond to the amino groups ($-NH_2$) available in APTES by their carboxyl groups (-COOH). The immobilization of protein via covalent linking on a microfluidic device surface is more stabilized, and the protein bio-affinity is not affected. Silanization has been shown to be a useful step for initiating PDMS modification for covalently binding enzymes. In one study by Yasukawa's group, glucose oxidase was immobilized on the PDMS surface after a

hydrophilization step using a plasma process and further silanization for generating glucose sensor [262]. Antibodies were also immobilized on a PDMS column for protein purification applications after applying plasma and silanization by Sandison et al. [299].

In addition, for applications involving the stretch of a PDMS culture surface, chemical modification may be preferable since it would seem to be mechanically stronger at the interface between PDMS and the hydrophilic coating. A study by Shafieyan et al. showed that covalently binding of collagen after surface silinization of PDMS is an effective way to promote osteoclast differentiation on extendable PDMS substrates [300]. Mahlstedt et al. demonstrated that the pluripotency of human ES cell culturing can be improved via physicochemical modification of polystyrene by plasma etching technique [277]. Chemical properties of surfaces can have a profound influence on cellular response, whether that effect is directly because of surface chemistry, or mediated through adsorbed proteins. Utilisation of silane-modified surfaces provided a controlled method to investigate the effect of specific surface chemistries on MSC adherence, viability, proliferation and differentiation.

Curran et al. demonstrated that mesenchymal stem cells showed increased viability and osteogenic differentiation on surfaces chemically modified with amine-terminated silanes, as opposed to chondrocytic differentiation on carboxylic acid-terminated silanes [301]. Low et al. investigated the surface chemistry effect of porous silicon (pSi) through chemical modification of pSi on mammalian cell attachment [302]. Cell attachment to ozone-oxidized, aminosilane-functionalized, and collagen-coated pSi surfaces was compared to ozone oxidised pSi. The results revealed that amino-silane and a collagen coating enhanced cell attachment to pSi surfaces whereas cells attached poorly to ozone oxidised surfaces. In another study, the surface of micropatterned PDMS film was functionalized using plasma oxidation coupled with aluminium deposition, followed by silanization with solutions of 3- aminopropyltrimethoxy silane (3-APTMS) and 3-mercaptopropyltrimethoxy silane (3-MPTMS), to obtain patterned amine and thiol functionalities, respectively. The modified substrate was shown to successfully selectively immobilize IgG molecules by protein A to the surface, and for the cellular arrays. The amine functionalized surface was biocompatible with C2C12 rat endothelial cell growth and proliferation within a patterned array [292].

Utilizing polysaccharides has proven to be a potential alternative to poly(ethylene glycol), a well-known material for preventing the nonspecific adsorption of proteins, which also features biocompatibility and low toxicity. Polysaccharides, such as dextran, have the potential to be replaced by PEG as nonfouling materials to graft onto aminosilane functionalized glass surfaces [303, 304]. Chitosan and dextran have been physically deposited or covalently grafted onto PDMS surfaces for biomolecule separation, immunoassay, and protein non-fouling [305, 306]. In addition, polysaccharides have been shown to be advantageous in improving the cytocompatibility of native PDMS and in decreasing surface protein adsorption [307].

Carboxymethyl cellulose (CMC) is an alternative cross linker which is a derivative of cellulose and commonly used as a Food and Drug Administration (FDA)-approved disintegrate in pharmaceutical manufacturing [308]. It is water-soluble, biocompatible, and available abundantly at low cost, making it an attractive biomaterials candidate. In fact, CMC effectively controls protein binding by providing a hydrogel-like layer on the surface of substrates, which also prevents non-specific protein interactions. CMC has been also employed as a wound dressing material and co-excipient with drugs [309]. CMC has been demonstrated to inhibit postsurgical and postoperative adhesions [310-312]. It has been demonstrated that the presence of CMC on the surface of the substrates dramatically decreases the amount of bovine serum albumin's (BSA) adsorption [313].

1.4.2.1.2 Biofunctionalization of PDMS for embryonic stem cells culturing

Biofunctionalization refers to the use of biochemical coatings (e.g., a coating of extracellular matrix proteins such as fibronectin, vitronectin, and collagen) to allow for the enhancement of interactions between the materials and the cells through the promotion and regulation of cellular functions such as adhesion, migration, proliferation, and differentiation [314-316]. To use the potential of stem cells to obtain highly specialized and functional bioengineering tissues, there is usually a need to use artificial materials that mimic stem cell compartments. The benefit of having defined and artificial materials is enormous. Indeed, an ideal opportunity can be provided by artificial materials to control conditions for stem cell maintenance, instruction, and differentiation. For instance, by providing a better environment for stem cells growth, the conditions in which ES cells turn into adult stem cells will be discovered.

Artificial materials can be immobilized with bioactive molecules, such as growth factors, cytokines, ECM proteins and adhesive peptides, and provide precise biological functionalities. These bioactive molecules can be adsorbed on the surface of polymeric substrates via physical or covalently chemical groups previously created on the surface. Cell attachment and growth are then influenced by the structural parameters of the bio-functionalized surface, such as the density of the ligands, their spatial distribution, their colocalization with synergistic ligands, etc. Agarose, alginate, hyaluronic acid, gelatin, fibrin glue, collagen derivatives, and acellular tissue matrices are examples of a various number of natural materials, which have also been used to support the differentiation for ESCs. In many different fundamental biological processes, such as guiding cells into their appropriate locations in the body, providing an attachment surface, and controlling cell proliferation, differentiation, and apoptosis ECM-cell and cell-cell interactions vital functions. ECMs can be employed to trigger ES cell differentiation toward a preferred cell lineage by incorporating tissue-specific ECM signals. ECM is established as a potent regulator of cell function and differentiation [317], and there is already evidence that ECM affects differentiation in stem cells.

A mixture of ECM molecules (Fibrotectin, laminin, collagen I, collagen III, collagen IV) was used by Flaim and co-workers to understand their cooperation in cardiac differentiation of murine ES cells [318]. Lee et al. found that physisorption of extra-cellular matrix (ECM) proteins, such as fibronectin, could increase mammalian cell attachment on PDMS[319]. Mouse ES cells were also cultured on an Ecadherin-coated surface, and the result showed that ES cells maintained their morphological characteristics while keeping their ES cell features. ES cells showed higher proliferative ability and transfection efficiency than those grown under conventional conditions [320]. In another report, Goetz et al.[321] described how environmental interactions alone can modify the development of neurogenic precursor cells. They showed the direct differentiation of stem cells into neural lineages by using laminin, fibronectin, and gelatin. Evans's group used decellularized bone-specific ECM to promote osteogenic differentiation of mouse ES cells [322].

Gelatin, a derivative of collagen, is a natural renewable and biodegradable material that has been used for coating formulations, and in pharmaceutical and medical applications for its outstanding properties such as availability, cost-effectiveness, excellent biodegradability and biocompatibility, and non-immunogenic properties [323, 324]. Gelatin can have positive or negative charge in an appropriate physiological environment or during the fabrication based on its isoelectric point, which is a very attractive property for many pharmaceutical researchers. Gelatin is among the natural polymers that have been used as a support material for gene delivery, cell culture, and more recently tissue engineering. The release of bioactive agents such as drugs, protein, and dual growth factors has been controlled by gelatin-based systems [325].

It is known that gelatin contains arginine–glycine–aspartate (RGD) motifs; RGD peptides provide a high-affinity site for cell binding, and are often incorporated in biomaterials to promote cell adhesion [326, 327]. Chemical grafting or cross-linking of gelatin is an effective way to introduce stable covalent bonds between protein segments to obtain a modified product that provides greater control of chemical and physical properties compared to natural polymers [328].

Overall, it is worth mentioning that since the number of the stem cells in each tissue is generally very small, they require culture and expansion *in vitro* for clinical use. Currently, a variety of micro-bioreactor systems made of biomaterials are being developed that enable cell growth in a tightly controlled microenvironment. The properties of micro-bioreactor surfaces have a strong influence on cell attachment and spreading, which are generally greater on certain hydrophilic surfaces relative to hydrophobic surfaces [199, 228]. As mentioned previously, the ability to support cell growth and the potential to resist protein adsorption in order to prevent undesired adsorption of analyte molecules, such as protein and DNA, are important characteristics of effective micro-bioreactor surfaces. Native PDMS, the most common polymer used in micro-bioreactor fabrication, is not suitable for stem cell cultivation. When using a PDMS based micro-bioreactor, the PDMS surface should be effectively functionalized to prevent protein adsorption, to avoid contamination and to minimize loss of precious

samples that are of micro/nano volume [259]. In this regard, improving the wetting characteristics of PDMS is an essential step to control nonspecific binding of proteins and increase cell adhesion and expansion for further applications in microfluidics and bioengineering [329, 330].

To fulfil the first aim of this study, which is improving the ability of cell attachment and proliferation, an effective and stable physiochemical modification method is provided. In this regard, Trimethoxysilylpropyl(polyethylene imine), as one of the effective silane solutions, is applied to introduce amine groups on the surface of PDMS for surface immobilization. CMC is further conjugated to control the protein adsorption by providing hydroxyl active groups on the aminized surface. Presence of these active groups makes further biofunctionalization easier. Gelatin is finally attached to increase the cell adhesion and growth because of its outstanding properties such as biodegradability, biocompatibility, and low antigenicity. This method enhances the adhesion of stem cells to the PDMS and improves proliferation of stem cell while retaining their pluripotency and normal morphology (Chapter 3).

1.5 Culture of cells as three-dimensional (3D) structures

Differentiation of pluripotent stem cells as a unique source of cells has been conducted in both two- and three dimensions; however, a recent study revealed that although both systems support differentiation of mESCs, the kinetics of differentiation differed greatly for cells cultured in 2D versus 3D [331]. Differentiation studies of several stem cell phenotypes have successfully shown the potential of 2D systems to spatially and temporally control the presentation of molecules for the differentiation. Besides providing some bound proteins, culturing stem cells on adherent surfaces (2D culturing) can provide well controlled exogenous physical cues such as cyclic tension and shear stress. For example, different studies have reported the observation of beating areas after plating down the spontaneously differentiating EBs (stem cell 3D structure) on an adherent substrate that exhibit structural and functional properties of early stage cardiomyocytes [332-334].

However, 2D culturing restricts cell growth to a single geometric plane [331]. Considering that in most of the cases, the differentiation of cells may require the effects of cell-cell and cell-ECM interactions provided within the context of embryonic bodies (EBs) in 3D, therefore introducing another dimension is essential.

In fact, although culture of ESCs in monolayer or co-culture provides a more defined condition for cell attachment and uniform exposure to soluble components in media, EB as the 3D aggregate of ESCs more accurately recapitulate the complex assembly of cell adhesions and intercellular signalling of early embryogenesis. In principle, 3D cultures can be obtained either by exploiting spontaneous cell aggregation and by generating more or less spherical cellular conglomerates (using various type

of bioreactors) or by culturing cells on artificial substrates (natural and synthetic scaffolds or hydrogels) that induce cellular differentiation and maintain cellular function [105, 108, 335-337]. (Different methods for EB formation will be discussed in more detail in the following sections)

Beside EBs as stem cells aggregates, different types of cell spheroids could serve as very useful models to understand the mechanisms of cell proliferation and cell death since spheroids mimic the solid tumors more closely than the monolayer culture.

1.5.1 Cancer cells as 3D structures (Spheroids)

In living systems, the responsibility of cells as the basic structural and functional units is to mediate various biochemical reactions, such as catabolism and anabolism, which help cells to grow and divide. Communication of cells throughout the whole living system is being done in a highly intelligent way despite very simple structure of cells. During the last decades, aggregates of cancer cells have been subjected to plenty of *in vitro* studies for the better understanding of the principle of morphogenesis and tissue formation. These aggregates, called "spheroids" with 3-dimensional (3D) structures, are of paramount importance in biomedical science as they literally mimic the *in vivo* tumour tissue structure and microenvironment. These 3D structures often consist of stem cells or tumour cells from malignant cell lines or fragments of human tumours [338], which are normally used to study the cell-cell interactions and communication, metabolic gradients, position dependent proliferation, or gene expression patterns. Mimicking the behaviour of tumours can be done more effectively in aggregated form rather than regular 2D cell cultures because spheroids, much like tumours, usually contain both surface-exposed and deeply buried cells, proliferating and non-proliferating cells, and well-oxygenated and hypoxic cells [339].

In fact, although monolayer cultures of tumours have been widely used for studying the various molecular processes, evaluation of some of the therapeutic strategies cannot be carried out with this most widely used laboratory system. Indeed, the 3-dimensional organization of solid tumours provides some complexities, which are not provided in the monolayer cultures derived from tumour cells. In contrast, multicellular spheroids of tumour cells provide an excellent three dimensional *in vitro* model in which hypoxic conditions can be generated to facilitate detailed investigations, including the response to various chemical agents and radiation [340].

Stuschke and colleagues reported a systematic study in which they identified the degree of differentiation as an important determinant of radio-responsiveness in various spheroid types of human origin [341]. Thus, spheroids mirror the radio-sensitivity of differentiating tumours *in vivo* more closely than conventional cell cultures. The Kerbel and Teicher groups, in a collaborative study, showed that after the cancer cells were isolated and grown in monolayers, they lost their drug

resistance to alkylating, while they could be fully recapitulated when cells were cultured as multicellular spheroids [342-344]. Spheroids can also be used to study the adhesive properties of tumour cells [345]. Tumour-induced angiogenic responses can be modelled using cultures in which tumour spheroids interact with vascular cells generated from embryonic stem cells, also showed the feasibility of analysing the interaction between different cell types in spheroids [346].

In fact, such efforts that have been made to study the different aspects of tumour cells as 3D multicellular spheroids highlighted the need for improved and more effective *in vitro* systems models, which more closely resemble the *in vivo* situation and the biological behaviour of the cells.

1.5.2 Embryonic stem cells as 3D structures (Embryoid Bodies)

The generation of populations of undifferentiated stem cells, without diminishing their characteristics through scalable and affordable culture systems, is the initial requirement for using the stem cells to fulfil the promise of TE for repairing/replacing damage organs. This aim can be achieved either through different conventional or small-scale techniques that mentioned in previous sections. However, the next important step for using stem cells in clinical application includes the generation of particular cell types for specific applications, which can be achieved through cell differentiation. Regarding clinical applications, it is very critical to generate differentiated ES cells prior to transplantation due to the fact that undifferentiated ES cells could cause teratoma (tumour) formation *in vivo*. The therapeutic potential of embryonic stem cells (ESCs) lies in their ability to differentiate into a variety of clinically useful cell types, such as hepatocytes [347], cardiomyocytes [41], osteoblasts [348], and neural cells [349]. This superior potential, in addition to providing unlimited number of cells, has drawn much attention to use them as integral parts of modern clinical treatment.

In vitro differentiation of ESCs, as an important characteristic of these cells, is mostly achieved by spontaneously self-assembling 3D cell aggregates called embryoid bodies (EBs) through culturing stem cells in low adhesion culture condition [350, 351]. Aggregation of embryonic cells has clearly been distinguished by formation of embryoid bodies that represent 3D cultures of pluri- or totipotent embryonic stem cells. EB formation is the initial step for many pluripotent stem cells differentiation protocols. Although there have been different approaches for differentiation from pluripotent stem cells such as END-2 approach and direct cardiac differentiation, EB formation is one of the most utilized method for generating beating cardiomyocytes and facilitating the differentiation process [352]. EBs are three-dimensional cell aggregates that can mimic some structures of the developing embryo and can provide temporal and spatial cues that control differentiation into all three germ layers (Figure1.12).

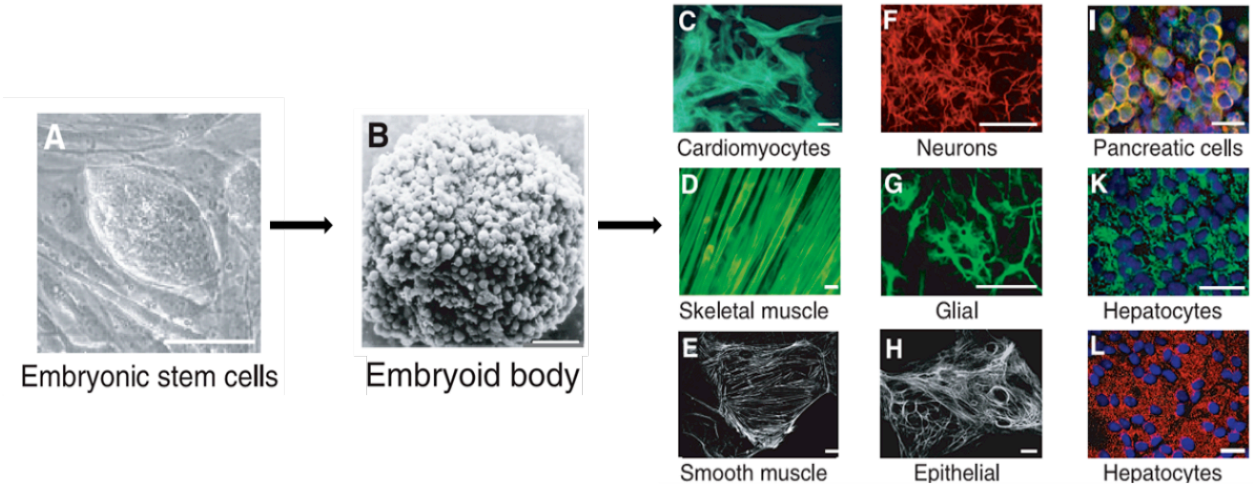

Figure (1.12): In vitro differentiation of ES cells. Undifferentiated mouse ES cells (*A*) develop *in vitro* via three-dimensional aggregates (embryoid body, *B*) into differentiated cell types of all three primary germ layers [353]

In fact, when stem cells transferred into EB formation conditions (such as a suspension dish), small aggregates can be observed after 1-3 days of culturing. In mouse ESCs, the tendency of forming EBs with a special structure consisting of an internal endoderm layer and an external ectoderm layer; is higher than human pluripotent stem cells. Over time, some EBs become cavitated and some become cystic [350]. Figure 1.13 shows the formation of EBs over time.

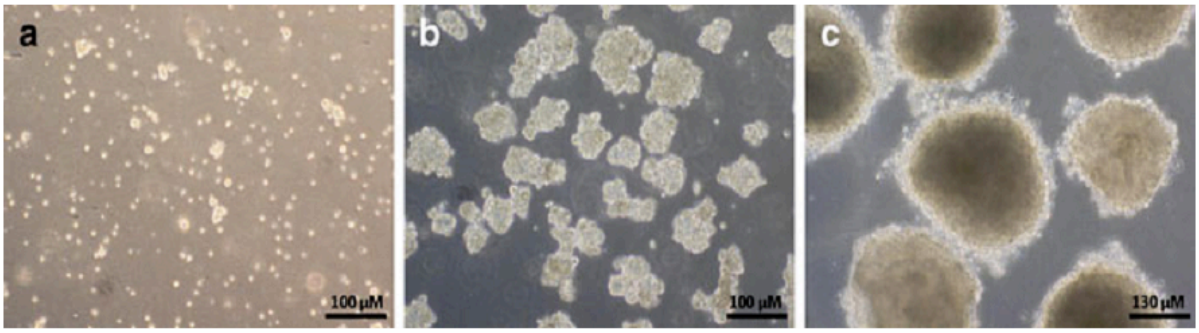

Figure (1.13): EB formation via suspension culture after one (a), three (b) and five days (c) after dissociation

Studies have shown that differentiation of ESCs through EB formation resembles embryonic development, in which EBs recapitulate early embryonic developmental phases [350, 354]. In fact, cells inside the developing EBs possess the capability of differentiating to a more developed phase of embryogenesis, contributing to various types of cells such as cardiomyocytes, skeletal muscle cells and endothelial cells [40, 355, 356].

Embryoid bodies have been broadly subjected to numerous studies during the last years following the landmark research of Evans and Kaufman [33], and Martin and Evans [34, 357]. The ability of EBs to recapitulate the developing embryo makes them a valuable tool for studying embryonic development in addition to their therapeutic usage [44, 354, 358]. The *in vitro* differentiation of both mouse and human ES cells can be triggered by formation of embryoid bodies as a widely employed method.

For instance, Serra et al. showed that the differentiation process of human embryonal teratocarcinoma stem cells into neurons is highly improved when cells are cultivated as 3D aggregates using stirred bioreactors. The result showed the significant increase in the neuronal differentiation efficiency and decrease in the time required for the differentiation process [118, 359]. Investigation of different aspects of mouse and human development *in vitro* has been shown to be facilitated by establishing EBs. Considering that the isolation of early stage cells from developing embryos *in vivo* is almost impossible, EBs plays a powerful role for characterising the function of precursor cells. In addition, studies showed that when targeted mutagenesis causes disruption in both alleles of a specific gene in ESCs, EBs derived from ESCs have often represent a fast alternative for investigating the impact of a given null mutation [360, 361]. Much progress has been made in different aspects of embryoid bodies as powerful models *in vivo* and *in vitro*, such as mechanistic and molecular work. Research undertaken by Weiss and colleagues highlighted the potential of targeted mutations in embryoid bodies [362]. Embryoid bodies were investigated for the mechanisms of vasculogenesis in different studies [40, 363, 364]. Several researchers have studied the mechanisms of vasculogenesis in embryoid bodies and analysed the role of cell adhesion molecules for the development of vessels and their response to inflammatory stimuli [40, 364-366]. Another study, done by Rohwedel et al. [367], showed that the development of skeletal muscle myocytes from mESCs is very similar in embryoid bodies and *in vivo* with regard to the activation of muscle-related genes. Wobus and Hescheler studied the capability of cardiomyocyte differentiation of EBs. They generated beating embryoid bodies with cardiospecific receptors, ionic channels, and action potentials [368, 369]. Three-dimensional structure has been shown to be advantageous for cardiac differentiation, given that close interaction with endodermal derivatives supports cardiomyogenic induction [370]. The oxygenation and oxygen-regulated gene expression in embryoid bodies in different oxygen environments were studied by Gassmann et al. [371]. EB formation has been demonstrated to help in facilitating the investigation of several aspects of ES cells *in vitro*, including the neutralisation of their potential to form tumours. Studies on embryoid bodies represent perhaps one of the most exciting fields of research with 3-D culture systems, and much progress with regard to our understanding of embryonic development and carcinogenesis may come from this research area in the near future. The importance of formation of cell aggregates encouraged us to engineer 3D culture system technologies capable of providing a higher degree of efficiency, robustness, consistency and more predictive cultures.

1.6 Methods for *in vitro* formation of EBs

So far, different methodologies have been utilized for EB formation, as schematically shown in Figure 1.14.

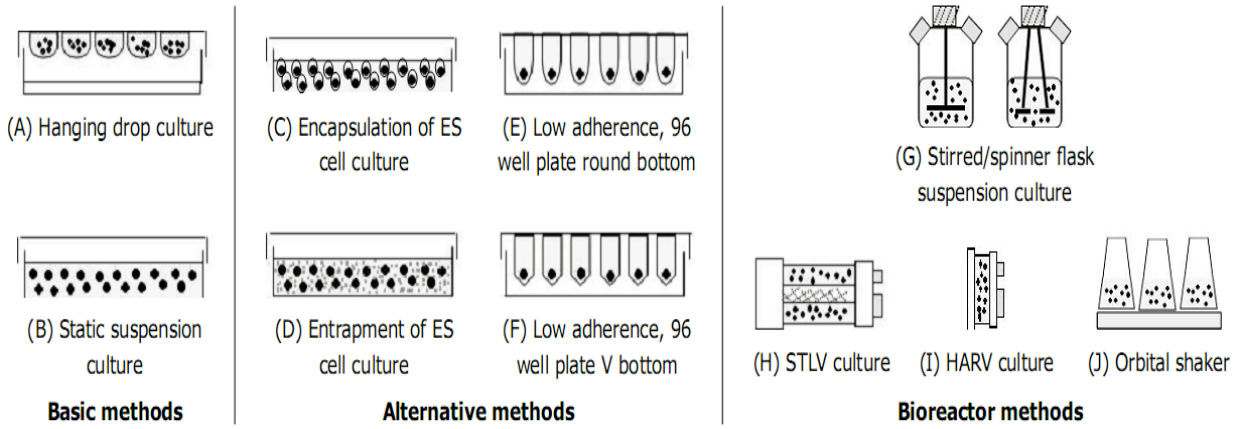

Figure (1.14): Schematic representation for vessels used in methods to form EBs from ES cells [372]

Traditionally, hanging drop and suspension culture methods were being used as the most widespread methods for EB formation and for inducing differentiation. Although EBs have successfully been generated to produce various differentiated cell types through these methods, these techniques allow only limited control over aggregate size and shape and present practical difficulties with scale-up. In the hanging drop technique, several droplets of media with identical cell density are suspended from the lid of a petri dish, resulting in the formation of uniform size EBs. EBs formed by the hanging drop method have been used to generate a broad spectrum of cell types, such as neuronal cells [373], hematopoietic cells, cardiomyocytes [355, 374, 375], and smooth muscle cells [376]. It is worth mentioning that this technique is mainly used for research applications and is practically not suitable for large scale EB production due to its laborious nature, and its low efficiency (each drop could contain just one EB) [123].

The inherent experimental challenge of the method appears when, in order to form a sufficiently stable hanging drop for easy experimental handling, the volume of the drop must be carefully controlled. Because the stability of a hanging drop is governed by the balance of the liquid surface tension force, and the gravitational force of the drop, it can be pulled off the well if it is too large [377]. Although efficient in yielding spheroids, the hanging drop technique is well known to be laborious, and requires a great deal of manipulation. In addition, the hanging drop method cannot easily be scaled up for large EB production, restricting its practical effectiveness. For example, for the

biochemical characterization of protein interactions and the interrogation of signalling pathways, over 100 dishes of hanging drops have to be pipetted, sometimes more depending on the experimental setup.

Alternative techniques, such as those utilizing round-bottom 96-well plate and conical tubes, have been adopted to form uniform EBs from certain numbers of ES cells [378, 379]. Although round-bottomed 96-well plates and conical tubes induce aggregation more rapidly than hanging drops, these methods still result in generation of a single EB in each well.

Using suspension bacterial-grade dishes is another approach developed in 1985 by Doetschman et al. [380]. The suspension method, unlike hanging drop methods, is carried out by adding a suspension of ESCs to a bacteriological grade dish or other hydrophilic polymer-coated vessel, which inhibits cell adhesion to the surface of the dish and consequently helps cells to spontaneously aggregate via cell-cell adhesions [381]. Cells naturally stick to each other and form aggregates without any shaking. The suspension method has been used to initiate the differentiation of ESCs into a variety of differentiated cell types. For instance, mouse ES cells have been induced to neural progenitors [382], vascular cells [383], cardiomyocytes [77], hepatic cells [384], and germ cells [385] from EBs formed in the bacterial-grade dishes.

As a result of spontaneous aggregation in the suspension method, the number and the size of each aggregate varies; therefore, it produces a large variety in EB sizes [351]. Another limitation of this method is the possibility of EB attachment to the plate due to surface chemistry deficiency, leading to a greater heterogeneity and loss of EBs from the suspension culture. One of the obstacles of this method is the formation of larger aggregates, which has negative effects on cell proliferation and differentiation, along with causing considerable cell death [351, 386]. Indeed, complicated and difficulties in manageability of the suspension method has limited its practical industrial applications [387].

Conventional techniques, such as hanging drop and suspension cultures, exhibit lower control over the size of ES cell aggregates. In fact, although suspension methods produce large numbers of EBs the major issue limiting cell proliferation in suspension culture is aggregation of EBs when one or more individual EBs fuse and form bigger aggregates [388].

Bioreactor methods have been shown to be effective methods for the production of large numbers of EBs [138, 389, 390]. It has been proven that these strategies are more advantageous than suspension and hanging drop methods since they have the capability of providing nutrient and oxygen to cells more effectively. As a result of the mixing environment, dispensing of media components is more homogenous throughout the culture volume, and consequently EBs experience a more uniform concentration of soluble factors and environmental conditions [391]. These systems fall into two categories; stirred vessels and rotational vessels. The former category has been used more frequently in large-scale production of cells for its high success rate in mass transfer [143, 390, 392, 393].

Krawetz et al. [394] developed a protocol for the expansion of hESCs in stirred suspension bioreactors, which yielded a 25-fold expansion of pluripotent hESCs over 6 days. Furthermore, Taiani et al. found that bioreactor culture may induce pluripotency, and reduce the differentiation efficiency of mESCs, in serum-containing media through fluid shear stress [395].

Sargent et al. found that a rotary bioreactor increased the fraction of cardiomyocytes generated from mESCs compared with hanging-drop and static-suspension cultures [396].

Lu et al. [392, 397] reported that rotating bioreactors were beneficial for generating spontaneously beating cardiomyoyctes. Controlling excessive cell aggregation is critical for this approach due to the formation of a few large cell clumps, or aggregation between EBs (agglomeration), that sometimes happens. For addressing this issue and controlling the interactions between cells and EBs, some strategies, such as transferring EBs to stirred-suspension cultures or encapsulating them in hydrogel capsules, have been proposed [138, 390, 398]. More importantly, generating shear forces due to the rotation and consuming relatively huge amount of reagents are other important parameters that should be concerned in using bioreactor techniques. The possibility of formation of bigger aggregates is enhanced in stirred culture since dynamic conditions boost the likelihood of cell collision and aggregation.

Recently, several studies have described the formation of uniformly sized cellular spheroids using microfluidic technologies [224, 399, 400]. Microwell arrays are developed through the merging of microfabrication and biomaterials technologies that facilitate ES cell culture and EB formation. For instance, ES cells have been patterned on the microfabricated adhesive stencils for better controlling on initial mouse ES cell aggregate sizes, which influenced the early differentiation to different germ layers [388].

In another study, islands of ES cells were generated on microcontact printed substrates for regulation of the self-renewal of ES cells by local modulation of self-renewal signalling molecules [401]. Mouse ESCs were also micropatterned on defined size substrate to be analysed for cardiac differentiation [402]. Photolithography has been used for making a 3-D cuboidal microwell plates to culture hESCs and form EBs of defined sizes in order to regulate cardiac differentiation. It is reported that differentiation of ES cells to cardiomyocyte lineage is more likely via EBs with smaller sizes (100–500μm) [403]. Recently, the agarose microwell plates (non-adhesive substrate) generated by a soft lithography strategy were used for aggregation of murine induced pluripotent stem cells EBs and cardiac differentiation [404]. Although the microwell-approach gives more homogeneous EBs and can be scaled up, commercially available single use microwell-based consumables are still very costly; therefore, large-scale experiments may be hardly affordable for most researchers. Furthermore, the need for the clean room facilities and using soft lithography procedures published so far proved to be technically complicated and time consuming [405, 406].

Each of the abovementioned methods suffers from at least one of the drawbacks, such as time-consuming, labour-intensive, complicated production process, inability to scale up, low efficiency of EB formation, or economical impracticality. The conditions vary between methods; therefore, the size and shape of EBs produced may also vary. Formation of heterogeneous EBs depends on the different sizes and shapes of the EB [407]. The lack of homogeneity in the EB results in asynchronous differentiation of the cells within. Most current methods aim to produce homogenous or uniform EBs. In order to consider embryoid bodies more efficiently, problems associated with death, adhesion to the culture dish, uncontrolled agglomeration, and dissolved EBs need to be solved. To physically separate and encapsulate the EBs in a three-dimensional (3D) semi solid matrix during culture is one way to cope these problems. Culturing in 3D system has the potential to facilitate the cellular differentiation and form an *in vitro* supplement for the 3D supportive tissues that evolves during embryogenesis *in vivo* [408, 409].

To create *in vivo*-like aggregates, mES cells can be cultured on 2D flat substrates and cell aggregation can be induced over time. However, moving stem cell culture protocols from 2D cell monolayers to 3D environments has been reported to enhance embryonic stem cells performance *in vitro* and help to exploit their potential more effectively [410, 411]. In fact, keeping and differentiating EBs inside three-dimensional culture could possibly persuade better cell–cell interactions, help to entrap secreted extra cellular matrix, and assist to maintain the spherical cellular morphologies [412, 413]. The importance of providing the spatiotemporal cell environment for cell behaviour is due to the fact that 3D provides a cellular situation closer to what actually takes place *in vivo*.

Another attractive development in EB formation techniques is utilizing porous hydrogel-scaffolds as more controlled systems that are capable of modulating EB size in order to begin to determine the effects on subsequent differentiation of the cells. Various tissue-engineering studies have pointed out that 3D scaffolds are well-suited to ESC based tissue engineering applications [410, 414, 415]. The confined environment of the pore structure in the scaffold would enable the formation of a more homogeneous population of EBs, minimize agglomeration of EBs, and eventually lead to efficient cell proliferation and differentiation. In addition, the porous structure of hydrogel fabricated from natural or synthetic extracellular matrix components, more closely resembles the extracellular matrix, enables efficient cell seeding and tissue engineering. Moreover, because of their high water-content structure, hydrogels provide high permeability for oxygen, nutrients and other water-soluble metabolites, which is an excellent environment for cell growth and tissue regeneration [416, 417].

Considering that EB formation remains important in the *in vitro* differentiation of stem cells, more attention needs to be given to the techniques, devices, and procedures used for EB formation. In fact, to produce a controlled differentiation pattern for ES cells, there is still the need for reliable methods to produce uniform aggregate sizes. In this regard, developing a novel technique in terms of the ease of operation, cost, and efficiency is necessary. Furthermore, the difficulties associated with the

common methods regarding the low yield of the formation of 3D cell structures have led to the development of approaches capable of forming larger and more homogeneous numbers of cell aggregates. To meet the aim of this project, two novel effective bioreactors with miniaturized scale will be proposed for generating stem cell aggregates: liquid marble and a biodegradable porous scaffold, which will be discussed in detail in sections 1.6.1 and 1.6.2, respectively. This part of the thesis is dedicated to the introduction of principles and properties and novel biomedical applications of liquid marble.

1.6.1 Liquid marble, Principles and properties

Wettability is described as the ability of a liquid to maintain contact with a solid surface, resulting from intermolecular interactions once the two are taken together. This is an important property of the surface, which is highly influenced by both chemical composition and geometrical microstructure of the surface [418].

This phenomenon has a large impact on other physical and chemical processes, such as adhesion, lubrication, catalysis, and friction. Nature, as a valuable and innovative source, always has been an excellent inspiration to mimic the bio-structures for studying the properties of biological systems.

Formation of water droplets on a lotus leaf due to the low surface energy of the botanical wax on the leaf is one of the well-known examples of Super-hydrophobicity [419]; the lotus leaf acts as a superhydrophobic surface, which is defined as a surface with a water contact angle larger than 150° [420]. The honeydew waste excreted from Phloem-feeders is life threatening for galling aphids. This waste can act as a trap for the insects to become stuck. However, these insects can avoid the sticking problem by secreting a hydrophobic powder wax to cover the honeydew. The wax-covered sphere is then rolled or kicked out of a hole in the gall by the soldier aphids [421]. Butterfly wings are another example of a superhydrophobic surface that direct drops of water away from the body of the butterfly [422].

Superhydrophobic surfaces exhibit extreme water-repellency, with water droplets resting on them with high contact angles. Creating the appropriate rough and low surface energy surfaces is the aim of different methodologies and instruments for the fabrication of artificial superhydrophobic surfaces. Various applications take advantage of superhydrophobic surfaces, especially in the last two decades, just like production of self-cleaning, drag reduction, energy restoration, and antifouling [423-426]. Superhydrophobic surfaces and their applications have attracted astounding attention since the 1990s, when photolithography technology matured, and it turned out to be possible to build superhydrophobic surfaces with desired properties [427-429]. In 2006, by hydrophobic silicon coating, superhydrophobic fabric fibres were created [430]. Furthermore, superhydrophobic surfaces

could have a number of potential marine applications, where it can prevent marine fouling and be involved in defence against adhesion and the growth of marine organisms[431].

When a drop of liquid comes into contact with a solid powder surface, based on the surface tension of the liquid-solid adhesion, the powder particles cover the surface of the liquid, leading to formation of a liquid marble Figure 1.15. An encapsulated liquid marble can easily form by rolling a drop of liquid on a bed of micro- or nano-hydrophobic or hydrophilic powder particles. By transferring this drop to any surface, it is observed to be in a pure non-wetting situation, since the grains prevent any contact from taking place. This liquid marble can behave as a micro-reservoir capable of moving quickly without any leakage [432].

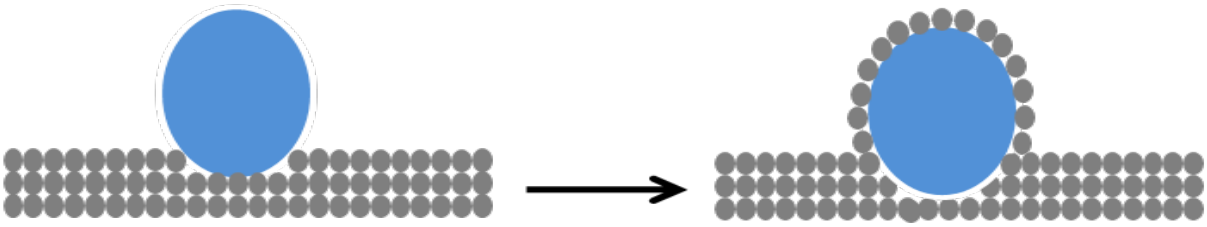

Figure (1.15): Covering a drop of liquid with the hydrophobic powder and formation of a liquid marble

The phenomenon of liquid marbles was introduced by the pioneering work of Aussillous and Quéré in 2001 and since then, intensive theoretical and experimental research has been directed toward miniaturization technology [433-435]. An interest in liquid marbles arises from both their very unusual physical properties and their promising applications. Liquid marbles present an alternative approach to superhydrophobicity, i.e., creating a non-stick situation for a liquid–solid pair. The hydrophobic powder particles have been poorly wetted by the liquid; therefore; they weakly adhere onto the surface of the liquid drop in a loose and rather random fashion, forming a porous shell over the liquid drop. The presence of a porous shell around the liquid marble was observed by optical microscopy [433, 436]. This kind of structure helps the liquid marble to endure a certain degree of mechanical force and deformation, considering that the porous shell is stretchable. The presence of the hydrophobic shell provides a barrier to direct contact between a liquid core and any surface outside of the liquid marble, while allowing air and other gases to freely transport into the liquid marble [437]. Such a structure makes a liquid marble an ideal respirable micro reactor for biological applications.

Despite the suggestion of Aussillous and Quéré for using hydrophobic and high surface tension powder particles for making a stable liquid marble, today hydrophilic powder has also been used for

making liquid marbles [438, 439] Figure 1.16. It should be mentioned that the covering powder could be more or less hydrophobic (e.g., marbles coated by graphite and carbon black, which are not strongly hydrophobic) [438-442]. The covering powder could be made of natural substances, such as soot or lycopodium, or from artificial substances, such as silica beads by a fluorosilane; the size of the powder can be varied from 0.1-100micrometre [443].

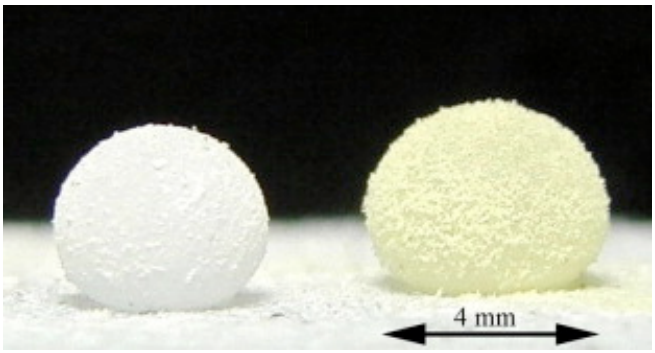

Figure (1.16): Liquid marble covered with hydrophobic polyvinylidene fluoride (PVDF) particles and lycopodium powder (yellow) [443]

It is worth mentioning that liquid marbles can be formed using a variety of low and high surface tension liquids. For microfluidic application, liquid marbles need to be formed with low surface tension and volatile liquids as well. For example, Xue et al. reported the formation of stable liquid marbles from both aqueous solution and organic liquids covered by fluorinated decyl polyhedral oligomeric silsesquioxane (FD-POSS) particles [444]. In another study, Gao and McCarthy made encapsulated ionic liquids marbles, which are non-volatile and versatile solvents, by fluoropolymer oligomerictetrafluoroethylene (OTFE) [445]. Liquid marbles have been manufactured using some other organic solvents such as dimethyl sulfoxide (DMSO), toluene, hexadecane, and ethanol. However, it should be mentioned that in a majority of studies, using high surface tension liquid marbles have been reported [433, 445-447]. The Zhang group reported the fabrication of highly water repellent micro-particles in a mild condition by inspiration from the strong adhesion of mussel adhesive protein and the micro-nano hierarchical structure of the lotus leaf. His group also, for the first time, reported the formation of oil liquid marbles under water encapsulated by superhydrophobic magnetic particles under external magnetic field. The author suggested the great potential of oil liquid marble in future micro-reactor and sensing applications [448].

Inherently, hydrophobic powder consists of a large proportion of air between its particles. Environmental scanning electron microscopy (ESEM) images of the surface of liquid marbles showed that the shell consisted of particles with trapped air between them. The study conducted by

Bormashenko [449] showed that hydrophobic powder does not form a uniform shell around a liquid drop. The encapsulating layer of particles can create a loosely packed monolayer or a multilayer surrounding the droplet. Increasing the angle has a direct relation with the fraction of the air on the surface of the hydrophobic particles. Nguyen et al. used confocal microscopy technique to investigate the structure of the liquid marble shell. The images revealed that hydrophobic particles formed a loosely packed multilayer shell consisting of small and relatively large lumps of primary particles [434]. They showed that the liquid marble powder shell is composed of predominantly multi-layers of fine powders. These fine particles help the liquid core to avoid contact with a wetting surface, and hence increase the flexibility of the liquid marble in withstanding compression forces. The powder shell is clearly seen in Figure 1.17 with the presence of multi-layers within the powder shell, and particles can be viewed on the liquid marble surface. Therefore, it is worth noting that the hydrophobic powder creates a completely non wetting soft solid and forms a porous shell around a droplet, which is permeable for gases and vapours and enables the liquid marble to act as a gas sensor [437].

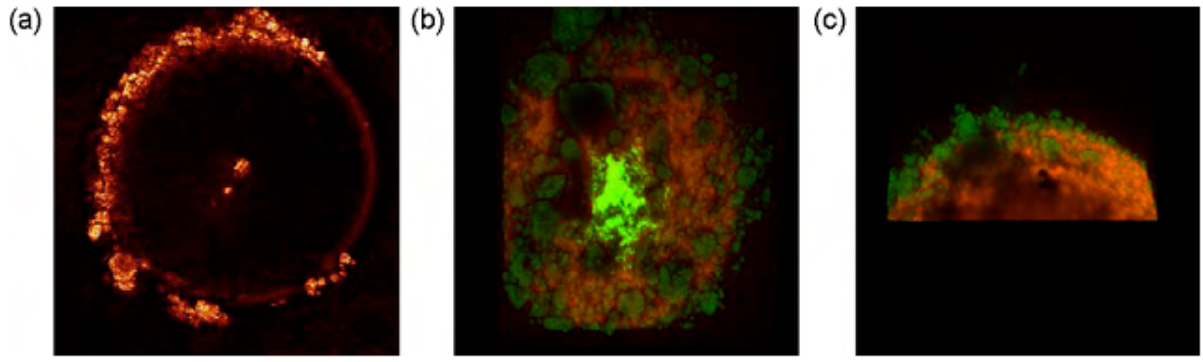

Figure (1.17): A cross-section of liquid marble produced from silica R974 powder and rhodamine B liquid core. (a) cross-sectional view of liquid marble; with the fluorescence artificially highlighted (b) aerial view of liquid marble; (c) side view of liquid marble [434]

Because of the hydrophobic nature of the powder, particles cannot be mixed, but instead cover the surface of the liquid droplet. This drop of liquid is considered as a non-wetting soft solid, and therefore behaves as a micro-bioreactor able to move easily across a surface by very weak forces and without any leakage and any residue [432]. Even at high speed, the hydrophobic powder acts as a preventer of leakages and any disruption. The low friction movement of liquid marble on the substrate requires low force to move it, making it important in microfluidic applications [440, 450]. Liquid marbles also can be formed with different particle sizes ranging from nano- to microns, which allow its use in both colorimetric and optical applications. Bhosale et al. [442] studied the stability of liquid marbles formed with nano- and micro particles. They showed that higher surface area of nano-particles creates more uniform shell and thereby more uniform coverage of liquid marbles. The

mechanical robustness of nano-particle liquid marbles was shown to be greater than the conventional liquid marbles made from larger particles. They believe that this robustness is due to the formation of an elastic nano-particle thin shell around the marble that self-assembles on the liquid-vapour interface. Atomic force microscopy images also showed that the presence of chain-shape particles, rather than spheres on the surface of droplets, allow the formation of particulate networks in the surface coating, which increased robustness against rupture under applied force. This effect also decreases the buckling of evaporating marbles made with smaller powder particle size. McEleney et al. studied the effect of powder density on liquid marble stability. The results of their study indicated that for the successful formation of liquid marbles, in addition to the hydrophobicity of the system, powder density and particle size (particle mass) are important parameters. It was also found that liquid marbles formed using low particle size have the most complete marbles, allow for the greatest ease of marble formation, and are more stable. Moreover, they provided a procedure to increase the mechanical strength of the liquid marble, by polymerising methylmethacrylate (MMA) on the surface of a PMMA [451].

Another interesting characteristic of the liquid marble is its low evaporation rate. The evaporation rate of a liquid marble depends on the size and the type of hydrophobic powder, and the type of encapsulated liquid. For example, for a volatile liquid, the life time is shorter and the deformation rate is higher [439]. The smaller particle size results in transparent liquid marbles, and therefore the content of liquid marbles can be monitored. This property makes the liquid marble a useful device in bio-fluidic applications, such as feasibility of optical monitoring of enwrapped biological fluids for checking the cell health, concentration or other characteristics [452]. The kinetics of evaporation of liquid marbles coated with PTFE has been also reported by Tosun et al.. The evaporation rate of chemically inert PTFE liquid marble was compared with that of pure water droplets in the identical conditions of relative humidity and temperature. The results showed that PTFE liquid marbles have longer lifetimes. They suggested that these life-times are sufficient for many promising applications in microfluidics, genetic analysis, antifouling, wear-free micro-machines, electromechanical actuators and valve fields under normal atmospheric conditions [453]. Dandan et al. also showed that the evaporation rate of graphic liquid marbles is half that for pure water droplets in the same conditions [439]. Small non-adhesive contact of a liquid marble with a substrate leads to relative robustness, and low resistance to motion provides potential for facile manipulation [446].

Another important characteristic of a liquid marble is its ability to deform in shape, which is dramatically influenced by the volume of liquid encapsulated. Although there is no direct contact between the internal liquid phase of a liquid marble and its substrate, the shape of the droplet is still affected by the presence of the powder particles. Since the marbles are soft, they will be deformed to minimize their potential energy. The marbles keep an approximately spherical shape until a certain

volume is reached. By increasing the volume of the encapsulated liquid, a quasi-spherical shape of a liquid marble transforms into a completely non-wetting puddle (Figure 1.18).

The skin of liquid marble exhibits shock resistance when two marbles impact each other, or when it hits the ground, they will deform during the shock, but not coalesce or explode. This property allows manipulation of the size of the marble by cutting it with a knife and dividing it in two parts. Conversely, a marble can be destroyed immediately by making it contact a liquid that penetrates the powder, such as oil or alcohol [446].

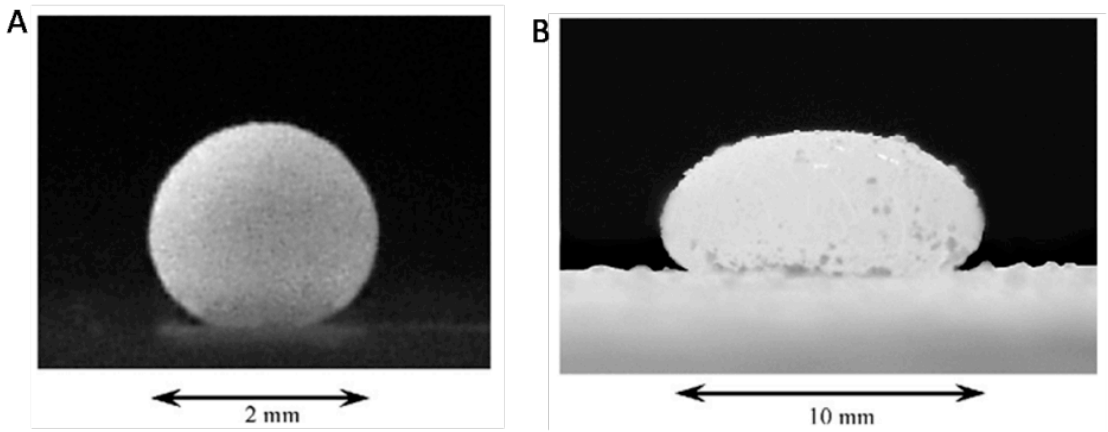

Figure (1.18): Pearland Puddle shapes of liquid marble, marbles were formed by PVDF powder of 10µ l (A) and 500µ l (B) [454]

1.6.1.1 Applications of liquid marbles as small-scaled bioreactors

Since Aussillous and Quere [433] proposed the unique potential of liquid marbles for the first time, this relatively new field of study has been subjected to a variety of practical applications during the past decades. Due to their unique physical and structural characteristics, liquid marbles have drawn the attention of researchers in a wide range of theoretical and experimental applications. The presence of a porous and superhydrophobic shell around the marble prevents contact of the liquid core with an outside surface, and allows gas and vapour permeability and its application for gas sensing. For example, NH_3 was successfully detected through Teflon-coated marbles [437, 455]. Recently, in another study, Fujii et al. [456] proposed a modified idea of using liquid marbles for gas sensing. In their study, liquid marbles were formed using PS latex particles carrying pH-sensitive PDEA hair (PDEA-PS particles). The liquid marbles were rapidly disintegrated upon exposure to HCl gas, presumably due to desorption of the latex particles from the surface of the liquid marbles. Arbatan et al. [457] demonstrated the use of liquid marbles as micro-bio-reactors, for diagnosis application for blood typing. Haemagglutination reaction happened after gentle shaking of the marble

containing the blood and antibody mixture. Tian et al. [437, 455] showed that the porous nature of the liquid marble shell could be used to allow gases to transport through the marble shell. They demonstrated the use of liquid marbles formed with gas-reactive indicator solutions to detect gases. In another recent study, liquid marbles made from lycopodium spores were used to encapsulate aqueous solutions 9-fluorenylmethoxycarbonyl-diphenylalanine (Fmoc-FF). The formation of the self-assembly of ribbon-like peptide fibrils into an ultrathin peptide membrane was as a result of the acidification of the Fmoc-FF solution at the liquid/air interface [458]. This study demonstrated the possible potential of liquid marbles as micro-bio-reactors applications. Polluted water with contaminations, such as oils, petroleum and its derivatives that decrease the surface tension of water, was effectively recognized by the liquid marble technique [459]. Bormashenko et al. showed that polyvinylidene fluoride (PVDF) marbles floating on the surface of contaminated water with silicon oil or kerosene will be destroyed because of the formation of low surface tension film on the surface of the water. They showed that liquid marbles could be effectively used for determination of water pollution from oils and petroleum [459]. The low evaporation rate of liquid marbles covered with graphite powder compared to uncovered ones showed that these marbles have sufficiently long life times to keep their spherical shape, which makes them an interesting choice for industrial and biological applications such as microfluidic, genetic analysis, and anti fouling. Evaporation rate was also decreased by increasing the humidity of the medium. From these studies it can be concluded that liquid marbles are also effective storage devices [460]. Wang et al. reported a gas storage system in which methane molecules were absorbed in the water of the marbles [461, 462].

Due to the ability of liquid marble to be merged, levitated and divided, liquid marbles are of interest in view of their micro-fluidic applications. Marble transportation could be achieved by exerting extra forces such as electric or magnetic fields or by tilting the supporting surface. Fe_3O_4 nanoparticle liquid marbles were formed, manipulated and transported using magnetic fields. Liquid marbles formed with magnetic particles exhibited considerable response to an external magnetic force and provide a straightforward alternative solution to conventional micro-fluidic systems [450, 463, 464]. Using liquid marbles in the pharmaceutical industry has drawn significant attention recently, where the formation and strength of the liquid marbles are seen to be advantageous in drug delivery. Studies have shown that the particle size enlargement process, and wet granulation, can produce liquid marbles. Liquid marbles in the pharmaceutical industry also offer the benefits of handling high drug loadings, simultaneous control of the size and structure of the granules, production of spherical granules with excellent flow, good compression properties, and fast drying periods [436, 460, 465]. An edible liquid marble formed by fatty acid crystals and triacylglycerol crystal was prepared in Kawamura's research group and has useful applications in food, cosmetic and medical areas [466]. Capsules containing drug components and stimulus-responsive liquid marbles were prepared by covering marbles with solid particles based on a copper substrate or polystyrene latex [451, 467]. Tian

et al. recently used the unique property of liquid marbles to build respirable micro-biological reactors to cultivate microorganisms. They found that this respirable bioreactor could provide a more suitable environment for the growth of an aerobe than that in McCartney bottles with shaking incubation; cell concentration increased more rapidly in liquid marbles [468].

The significant advantages of liquid marble bioreactors are the minimization of the consumption of chemical and biological reagents, more accurately controlled reaction conditions, and much shorter reaction times as a result of their small dimensions [444, 450]. For this reason, manipulating and dealing with the small populations of cells becomes cheaper while studying cell behaviour gets easier and in more details. Small volumes are also particularly important for minimizing waste when working with hazardous biological materials. Utilizing a liquid marble bioreactor reduces the risk of biohazard contaminations, since there is no direct contact between the liquid core and the underneath substrate bed. Liquid marble is an easy and simple method that does not need complicated equipment, except the regular cell culture facilities. More importantly, controlling the bio-microreaction can be possible by joining liquid marbles containing different reagents together or by adding different reagents into the marbles. The extraction, replenishment, or change of the liquid core of the liquid marble can be undertaken easily, due to the flexible structure of liquid marbles. Liquid marbles are also disposable.

In fact, all of the above mentioned properties of liquid marbles and specifically I) permeability of the porous shell, which allows the possibility of gas exchange between the medium and surrounding environment, II) Non-adhesiveness of hydrophobic powder particles, which encourages cells to suspend in the medium and form EBs more effectively, and III) a confined liquid core volume that promotes effective contact between cells, encouraged us to exploit these advantages for the first time for living cell applications.

Although there are several reports on the applications of liquid marbles [459, 469, 470], no practical applications considered such unique structures as miniaturized bioreactors for cell purposes. So far, the biological application of liquid marble for studying the behaviour of cells has not been discussed and there is still much to be discovered, characterized, and developed.

As part of the aim of this study, it will be shown that (Chapter 4,5,6) how the confined internal space of liquid marble bioreactors made of highly hydrophobic polytetrafluoroethylene powder can provide the necessary conditions for accommodating living cells and the formation of plenty of uniform EBs in a convenient growth condition. EBs will be shown to express all three germ markers associated with differentiation potential. Additionally, using this novel method provides the differentiation potential of EBs with features of cardiomyocytes and spontaneous beating. Advantages of this method over the existing technologies are mentioned and the high efficiency of the method is highlighted.

1.6.2 Scaffold bioreactors as 3D small-scaled cell culture system

Although the majority of our knowledge in modern biology has been provided by classical 2D cell culture techniques, it is now well accepted that cells reside, proliferate, and differentiate in complex 3D microenvironments. The concept of using 3D biodegradable scaffolds as alternatives for extracellular matrix (ECM), which more closely reform cells' native structure, is an interesting area of study in current tissue engineering. For having the unique function of stem cells, they need to reside in the specialized, three-dimensional microenvironment that surrounds them in native tissues. The microenvironment components need to be positioned in their physiological and functional locations; the interactions between those components are crucial for the purpose of controlling stem cell functions [471].

So far, various studies have demonstrated the significant role of the extracellular microenvironment (ECM) in controlling cellular behaviour [472-474]. A desired scaffold with proper biochemical and biophysical cues can provide structural stability for developing tissues as well as direct cellular behaviour and function. The biomaterial-based scaffold plays a temporary platform for cell activities [475]. Due to the important role of matrix composition in ES cell proliferation, differentiation and their behaviour toward specific lineages, extensive efforts have been devoted to constructing biomaterials that behave more like ECMs.

In this regard, hydrogels with structural and functional similarities to the natural ECM are the most attractive tissue engineering scaffolds in providing 3D environment to cells, both in culture and inside the body. In addition, hydrogel has the ideal potential of allowing the proper diffusion of nutrients and waste to and from tissue due to its high water content and provides an ideal 3D platform for cell-cell and cell-material communications [476]. Hydrogels are defined as three-dimensional stable networks of macroscopic dimensions formed from cross-linked hydrophilic polymers to form insoluble polymeric materials that are able to swell and retain large amounts of water [477]. In fact, different special characteristics of hydrogel, such as tuneable physical and chemical properties and spatially controlled distribution of biostimuli, have been proven to guide and affect stem cell fate [191, 478]. As a consequence of presenting highly hydrated three-dimensional networks of polymers in which cells can attach, grow, and differentiate, hydrogel scaffolds are appealing options for cell delivery and tissue development. It is also possible to manipulate the mechanical properties of the hydrogel material by providing chemical signals to the cells through the incorporation of growth factors, and mechanical signals. Currently, hydrogel scaffolds are being used in an attempt to engineer a wide range of tissues, including cartilage, bone, muscle, fat, liver, and neurons [479].

A study has shown that the combination of micro-scale technology with a 3D hydrogel resulted in more viable cells in the fabricated device than in microchannels without the scaffolds, which

demonstrates the importance of 3D scaffolds in cell proliferation and differentiation [184]. It is worth mentioning that different properties of hydrogel, such as morphology, mesh size, viscoelasticity, degradation behaviour, and biological activities, vary based on different chemical composition and the method of crosslinking [480].

1.6.2.1 Biomaterials for synthesizing hydrogel

Polymers are the commonly used materials for fabrication because of the ability to control their chemical and structural properties. Polymeric materials for scaffolding can be generally categorized into synthetic derived and naturally polymers derivatives [481].

Synthetic materials have been inspired by the understanding of the composition of the ECM in different stem cell niches. Synthetic hydrogels have been generated by polymerization of monomers with a wide range of properties. These materials offer advantages over natural ones as well as limitations. For instance, although synthetic materials are inherently less bioactive, they are mechanically strong and can be engineered with the desirable macro (shape) and micro structure (pore size and porosity), as well as being modified to possess desired bioactive properties that will facilitate cellular growth and organogenesis in a biomimetic manner [482, 483]. In addition, the surface properties of the synthetic polymers can be engineered to suit specific functions, and therefore be more beneficial for tissue engineering applications. Furthermore, since for many synthetic polymers, degradation rate and mechanical strength are known, therefore degradation time should not vary significantly between hosts.

PEG is the most popular synthetic polymer in the biomedical field due to its appealing properties, such as biocompatibility, low immunogenic polymers, protein-resistant properties, and good solubility in various solvents [484, 485]. Studies demonstrated that utilizing 3D degradable polyethylene glycol (PEG) and poly (lactic-coglycolic acid)/poly(l-lactic acid)-based hydrogels, which have been used to support complex tissue structures, could support the formation of structures with the characteristics of neural tissues, cartilage and liver, as well as a network of blood vessel-like tubules, and for cultivation and differentiation of stem cells [410]. In addition, the use of hydrogels represents another useful method for *in vitro* organogenesis. Moutos et al. (2006) showed that a three dimensional woven scaffold made from PGA can be designed to mimic the mechanical properties of a native articular cartilage [486]. Generally, in comparison with natural polymers, the synthetic ones, which are hydrophobic and mechanically strong, have comparatively slower degradation rates [475].

Poylacrylamide/acrylic acid copolymers and Poly(urethane)s (PU) are other examples of synthetic biomaterials with highly tunable properties to influence the behaviour of stem cells. Importantly, proteolytic sensitivity of these biomaterials can be conferred by using small peptides with enzyme-specific cleavage sequences as cross-linkers in polymer synthesis [487].

Examples of other synthetic polymers used for scaffold fabrication that have been approved by the USA Food and Drug Administration (FDA) are poly(acrylic amide) (PAAm), poly(acrylic acid) (PAA) and its derivates and poly(vinyl alcohol) (PVA). PVA has been used in pharmaceutical and biomedical applications or controlled drug release tests, regeneration of artificial articular cartilage and for a hybrid type artificial pancreas [488-490]. Despite the ability to control the surface characteristics of the synthetic polymers, as implied by their name "synthetic", they are deficient in the biological component of the native ECM [491, 492]. In addition, due to the degradation process of these polymers, weak acids will be produced that could be toxic and cause an adverse reaction if they accumulate locally [493].

Biomaterials derived from natural sources are the vast majority of the initial recorded cases of modern tissue engineering [494]. Natural biomaterials being used in scaffold fabrication usually consist of ECM components such as collagen, fibrinogen, agarose, alginate, hyaluronic acid, glycosaminoglycans (GAGs), hydroxyapatite (HA), etc., and therefore have the advantage of being bioactive, biocompatible, and with mechanical properties similar to native tissue. Natural biomaterials, being biologically similar to the native ECM, allow the cells to interact with these polymers in a natural manner through receptors and signals, and aids in the correct functioning of the cells, such as attachment, proliferation, and differentiation. A number of natural materials have been used to support the differentiation for ESCs, including agarose, alginate, chitosan, hyaluronic acid, gelatin, fibringlue, collagen derivatives, and acellular tissue matrices.

Polysaccharide and proteins are the naturally derived polymers have been shown to have the potential of biological recognition that might support cell development. Using polysaccharides for fabrication of hydrogel is beneficial not merely from a biomimetic prospective but also from a scaffold-processing point of view. These polysaccharides have abundant functional groups, such as hydroxyl groups and carboxylic acid groups, amenable to various types of chemical modifications. This provides the possibility to introduce cross-linkable, cell-specific ligands, or extracellular signalling molecules, such as peptides and oligosaccharides, into the polysaccharidic precursors of hydrogels that accelerate tissue reorganization.

Collagen, HA and alginate are some natural polymers that have been employed for tissue engineering to improve surface chemistry and to encourage cell growth and differentiation of embryonic and adult stem cells [476]. Collagen fibres or porous collagen 3D scaffolds with the potential of expressing structural and physiological features similar to the natural microenvironment have been used for mimicking native cardiac muscle. [495, 496]. Zimmerman et al. have created highly functional contracting constructs, which incorporate collagen and Matrigel™ along with neonatal rat heart cells.

Collagen is a structural component of typical engineered heart tissues (EHT), which has been used for generating of cardiac tissue with mechanical and electrophysiological properties similar to the native myocardium of rats, with the potential of integrating with host tissue [497].

However, natural collagen raises concern over potential immunogenicity and pathogen transmission, as well as exhibiting poor thermal stability, mechanical strength, water resistance, biodegradability and handling [498].

Matrigel™ is a commercially available product containing ECM components such as laminin and collagen IV, and heparansulfate proteoglycans, which have been used extensively in cell culture [50, 499]. However, since Matrigel is derived from Engelbreth–Holm–Swarm mouse sarcoma cells, it increases the tumourigenicity and hence is unsuitable for implantation [500].

Other examples of derived natural materials used for creating three-dimensional scaffolds and mESC differentiation are fibrinogen, fibrin [501, 502], and hyaluronic acid (HA), which are highly attractive natural biomaterials. This component has been shown to participate in cellular behaviour and cell signalling. Gerecht et al. (2007) reported the use of hyaluronic acid hydrogels for maintaining the pluripotency and undifferentiated state of hESCs, while by adding soluble factors to the scaffold, cells could be differentiated into specific lineage [411]. HA has also been used in a nano-structured self-assembling peptide scaffold to encourage osteogenic differentiation of mESCs [503]. Fibrinogen, fibrin and hyaluronic acid are available commercially; however, they are usually very costly.

Alginate is a well-known natural polysaccharide with broad applications in cell encapsulation and drug, antibody or growth factor delivery due to its biocompatibility and low toxicity [416, 504]. Alginate has also been used for the encapsulation and differentiation of hESCs and mESCs [105]. Another study showed that by encapsulating mESCs in alginate polyL-lysine (PLL), cells keep their proliferation ability [336]. Porous alginate as 3D matrices has been also associated with enhanced proliferation of embryonic, mesenchymal and neural stem cells [476]. In fact, alginate is considered to have the simplest gelling process as well as the most biocompatible one; lack of bio-active moieties and lack of diverse modification potential limit its practical applications [505]. Furthermore, since degradation of alginate includes a process that causes loss of divalent ions into the surrounding medium, discourages protein adsorption and has an uncontrollable and unpredictable degradation process, it is not the best biomaterial option [479].

Cellulose is the most widespread naturally occurring polysaccharide found in nature, consisting of glucose-based repeating units. Since cellulose and its derivatives can be degraded by microbial or fungal enzymes in nature, it is considered as an environmentally friendly component. In addition, it is inexpensive and biocompatible. The biocompatibility of cellulose and its derivatives is well established [506, 507]. It is easily machinable and thus available in a wide range of forms and shapes. Its mechanical properties have been shown to have a good match with those of hard and soft tissues [506, 508, 509]. The attractive characteristics of cellulose have promoted the widespread use of cellulose-based devices in biomedical applications, such as tissue regeneration and controlled release of drugs [510-512]. Entcheva et al. (2004) demonstrated the ability of a cellulose scaffold to promote cardiac cell growth, to enhance cell connectivity and electrical functionality, and to grow functional

cardiac cell constructs [511]. An early result on liver cells demonstrated superior adhesion properties of cellulose-based materials compared to most polymer surfaces [513]. Several studies report the applicability of cellulose-based materials for culturing cells and for implantation. Examples include bone regeneration [514], hepatocyte culturing for an artificial liver [515], and expansion of progenitor hematopoetic cells in culture [516]. Indeed, cellulosic material is a desirable material for tissue engineering applications since it is renewable, inexpensive, biodegradable, photo-crosslinkable, easy to functionalize, biocompatible to most stem cells, and possesses mechanical properties similar to soft tissues and organs. Besides, cellulose-based materials have very low water solubility, therefore allowing for better control over scaffold design. Hydrogen bonds from the hydroxyl groups, holding the cellulose chains together, account for the high degree of crystallinity, low solubility and poor cellulose degradation *in vivo* [507].

Commonly used cellulose derivatives include hydroxypropylcellulose (HPC), carboxymethycellulose (CMC) and hydroxypropylmethyl cellulose (HPMC)[517]. HPC is a commercial derivative of cellulose that has been approved by the US Food and Drug Administration (FDA) as an agent for drug delivery applications. HPC is soluble in water and many organic solvents, and it is also available abundantly at low cost. This has partly contributed to its use in biomedical and pharmaceutical applications. HPC has exhibited properties such as biocompatibility, biodegradability, and cell-responsiveness, which helps it to be used as a hydrogel for microscale tissue engineering applications. It also is patternable, flexible and has mechanical rigidity to be applied in paper substrates [500]. Although HPC has been modified with allylisocyanate to a biocompatible 3D interconnected porous scaffold, this product is not biodegradable, due to the lack of cellulose hydrolyses *in vivo* [518].

In general, materials from natural sources are advantageous because of their inherent properties of biological recognition, including presentation of receptor-binding ligands and susceptibility to cell-triggered proteolytic degradation and remodelling. However, common disadvantages of natural polymers include variations in degradation rates, batch-to-batch inconsistency, and poor mechanical strength [491, 493, 519].

1.6.2.2 Biodegradability and porosity

Biomaterials play an important role in the preparation of cell scaffolds. Basically, the scaffold should be porous and biodegradable. Biodegradability of polymers is one of the most important factors in pharmaceutical and biomaterials applications. Biodegradable materials are those can degrade or are water soluble by any process in the body to disappear from the site where they have been implanted. Ideally, for functional clinical application, biodegradable scaffolds are needed, which after implantation are remodelled by the body and replaced by native tissue to restore original function.

Therefore, the scaffold must support cell growth and differentiation. Furthermore, the scaffold should degrade into metabolites that do not have any toxicity or immunogenic response.

On the other hand, a 3D scaffold could perform a significant role as an *in vitro* model to help to expand our knowledge about a fundamental aspect of tissue biology or to generate systems for drug and cosmetics screening [520]. Considering that the main composition of extracellular matrix *in vivo* includes collagen, non-collagenous glyco-protein, amino-polysaccharides and proteoglycans, and elastin, the biocompatibility of synthetic scaffold materials has to be raised.

Scaffold pore size is another factor that has been shown to influence cell adhesion, growth and phenotype [521]. Nutrient and gas exchanges are important requirements for cellular aggregates. A cell death problem emerges when there is a limitation in the exchange of nutrients and waste metabolites [522]. This has been tackled by using highly porous scaffolds, where basic designs take into consider such as shape, cell adhesion sites and the flow of gases, nutrients, and metabolites [481]. In fact, the porosity and pore interconnectivity are two important parameters that need to be considered in fabrication of a functional hydrogel, because they play a significant role in cell survival, proliferation, migration and ECM secretion [523, 524]. There are different natural and synthetic materials derived from biodegradable polymers, such as PGA, PLA, PLGA, and collagen, which have been widely used for fabrication of porous three-dimensional scaffolds in the tissue engineering of cartilage, bone, skin, and ligament, etc [525]. Mass transport vascularization and tissue organization is being facilitated by using porous 3D scaffold. For instance, the induction of vessel networks became easier by seeding myoblasts, embryonic fibroblasts and endothelial cells in highly porous, biodegradable polymer scaffolds [526]. In fact, porosity of a scaffold should be sufficient to provide enough space for penetration and migration of cell suspension within the 3D structure, while simultaneously being small enough to let cells to give a critical total surface area for appropriate cell attachment.

It is worth mentioning that different cell types are embedded within matrices possessing distinctly different properties and shapes. For instance, the requirement for peripheral nerve is to be surrounded by a soft uniaxially aligned lipoprotein myelin sheath environment, while for osteoblasts, a hard surface of bone within cuboidal sheets need to be engineered. Therefore, the design of scaffolds must represent the tissue of interest, and a tremendous diversity exists in the design of scaffolds for the engineering of tissues. Using a porous hydrogel can provide an effective mass transfer through the scaffold and consequently provide better cell interactions and a more physiologically relevant environment for the cultivated cells, which make them proper candidates for tissue engineering applications [109, 527]. Indeed, porous gels improve cells functions by providing proper 3D structure [224, 349].

1.6.2.3 Thermo-responsive hydrogel

Smart materials, which are defined as materials with the ability to respond to external stimuli, are one of the most interesting classes of materials [528, 529]. Polymer-based thermo-responsive materials are a class of "smart" materials that have the ability to respond to a change in temperature; this property makes them attractive materials in a wide range of applications such as sensors, drug and gene delivery and tissue engineering [530, 531]. Thermo-responsive polymers in tissue engineering are commonly used for two purposes, one as substrates that enable the cell growth and proliferation as well as injectable gels, *in situ* of the scaffold. In the first application, the thermo-responsive ability of the polymers is used to regulate cell attachment and detachment from a surface [532, 533]. There are two main types of thermo-responsive polymers based on presenting a lower critical solution temperature (LCST) and an upper critical solution temperature (UCST). In fact, at different temperatures lower than LCST and higher than UCST points, the polymer and solvent are completely miscible [534].

Since thermo-responsive hydrogels only respond to temperature changes for their gelation and do not require chemical or environmental treatment, they have been classified as, and considered as, one of the important class of materials. They can be thus produced (e.g., upon injection to the body) when temperature is increased from ambient to physiological levels.

Poly(N,N-diethylacrylamide) (PDEAAm), poly(N-vinlycaprolactam) (PVCL), poly[2-(dimethylamino)ethyl methacrylate] (PDMAEMA), and poly(ethylene glycol) (PEG), also called poly(ethylene oxide) (PEO), are examples of synthetic thermo-reponsive polymers. Due to the fact that Poly(N-isopropylacrylamide) (PNIPAAm)'s LCST is close to body temperature and its fast on-off switching, it is one of the most used polymers for the development of thermo-responsive behaviour hydrogels. A major issue for PNIPAAm-based hydrogel is its biodegradability. PNIPAAm is non- degradable, which limits its application. Many studies have been carried out on PNIPAAm with the attempt to introduce degradable groups onto PNIIPAAm to render it biodegradable. PEG is an interesting synthetic polymer for fabricating thermo-responsive hydrogels. However, PEG and polyester based thermo-sensitive hydrogels release acid during degradation, which may provoke severe inflammatory response [535, 536].

Gelatin and chitosan are considered as natural biopolymers with thermo reversible properties. Cellulose is another natural polysaccharide that is insoluble in water. Some cellulose derivatives such as methylcellulose (MC), hydroxypropyl methylcellulose (HPMC) and hydroxypropyl cellulose have been extensively studied for biomedical and tissue engineering applications. Utilizing renewable cellulosic materials with new biochemical and physiochemical properties for developing a thermo-responsive hydrogel will bring attention to new applications in the biomedical field. As a result of many promising applications of thermo-responsive polymer, new thermo-responsive polymer systems

with new biochemical and physiochemical properties are still needed to provide multifunctional platforms.

1.6.2.4 Hydrogel for embryoid body formation

So far, different cell types have been successfully cultured on polymeric scaffold; however, these are usually single-cell-type cultures [7, 537, 538]. Embryonic stem cells (ESCs) are pluripotent cells with the ability to organize into multi-cell-type structures during embryonic like differentiation, which makes them powerful sources for therapeutic, drug discovery and cell replacement applications [33, 34, 38, 79, 405]. Generally, differentiation of ESCs is initiated through an intermediate step involving the formation of embryoid bodies (EBs) via complex three-dimensional aggregates of ESCs [539, 540]. As mentioned earlier, ESCs aggregates subsequently can undergo differentiation into all the somatic cell types. Therefore, EBs have the potential to serve as an omnipotent cell resource for cell therapy, including tissue engineering. One of the primary challenges in ES cell research is the development of a culture system to control cell aggregation and agglomeration during EB formation, which has a profound effect on the extent of cell proliferation and differentiation.

Currently, there are several methods with unique peculiarities used to form EBs from ES cells (as discussed in detail in section 1.6). These methods, such as forced aggregation, spinner flask, and reactor-based cultures, have been developed to generate a large scale of ES cell derivatives through the formation of EBs for further applications [119, 138, 541].

However, these methods suffer from several drawbacks, including generating shear forces, which although manageable, still damage the cells [133, 542]. Some other common techniques such as hanging drops and the liquid suspension culture may have one of the following limitations, such as being time-consuming or labour intensive, having a complicated production process, being unable to scale up, having low efficiency of EB formation, or being economically impractical [138, 143, 390, 543]. It is worth noting that the common disadvantage of all these methods is the lack of support from extra-cellular matrix, which plays an important role in cell growth and development. On the other hand, since multi-cellular structures require cells to be able to migrate in three dimensions and interact with their microenvironment, two dimensional culture environments are not adequate, and there is a need for proper 3D environment.

As it was mentioned earlier, effective mass transfer can be achieved by generating porous structure in the scaffolds or selecting highly permeable scaffold materials. Porous collagen sponges have been used in 3D culture conditions to influence rhesus ESC differentiation [544]. In that work, undifferentiated rhesus ESCs were seeded on top of the collagen sponges or at the bottom of the culture well, with or without co-culture of human dermal fibroblasts or keratinocytes. However, in this study, ES cells were not seeded in the collagen matrix and the process of EBs formation in the

whole ES cells differentiation was skipped. The research performed by Levenberge et al. (2003) showed the cultivation of undifferentiated ESCs and differentiated cells with the use Matrigel or fibronectin as an adhesive agent to prevent cells from leaking out [410]. They also used different growth factors to direct differentiation. In their study, a combination of porous polymeric scaffold and Matrigel or fibronectin coating of the scaffold were needed to enable the formation of tissue structures from differentiated ESCs, while Matrigel alone failed to support cell growth and 3D organization. The work was unsuccessful in generating EBs by seeding the ESC directly into porous PLLA/PLGA scaffolds with 250-500μm pore size. In another study, mESCs were induced to become neural progenitors using three-dimensional (3D) fibrin scaffolds and by adding retinoic acid. However, this study failed to form the EB-like structure after seeding mESC [501].

The presence of dense reactive hydroxyl groups on the surface makes cellulose surfaces suitable for immobilization of cell adhesive proteins such as fibronectin [545]. In addition, the densely packed glucan chain structure in cellulose fibres gives them sufficient mechanical strength to support cell aggregate structures [546]. Therefore, this natural biomaterial could be considered as one of the desired components for inducing EB formation. Methylcellulose (MC), one of the derivatives of cellulose, was employed to coat the surface of a polystyrene dish to cultivate human embryonic stem (hES) cell clumps for the formation of embryoid bodies (EBs) in liquid suspension culture; however, in this technique, cells were grown on top of the non porous scaffold [547]. Recently, it has been reported that biodegradable 3D hydrogel constructed from hydroxypropyl cellulose (HPC), modified with bio-functional methacrylic anhydride (MA), is biocompatible to human adipose-derived stem cells (ASCs). ASCs were successfully differentiated into the adipocytes inside the scaffolds, and therefore demonstrated the potential application of these HPC-MA scaffolds for adipose tissue engineering [548]. Overall, cellulose-based hydrogels have many favourable properties such as hydrophilicity, biodegradability, biocompatibility, transparency, low cost, and non-toxicity, which make them interesting options in tissue engineering [549], controllable delivery system [550],blood purification [551] and cell culturing.

To our knowledge, however, there have been few studies into the application of cellulose microfibres as scaffolds for cell culturing, direct formation of EBs inside cellulose-derived scaffolds and the cardiac differentiation potential of hydrogel-born EBs have not been reported. To achieve this goal, a modified macro-porous HPC hydrogel is used to study the capability of a 3D porous scaffold to support stem cell growth and, more importantly, the feasibility of embryoid body formation comprising the three embryonic germ layers is investigated. The potential of the EBs formed in hydrogel to differentiate into cardiac lineage cells will also be investigated.

There have been extensive studies on the efficacy of biocompatible natural and synthetic polymeric hydrogels as 3D tissue scaffolds, which have the ability to degrade and function as “smart” hydrogels,

as well as in the microfluidics field. However, the use of modified cellulose as a 3D tissue scaffold has yet to be fully exploited.

1.7 Scope of the Present Study

Embryonic stem cells (ESCs) are pluripotent cells capable of differentiating into all somatic and germ cell types. The intrinsic ability of pluripotent cells to generate a vast array of different cells makes ESCs a robust resource for a variety of cell transplantation and tissue engineering applications. Stem cell characteristics, such as proper proliferation and differentiation, are regulated not only by the stem cells themselves but also by their microenvironment.

To shed light on the mechanisms that regulate stem cells, it is important and indispensable to develop technologies and methodologies that allow the study of stem-cell function in response to isolated components of a complex system. Biomaterial approaches, in combination with other technologies such as microfabrication, are well suited to assist studies of stem-cell biology through the creation of evolving systems that allow key variables to be systematically altered, and their influence on stem-cell fate analysed. Biomaterial technologies provide the exciting possibility of deconstructing and then reconstructing niches, and play an important role in creation of a local environment that enhances and regulates proliferation and differentiation of stem cells and induces cell-based tissue regeneration. However, due to the inert nature of most of the biomaterials used in small-scale devices, they must undergo surface modification prior to cell attachment to promote adhesion and to prevent adsorption of proteins on the surfaces.

Stem cell adhesion is a prerequisite for eliciting pluripotency. Therefore, it is a crucial task to efficiently mimic stem cell microenvironments and niches using biopolymers (biomaterials) to control adhesion and spreading of cells, which can be effectively achieved by surface modification of the substrates and providing suitable microenvironment using proper biomaterials. Different techniques can be used to modify the surface of materials, which have the desired physical and chemical properties, but lack sufficient biocompatibility.

The object of the first part of this work is to engineer an effective surface functionalization method for enhancing the biocompatibility of a PDMS surface that is protein resistant while facilitating cell proliferation (expansion) and maintaining the pluripotency potential of cells. A bio-functionalized surface was fabricated in the form of a disposable micro-bioreactor with a microchannel reactor bed, which was shown to have the potential to be utilized as stem cell studying tool. (First part of the thesis study, Chapter 3)

To fulfil this aim, soft lithography was used to fabricate a PDMS micro-bioreactor. The inner surface of the channel was functionalized by an effective physiochemical modification method. We also investigated the potential of functionalizing PDMS with carboxylmethyl cellulose (CMC) as a low-cost non-fouling material to minimize protein adsorption. Different characterisation methods were applied to study the structural and chemical properties of the modified substrate. To investigate the composition and chemical properties of the composites, Fourier transform infrared (FTIR)

spectroscopy was used. Water contact measurements were performed to demonstrate the improvement in hydrophilicity and long term stability of the functionalized surface. Protein adsorption assay was also performed to demonstrate the protein-resistance of the surface. Biocompatibility of the modified surface on cell attachment and proliferation was also investigated through different characterization methods, and compared to the non-modified surface.

In order to use adult or embryonic stem cells for regenerative medicine applications, control over their self-renewal and differentiation properties must be attained. Differentiation of ESCs into a variety of cell types is an important characteristic of these types of cells, which is commonly achieved *in vitro* by spontaneously self-assembling in low adhesion culture condition into 3D cell aggregates called embryoid bodies (EBs). Formation of EBs, as a critical step to direct differentiation of the cells provides opportunities to mechanistically study early differentiation events of 3D assemblies of pluripotent cells. Miniaturized devices expand our ability to control material transport, and material manipulation, at smaller scale than their conventional counterparts. Miniature systems are especially beneficial for biological and medical applications. Indeed, small scale devices have the potential to create bio-mimetic structures that mimic the *in vivo* cellular microenvironment, enable experimental parallelization under well-controlled conditions, minimize the consumption of reagents and reduce sample analysis time. Engineering new culture-based approaches using advanced biomaterials in the form of artificial miniature reactors (liquid marble and porous hydrogel scaffold techniques), that more closely mimic what the body already does and promote the generation of more homogeneous EBs, is another major goal of this study. (Second part chapter 4,5,6 and the third part of this study, Chapter 7 and Appendix 7.3)

The second part of this study was accomplished by developing a novel, low cost, high-yield and easy-to-control strategy in the form of a miniaturized bioreactor. This novel method was first developed for formation of cancer cell spheroids inside liquid marbles, with immediate significance in biomedical and tissue engineering applications. Factors such as the powder particle size, the liquid marble volume and the cell seeding density inside each liquid marble were also investigated to evaluate the effects of varying experimental conditions on the efficiency of EB formation within a liquid marble. The efficiency of the method to support cell viability and to generate more homogeneous EBs was then compared to one of the most popular formation techniques called suspension culture. A bioreactor made of liquid marble was further investigated for its capability to induce EB differentiation into myocytes cells as an easy, cost effective and straightforward method. The loss of pluripotency of cells in EBs was investigated using the Fluorescence-activated cell sorting technique (FACS). The differentiation capability of marble-born EBs was investigated via presence of three germ layer markers. The expression of different stage cardiac genes was investigated using RT-PCR and RT-qPCR techniques. Cells were also immunostained for present of cardiac markers. Feasibility of spontaneous differentiation into beating cardiomyocytes was additionally investigated by plating

down the EBs. In this study, we proposed for the first time that liquid marble could greatly contribute to ES cardiac differentiation, which enhances biology and genetic studies.

It is now well accepted that cells reside, proliferate and differentiate in complex 3D microenvironments. Biomaterial-based scaffolds have been the most important tool in providing a 3D environment to cells, both in culture or inside the body. A proper supporting matrix can provide support for cell survival and functioning. The use of scaffolding materials as stem cell embedding biomaterials in a fixed bed micro-bioreactor is intriguing, since scaffolding materials can mimic the microenvironment of the extracellular matrix in a human body. In fact, scaffolds act as artificial extracellular matrices while providing the necessary support for cell proliferation and maintaining their differentiation functions.

On the other hand, since differentiation of embryonic stem (ES) cells typically requires cell–cell aggregation in the form of embryoid bodies (EBs), using functional a porous scaffold with the confined environment of the pore structure in the scaffold would effectively enable the formation of EBs, minimize the agglomeration of EBs, and eventually lead to efficient cell proliferation and desired differentiated lineage

In the third part, we further studied the feasibility of using a novel biodegradable porous cellulose scaffold to create a 3D supportive environment for generating stem cell spheroids (known as embryonic bodies (EBs)). The morphology and structural characteristics of porous scaffolds and the formation of EBs inside a 3D scaffold were investigated by scanning electron microscopy (SEM) and confocal imaging. The efficiency of formed EBs in terms of uniformity and cell viability was compared with those formed in suspension culture method. The differentiation capability of scaffold-born EBs was investigated via presence of three germ layers markers by conducting immunostaining as well as RT-PCR analysis. The level of expression of the three germ layer markers in scaffold-born EBs over a certain period of time was also compared to those formed via suspension culture. To determine the capability of EBs formed in scaffold to differentiate into cardiac lineage cells, they were subsequently plated down to study the development of this lineage. Immunostaining for NKx2.5 as a cardiac transcription factor and the expression of cardiomyocyte filament proteins, cardiac troponin I (cTnI) as a mature cardiac specific transcript factor was conducted. The capability of the hydrogel for promoting spontaneous cardiac-like action potentials, which shows the maturation of EBs, was also investigated.

1.8 Thesis Overview

This thesis is presented in a "Thesis Partially Based on Conjointly Published and Unpublished Work" format. It is made up of four published journal articles, one submitted article and one drafted article. Each chapter contains a brief introduction in which the articles are placed within the context of the thesis as a whole. The outline of the present PhD thesis is as follows:

Chapter 1 provides an introduction on cell and tissue engineering, information about stem cells and their different types, their applications and a literature review on the technologies developed for supporting stem cell proliferation and differentiation including conventional bioreactors. In this chapter, we will pay special consideration to miniaturized technologies for stem cell growth and expansion, including the bio-functionalized PDMS micro-bioreactor (as a 2D model), the liquid marble bioreactor and the macro-porous scaffold (as 3D models). The most common techniques for functionalization of a PDMS surface will be discussed and the best one will be selected for our study. The liquid marble will be introduced as a novel mini-bioreactor and its principles, properties and applications will be discussed. Novel applications are proposed and investigated to demonstrate the great capability of liquid marbles, particularly as microreactors in biological studies. A novel scaffold integrated bioreactor will also be used for studying the feasibility of formation of embryoid bodies.

Chapter 2 describes the experimental and characterisation methods used in this thesis.

Chapter 3 concerns the physio-chemical bio-functionalization of PDMS surface. In this chapter, we present a novel and inexpensive method to prepare a disposable micro-bioreactor for stem cell expansion. The micro-bioreactor was fabricated in the form of a fixed bed bioreactor with a microchannel reactor bed. The functionalized surface was found to be biocompatible with MDA-MB-231 and Oct4b2 cells, and was demonstrated to facilitate cell proliferation. The expanded Oct4b2 cells retained their proliferation potential, undifferentiated phenotype and pluripotency.

The results were published in Journal of Materials and Chemistry.

- Publication: Surface-functionalization of PDMS for potential micro-bioreactor and embryonic stem cell culture applications

The novel concept of small-scale bioreactors made of liquid marbles is demonstrated in Chapter 4. The idea of using liquid marbles as bioreactors is discussed in this chapter through studying a typical, yet important, biological assay. Liquid marbles are shown to be capable of accommodating living cells, in a convenient growth condition. A case study is then done including investigation of the formation of cancer cell spheroids inside liquid marbles made of polytetrafluoroethylene powder and cell culture medium. Advantages of the method over the existing technologies are mentioned and the high efficiency of the method is highlighted.

The published result is listed below:

- Publication : Tumor inside a pearl drop

In chapter 5, we provide a novel application of liquid marbles for formation of three dimensional (3D) structures of stem cells, which are called embryoid bodies (EBs), inside liquid marbles. In this part, we also discuss factors including liquid marble shell properties, liquid marble size and the cell seeding density and their effects on the size, uniformity and quality of the EBs formed. By using liquid marble bioreactors, we showed that this method provides a quick aggregate formation method with time similar to the hanging drop method, which is the most common method. The liquid marble method also minimized human involvement; once the medium marbles containing cells are prepared, they can be placed in an incubator until the spheroids are formed. In addition, as a result of producing several EBs in each individual marble, this method is more efficient. In this part, we also showed that the EBs that formed using the liquid marble technique are capable of further *in vitro* differentiation potential.
The published result is listed below:

- Publication : A novel technique for formation of Embryoid Bodies inside liquid marbles

In chapter 6, we further develop the idea of using liquid marble bioreactors for cardiomyocyte differentiation of mouse ES (mES) cells after formation of EBs inside the liquid marble. The results demonstrate that ES cells can differentiate into myocytes cells through the liquid marble technique as a facile, cost effective, and straightforward method. We propose for the first time that liquid marbles greatly contribute to ES cardiac differentiation, which leads to better exploration of ES biology and genetic studies.
The results are presented as a submitted paper:

- Publication (Submitted) : Cardiogenesis of Embryonic Stem Cells with Liquid Marble Micro-bioreactor

Chapter 7 concerns the feasibility of generating homogeneous embryonic bodies (EBs) inside a novel biodegradable porous hydrogel. The efficiency of hydrogel-born EBs in term of size uniformity and cell viability are compared with EBs formed through liquid suspension method. Hydrogel born EBs are further studied for the capability of *in vitro* differentiation for expressing the three germ markers. The cardiomyocytes differentiation capability of EBs, which is formed inside hydrogel, is also examined by conducting PCR and immunostaining for presence of cardiac markers.
The findings of this study is presented in the following submitted publication,

- Publication (submitted) : Stem cells inside Hydrogel Micro-bioreactor

In Appendix 7.3, the use of thermo-responsive HPC-MA hydrogels for the engineering of tissues with cell-releasing behaviour is examined. The thermo-responsive properties (such as turbidity, water contact angle, swelling ratio, dynamic mechanical analysis and thermal analysis) of these HPC-MA hydrogels were evaluated. Temperature-modulated cell-releasing characteristics were studied using African green monkey kidney cells (COS-7 cells) and murine-derived embryonic stem (mES) cells.
The findings of this study is presented in the following publication,

- Publication : Thermoresponsive Cellulosic Hydrogels with Cell-Releasing Behaviour

Chapter 8 provides a summary of the concluding remarks in this work and discusses some possible avenues for future research.

Chapter 2: Experimental Methodology

An experimental section is given in each of the papers that follow but the detailed experimental methods have been collected together in this chapter for completeness and convenience.

2.1 Materials and Method

PDMS substrates were prepared using a silicon elastomer kit (Sylgard 184, Dow Corning, MI) and mixed at a 1:10 curing agent to base ratio. Trimethoxysilylpropyl(polyethyleneimine) (50% in isopropanol) (Mw= 2000–4000) was purchased from GelestInc, USA. N-Hydroxysuccinimide (NHS), 1-ethyl-3-(3-dimethylaminopropyl) carbodiimide hydrochloride (EDC), carboxymethyl cellulose sodium salt (CMC, Mw~90 kDa), albumin–fluorescein isothiocyanate conjugate (BSA–FITC), bovine serum albumin (BSA), acid orange II, and 2-(N-morpholiino) ethane sulfonic acid (MES) were purchased from Sigma-Aldrich, Australia. Calcein AM, 4',6-diamidino-2-phenylindole, dilactate (DAPI), Texas Red-X phalloidin, Dulbecco's modified Eagle's medium (DMEM), non-essential amino acids, GlutaMAX, and penicillin–streptomycin were obtained from Life Technologies, Australia. n-Hexane was obtained from Merck. Gelatin (Mw=80–140 kDa) was obtained from Wako. Unless stated otherwise, all other chemicals were purchased from Sigma-Aldrich, Australia.

2.1.1 PDMS microchannel design and preparation

Preparing the PDMS is very straightforward. Sylgard 184 silicone base and curing agent are mixed in a 10:1 ratio by weight. Then the mixture is degassed to remove any bubbles and poured over the PDMS master. The PDMS is then baked under vacuum, causing it to cure and ensuring all entrapped gasses are evacuated. After cooling, the PDMS is easily peeled and cut.

Fabrication of the microchannels was successfully performed at the Melbourne Nano Fabrication centre next to Monash University. A dark field photomask with a microchannel pattern of 200 mm width, 50 mm height and 3 cm length was designed using AutoCAD. Standard photolithography was employed to fabricate the Si master mold for PDMS replication. Spin-coating is a conventional technique for the preparation of polymer thin films. The wafer was positioned on the centre of the spin coater, and SU8-2050 (Microchem) was spin coated on a wafer at 500 and 1500 rpm for 5s and 30s, respectively. The high centrifugal force is critical for generating a uniform thickness of the polymer. The spun coated wafer was placed on a hotplate at 65°C and 95°C in sequence for 5 min and 20 min, respectively. The wafer was then allowed to cool to RT. The photomask was lowered over the photoresist coated wafer to form a sandwich assembly, and was irradiated under UV at 240 mJ cm^2 in

a Contact Aligner (Mask Aligner, EVG 620). The mask aligner exposes and transfers the pattern of the mask onto the SU-8 covered silicon substrate.

After UV-irradiation, the wafer was baked at 65 °C for 5 min followed by 95°C for 10 min and then cooled down to RT. The wafer was subsequently developed for 15 min, followed by rinsing in acetone and isopropyl alcohol (IPA) before drying with dry nitrogen. The thickness of the patterned photoresist film was determined using the surface profilometer. PDMS is cast from the most more commonly used Dow Corning Sylgard184, containing PDMS with two components, Elastomer (Component A) and the curing agent (Component B). PDMS precursors were combined in a 10:1massratio. Sylgard is a two part resin system containing vinyl groups (Part A) and hydroxysilane groups (Part B), shown in Figure 2.1.

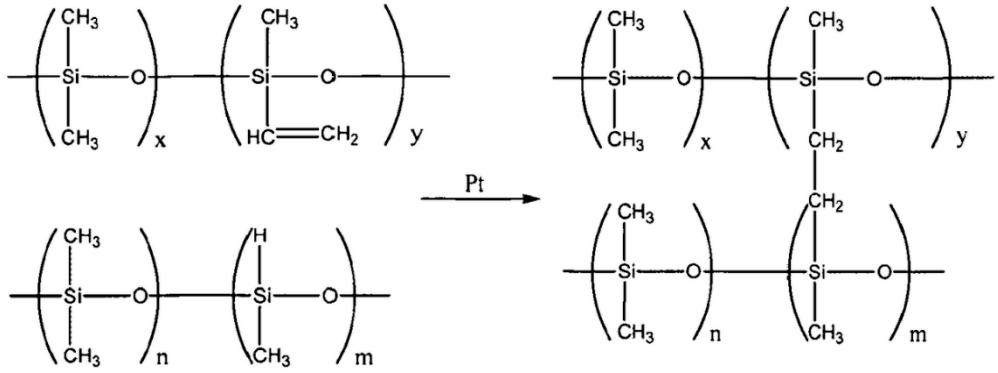

Figure (2.1): Schematic reaction between two parts of PDMS [552]

A cross-linked network of dimethylsiloxane groups is created by mixing the two resin components together. Because this material is flexible, it can be peeled off from the SU-8master, leaving them to interact and ready to produce another device. After mixing the PDMS components, PDMS is poured on each mold and degassed using a vacuum chamber for 30 minutes to remove air bubbles. Then the molds are heated at 85°C for 4 hours. As the baking of PDMS is done, a scalpel is used to cut out the required shape and peel off the silica wafer. The PDMS microchannel replica is gently peeled off from the master mold and cut into a rectangular plate of dimension 2×3 cm^2 to prepare microbioreactor assemblies. A biopsy punch is used to cut out the holes for the ports. The PDMS substrates are then washed with hexane for 2 days to remove the uncured prepolymer, followed by isopropanol to remove contaminants. Figure 2.2 shows the schematic steps for preparing PDMS microchannel.

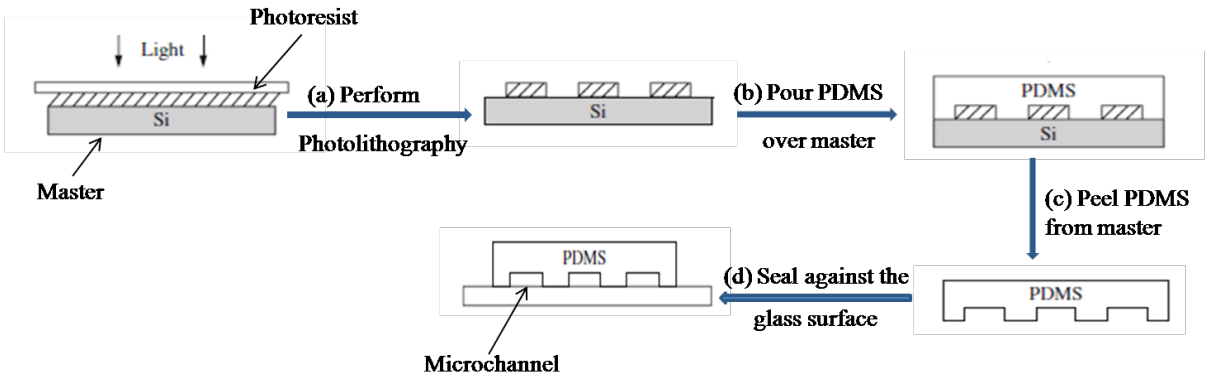

Figure (2.2): Scheme describing of prototyping of microfluidic systems. A system of channels is designed in a CAD program. A photomask was used in contact photolithography to produce a master. (a) A master consists of a positive relief of photoresist on a silicon wafer and serves as a mold for PDMS. (b) Liquid PDMS prepolymer is poured over the master and cured for 4 h at 85°C. (c) The PDMS replica is peeled from the master. (d) The replica is sealed to a flat surface to enclose the channels [553]

2.1.2 PDMS surface functionalization

The immobilization of biological entities - such as proteins, enzymes, and cells - is of great importance for the development of biosensors, immunoassays and bio- microfluidic devices. In this work, we study the *in-situ* bio-functionalization and cell adhesion in microfluidic channels. The most common surface functionalization technique for any silicon-based material is Oxygen plasma treatment. The glass substrates were soaked in acetone for 10 min and rinsed in isopropanol followed by drying with compressed air to remove any residual. The glass substrates and the microchannel PDMS were placed inside the plasma cleaner (Harrick Plasma, PDC-001/002, USA) system. The PDMS chip surface was placed face up. A plasma cleaner was used to create activated silanol groups on the surface of glass, and PDMS microchannels. O xygen plasma treatment was applied at 1000 mTorr for 60s. By applying oxygen plasma treatment, we were able to create oxygen free radicals on the surface of glass and PDMS, and then place the surfaces together for a permanent bond. To ensure a better seal between PDMS with glass, the PDMS microchannels were heated at 85° C for an extra 20 minutes.

Immediately after sealing the PDMS channel with the glass substrate, the microchannel was filled with 4% (v/v) trimethoxysilylpropyl (polyethyleneimine) in acetone in a single injection using a syringe, and allowed to react for 2 h at RT. The modified microchannel was rinsed with ethanol and deionized (DI) water to remove any unbound polymer, and dried at 65° C for 3 h. The microchannel was then equilibrated with MES buffer (50 mM, pH 5.0) for the next step of modification. The amine group is created on the surface of the PDMS channel and the aminized PDMS substrate is denoted as PDMS–NH2. CMC was conjugated onto the aminated PDMS substrates in the presence of EDC and

NHS. To graft CMC onto the aminated substrates, 0.6 mg/ml CMC was dissolved in 50mM MES buffer, pH 5.0, to obtain the final concentration of 2mg/ml. For activating the CMC, NHS powder was added to the CMC solution to a final concentration of 2.0 mg/ml until fully dissolved. EDC powder was then added to the NHS and CMC solution to a final concentration of 2.0mg/ml, and stirred at room temperature for 30min. Once weighed, EDC powder was added immediately to the NHS and CMC solution to a final concentration of 2.0mg/ml, stirred at room temperature for 30min. The activated CMC solution, prepared according to the above procedures, was injected into the PDMS–NH2 microchannel until the microchannel was fully filled, and was allowed to react at RT overnight. The CMC grafted PDMS microchannels were then washed with DI water and with MES 0.1M buffer to remove residual reagents. The samples were dried in an oven at 65°C for 3 h. The CMC grafted substrate is denoted as PDMS–NH–CMC. Gelatin conjugation was performed in a biosafety cabinet and under aseptic conditions. PDMS–NH–CMC microchannels were first sterilized in 70% ethanol overnight. 0.1M MES buffer (pH 5, 1ml per sample) was prepared and autoclaved to sterilize MES. Gelatin was dissolved in PBS (300µg/ml) at 60°C, and once fully dissolved, it was allowed to cool to room temperature. Gelatin solution was sterilized with 0.22µm sterile filter. NHS was added followed by EDC at a final concentration of 2mg/ml to PDMS-NH-CMC. One ml of EDC (2.0 mg/ml) and NHS (2.0 mg/ml) in MES buffer (pH= 5) was filter sterilized before injecting into a PDMS–NH–CMC microchannel in a single-injection until the microchannel was fully filled. After reacting for 30 min at RT, sterile gelatin was injected into the activated microchannel in a single-injection until the microchannel was fully filled, and allowed to react overnight at RT. The microchannel was then rinsed by injecting sterile MilliQ water followed by PBS. The gelatin-grafted substrate is denoted as PDMS–NH–CMC-GEL.

2.1.3 PDMS surface characterization

2.1.3.1 Amine adsorption by Acid orange II

Acid orange II is a negatively charged dye that can combine with positively charged amino groups on a material surface under acidic condition by an ion exchange mechanism, as shown in Figure 2.3. The number of surface accessible amines was quantified using an Acid Orange II [554]. Each sample of defined size (2.0 cm^2) was incubated in 1 mL of Acid Orange II solution in deionised water (500 mM, pH 3.0, adjusted with HCl) at RT overnight. The residual Acid Orange II was removed by washing the films with copious water at pH 3.0, and the films were incubated in 1mL of deionised water at pH 12.0 (adjusted with NaOH) overnight for detachment. The amount of bound dye was quantified by measuring the solution optical density at 492 nm. PDMS films served as controls. A standard curve

was created for 100 µM, 200 µM, 300 µM, 400 µM and 500 µM concentrations of Acid orange in deionised water at pH 12.0. The number of surface amine groups was determined based upon the assumption that Acid Orange II complexes with amine at a molar ratio of 1:1.

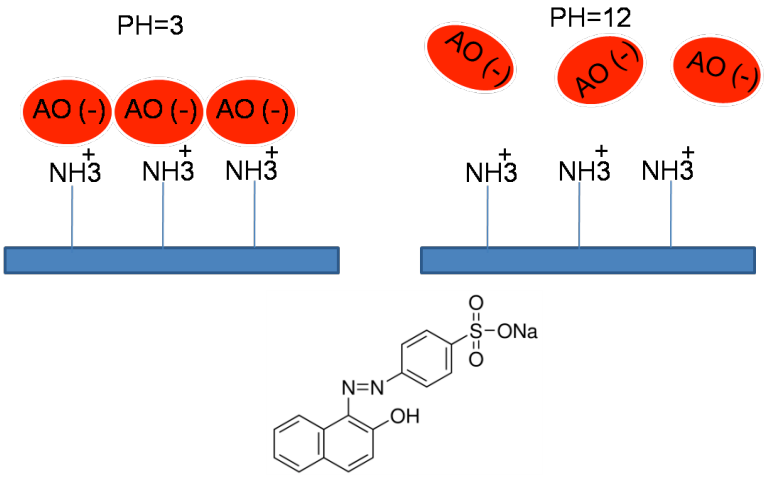

Figure (2.3): Quantitative analysis of amino group on aminated PDMS surface. (a) In acidic solution (pH~3), negatively charged Acid orange forms complex with $–NH3^+$; (b) in basic solution (pH~12) or organic solvents, the Acid Orange molecules are released from the material surface; (c) molecular structure of Acid Orange.

2.1.3.2 Contact angle measurement (Wettability)

As a result of oxygen plasma treatment on the surface of silicon based materials, siloxane bonds on the polymer surface. Atoms and molecules on the surface of polymers are in a different environment with their bulk molecules. They are subjected to intermolecular attraction from one side only. Wettability of the surface has a direct relation with the surface energy of the surface and has often correlated strongly with biological interaction. Hydrophilicity of a surface is measured by the water contact angle, which shows how much a droplet of water spreads on a surface. The lower the contact angle, the more hydrophilic the surface is. Oxidation or ionization of the surface introduces more hydrophilic bonds to the surface, which makes it easier for a drop of water to spread along the hydrophilic surface, resulting in a lower contact angle. Surfaces that are considered hydrophobic have a contact angle with water greater than 90^o. On the other hand, when the contact angle is less than 90^o, the surfaces are considered hydrophilic [555] Figure 2.4.

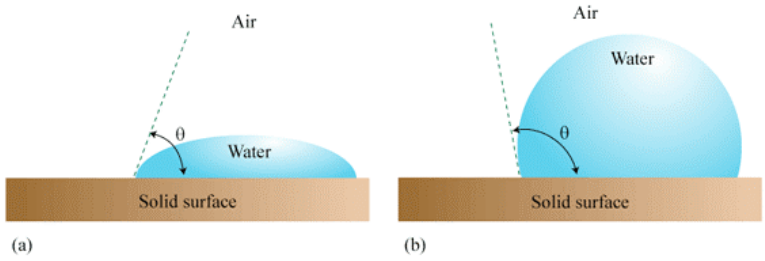

Figure (2.4): (a) Water spreading over a hydrophilic surface and the contact angle is less than 90°, while (b) in a hydrophobic surface, water forming a droplet.

Static contact angle measurements were made using OCA20, Dataphysics Instruments GmbH, Germany. 2 µL drops of deionized water were placed on the sample surfaces, after 5 s the data were collected to obtain the static contact angle. The measurements were performed on at least three different areas on each substrate and the values were averaged. PDMS–NH2 and PDMS–NH–CMC surfaces were immersed in water for up to 25 days for measuring the hydrophilic stability. After a certain period of time, samples of each surface type were removed from water and dried under a stream of air and static water contact angle for at least three different areas were measured.

2.1.3.3 Protein adsorption

Due to inherent affinity of PDMS to adsorb proteins and hydrophobic molecules, it usually requires some modification for use as a micro-bioreactor substrate to prevent the loss of attachment of the targeted cells and also clogging of the microfluidic channels [556]. Protein adsorption of the surface was done using qualitative and quantitative methods.

The BCA protein assay kit is a detergent-compatible formulation based on bicinchoninic acid (BCA) for the colourimetric detection and quantitation of total protein. This method combines the well-known reduction of Cu^{+2} to Cu^{+1} by protein in an alkaline medium (the biuret reaction) with the highly sensitive and selective colourimetric detection of the cuprous cation (Cu+1) using a unique reagent containing bicinchoninic acid [557]. The purple-coloured reaction product of this assay is formed by the chelation of two molecules of BCA with one cuprous ion. This water-soluble complex exhibits a strong absorbance at 562nm that is nearly linear with increasing protein concentrations over a broad working range (20-2000µg/mL). The BCA method is not a true end-point method; that is, the final colour continues to develop. However, following incubation, the rate of continued colour development is sufficiently slow to allow large numbers of samples to be assayed together. The macromolecular structure of protein, the number of peptide bonds and the presence of four particular amino acids (cysteine, cystine, tryptophan and tyrosine) are reported to be responsible for colour

formation with BCA. Studies with di-, tri- and tetra peptides suggest that the extent of colour formation is caused by more than the mere sum of individual colour producing functional groups. Accordingly, protein concentrations generally are determined and reported with reference to standards of a common protein, such as bovine serum albumin (BSA). A series of dilutions of known concentration are prepared from the protein and assayed alongside the unknown(s) before the concentration of each unknown is determined based on the standard curve.

After being equilibrated in PBS at RT overnight, samples with a defined size (4.0 cm^2) were immersed in a freshly prepared BSA solution (3 mg/ ml, 1 ml per sample). Adsorptions were allowed to proceed at RT overnight under gentle shaking. The samples were then rinsed with PBS and treated with 1% sodium dodecyl sulphate (SDS) (1 ml per sample) for 20 min to remove the adsorbed protein. The amount of adsorbed protein was quantified using a Micro BCA protein assay kit (Thermo Scientific, Australia). Figure 2.5 shows the schematic stages of protein assay. The surfaces of PDMS were treated by FITC labeled BSA in PBS at 37°C for 1h, and washed by PBS. The amount of protein adsorption was measured by the fluorescence intensity using confocal microscopy.

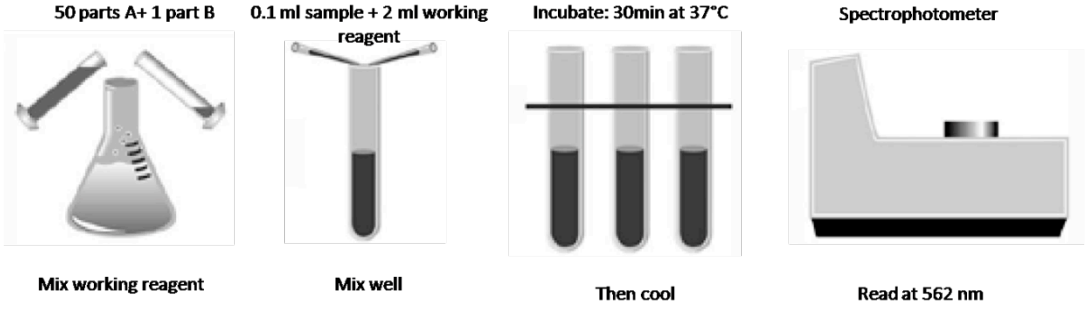

Figure (2.5): Protein adsorption assay procedure summary [558]

2.1.3.4 Fourier Transform Infrared spectroscopy (ATR-FTIR)

FTIR is a chemical analytical technique for identifying the functional groups on the surface of materials by measuring the infrared intensity versus wavelength (wavenumber) of light. This technique uses infrared radiation to determine the chemical functionalities present in a sample. By directing an infrared (IR) beam to the sample, chemical bonds stretch, contract, and bend. As a result, infrared radiation will absorb in specific wave number based on the type of surface functional groups. Attenuated total reflectance (ATR) FTIR is used for surface analysis of soft samples and liquids. In this method, the sample is placed on top of the blue crystal and the IR beam passes a few micron into the sample. For a better result, there should be a good contact between the sample and crystal. Despite a relatively deep sampling depth of ATR-FTIR, it does not require ultra high vacuum conditions, as

do XPS and EDS, and an analysis can therefore be conducted in less than ten minutes[559]. Figure 2.6 shows the schematic concept of ATR-FTIR system.

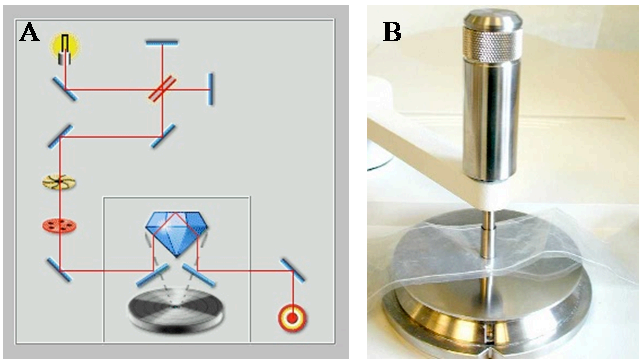

Figure (2.6): The basic ATR-FTIR concept (A), equipment to push the sample on to the crystal (B)

2.1.4 Cell handling and protocols

2.1.4.1 Cell lines and reagents

Feeder free murine Oct4B2 ES (129/Sv) cells containing the Oct4-GFP-IRES-puromycin and hygromycin resistance cassettes were used. Oct4 drove the expression of GFP, hence the EGFP expression was an indicator of cell pluripotency. ES cell medium was prepared by supplementing Dulbecco's modified Eagle medium [cat # 11995, Gibco] with 10% FBS (JRH Biosciences, Australia), 1% non-essential amino acids (NEAA) [cat#11140-050, Invitrogen], 1% GlutaMAX™ [cat# 35050061, Invitrogen], 0.5% penicillin-streptomycin [cat# 15070-063, Invitrogen], 0.1mMβ-mercaptoethanol [cat# 21985-023, Invitrogen], and 1,000 U/ml ESGRO leukemia inhibitory factor (mLIF, Chemicon, Australia). Medium was 0.22um filter sterilized and stored at 4 C for up to a fortnight. EBs were cultured in differentiation medium that is without LIF. mESC expansion medium consisted of high glucose DMEM (cat#11995, Gibco) supplemented with 10% FBS (JRH Biosciences, Australia), 1% non-essential amino acids, 1% GlutaMAX™, 0.5% penicillin-streptomycin, 0.1 mMβ-mercaptoethanol, Tryple^{tm} express (cat#12605, Gibco), and 1,000 U/ml ESGRO leukemia inhibitory factor (mLIF, Chemicon, Australia). An MDA-MB-231 cell line was also used as a model of study. The MDA-MB-231 human breast cancer cell with epithelial-like morphology was isolated as one of a series of breast tumour lines from a 50 year old patient in 1973. This type of cancer cell phenotypically is a spindle shaped cell. MDA-MB-231 cells were maintained

in high glucose DMEM (cat#11965, Gibco) supplemented with 10% fetal bovine serum (FBS), and 1% penicillin–streptomycin at 37°C in a humidified 5% CO_2 incubator [560].

2.1.4.2 Cell attachment and growth

ES cells were plated at a density of 2.5×10^4 cells/cm^2 on gelatinized plates. A 0.1% gelatin solution was prepared by diluting gelatin 2% Solution Type B: From Bovine Skin (Sigma, cat# G1393) to 0.1% using PBS. The gelatin solution was then sterilized through 0.22 µm PVDF filter (cat# SLGV033RS, Millipore) and stored at 4°C fridge. A10 cm petri dish was used for maintaining mES cells. For coating the surface of the petri dish, 5.0 mL of 0.1% gelatin solution was used. The petri dish was then placed inside the incubator for at least 30 min. The gelatin was then removed and 10 ml of medium was added to the petri dish. Unless otherwise stated, all cell handling protocols were conducted in a sterile biological safety cabinet using aseptic techniques. All mES and cancer cell cultures were cultured in a humidified, 37°C and 5% C0 2 incubator. In the case of cancer cells, there is no need to use the gelatinized dish. The rest is similar to the stem cell.

2.1.4.3 Leukemia Inhibitory Factor

The maintenance medium (for stem cells) was also supplemented with murine Leukemia Inhibitory Factor (mLIF, Chemicon, Australia) at 1000 U/ml to maintain the undifferentiated state of mES cells. The working dilution of LIF was 10^6 U/ml in high glucose DMEM (11995, Gibco). This working dilution was stored at 4°C in sterile microcentrifuge tubes and added to the mES cell maintenance medium prior to use.

2.1.4.4 Thawing cells

A gelatin-coated dish was prepared and kept inside the incubator before thawing cells. The maintenance media was also warmed up prior to thawing cells. The 2 ml cryogenic vial containing the desired cells from the liquid nitrogen tank was removed and quickly was submerged in a 37°C water bath. Care was taken to avoid the water level reaching the lid of the vial, to prevent contamination. The vial was thawed rapidly. The outer surfaces of the vial were wiped with a Kim Wipe soaked in 70% ethanol, and the vial was quickly moved into a sterile biological safety cabinet. The content of vial was added drop wise into 9 ml of maintenance medium (in a 15 ml falcon tube). The falcon tube was sealed and centrifuged at 1200 rpm for 2 min. Following centrifugation, the supernatant was aspirated out, leaving the cell pellet in the Falcon tube. One ml of pre-warmed

maintenance medium was added to the falcon tube to resuspend the cell pellet. The contents of the Falcon tube were added to the 10 cm petri dish with 9 ml of medium, and the dish was returned to the humidified incubator. The same protocol was used for thawing cancer cells, except cancer cells do not need gelatinization of dish before use. The thawing protocol is the same for cancer cells except using cancer cell medium.

2.1.4.5 Cryopreservation

After centrifugation of cell suspension, the supernatant was discarded and the cell pellet was resuspended in 1.0 ml of a freezing medium, which consisted of 90% FBS and 10% dimethylsulfoxide (DMSO, Sigma, cat# D-5879). The freezing medium was filter sterilized prior to use, using a 0.22 µm syringe filter. Cells stocks were prepared in 1.5ml cryovials (Nunc, Denmark) and slowly frozen in a cryo freezing container "Mr Frosty" containing isopropanol (BDH) in a -80 freezer overnight. For long-term storage, vials were transferred to liquid nitrogen tanks.

2.1.4.6 Cell counting

Cells were tryptinized into single cells and the cell density was assessed by cell counts a haemocytometer and the trypan blue (Sigma, cat# T8154) method. Around 15 µl of cell suspension were taken out and injected into the chamber of the haemocytometer. Trypan blue and 1x PBS were added to each sample at a 1:2 ratio. Non viable cells turn blue. The number of viable cells in each of the four corner squares was counted. The mean number of the total viable cells per four corner squares was calculated. The concentration per ml of vial cells was calculated using the following formula:

$$C_1 = (N \times tb \times 10^4)/4$$

N = total viable cell count of four corner squares, tb = correction for the trypan blue dilution (counting dilution was 1/tb), 1/4 = correction to give mean cells per corner square, 10^4 = conversion factor for counting chamber, C_1 = initial cell concentration per ml. Figure 2.7 shows the Cell counting using a haemocytometer.

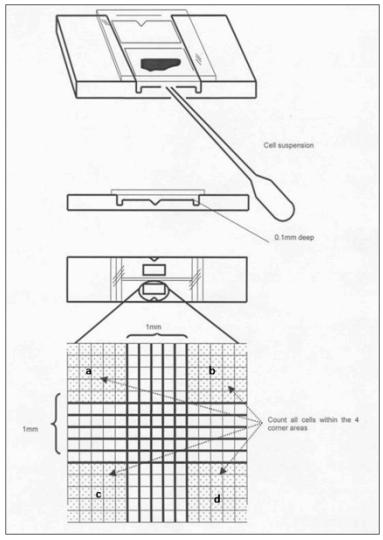

Figure (2.7): Cell counting using a haemocytometer

2.1.4.7 Cell viability assay

CellTitre-Glu^{R} Luminescent cell viability assay (Promega) is an assay that measures ATP levels. ATP is indicative of the number of metabolically active cells in culture. This cell viability assay was conducted according to the manufacturer's instructions. Cells (including EBs) were collected from inside the hydrogel or low suspension well plates. A volume of CellTitre-Glu^{R} equal to the volume of cell culture medium was added. The contents were manually mixed for 2 mins to induce cell lysis. After 5 min incubation time at RT to stabilize the luminescent signal, the cell solutions were seeded in a white opaque-walled 96-multiwell assay plate. Control wells readout contained medium without cells for background luminescence. The plate was analysed at the appropriate time points by a stable glow-type luminescent signal on a Fluostar Optima (BMG Labtech, Australia).

2.1.4.8 Passaging of mouse ES cells

Passaging by trypsinization was done when cells reached around 70% confluency. After aspiration of the culture medium, a wash with DPBS was given. A sufficient amount of Tryple was added to cover the entire dish surface and left in the incubator at 37°C for minutes. Tryple was inactivated by addition of ES media at 2 times the volume of Tryple and the entire cell suspension was transferred to a 15 ml centrifugation tube. The cell suspension was centrifuged for 5 mins at 400 g (Eppendorf Centrifuge 5702), the supernant was aspirated and the cell pellet was resuspended in appropriate amount of ES medium, counted and replated at an appropriate dilution.

2.1.4.9 Culturing cells on PDMS modified surfaces

For PDMS experiments, cells were collected from the plate with Tryple after reaching 70-80% confluence. MDA-MB-231 and Oct4b2 cell suspensions were plated on different type of PDMS substrates at densities of 80×10^3 and 40×10^3 cell/cm^2, respectively. Before seeding cells, all substrates were sterilized in 70% ethanol overnight followed by rinsing with sterile PBS. Cell proliferation was calculated at different time points by counting the number of viable cells.

2.1.4.10 Culturing cells in PDMS microchannel

The PDMS microchannels were sterilized using a 30 minute ultraviolet (UV) light treatment. Prior to cell seeding, all substrates were sterilized in 70% ethanol overnight followed by rinsing with sterile PBS. Channels were then loaded with the desired density of cell solution using a syringe, and a drop of medium was placed in the inlet and outlet ports to reduce evaporation and the risk of contamination. The microchannel was placed in a 37°C, 5% CO_2 incubator. The cells were cultured for four days in the microchannels, and their growth was monitored over this period. To avoid medium evaporation inside the microchannel, every 5-6 hours, two drops of medium were placed in the inlet and outlet ports.

2.1.4.11 Immunocytochemistry

After 4 days in culture, the MDA.MB 231 breast cancer cells were stained using a fluorescent dye (Calcein^{AM}) for visualization of viable of cells inside microchannels.

Nuclei were stained with Hoechst or DAPI (Invitrogen, 1:1000dilution) for 5 minutes at room temperature, followed by three washes with PBS. The nucleus of cells was stained with DAPI, for 5min. Cytoskeleton protein F-actin was examined with Texas Red -X phalloidin. Cells grown on modified and native PDMS surfaces were fixed using 4% formaldehyde for 20 min at RT and washed 3 times with 1 PBS buffer, permeated with 0.1% Triton X-100-PBS for 2 min, and washed with PBS. The samples were further blocked by incubating with 1% bovine serum albumin in PBS (BSA–PBS) for 15 min, followed by Texas Red-X phalloidin (1/1000 in 1% BSA–PBS) staining for 1 hour.

For immunostaining, we examined Nkx2.5 as a cardiac transcription factor and myofilament protein gene such as cardiac troponin T (cTnT). Nkx-2.5, which is also designated cardiac specific homeobox protein (Csx), is a homeodomain-containing nuclear transcription protein of the Nkx-2 gene family. Nkx-2.5 is essential for normal cardiovascular development. Troponin T is a thin filament regulatory protein of striated muscle that binds to troponin C and I to tropomyosin and is required for calcium-

dependent ATPase activity of myofibrillar proteins. It is important in proper muscle function and myofibril formation.

Cells were fixed in 4% paraformaldehyde for 30 min and washed three times with 1% BSA in DPBS. For NKx2.5 (Sc-14033, Santa Cruz) and cTnT immunostaining (ab10214, abcam), fixed cells were incubated with blocking solution (5% goat serum, 1% BSA in DPBS) for 1 h at room temperature . Cells were then incubated overnight with the primary antibodies diluted (1:500) in blocking solution at 4°C. Next, cells were washed three times with 1% BSA in DPBS and then incubated at room temperature for 1 h with secondary antibodies (goat PAb to RbIgG Alexa 594, goat anti-mouse Alexa 594, Invitrogen Australia) at a concentration of 1:400 in blocking solution. Cells were washed three times with 1% BSA in DPBS for 10min. Nuclei were counterstained with Hoechst (1µg/ml, Sigma) dye. For determining the expression of three germ layers, Nestin (MAB 353, Ectoderm marker), Brachyury (ab20680, Mesoderm marker) and Foxa2 (SC-6554, Endoderm marker) were selected as primary antibodies. Fixed cells were incubated for 1 h at room temperature with blocking solution [(5% goat serum (for Nestin and Brachyury), 1% BSA in DPBS and 5% donkey serum (for Foxa2), 1% BSA in DPBS)]. Cells were then incubated overnight with the primary antibodies diluted (1:1000) in blocking solution at 4°C. Next, cells were washed three times with 1% BSA in DPBS and then incubated at room temperature for 1h with appropriate secondary antibodies (for Nestin goat anti-mouse, goat anti-rabbit for Brachyury and for Foxa2 donkey anti-goat IgG Alexa-Fluor 594, Invitrogen Australia) at a concentration of (1:400) in appropriate blocking solution.

2.1.4.12 Cell Imaging

Fluorescent and phase-contrast microscopy

Fluorescent and transmitted microscopy was performed with optical and epifluorescence microscopy (Olympus 1X70 microscope).

2.1.4.1.1 Confocal Microscopy

Observation of EBs inside the hydrogel, and also stained CCSs in marble was done using laser scanning confocal microscopy (LSCM, Nikon A1Rsi, Nikon Instruments INC., NY, USA.). The captured images were converted to grayscale using ImageJ for further image analysis.

2.1.4.1.2 Scanning Electron Microscopy

For observation of EBs inside scaffolds and the surface and cross-sectional morphologies of the scaffolds as well, gels were fixed for 30 min in 4% paraformaldehyde. The samples were then quickly soaked in liquid nitrogen and kept at-80^{0}C overnight. The samples were then freeze dried for 72 hr. The freeze-dried samples were sputter-coated with platinum-gold alloy and examined using JEOL JSM-7001F FEG SEM (Japan). An acceleration voltage of 5 kV was used and images were obtained at different magnifications.

2.1.5 Molecular biology

2.1.5.1 Reverse transcription polymerase chain reaction (RT-PCR)

Samples used for RNA extraction were snap frozen using dry ice and stored at -80°C. RNA extraction was performed using the RNeasy kit (Qiagen) according to manufacturer's instructions. Briefly, cells were homogenised in lysis buffer and 70% ethanol added to promote selective binding of RNA to the RNeasy membrane. Contaminants were eliminated by successive washes through the RNeasy membrane column. RNA was eluted by the addition of RNase free water and stored at -20°C. The amount and purity of extracted RNA was measured by absorbance at 260/280 nM on a nanodrop ND 1000 Spectrophotometer (Nanodrop^{TM}, ThermoScientific). 1 µg of RNA was used for subsequent cDNA generation. Total RNA was first treated with RQ1 DNase at 37°C for 30 mins to remove contaminating gemonic DNA. DNase treatment was stopped by the addition of the stop buffer and incubated at 65°C for 1 min. To further exclude the possibility of genomic DNA contamination, control reactions without reverse transcriptase enzyme (RT-) were concluded in parallel. Next, random primers, RNase out and MQ water were added to the reverse transcriptase (RT) reaction and incubated at 65°C for 5 mins. The RT reaction was cooled on ice for 5 mins and then Superscript buffer, 0.1 mM dithioreitol (DTT), 10 mM dNTP mix and Superscript III reverse transcriptase added. This RT reaction was incubated at 50°C for 50 mins and the enzyme subsequently inactivated by incubating the mixture at 37°C for 20 mins. cDNA (complementary DNA) was stored at -20°C and 1-2 µg was used for subsequent PCR reactions.

2.1.5.2 Real time reverse transcription polymerase chain reaction (RT-qPCR)

Real-time PCR analysis was performed on the 7900HT Fast Real-Time PCR system (Applied Biosystems) at standard reaction conditions using Power SYBR Green PCR Master Mix (Applied Biosystems) in triplicate for each sample and each gene.

A PCR master mix was prepared in 1.5-ml microcentrifuge tubes. This master mix contained reverse and forward primers, H_2O and Syber green in a 10 µl final volume. 9 µl of the PCR mix above was added into individual wells on a 384-well plate. 1 µl of each cDNA sample was added to separate wells in the plate. And the plate was subjected to the following cycling. Briefly, after a 2 min denaturation at 95°C, 35 cycles carried out at 95°C for 15 s, 58°C for 30 s and 72°C for 30 s following by a dissociation stage. Relative mRNA levels were calculated using the ΔΔCT method and were analysed using SDS Version 2.4.1 software. Primers sequences were obtained from the online NCBI Primer-Blast databank as depicted in Table 2.1 below. The β-actin was used as an internal control.

Table (2.1): PCR primer sequences and the NCBI accession numbers for the corresponding genes.

Gene Name	Forward/ Reverse (5'→3')	NCBI accession no.
Flk-1	GGCGGTGGTGACAGTATCTT/CTCGGTGATGTACACGATGC	NM_010612.2
Nkx2.5	ACACCCACGCCTTTCTCAGTCAAA/CGACAGGTACCGCTGTTGCTTGAA	NM_008700.2
Gata4	TCTCACTATGGGCACAGCAG/GCGATGTCTGAGTGACAGGA	NM_008092
MLC2a	TCAGCTGCATTGACCAGAAC/AAGACGGTGAAGTTGATGGG	NM_022879.2
MLC2v	AAAGAGGCTCCAGGTCCAAT/CCTCTCTGCTTGTGTGGTCA	NM_010861.3
α-actinin	ATGAGGATTGGCTGCTTT/ TGTTCCACCCGGTCTTG	NM_013456
β-actin	CACCACACCTTCTACAATGAGC/TCGTAGATGGGCACAGTGTGGG	NM_007393.3
Nestin	TCTGGAAGTCAACAGAGGTGG/ACGGAGTCTTGTTCACCTGC	NM_016701.3
Brachyury	CATGTACTCTTTCTTGCTGG/GGTCTCGGGAAAGCAGTGGC	NM_009309.2
Foxa2	TGGTCACTGGGGACAAGGGAA/GCAACAACAGCAATAGAGAAC	NM_010446.2

2.1.6 Embryoid body formation

2.1.6.1 Inside liquid marble

In a typical cell spheroid formation experiment, 300 µL drops of medium containing Hep G2 cells or ESCs (~10^4 cells/marble) were placed onto a Poly Tetrafluoroethylene (PTFE, 35 µm or 100 µm

particle size) powder bed inside a petri dish (60 mm diameter) using a micropipette. The liquid drops were then gently rolled on the powder bed until they were covered completely with powder particles to form liquid marbles. This Petri dish containing the liquid marbles on a powder bed was then placed in a larger Petri dish (10 cm), half filled with water or PBS, to provide an atmosphere saturated with water vapour to suppress the evaporation of the medium in the liquid marbles. This experimental setup minimises the problem of water core evaporation from liquid marbles reported in the literature. The petri dish was then capped and placed inside an incubator to provide the cells with suitable growth conditions. In order to monitor cell aggregation, the liquid core of a marble was extracted out of the marble using a micropipette for confocal imaging. Figure 2.8 shows the steps in preparation of liquid marble bioreactor.

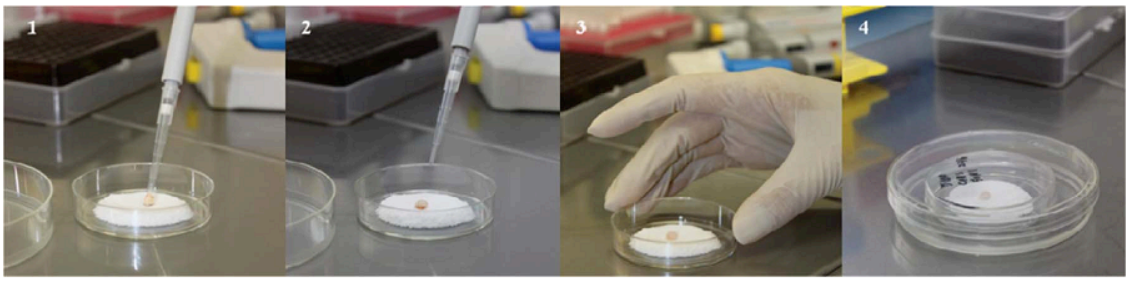

Figure (2.8): Steps towards the formation o f liquid marbles containing stem cells.

2.1.6.2 Inside porous scaffold

Prior to cell seeding, the scaffolds were first soaked in PBS overnight and then sterilized with 70% ethanol for 5 hr by changing ethanol three times. Each scaffold was then rinsed with PBS for 5 hr. PBS was then removed from the scaffold, and the well plate kept inside the hood overnight. The next day, 0.1% gelatin was added and incubated for 24 hr for better cell attachment before cell seeding. For EB formation, the undifferentiated ESCs were collected, counted and were resuspended in DMEM medium supplemented with 10% FBS, 1% NEAA, 1% mM L-glutamine, 1% penicillin-streptomycin (EB formation medium). It is worth noting that EB-forming medium does not have LIF. For EB formation, 2.5×10^5 cells in approximately 40 µl of EB medium was then added drop-wise on top of the hydrogel surface in each 48-well plate. Immediately after cell seeding, the cell-seeded hydrogel was placed in the incubator in 5% CO_2 incubator at 37°C for 15-20 min to allow swelling equilibration. Fresh medium was then added to cover the scaffolds.

2.1.7 Reference

1. Vacanti, C.A., *The history of tissue engineering.* Journal of Cellular and Molecular Medicine, 2006. **10**(3): p. 569-576.
2. Alsberg, E., et al., *Engineering growing tissues.* Proceedings of the National Academy of Sciences of the United States of America, 2002. **99**(19): p. 12025-12030.
3. Bisceglie V., *Uber die antineoplasticscshe Immunitat; heterologe Einpflanzung von Tumoren in Huhner-embryonen. Z Krebsforsch*1933. **40**: p. 122–40.
4. Bell, E., et al., *Living tissue formed in vitro and accepted as skin-equivalent tissue of full thickness.* Science, 1981. **211**(4486): p. 1052-1054.
5. Burke, J.F., et al., *Successful use of a physiologically acceptable artificial skin in the treatment of extensive burn injury.* Annals of Surgery, 1981. **194**(4): p. 413-428.
6. Vacanti, J.P., et al., *Selective cell trasplantation using bioabsorbable atrificial polymers as matrices* Journal of Pediatric Surgery, 1988. **23**(1): p. 3-9.
7. Langer, R. and J.P. Vacanti, *Tissue engineering* Science, 1993. **260**(5110): p. 920-926.
8. Griffith, L.G. and G. Naughton, *Tissue engineering - Current challenges and expanding opportunities.* Science, 2002. **295**(5557): p. 1009.
9. Khademhosseini, A., J.P. Vacanti, and R. Langer, *Progress in tissue engineering* Scientific American, 2009. **300**(5): p. 64-+.
10. Macchiarini, P., et al., *Clinical transplantation of a tissue-engineered airway.* Lancet, 2008. **372**(9655): p. 2023-2030.
11. Atala, A., et al., *Tissue-engineered autologous bladders for patients needing cystoplasty.* Lancet, 2006. **367**(9518): p. 1241-1246.
12. Ryu, W., et al., *Microfabrication technology of biodegradable polymers for interconnecting microstructures.* Journal of Microelectromechanical Systems, 2006. **15**(6): p. 1457-1465.
13. Whitesides, G.M., et al., *Soft lithography in biology and biochemistry.* Annual Review of Biomedical Engineering, 2001. **3**: p. 335-373.
14. Norbert Pallua and Christoph V. Suschek, *Tissue Engineering From Lab to Clinic*2011: Springer.
15. Lavik, E. and R. Langer, *Tissue engineering: current state and perspectives.* Applied Microbiology and Biotechnology, 2004. **65**(1): p. 1-8.
16. Cascalho, M. and J.L. Platt, *New technologies for organ replacement and augmentation.* Mayo Clinic Proceedings, 2005. **80**(3): p. 370-378.
17. Jungebluth, P., et al., *Tissue-Engineered Airway: A Regenerative Solution.* Clinical Pharmacology & Therapeutics, 2012. **91**(1): p. 81-93.
18. Thomson, J.A., et al., *Embryonic stem cell lines derived from human blastocysts.* Science, 1998. **282**(5391): p. 1145-1147.
19. Reubinoff, B.E., et al., *Erratum: Embryonic stem cell lines from human blastocysts: Somatic differentiation in vitro (Nature Biotechnology) (April 2000) (402)).* Nature Biotechnology, 2000. **18**(5): p. 559.
20. Fiona M. Watt and Ryan R. Driskell, *The therapeutic potential of stem cells.* Phil. Trans. R. Soc. B, 2010. **365**: p. 155–163.
21. Lou, Y.J. and X.G. Liang, *Embryonic stem cell application in drug discovery.* Acta Pharmacologica Sinica, 2011. **32**(2): p. 152-159.
22. Pouton, C.W. and J.M. Haynes, *Pharmaceutical applications of embryonic stem cells.* Advanced Drug Delivery Reviews, 2005. **57**(13): p. 1918-1934.
23. Gorba, T. and T.E. Allsopp, *Pharmacological potential of embryonic stem cells.* Pharmacological Research, 2003. **47**(4): p. 269-278.
24. Zandstra, P.W., *Stem cell bioengineering* Annu. Rev. Biomed. Eng., 2001. **3**: p. 275-305.

25. Pillow, R.P., et al., *Treatment of bone- marrow failure by isogeneic marrow infusion* New England Journal of Medicine, 1966. **275**(2): p. 94-&.
26. Presnell, S.C., B. Petersen, and M. Heidaran, *Stem cells in adult tissues.* Seminars in Cell & Developmental Biology, 2002. **13**(5): p. 369-376.
27. Hodgkinson, T., X.-F. Yuan, and A. Bayat, *Adult stem cells in tissue engineering.* Expert Review of Medical Devices, 2009. **6**(6): p. 621-640.
28. Lagasse, E., et al., *Purified hematopoietic stem cells can differentiate into hepatocytes in vivo.* Nature Medicine, 2000. **6**(11): p. 1229-1234.
29. Bittner, R.E., et al., *Recruitment of bone-marrow-derived cells by skeletal and cardiac muscle in adult dystrophic mdx mice.* Anatomy and Embryology, 1999. **199**(5): p. 391-396.
30. Orlic, D., et al., *Transplanted adult bone marrow cells repair myocardial infarcts in mice*, in *Hematopoietic Stem Cells 2000 Basic and Clinical Sciences*, D. Orlic, et al., Editors. 2001. p. 221-230.
31. Krause, D.S., et al., *Multi-organ, multi-lineage engraftment by a single bone marrow-derived stem cell.* Cell, 2001. **105**(3): p. 369-377.
32. Puri, M.C. and A. Nagy, *Concise Review: Embryonic Stem Cells Versus Induced Pluripotent Stem Cells: The Game Is On.* Stem Cells, 2012. **30**(1): p. 10-14.
33. Evans, M.J. and M.H. Kaufman, *Establishment in culture of pluripotential cells from mouse embryos* Nature, 1981. **292**(5819): p. 154-156.
34. Martin, G.R., *Isolation of a pluripotent cell-line from early mouse embryos cultured in medium conditioned by teratocarcinoma stem-cells* Proceedings of the National Academy of Sciences of the United States of America-Biological Sciences, 1981. **78**(12): p. 7634-7638.
35. Fong, C.Y., et al., *Blastocyst transfer after enzymatic treatment of the zona pellucida: improving in-vitro fertilization and understanding implantation.* Human Reproduction, 1998. **13**(10): p. 2926-2932.
36. *Stem cell information* National Institues of Health, 2001.
37. Ulloa-Montoya, F., C.M. Verfaillie, and W.S. Hu, *Culture systems for pluripotent stem cells.* Journal of Bioscience and Bioengineering, 2005. **100**(1): p. 12-27.
38. Palacios, R., E. Golunski, and J. Samaridis, *In vitro generation of hematopoietic stem cells from an embryonic stem cell line.* Proceedings of the National Academy of Sciences of the United States of America, 1995. **92**(16): p. 7530-7534.
39. Wiles, M.V. and G. Keller, *Multiple hematopoitic lineages develop from embryonic stem (Es) cells in culture* Development, 1991. **111**(2): p. 259-&.
40. Wang, R., R. Clark, and V.L. Bautch, *Embryonic stem cell-derived cystic embryoid bodies form vascular channels: An in vitro model of blood vessel development.* Development, 1992. **114**(2): p. 303-316.
41. Mummery, C., et al., *Cardiomyocyte differentiation of mouse and human embryonic stem cells.* Journal of Anatomy, 2002. **200**(3): p. 233-242.
42. Maltsev, V.A., et al., *Cardiomyocytes differentiation in vitro from embryonic stem-cells developmentally express cardiac-specific genes and ionic currents* Circulation Research, 1994. **75**(2): p. 233-244.
43. Bain, G., et al., *Embryonic stem cells express neuronal properties in vitro.* Developmental Biology, 1995. **168**(2): p. 342-357.
44. Smith, A.G., *Embryo-derived stem cells: Of mice and men.* Annual Review of Cell and Developmental Biology, 2001. **17**: p. 435-462.
45. Stojkovic, M., et al., *Derivation, growth and applications of human embryonic stem cells.* Reproduction, 2004. **128**(3): p. 259-267.
46. Thomson, J.A., et al., *Isolation of a primate embryonic stem-cell line* Proceedings of the National Academy of Sciences of the United States of America, 1995. **92**(17): p. 7844-7848.
47. Laslett, A.L., A.A. Filipczyk, and M.F. Pera, *Characterization and culture of human embryonic stem cells.* Trends in Cardiovascular Medicine, 2003. **13**(7): p. 295-301.
48. Martin, M.J., et al., *Human embryonic stem cells express an immunogenic nonhuman sialic acid.* Nature Medicine, 2005. **11**(2): p. 228-232.

49. Xu, R.H., et al., *Basic FGF and suppression of BMP signaling sustain undifferentiated proliferation of human ES cells.* Nature Methods, 2005. **2**(3): p. 185-190.
50. Xu, C.H., et al., *Feeder-free growth of undifferentiated human embryonic stem cells.* Nature Biotechnology, 2001. **19**(10): p. 971-974.
51. Sato, N., et al., *Maintenance of pluripotency in human and mouse embryonic stem cells through activation of Wnt signaling by a pharmacological GSK-3-specific inhibitor.* Nature Medicine, 2004. **10**(1): p. 55-63.
52. Wong, C.-W., et al., *Kruppel-Like Transcription Factor 4 Contributes to Maintenance of Telomerase Activity in Stem Cells.* Stem Cells, 2010. **28**(9): p. 1510-1517.
53. Ehrnhoefer, D.E., et al., *Mouse models of Huntington disease: variations on a theme.* Disease Models & Mechanisms, 2009. **2**(3-4): p. 123-129.
54. Peters, L.L., et al., *The mouse as a model for human biology: a resource guide for complex trait analysis.* Nature Reviews Genetics, 2007. **8**(1): p. 58-69.
55. Pauklin, S., R.A. Pedersen, and L. Vallier, *Mouse pluripotent stem cells at a glance.* Journal of Cell Science, 2011. **124**(22): p. 3727-3732.
56. Lumelsky, N., et al., *Differentiation of embryonic stem cells to insulin-secreting structures similar to pancreatic islets.* Science, 2001. **292**(5520): p. 1389-1394.
57. Studer, L., V. Tabar, and R.D.G. McKay, *Transplantation of expanded mesencephalic precursors leads to recovery in parkinsonian rats.* Nature Neuroscience, 1998. **1**(4): p. 290-295.
58. McDonald, J.W., et al., *Transplanted embryonic stem cells survive, differentiate and promote recovery in injured rat spinal cord.* Nature Medicine, 1999. **5**(12): p. 1410-1412.
59. Guasch, G. and E. Fuchs, *Mice in the world of stem cell biology.* Nature Genetics, 2005. **37**(11): p. 1201-1206.
60. Bjorklund, L.M., et al., *Embryonic stem cells develop into functional dopaminergic neurons after transplantation in a Parkinson rat model.* Proceedings of the National Academy of Sciences of the United States of America, 2002. **99**(4): p. 2344-2349.
61. Aboody, K., et al., *Translating Stem Cell Studies to the Clinic for CNS Repair: Current State of the Art and the Need for a Rosetta Stone.* Neuron, 2011. **70**(4): p. 597-613.
62. Dawson, T.M. and V.L. Dawson, *Neuroprotective and neurorestorative strategies for Parkinson's disease.* Nature Neuroscience, 2002. **5**: p. 1058-1061.
63. Navarro-Alvarez, N., A. Soto-Gutierrez, and N. Kobayashi, *Stem Cell Research and Therapy for Liver Disease.* Current Stem Cell Research & Therapy, 2009. **4**(2): p. 141-146.
64. Dinsmore, J., et al., *Embryonic stem cells differentiated in vitro as a novel source of cells for transplantation.* Cell Transplantation, 1996. **5**(2): p. 131-143.
65. Liu, S., et al., *Embryonic stem cells differentiate into oligodendrocytes and myelinate in culture and after spinal cord transplantation.* Proceedings of the National Academy of Sciences of the United States of America, 2000. **97**(11): p. 6126-6131.
66. Blyszczuk, P., et al., *Expression of Pax4 in embryonic stem cells promotes differentiation of nestin-positive progenitor and insulin-producing cells.* Proceedings of the National Academy of Sciences of the United States of America, 2003. **100**(3): p. 998-1003.
67. Shim, J.H., et al., *Directed differentiation of human embryonic stem cells towards a pancreatic cell fate.* Diabetologia, 2007. **50**(6): p. 1228-1238.
68. Wakitani, S., et al., *Autologous bone marrow stromal cell transplantation for repair of full-thickness articular cartilage defects in human patellae: Two case reports.* Cell Transplantation, 2004. **13**(5): p. 595-600.
69. Cohen, I., et al., *Use of a novel joint-simulating culture system to grow organized ex-vivo three-dimensional cartilage-like constructs from embryonic epiphyseal cells.* The Iowa orthopaedic journal, 2005. **25**: p. 102-7.
70. Ikeda, T., et al., *The combination of SOX5, SOX6, and SOX9 (the SOX trio) provides signals sufficient for induction of permanent cartilage.* Arthritis and Rheumatism, 2004. **50**(11): p. 3561-3573.

71. Ohba, S., et al., *Identification of a potent combination of osteogenic genes for bone regeneration using embryonic stem (ES) cell-based sensor.* Faseb Journal, 2007. **21**(8): p. 1777-1787.
72. Sinz, M.W. and S. Kim, *Stem cells, immortalized cells and primary cells in ADMET assays.* Drug Discovery Today: Technologies, 2006. **3**(1): p. 79-85.
73. Rohwedel, J., et al., *Embryonic stem cells as an in vitro model for mutagenicity, cytotoxicity and embryotoxicity studies: present state and future prospects.* Toxicology in Vitro, 2001. **15**(6): p. 741-753.
74. Zhang, F. and K.B.S. Pasumarthi, *Embryonic Stem Cell Transplantation Promise and Progress in the Treatment of Heart Disease.* Biodrugs, 2008. **22**(6): p. 361-374.
75. Maltsev, V.A., et al., E*mbryonic stem cells differentiate in vitro into cardiomyocytes representing sigusnodal, atrial and ventricular cell types.* Mechanisms of Development, 1993. **44**(1): p. 41-50.
76. Maltsev, V.A., et al., *Embryonic stem-cell differentiate in vitro into cardiomyocytes representing sinusnodal, atrial and ventricular cell types.* Mechanisms of Development, 1993. **44**(1): p. 41-50.
77. Klug, M.G., et al., *Genetically selected cardiomyocytes from differentiating embryonic stem cells form stable intracardiac grafts.* Journal of Clinical Investigation, 1996. **98**(1): p. 216-224.
78. Wobus, A.M., *Potential of embryonic stem cells.* Molecular aspects of medicine, 2001. **22**(3): p. 149-64.
79. Kehat, I., et al., *Human embryonic stem cells can differentiate into myocytes with structural and functional properties of cardiomyocytes.* Journal of Clinical Investigation, 2001. **108**(3): p. 407-414.
80. Kehat, I., et al., *Electromechanical integration of cardiomyocytes derived from human embryonic stem cells.* Nature Biotechnology, 2004. **22**(10): p. 1282-1289.
81. Laflamme, M.A., et al., *Cardiomyocytes derived from human embryonic stem cells in pro-survival factors enhance function of infarcted rat hearts.* Nature Biotechnology, 2007. **25**(9): p. 1015-1024.
82. Mauritz, C., et al., *Generation of functional murine cardiac myocytes from induced pluripotent stem cells.* Circulation, 2008. **118**(5): p. 507-517.
83. Mayhall, E.A., N. Paffett-Lugassy, and L.I. Zon, *The clinical potential of stem cells.* Current Opinion in Cell Biology, 2004. **16**(6): p. 713-720.
84. Nirmalanandhan, V.S. and G.S. Sittampalam, *Stem Cells in Drug Discovery, Tissue Engineering, and Regenerative Medicine: Emerging Opportunities and Challenges.* Journal of Biomolecular Screening, 2009. **14**(7): p. 755-768.
85. Krtolica, A., et al., *Human embryonic stem cells as a model for embryotoxicity screening.* Regenerative Medicine, 2009. **4**(3): p. 449-459.
86. Parson, A.B., *Stem cell biotech: Seeking a piece of the action.* Cell, 2008. **132**(4): p. 511-513.
87. Vazin, T. and D.V. Schaffer, *Engineering strategies to emulate the stem cell niche.* Trends in Biotechnology, 2010. **28**(3): p. 117-124.
88. Placzek, M.R., et al., *Stem cell bioprocessing: fundamentals and principles.* Journal of the Royal Society Interface, 2009. **6**(32): p. 209-232.
89. Sodian, R., et al., *Tissue-engineering bioreactors: A new combined cell-seeding and perfusion system for vascular tissue engineering.* Tissue Engineering, 2002. **8**(5): p. 863-870.
90. Zeltinger, J., et al., *Development and characterization of tissue-engineered aortic valves.* Tissue Engineering, 2001. **7**(1): p. 9-22.
91. Howard, D., et al., *Tissue engineering: strategies, stem cells and scaffolds.* Journal of Anatomy, 2008. **213**(1): p. 66-72.
92. Higuchi, A., et al., *Biomimetic Cell Culture Proteins as Extracellular Matrices for Stem Cell Differentiation.* Chemical Reviews, 2012. **112**(8): p. 4507-4540.
93. Higuchi, A., et al., *Biomaterials for the Feeder-Free Culture of Human Embryonic Stem Cells and Induced Pluripotent Stem Cells.* Chemical Reviews, 2011. **111**(5): p. 3021-3035.

94. Grinnell, F., *Cellular adhesiveness and extracellular substrata.* International review of cytology, 1978. **53**: p. 65-144.
95. Vonarbourg, A., et al., *Parameters influencing the stealthiness of colloidal drug delivery systems.* Biomaterials, 2006. **27**(24): p. 4356-4373.
96. Goddard, J.M. and J.H. Hotchkiss, *Polymer surface modification for the attachment of bioactive compounds.* Progress in Polymer Science, 2007. **32**(7): p. 698-725.
97. Kleinman, H.K., D. Philp, and M.P. Hoffman, *Role of the extracellular matrix in morphogenesis.* Current Opinion in Biotechnology, 2003. **14**(5): p. 526-532.
98. Zhang, S.G., *Fabrication of novel biomaterials through molecular self-assembly.* Nature Biotechnology, 2003. **21**(10): p. 1171-1178.
99. Kane, R.S., et al., *Patterning proteins and cells using soft lithography.* Biomaterials, 1999. **20**(23-24): p. 2363-2376.
100. Samira M. Azarina and Sean P. Paleceka, *Development of scalable culture systems for human embryonic stem cells.* Biochemical Engineering 2010. **48**: p. 378-384.
101. Jinno, S., et al., *Macrefabricated multilayer parylene-C stencils for the generation of patterned dynamic co-cultures.* Journal of Biomedical Materials Research Part A, 2008. **86A**(1): p. 278-288.
102. Ostuni, E., et al., *A survey of structure-property relationships of surfaces that resist the adsorption of protein.* Langmuir, 2001. **17**(18): p. 5605-5620.
103. Ostuni, E., et al., *Selective deposition of proteins and cells in arrays of microwells.* Langmuir, 2001. **17**(9): p. 2828-2834.
104. Ling, Y., et al., *A cell-laden microfluidic hydrogel.* Lab on a Chip, 2007. **7**(6): p. 756-762.
105. Dean, S.K., et al., *Differentiation of encapsulated embryonic stem cells after transplantation.* Transplantation, 2006. **82**(9): p. 1175-1184.
106. Murua, A., et al., *Cell microencapsulation technology: Towards clinical application.* Journal of Controlled Release, 2008. **132**(2): p. 76-83.
107. Wang, N., et al., *Alginate encapsulation technology supports embryonic stem cells differentiation into insulin-producing cells.* Journal of Biotechnology, 2009. **144**(4): p. 304-312.
108. Xing, Q., et al., *Porous biocompatible three-dimensional scaffolds of cellulose microfiber/gelatin composites for cell culture.* Acta Biomaterialia, 2010. **6**(6): p. 2132-2139.
109. Slaughter, B.V., et al., *Hydrogels in Regenerative Medicine.* Advanced Materials, 2009. **21**(32-33): p. 3307-3329.
110. Yue, Z., et al., *Preparation of three-dimensional interconnected macroporous cellulosic hydrogels for soft tissue engineering.* Biomaterials, 2010. **31**(32): p. 8141-8152.
111. Rodrigues, C.A.V., et al., *Stem cell cultivation in bioreactors.* Biotechnology Advances, 2011. **29**(6): p. 815-829.
112. Dexter, T.M., T.D. Allen, and L.G. Lajtha, *Conditions controlling the proliferation of haemopoietic stem cells in vitro.* Journal of Cellular Physiology, 1977. **91**(3): p. 335-344.
113. Bilodeau, K. and D. Mantovani, *Bioreactors for tissue engineering: Focus on mechanical constraints. A comparative review.* Tissue Engineering, 2006. **12**(8): p. 2367-2383.
114. Kasper Cornelia , Van Griensven Martijn , and Pörtner Ralf, *Bioreactor Systems for Tissue Engineering.* Advances in Biochemical Engineering/Biotechnology, 2009. **112**.
115. Eibl, R., et al., *Cell and Tissue Reaction Engineering*, 2008, Springer.
116. Portner, R., et al., *Bioreactor Design for tissue Engineering.* Journal of Bioscience and Bioengineering, 2005. **100**(3): p. 235-245.
117. T. Liu, *Expansion of hematopoietic stem/progenitor cells,.* Comprehensive Biotechnology (2nd edition), 2011. **5**: p. 389-396.
118. Serra, M., et al., *Integrating human stem cell expansion and neuronal differentiation in bioreactors.* BMC Biotechnology, 2009. **9**: p. 82.
119. Zandstra, P.W., et al., *Scalable production of embryonic stem cell-derived cardiomyocytes.* Tissue Engineering, 2003. **9**(4): p. 767-778.
120. *SKS Science.* 2013.

121. Cormier, J.T., et al., *Expansion of undifferentiated murine embryonic stem cells as aggregates in suspension culture bioreactors.* Tissue Engineering, 2006. **12**(11): p. 3233-3245.
122. zur Nieden, N.I., et al., *Embryonic stem cells remain highly pluripotent following long term expansion as aggregates in suspension bioreactors.* Journal of Biotechnology, 2007. **129**(3): p. 421-432.
123. Kehoe, D.E., et al., *Scalable Stirred-Suspension Bioreactor Culture of Human Pluripotent Stem Cells.* Tissue Engineering Part A, 2010. **16**(2): p. 405-421.
124. Fok Y.L, E. and P. Zandstra W., *Shear-controlled single-step mouse embryonic stem cell expansion and embryoid body-based differentiation.* Stem Cells, 2005. **23**(9): p. 1333-1342.
125. Schroeder, M., et al., *Differentiation and lineage selection of mouse embryonic stem cells in a stirred bench scale bioreactor with automated process control.* Biotechnology and Bioengineering, 2005. **92**(7): p. 920-933.
126. Ling-Ling, E., et al., *Enrichment of cardiomyocytes derived from mouse embryonic stem cells.* Journal of Heart and Lung Transplantation, 2006. **25**(6): p. 664-674.
127. McLeod, M., et al., *Transplantation of bioreactor-produced neural stem cells into the rodent brain.* Cell Transplantation, 2006. **15**(8-9): p. 689-697.
128. Sen, A., M.S. Kallos, and L.A. Behie, *Effects of hydrodynamics on cultures of mammalian neural stem cell aggregates in suspension bioreactors.* Industrial & Engineering Chemistry Research, 2001. **40**(23): p. 5350-5357.
129. Alfred, R., et al., *Serum-free scaled Up expansion and differentiation of murine embryonic stem cells to osteoblasts in suspension bioreactors.* Biotechnology and Bioengineering, 2010. **106**(5): p. 829-840.
130. Niebruegge, S., et al., *Generation of Human Embryonic Stem Cell-Derived Mesoderm and Cardiac Cells Using Size-Specified Aggregates in an Oxygen-Controlled Bioreactor.* Biotechnology and Bioengineering, 2009. **102**(2): p. 493-507.
131. Carrier, R.L., et al., *Cardiac tissue engineering: Cell seeding, cultivation parameters, and tissue construct characterization.* Biotechnology and Bioengineering, 1999. **64**(5): p. 580-589.
132. Gooch, K.J., et al., *Effects of mixing intensity on tissue-engineered cartilage.* Biotechnology and Bioengineering, 2001. **72**(4): p. 402-407.
133. Chisti, Y., *Hydrodynamic damage to animal cells.* Critical Reviews in Biotechnology, 2001. **21**(2): p. 67-110.
134. Zandstra, P.W., C.J. Eaves, and J.M. Piret, *Expansion of hematopoietic Progenitor cell populations in stirred suspension bioreactor of normal himan bone marrow cells.* Biotecnology, 1994. **12**: p. 909-914.
135. King, J.A. and W.M. Miller, *Bioreactor development for stem cell expansion and controlled differentiation.* Current Opinion in Chemical Biology, 2007. **11**: p. 394-398.
136. Youn, B.S., et al., *Large-scale expansion of mammary epithelial stem cell aggregates in suspension bioreactors.* Biotechnology Progress, 2005. **21**(3): p. 984-993.
137. Bauwens, C., et al., *Development of a perfusion fed bioreactor for embryonic stem cell-derived cardiomyocyte generation: Oxygen-mediated enhancement of cardiomyocyte output.* Biotechnology and Bioengineering, 2005. **90**(4): p. 452-461.
138. Dang, S.M., et al., *Controlled, scalable embryonic stem cell differentiation culture.* Stem Cells, 2004. **22**(3): p. 275-282.
139. Abranches, E., et al., *Expansion of mouse embryonic stem cells on microcarriers.* Biotechnology and Bioengineering, 2007. **96**(6): p. 1211-1221.
140. Fernandes, A.M., et al., *Mouse embryonic stem cell expansion in a microcarrier-based stirred culture system.* Journal of Biotechnology, 2007. **132**(2): p. 227-236.
141. Freed, L.E. and G. Vunjaknovakovic, *Cultivation of cell-ploymer tissue constructs in simulated microgravity* Biotechnology and Bioengineering, 1995. **46**(4): p. 306-313.
142. Begley, C.M. and S.J. Kleis, *The fluid dynamic and shear environment in the NASA/JSC rotating-wall perfused-vessel bioreactor.* Biotechnology and Bioengineering, 2000. **70**(1): p. 32-40.

143. Gerecht-Nir, S., S. Cohen, and J. Itskovitz-Eldor, *Bioreactor cultivation enhances the efficiency of human embryoid body (hEB) formation and differentiation.* Biotechnology and Bioengineering, 2004. **86**(5): p. 493-502.
144. Unsworth, B.R. and P.I. Lelkes, *Growing tissues in microgravity.* Nature Medicine, 1998. **4**(8): p. 901-907.
145. E, L.-L., et al., *Enrichment of cardiomyocytes derived from mouse embryonic stem cells.* The Journal of heart and lung transplantation : the official publication of the International Society for Heart Transplantation, 2006. **25**(6): p. 664-74.
146. Liu, Y., et al., *Ex vivo expansion of hematopoietic stem cells derived from umbilical cord blood in rotating wall vessel.* Journal of Biotechnology, 2006. **124**(3): p. 592-601.
147. Lin, H.J., et al., *Neural stem cell differentiation in a cell-collagen-bioreactor culture system.* Developmental Brain Research, 2004. **153**(2): p. 163-173.
148. Carlsson, S.I.M., et al., *Modulation of human endothelial cell behaviour in simulated microgravity.* Proceedings of the European Symposium on Life in Space for Life on Earth, 2002. **501**: p. 281-282.
149. Rhiel, M.H., et al., *On-line monitoring of human prostate cancer cells in a perfusion rotating wall vessel by near-infrared spectroscopy.* Biotechnology and Bioengineering, 2004. **86**(7): p. 852-861.
150. Turhani, D., et al., *Analysis of Cell-Seeded 3-Dimensional Bone Constructs Manufactured In Vitro With Hydroxyapatite Granules Obtained From Red Algae.* Journal of Oral and Maxillofacial Surgery, 2005. **63**(5): p. 673-681.
151. Qiu, Q.Q., P. Ducheyne, and P.S. Ayyaswamy, *3D Bone tissue engineered with bioactive microspheres in simulated microgravity.* In Vitro Cellular & Developmental Biology-Animal, 2001. **37**(3): p. 157-165.
152. Obradovic, B., et al., *Gas exchange is essential for bioreactor cultivation of tissue engineered cartilage.* Biotechnology and Bioengineering, 1999. **63**(2): p. 197-205.
153. Botchwey, E.A., et al., *Bone tissue engineering in a rotating bioreactor using a microcarrier matrix system.* Journal of Biomedical Materials Research, 2001. **55**(2): p. 242-253.
154. Ikada, Y., *Tissue Engineering: Fundamentals and Applications, Chapter 1 Scope of Tissue Engineering*, in *Interface Science and Technology*, I. Yoshito, Editor 2006, Elsevier. p. 1-89.
155. Wendt, D., et al., *Oscillating perfusion of cell suspensions through three-dimensional scaffolds enhances cell seeding efficiency and uniformity.* Biotechnology and Bioengineering, 2003. **84**(2): p. 205-214.
156. Oh, S.K.W., et al., *High density cultures of embryonic stem cells.* Biotechnology and Bioengineering, 2005. **91**(5): p. 523-533.
157. Zhao, F., et al., *Effects of oxygen transport on 3-D human mesenchymal stem cell metabolic activity in perfusion and static cultures: Experiments and mathematical model.* Biotechnology Progress, 2005. **21**: p. 1269-1280.
158. Zhao, F. and T. Ma, *Perfusion bioreactor system for human mesenchymal stem cell tissue engineering: Dynamic cell seeding and construct development.* Biotechnology and Bioengineering, 2005. **91**(4): p. 482-493.
159. Xie, Y.Z., et al., *Three-dimensional flow perfusion culture system for stem cell proliferation inside the critical-size beta-tricalcium phosphate scaffold.* Tissue Engineering, 2006. **12**(12): p. 3535-3543.
160. Zhao, F., R. Chella, and T. Ma, *Effects of shear stress on 3-D human mesenchymal stem cell construct development in a perfusion bioreactor system: Experiments and hydrodynamic modeling.* Biotechnology and Bioengineering, 2007. **96**(3): p. 584-595.
161. Dvir, T., et al., *A novel perfusion bioreactor providing a homogenous milieu for tissue regeneration.* Tissue Engineering, 2006. **12**(10): p. 2843-2852.
162. Fong, W.J., et al., *Perfusion cultures of human embryonic stem cells.* Bioprocess and Biosystems Engineering, 2005. **27**(6): p. 381-387.
163. Braccini, A., et al., *Three-dimensional perfusion culture of human bone marrow cells and generation of osteoinductive grafts.* Stem Cells, 2005. **23**(8): p. 1066-1072.

164. Palsson, B.O., et al., *Expansion of human bone marrow progenitor cells in a high cell density continuous perfusion system.* Bio/Technology, 1993. **11**(3): p. 368-372.
165. Gerlach, J.C., et al., *Dynamic 3D Culture Promotes Spontaneous Embryonic Stem Cell Differentiation In Vitro.* Tissue Engineering Part C-Methods, 2010. **16**(1): p. 115-121.
166. Gerlach, J.C., et al., *Interwoven Four-Compartment Capillary Membrane Technology for Three-Dimensional Perfusion with Decentralized Mass Exchange to Scale Up Embryonic Stem Cell Culture.* Cells Tissues Organs, 2010. **192**(1): p. 39-49.
167. Stachelscheid, H., et al., *Teratoma formation of human embryonic stem cells in three-dimensional perfusion culture bioreactors.* Journal of Tissue Engineering and Regenerative Medicine, 2012: p. n/a-n/a.
168. Ikada, Y., *Tissue Engineering: Fundamentals and Applications, Chapter 3 Basic Technologies Developed for Tissue Engineering*, in *Interface Science and Technology*, I. Yoshito, Editor 2006, Elsevier. p. 235-421.
169. Dhawan, A., R.R. Mitry, and R.D. Hughes, *Hepatocyte transplantation for liver-based metabolic disorders.* Journal of Inherited Metabolic Disease, 2006. **29**(2-3): p. 431-435.
170. Mizuno, S., F. Allemann, and J. Glowacki, *Effects of medium perfusion on matrix production by bovine chondrocytes in three-dimensional collagen sponges.* Journal of Biomedical Materials Research, 2001. **56**(3): p. 368-375.
171. Dahlin, R.L., et al., *Design of a High-Throughput Flow Perfusion Bioreactor System for Tissue Engineering.* Tissue Engineering Part C-Methods, 2012. **18**(10): p. 817-820.
172. Godara, P., C.D. McFarland, and R.E. Nordon, *Design of bioreactors for mesenchymal stem cell tissue engineering.* Journal of Chemical Technology and Biotechnology, 2008. **83**(4): p. 408-420.
173. Cabrita, G.J.M., et al., *Hematopoietic stem cells: from the bone to the bioreactor.* Trends in Biotechnology, 2003. **21**(5): p. 233-240.
174. Kallos, M.S., A. Sen, and L.A. Behie, *Large-scale expansion of mammalian neural stem cells: a review.* Medical & Biological Engineering & Computing, 2003. **41**(3): p. 271-282.
175. Cimetta, E., et al., *Micro-bioreactor arrays for controlling cellular environments: Design principles for human embryonic stem cell applications.* Methods, 2009. **47**(2): p. 81-89.
176. Yeo, L.Y., et al., *Microfluidic Devices for Bioapplications.* Small, 2011. **7**(1): p. 12-48.
177. Weibel, D.B. and G.M. Whitesides, *Applications of microfluidics in chemical biology.* Current Opinion in Chemical Biology, 2006. **10**(6): p. 584-591.
178. Xu, N., et al., *MicroRNA-145 Regulates OCT4, SOX2, and KLF4 and Represses Pluripotency in Human Embryonic Stem Cells.* Cell, 2009. **137**(4): p. 647-658.
179. Pasirayi, G., et al., *Microfluidic bioreactors for cell culturing: A review.* Micro and Nanosystems, 2011. **3**(2): p. 137-160.
180. Kim, L., et al., *Microfluidic arrays for logarithmically perfused embryonic stem cell culture.* Lab on a Chip, 2006. **6**(3): p. 394-406.
181. Figallo, E., et al., *Micro-bioreactor array for controlling cellular microenvironments.* Lab on a Chip, 2007. **7**(6): p. 710-719.
182. Korin, N., et al., *Periodic "flow-stop" perfusion microchannel bioreactors for mammalian and human embryonic stem cell long-term culture.* Biomedical Microdevices, 2009. **11**(1): p. 87-94.
183. Chin, V.I., et al., *Microfabricated platform for studying stem cell fates.* Biotechnology and Bioengineering, 2004. **88**(3): p. 399-415.
184. Lee, W., et al., *On-Demand Three-Dimensional Freeform Fabrication of Multi-Layered Hydrogel Scaffold With Fluidic Channels.* Biotechnology and Bioengineering, 2010. **105**(6): p. 1178-1186.
185. Park, J.Y., et al., *Differentiation of Neural Progenitor Cells in a Microfluidic Chip-Generated Cytokine Gradient.* Stem Cells, 2009. **27**(11): p. 2646-2654.
186. Kim, C., et al., *Three dimensional perfusion culture of encapsulated embryonic stem cells in microfluidic chip*. Transducers '07 & Eurosensors Xxi, Digest of Technical Papers, Vols 1 and 22007. U671-U671.

187. Moeller, H.C., et al., *A microwell array system for stem cell culture.* Biomaterials, 2008. **29**(6): p. 752-763.
188. Kang, E., et al., *Development of a multi-layer microfluidic array chip to culture and replate uniform-sized embryoid bodies without manual cell retrieval.* Lab on a Chip, 2010. **10**(20): p. 2651-2654.
189. Fernandes, T.G., et al., *High-throughput cellular microarray platforms: applications in drug discovery, toxicology and stem cell research.* Trends in Biotechnology, 2009. **27**(6): p. 342-349.
190. Abranches, E., et al., *Neural Differentiation of Embryonic Stem Cells In Vitro: A Road Map to Neurogenesis in the Embryo.* Plos One, 2009. **4**(7).
191. Hwang, N.S., S. Varghese, and J. Elisseeff, *Controlled differentiation of stem cells.* Advanced Drug Delivery Reviews, 2008. **60**(2): p. 199-214.
192. Amit, M., et al., *Human feeder layers for human embryonic stem cells.* Biology of Reproduction, 2003. **68**(6): p. 2150-2156.
193. Richards, M., et al., *Human feeders support prolonged undifferentiated growth of human inner cell masses and embryonic stem cells.* Nature Biotechnology, 2002. **20**(9): p. 933-936.
194. Lebkowski, J.S., et al., *Human embryonic stem cells: Culture, differentiation, and genetic modification for regenerative medicine applications.* Cancer Journal, 2001. **7**: p. S83-S93.
195. Takahashi Kazutoshi , et al., *Induction of Pluripotent Stem Cells from Adult Human Fibroblasts by Defined Factors.* cell, 2007. **131**: p. 861-872.
196. Takahashi, K. and S. Yamanaka, *Induction of pluripotent stem cells from mouse embryonic and adult fibroblast cultures by defined factors.* Cell, 2006. **126**(4): p. 663-676.
197. Groth, T., et al., *Contact activation of plasmatic coagulation on polymeric membranes measured by the activity of kallikrein in heparinized plasma.* Journal of Biomaterials Science-Polymer Edition, 1997. **8**(10): p. 797-807.
198. Duncan, R., *The dawning era of polymer therapeutics.* Nature Reviews Drug Discovery, 2003. **2**(5): p. 347-360.
199. Altankov, G., F. Grinnell, and T. Groth, *Studies on the biocompatibility of materials: Fibroblast reorganization of substratum-bound fibronectin on surfaces varying in wettability.* Journal of Biomedical Materials Research, 1996. **30**(3): p. 385-391.
200. Hierlemann, A., et al., *Microfabrication techniques for chemical/biosensors.* Proceedings of the Ieee, 2003. **91**(6): p. 839-863.
201. Martins, A., et al., *Electrospun nanostructured scaffolds for tissue engineering applications.* Nanomedicine, 2007. **2**(6): p. 929-942.
202. Wilbur, J.L., et al., *Lithographic modeling - A convenient route to structures with submicrometer dimensions* Advanced Materials, 1995. **7**(7): p. 649-652.
203. Wilbur, J.L., et al., *Microfabrication by microcontact printing of self-assembled monolayers* Advanced Materials, 1994. **6**(7-8): p. 600-604.
204. Chen, Y. and A. Pepin, *Nanofabrication: Conventional and nonconventional methods.* Electrophoresis, 2001. **22**(2): p. 187-207.
205. Dolnik, V., S.R. Liu, and S. Jovanovich, *Capillary electrophoresis on microchip.* Electrophoresis, 2000. **21**(1): p. 41-54.
206. Kalkandjiev, K., et al., *Microfluidics in silicon/polymer technology as a cost-efficient alternative to silicon/glass.* Journal of Micromechanics and Microengineering, 2011. **21**(2).
207. Mery, E., et al., *A silicon microfluidic chip integrating an ordered micropillar array separation column and a nano-electrospray emitter for LC/MS analysis of peptides.* Sensors and Actuators B-Chemical, 2008. **134**(2): p. 438-446.
208. Makamba, H., et al., *Stable permanently hydrophilic protein-resistant thin-film coatings on poly(dimethylsiloxane) substrates by electrostatic self-assembly and chemical cross-linking.* Analytical Chemistry, 2005. **77**(13): p. 3971-3978.
209. Melin, J., et al., *Thermoplastic microfluidic platform for single-molecule detection, cell culture, and actuation.* Analytical Chemistry, 2005. **77**(22): p. 7122-7130.
210. Heyries, K.A., et al., *"Macromolecules to PDMS transfer" as a general route for PDMS biochips.* Biosensors & Bioelectronics, 2009. **24**(5): p. 1146-1152.

211. Shadpour, H., et al., *Physiochemical properties of various polymer substrates and their effects on microchip electrophoresis performance.* Journal of Chromatography A, 2006. **1111**(2): p. 238-251.
212. Vickers, J.A., M.M. Caulum, and C.S. Henry, *Generation of hydrophilic poly(dimethylsiloxane) for high-performance microchip electrophoresis.* Analytical Chemistry, 2006. **78**(21): p. 7446-7452.
213. Aizawa, P., et al., *Effect of Different Materials used in Bioreactor Equipments on Cell Growth of Human Embryonic Kidney (HEK293) Cells Cultivated in a Protein-free Medium.* cell technology for cell products, 2007: p. 459-462.
214. McDonald, J.C. and G.M. Whitesides, *Poly(dimethylsiloxane) as a material for fabricating microfluidic devices.* Accounts of Chemical Research, 2002. **35**(7): p. 491-499.
215. Sia, S.K. and G.M. Whitesides, *Microfluidic devices fabricated in poly(dimethylsiloxane) for biological studies.* Electrophoresis, 2003. **24**(21): p. 3563-3576.
216. Park, J., et al., *A microsystem for sensing and patterning oxidative microgradients during cell culture.* Lab on a Chip, 2006. **6**(5): p. 611-622.
217. Skolimowski, M., et al., *Microfluidic dissolved oxygen gradient generator biochip as a useful tool in bacterial biofilm studies.* Lab on a Chip, 2010. **10**(16): p. 2162-2169.
218. Biehl, J.K., et al., *Proliferation of Mouse Embryonic Stem Cell Progeny and the Spontaneous Contractile Activity of Cardiomyocytes Are Affected by Microtopography.* Developmental Dynamics, 2009. **238**(8): p. 1964-1973.
219. Leclerc, E., et al., *Study of osteoblastic cells in a microfluidic environment.* Biomaterials, 2006. **27**(4): p. 586-595.
220. Borenstein, J.T., et al., *Microfabrication technology for vascularized tissue engineering.* Biomedical Microdevices, 2002. **4**(3): p. 167-175.
221. Leclerc, E., Y. Sakai, and T. Fujii, *Cell culture in 3-dimensional microfluidic structure of PDMS (polydimethylsiloxane).* Biomedical Microdevices, 2003. **5**(2): p. 109-114.
222. Leclerc, E., Y. Sakai, and T. Fujii, *Microfluidic PDMS (polydimethylsiloxane) bioreactor for large-scale culture of hepatocytes.* Biotechnology Progress, 2004. **20**(3): p. 750-755.
223. Jeon, K., et al., *Self-renewal of embryonic stem cells through culture on nanopattern polydimethylsiloxane substrate.* Biomaterials, 2012. **33**(21): p. 5206-5220.
224. Khademhosseini, A., et al., *Co-culture of human embryonic stem cells with murine embryonic fibroblasts on microwell-patterned substrates.* Biomaterials, 2006. **27**(36): p. 5968-5977.
225. Khetani, S.R. and S.N. Bhatia, *Microscale culture of human liver cells for drug development.* Nature Biotechnology, 2008. **26**(1): p. 120-126.
226. Lin, X. and B.P. Helmke, *Micropatterned structural control suppresses mechanotaxis of endothelial cells.* Biophysical Journal, 2008. **95**(6): p. 3066-3078.
227. Betancourt, T. and L. Brannon-Peppas, *Micro- and nanofabrication methods in nanotechnological medical and pharmaceutical devices.* International Journal of Nanomedicine, 2006. **1**(4): p. 483-495.
228. Healy, K.E., et al., *Kinetics of bone cell organization and mineralization on materials with patterned surface chemistry.* Biomaterials, 1996. **17**(2): p. 195-208.
229. Britland, S., et al., *Micropatterned substratum adhesiveness: A model for morphogenetic cues controlling cell behavior.* Experimental Cell Research, 1992. **198**(1): p. 124-129.
230. Goubko, C.A. and X.D. Cao, *Patterning multiple cell types in co-cultures: A review.* Materials Science & Engineering C-Materials for Biological Applications, 2009. **29**(6): p. 1855-1868.
231. Xia, Y.N. and G.M. Whitesides, *Soft lithography.* Annual Review of Materials Science, 1998. **28**: p. 153-184.
232. Manz, A., N. Graber, and H.M. Widmer, *Miniaturized total chemical-analysis systems - A novel concept for chemical sensing* Sensors and Actuators B-Chemical, 1990. **1**(1-6): p. 244-248.
233. Angell, J.B., S.C. Terry, and P.W. Barth, *Silicon micromechanical devices.* Scientific American, 1983. **248**(4): p. 44-&.

234. Unger, M.A., et al., *Monolithic microfabricated valves and pumps by multilayer soft lithography.* Science, 2000. **288**(5463): p. 113-116.
235. Gates, B.D., et al., *Unconventional nanofabrication.* Annual Review of Materials Research, 2004. **34**: p. 339-372.
236. Zhang, X. and S.-T. Yang, *High-throughput 3-D cell-based proliferation and cytotoxicity assays for drug screening and bioprocess development.* Journal of Biotechnology, 2011. **151**(2): p. 186-193.
237. Lee, J., et al., *Effect of thermal treatment on the chemical resistance of polydimethylsiloxane for microfluidic devices.* Journal of Micromechanics and Microengineering, 2013. **23**(3).
238. Backovic, A., et al., *Simultaneous analysis of multiple serum proteins adhering to the surface of medical grade polydimethylsiloxane elastomers.* Journal of Immunological Methods, 2007. **328**(1-2): p. 118-127.
239. Motomura, T., et al., *Development of silicone rubber hollow fiber membrane oxygenator for ECMO.* Artificial Organs, 2003. **27**(11): p. 1050-1053.
240. Giang, U.B.T., M.R. King, and L.A. DeLouise, *Microfabrication of Bubbular Cavities in PDMS for Cell Sorting and Microcell Culture Applications.* Journal of Bionic Engineering, 2008. **5**(4): p. 308-316.
241. Paranjape, M., et al., *A PDMS dermal patch for non-intrusive transdermal glucose sensing.* Sensors and Actuators a-Physical, 2003. **104**(3): p. 195-204.
242. Gao, Z.M., et al., *Poly(dimethylsiloxane) coatings for controlled drug release. I. Preparation and characterization of pharmaceutically acceptable materials.* Journal of Applied Polymer Science, 2003. **90**(3): p. 658-666.
243. Ertel, S.I., et al., *In-vitro study of the intrinsic toxicity of synthetic surfaces to cells* Journal of Biomedical Materials Research, 1994. **28**(6): p. 667-675.
244. Toepke, M.W. and D.J. Beebe, *PDMS absorption of small molecules and consequences in microfluidic applications.* Lab on a Chip, 2006. **6**(12): p. 1484-1486.
245. Abate, A.R., et al., *Glass coating for PDMS microfluidic channels by sol-gel methods.* Lab on a Chip, 2008. **8**(4): p. 516-518.
246. Lee, J.N., C. Park, and G.M. Whitesides, *Solvent compatibility of poly(dimethylsiloxane)-based microfluidic devices.* Analytical Chemistry, 2003. **75**(23): p. 6544-6554.
247. Wong, I. and C.-M. Ho, *Surface molecular property modifications for poly(dimethylsiloxane) (PDMS) based microfluidic devices.* Microfluidics and Nanofluidics, 2009. **7**(3): p. 291-306.
248. Norde, W., Buijs, J., Lyklema, J. , *Biopolymers in Solution and on Surfaces,* . Fundamentals of Interface and Colloid Science , Soft Colloids, Elsevier Ltd. , 2005. **Vol. V**.
249. Grinnell, F. and M.K. Feld, *Adsorption characteristics of plasma fibronectin in relationship to biological-activity* Journal of Biomedical Materials Research, 1981. **15**(3): p. 363-381.
250. Pettit, D.K., A.S. Hoffman, and T.A. Horbett, *Correlation between corneal epithelial-cell out growth and monoclonal-antibody binding to the cells-binding domain of adsorbed fibronectin* Journal of Biomedical Materials Research, 1994. **28**(6): p. 685-691.
251. Keselowsky, B.G., D.M. Collard, and A.J. Garcia, *Surface chemistry modulates fibronectin conformation and directs integrin binding and specificity to control cell adhesion.* Journal of Biomedical Materials Research Part A, 2003. **66A**(2): p. 247-259.
252. van Kooten, T.G., H.T. Spijker, and H.J. Busscher, *Plasma-treated polystyrene surfaces: model surfaces for studying cell-biomaterial interactions.* Biomaterials, 2004. **25**(10): p. 1735-1747.
253. Groth, T., et al., *Chemical and Physical Modifications of Biomaterial Surfaces to Control Adhesion of Cells*, in *Advances in Regenerative Medicine: Role of Nanotechnology and Engineering Principles*, V.P. Shastri, G. Altankov, and A. Lendlein, Editors. 2010. p. 253-284.
254. Cretich, M., et al., *Functionalization of poly(dimethylsiloxane) by chemisorption of copolymers: DNA microarrays for pathogen detection.* Sensors and Actuators B-Chemical, 2008. **132**(1): p. 258-264.

255. Waddell, E.A., et al., *Surface modification of Sylgard 184 polydimethylsiloxane by 254 nm excimer radiation and characterization by contact angle goniometry, infrared spectroscopy, atomic force and scanning electron microscopy.* Applied Surface Science, 2008. **254**(17): p. 5314-5318.
256. Dhara, S.K. and S.L. Stice, *Neural differentiation of human embryonic stem cells.* Journal of Cellular Biochemistry, 2008. **105**(3): p. 633-640.
257. Velve-Casquillas, G., et al., *Microfluidic tools for cell biological research.* Nano Today, 2010. **5**(1): p. 28-47.
258. Ma, Z., Z. Mao, and C. Gao, *Surface modification and property analysis of biomedical polymers used for tissue engineering.* Colloids and Surfaces B-Biointerfaces, 2007. **60**(2): p. 137-157.
259. Yan, H., B. Zhang, and H. Wu, *Chemical cytometry on microfluidic chips.* Electrophoresis, 2008. **29**(9): p. 1775-1786.
260. Huang, B., et al., *Coating of poly(dimethylsiloxane) with n-dodecyl-beta-D-maltoside to minimize nonspecific protein adsorption.* Lab on a Chip, 2005. **5**(10): p. 1005-1007.
261. Bai, Y., et al., *Surface modification for enhancing antibody binding on polymer-based microfluidic device for enzyme-linked immunosorbent assay.* Langmuir, 2006. **22**(22): p. 9458-9467.
262. Yasukawa, T., E. Maekawa, and F. Mizutani, *Immobilization of Glucose Oxidase on a Poly(dimethylsiloxane) Layer by Using Poly(L-lysine) as a Polymer Backbone.* Analytical Sciences, 2009. **25**(9): p. 1159-1162.
263. Doherty, E.A.S., et al., *Microchannel wall coatings for protein separations by capillary and chip electrophoresis.* Electrophoresis, 2003. **24**(1-2): p. 34-54.
264. Klee, D., et al., *Surface modification of poly(vinylidenefluoride) to improve the osteoblast adhesion.* Biomaterials, 2003. **24**(21): p. 3663-3670.
265. Croll, T.I., et al., *A blank slate? Layer-by-layer deposition of hyaluronic acid and chitosan onto various surfaces.* Biomacromolecules, 2006. **7**(5): p. 1610-1622.
266. Brown, X.Q., K. Ookawa, and J.Y. Wong, *Evaluation of polydimethylsiloxane scaffolds with physiologically-relevant elastic moduli: interplay of substrate mechanics and surface chemistry effects on vascular smooth muscle cell response.* Biomaterials, 2005. **26**(16): p. 3123-3129.
267. Wang, A.-J., J.-J. Xu, and H.-Y. Chen, *In-situ grafting hydrophilic polymer on chitosan modified poly (dimethylsiloxane) microchip for separation of biomolecules.* Journal of Chromatography A, 2007. **1147**(1): p. 120-126.
268. Mehta, G., et al., *Polyelectrolyte-clay-protein layer films on microfluidic PDMS bioreactor surfaces for primary murine bone marrow culture.* Advanced Functional Materials, 2007. **17**(15): p. 2701-2709.
269. Park, J.Y., et al., *Surface chemistry modification of PDMS elastomers with boiling water improves cellular adhesion.* Sensors and Actuators B-Chemical, 2012. **173**: p. 765-771.
270. Duffy, D.C., et al., *Rapid prototyping of microfluidic systems in poly(dimethylsiloxane).* Analytical Chemistry, 1998. **70**(23): p. 4974-4984.
271. Efimenko, K., W.E. Wallace, and J. Genzer, *Surface modification of Sylgard-184 poly(dimethyl siloxane) networks by ultraviolet and ultraviolet/ozone treatment.* Journal of Colloid and Interface Science, 2002. **254**(2): p. 306-315.
272. Romero-Sanchez, M.D., M.M. Pastor-Blas, and J.M. Martin-Martinez, *Treatment of a styrene-butadiene-styrene rubber with corona discharge to improve the adhesion to polyurethane adhesive.* International Journal of Adhesion and Adhesives, 2003. **23**(1): p. 49-57.
273. Wu, Z.Y., et al., *Polymer microchips bonded by O-2-plasma activation.* Electrophoresis, 2002. **23**(5): p. 782-790.
274. Hillborg, H., et al., *Crosslinked polydimethylsiloxane exposed to oxygen plasma studied by neutron reflectometry and other surface specific techniques.* Polymer, 2000. **41**(18): p. 6851-6863.

275. Hillborg, H., M. Sandelin, and U.W. Gedde, *Hydrophobic recovery of polydimethylsiloxane after exposure to partial discharges as a function of crosslink density.* Polymer, 2001. **42**(17): p. 7349-7362.
276. Owen, M.J. and P.J. Smith, *Plasma treatment of polydimethylsiloxane* Journal of Adhesion Science and Technology, 1994. **8**(10): p. 1063-1075.
277. Mahlstedt, M.M., et al., *Maintenance of Pluripotency in Human Embryonic Stem Cells Cultured on a Synthetic Substrate in Conditioned Medium.* Biotechnology and Bioengineering, 2010. **105**(1): p. 130-140.
278. Kim, H.T. and O.C. Jeong, *PDMS surface modification using atmospheric pressure plasma.* Microelectronic Engineering, 2011. **88**(8): p. 2281-2285.
279. Bodas, D. and C. Khan-Malek, *Hydrophilization and hydrophobic recovery of PDMS by oxygen plasma and chemical treatment - An SEM investigation.* Sensors and Actuators B-Chemical, 2007. **123**(1): p. 368-373.
280. Kim, J., et al., *The mechanisms of hydrophobic recovery of polydimethylsiloxane elastomers exposed to partial electrical discharges.* Journal of Colloid and Interface Science, 2001. **244**(1): p. 200-207.
281. Morra, M., et al., *The characterization of plasma-modified polydimethylsiloxane interfaces with media of different surface energy.* Clinical materials, 1990. **5**(2-4): p. 147-56.
282. Morra, M., et al., *On the aging of oxygen plasmas-treated polydimethylsiloxane surfaces* Journal of Colloid and Interface Science, 1990. **137**(1): p. 11-24.
283. Eddington, D.T., J.P. Puccinelli, and D.J. Beebe, *Thermal aging and reduced hydrophobic recovery of polydimethylsiloxane.* Sensors and Actuators B-Chemical, 2006. **114**(1): p. 170-172.
284. Wang, L., et al., *Chemical and physical modifications to poly(dimethylsiloxane) surfaces affect adhesion of Caco-2 cells.* Journal of Biomedical Materials Research Part A, 2010. **93A**(4): p. 1260-1271.
285. Singh, N., et al., *The role of independently variable grafting density and layer thickness of polymer nanolayers on peptide adsorption and cell adhesion.* Biomaterials, 2007. **28**(5): p. 763-771.
286. Pallandre, A., et al., *Surface treatment and characterization: Perspectives to electrophoresis and lab-on-chips.* Electrophoresis, 2006. **27**(3): p. 584-610.
287. Wheeler, B.C., et al., *Microcontact printing for precise control of nerve cell growth in culture.* Journal of Biomechanical Engineering-Transactions of the Asme, 1999. **121**(1): p. 73-78.
288. Ciampi, S., J.B. Harper, and J.J. Gooding, *Wet chemical routes to the assembly of organic monolayers on silicon surfaces via the formation of Si-C bonds: surface preparation, passivation and functionalization.* Chemical Society Reviews, 2010. **39**(6): p. 2158-2183.
289. Gooding, J.J. and S. Ciampi, *The molecular level modification of surfaces: from self-assembled monolayers to complex molecular assemblies.* Chemical Society Reviews, 2011. **40**(5): p. 2704-2718.
290. Slentz, B.E., et al., *Nanoliter capillary electrochromatography columns based on collocated monolithic support structures molded in poly(dimethyl siloxane).* Electrophoresis, 2001. **22**(17): p. 3736-3743.
291. Wipff, P.J., et al., *The covalent attachment of adhesion molecules to silicone membranes for cell stretching applications.* Biomaterials, 2009. **30**(9): p. 1781-1789.
292. Seguin, C., et al., *Surface modification of poly(dimethylsiloxane) for microfluidic assay applications.* Applied Surface Science, 2010. **256**(8): p. 2524-2531.
293. Cortese, G., et al., *Modification of micro-channel filling flow by poly(dimethylsiloxane) surface functionalization with fluorine-Substituted aminonaphthols.* Journal of Fluorine Chemistry, 2010. **131**(3): p. 357-363.
294. Zhang, Z., et al., *"Click" chemistry-based surface modification of poly(dimethylsiloxane) for protein separation in a microfluidic chip.* Electrophoresis, 2010. **31**(18): p. 3129-3136.

295. Tebbe, D., R. Thull, and U. Gbureck, *Influence of spacer length on heparin coupling efficiency and fibrinogen adsorption of modified titanium surfaces.* Biomedical Engineering Online, 2007. **6**.
296. Ruegg, U.T. and F. Hefti, *Growth of dissociated neurons in culture dishes coated with synthetic polymeric amines.* Neuroscience Letters, 1984. **49**(3): p. 319-324.
297. Bledi, Y., A.J. Domb, and M. Linial, *Culturing neuronal cells on surfaces coated by a novel polyethyleneimine-based polymer.* Brain Research Protocols, 2000. **5**(3): p. 282-289.
298. Yue, Z., et al., *Bio-functionalisation of polydimethylsiloxane with hyaluronic acid and hyaluronic acid - Collagen conjugate for neural interfacing.* Biomaterials, 2011. **32**(21): p. 4714-4724.
299. Sandison, M.E., et al., *On-chip immunoprecipitation for protein purification.* Lab on a Chip, 2010. **10**(20): p. 2805-2813.
300. Shafieyan, Y., et al., *Monocyte proliferation and differentiation to osteoclasts is affected by density of collagen covalently bound to a poly(dimethyl siloxane) culture surface.* Journal of Biomedical Materials Research Part A, 2012. **100A**(6): p. 1573-1581.
301. Curran, J.M., R. Chen, and J.A. Hunt, *The guidance of human mesenchymal stem cell differentiation in vitro by controlled modifications to the cell substrate.* Biomaterials, 2006. **27**(27): p. 4783-4793.
302. Low, S.P., et al., *Evaluation of mammalian cell adhesion on surface-modified porous silicon.* Biomaterials, 2006. **27**(26): p. 4538-4546.
303. Osterberg, E., et al., *Protein-rejecting ability of surface-bound dextran in end-on and side-on configurations - comparison to PEG.* Journal of Biomedical Materials Research, 1995. **29**(6): p. 741-747.
304. Martwiset, S., A.E. Koh, and W. Chen, *Nonfouling characteristics of dextran-containing surfaces.* Langmuir, 2006. **22**(19): p. 8192-8196.
305. Hu, S.G., C.H. Jou, and M.C. Yang, *Protein adsorption, fibroblast activity and antibacterial properties of poly(3-hydroxybutyric acid-co-3-hydroxyvaleric acid) grafted with chitosan and chitooligosaccharide after immobilized with hyaluronic acid.* Biomaterials, 2003. **24**(16): p. 2685-2693.
306. Yu, L., et al., *Flow-through functionalized PDMS microfluidic channels with dextran derivative for ELISAs.* Lab on a Chip, 2009. **9**(9): p. 1243-1247.
307. Yang, L.Y., et al., *Photocatalyzed Surface Modification of Poly(dimethylsiloxane) with Polysaccharides and Assay of Their Protein Adsorption and Cytocompatibility.* Analytical Chemistry, 2010. **82**(15): p. 6430-6439.
308. Reza, A.T. and S.B. Nicoll, *Characterization of novel photocrosslinked carboxymethylcellulose hydrogels for encapsulation of nucleus pulposus cells.* Acta Biomaterialia, 2010. **6**(1): p. 179-186.
309. Ramli, N.A. and T.W. Wong, *Sodium carboxymethylcellulose scaffolds and their physicochemical effects on partial thickness wound healing.* International Journal of Pharmaceutics, 2011. **403**(1–2): p. 73-82.
310. Ryan, C.K. and H.C. Sax, *Evaluation of a carboxymethyl cellulose sponge for prevantion of postoperative adhesions* American Journal of Surgery, 1995. **169**(1): p. 154-160.
311. Ma, J., et al., *Preparation and characterization of sodium carboxymethylcellulose/poly(N-isopropylacrylamide)/clay semi-IPN nanocomposite hydrogels.* European Polymer Journal, 2007. **43**(6): p. 2221-2228.
312. Lalountas, M.A., et al., *Preventing intraperitoneal adhesions with atorvastatin and sodium hyaluronate/carboxymethylcellulose: a comparative study in rats.* American Journal of Surgery, 2010. **200**(1): p. 118-123.
313. Orelma, H., et al., *Modification of Cellulose Films by Adsorption of CMC and Chitosan for Controlled Attachment of Biomolecules.* Biomacromolecules, 2011. **12**(12): p. 4311-4318.
314. Dalsin, J.L., et al., *Mussel adhesive protein mimetic polymers for the preparation of nonfouling surfaces.* Journal of the American Chemical Society, 2003. **125**(14): p. 4253-4258.

315. Kim, T.H., et al., *Differential expression and distribution of focal adhesion and cell adhesion molecules in rat hepatocyte differentiation.* Experimental Cell Research, 1998. **244**(1): p. 93-104.
316. Perantoni, A.O., *Adhesion molecules in the kidney: From embryo to adult.* Experimental Nephrology, 1999. **7**(2): p. 80-102.
317. Adams, J.C. and F.M. Watt, *Regulation of development and differentiation by the extracellular-matrix.* Development, 1993. **117**(4): p. 1183-1198.
318. Flaim, C.J., et al., *Combinatorial signaling microenvironments for studying stem cell fate.* Stem Cells and Development, 2008. **17**(1): p. 29-39.
319. Lee, J.N., et al., *Compatibility of mammalian cells on surfaces of poly(dimethylsiloxane).* Langmuir, 2004. **20**(26): p. 11684-11691.
320. Nagaoka, M., et al., *E-Cadherin-Coated Plates Maintain Pluripotent ES Cells without Colony Formation.* Plos One, 2006. **1**(1).
321. Goetz, A.K., et al., *Temporally restricted substrate interactions direct fate and specification of neural precursors derived from embryonic stem cells.* Proceedings of the National Academy of Sciences of the United States of America, 2006. **103**(29): p. 11063-11068.
322. Evans, N.D., et al., *Extracellular matrix-mediated osteogenic differentiation of murine embryonic stem cells.* Biomaterials, 2010. **31**(12): p. 3244-3252.
323. Young, S., et al., *Gelatin as a delivery vehicle for the controlled release of bioactive molecules.* Journal of Controlled Release, 2005. **109**(1-3): p. 256-274.
324. Zhang, X., et al., *Chemical Cross-Linking Gelatin with Natural Phenolic Compounds as Studied by High-Resolution NMR Spectroscopy.* Biomacromolecules, 2010. **11**(4): p. 1125-1132.
325. Mufamadi, M.S., et al., *A review on composite liposomal technologies for specialized drug delivery.* Journal of drug delivery, 2011. **2011**: p. 939851-939851.
326. Shin, H., S. Jo, and A.G. Mikos, *Biomimetic materials for tissue engineering.* Biomaterials, 2003. **24**(24): p. 4353-4364.
327. Wang, L.S., et al., *Injectable biodegradable hydrogels with tunable mechanical properties for the stimulation of neurogenesic differentiation of human mesenchymal stem cells in 3D culture.* Biomaterials, 2010. **31**(6): p. 1148-1157.
328. Hellio-Serughetti, D. and M. Djabourov, *Gelatin hydrogels cross-linked with bisvinyl sulfonemethyl. 2. The physical and chemical networks.* Langmuir, 2006. **22**(20): p. 8516-8522.
329. Ruardy, T.G., et al., *Adhesion and spreading of human skin fibroblasts on physicochemically characterized gradient surfaces* Journal of Biomedical Materials Research, 1995. **29**(11): p. 1415-1423.
330. Iuliano, D.J., S.S. Saavedra, and G.A. Truskey, *Effect of the conformation and orientation of adsorbed fibronectin on endothelial-cell spreading and the strength of adhesion* Journal of Biomedical Materials Research, 1993. **27**(8): p. 1103-1113.
331. Pineda, E.T., R.M. Nerem, and T. Ahsan, *Differentiation Patterns of Embryonic Stem Cells in Two- versus Three-Dimensional Culture.* Cells Tissues Organs, 2013. **197**(5): p. 399-410.
332. Germanguz, I., et al., *Molecular characterization and functional properties of cardiomyocytes derived from human inducible pluripotent stem cells.* Journal of Cellular and Molecular Medicine, 2011. **15**(1): p. 38-51.
333. Zwi, L., et al., *Cardiomyocyte Differentiation of Human Induced Pluripotent Stem Cells.* Circulation, 2009. **120**(15): p. 1513-1523.
334. Tanaka, T., et al., *In vitro pharmacologic testing using human induced pluripotent stem cell-derived cardiomyocytes.* Biochemical and Biophysical Research Communications, 2009. **385**(4): p. 497-502.
335. Maguire, T., et al., *Control of hepatic differentiation via cellular aggregation in an alginate microenvironment.* Biotechnology and Bioengineering, 2007. **98**(3): p. 631-644.
336. Maguire, T., et al., *Alginate-PLL microencapsulation: Effect on the differentiation of embryonic stem cells into hepatocytes.* Biotechnology and Bioengineering, 2006. **93**(3): p. 581-591.

337. Trappmann, B., et al., *Extracellular-matrix tethering regulates stem-cell fate.* Nature Materials, 2012. **11**(7): p. 642-649.
338. Kunz-Schughart, L.A., et al., *The use of 3-D cultures for high-throughput screening: The multicellular spheroid model.* Journal of Biomolecular Screening, 2004. **9**(4): p. 273-285.
339. Frieboes, H.B., et al., *An integrated computational/experimental model of tumor invasion.* Cancer Research, 2006. **66**(3): p. 1597-1604.
340. Santini, M.T., G. Rainaldi, and P.L. Indovina, *Multicellular tumour spheroids in radiation biology.* International Journal of Radiation Biology, 1999. **75**(7): p. 787-799.
341. Stuschke, M., et al., *Heterogeneity in the fraction sensitivities of human tumor-cell lines - studies in a 3-dimensional model system* International Journal of Radiation Oncology Biology Physics, 1995. **32**(2): p. 395-408.
342. Graham, C.H., et al., *Rapid aquisition of multicellular drug-resistance after a single exposure of mammary-tumor cells to antitumor Alkylating-agents.* Journal of the National Cancer Institute, 1994. **86**(13): p. 975-982.
343. Kobayashi, H., et al., *Acquired multicellular- mediated resistance to alkylating -agents in cancer* Proceedings of the National Academy of Sciences of the United States of America, 1993. **90**(8): p. 3294-3298.
344. Graham, C.H., et al., *Rapid acuisition of multicellular drug-resistance after a single exposure of mammary-tumor cells to antitumor alkylating-agents* Journal of the National Cancer Institute, 1994. **86**(13): p. 975-982.
345. Winters, B.S., S.R. Shepard, and R.A. Foty, *Biophysical measurement of brain tumor cohesion.* International Journal of Cancer, 2005. **114**(3): p. 371-379.
346. Wartenberg, M., et al., *Tumor-induced angiogenesis studied in confrontation cultures of multicellular tumor spheroids and embryoid bodies grown from pluripotent embryonic stem cells.* Faseb Journal, 2001. **15**(6): p. 995-1005.
347. Ishii, T., et al., *In vitro differentiation and maturation of mouse embryonic stem cells into hepatocytes.* Experimental Cell Research, 2005. **309**(1): p. 68-77.
348. Bielby, R.C., et al., *In vitro differentiation and in vivo mineralization of osteogenic cells derived from human embryonic stem cells.* Tissue Engineering, 2004. **10**(9-10): p. 1518-1525.
349. Kim, J.H., et al., *Dopamine neurons derived from embryonic stem cells function in an animal model of Parkinson's disease.* Nature, 2002. **418**(6893): p. 50-56.
350. Itskovitz-Eldor, J., et al., *Differentiation of human embryonic stem cells into embryoid bodies comprising the three embryonic germ layers.* Molecular Medicine, 2000. **6**(2): p. 88-95.
351. Dang, S.M., et al., *Efficiency of embryoid body formation and hematopoietic development from embryonic stem cells in different culture systems.* Biotechnology and Bioengineering, 2002. **78**(4): p. 442-453.
352. Rajala, K., et al., *Cardiac Differentiation of Pluripotent Stem Cells.* Stem Cells International, 2011. **2011**.
353. Wobus, A.M. and K.R. Boheler, *Embryonic stem cells: Prospects for developmental biology and cell therapy.* Physiological Reviews, 2005. **85**(2): p. 635-678.
354. Desbaillets, I., et al., *Embryoid bodies: an in vitro model of mouse embryogenesis.* Experimental Physiology, 2000. **85**(6): p. 645-651.
355. Wobus, A.M., G. Wallukat, and J. Hescheler, *Pluripotent mouse embryonic stem-cellsare able to differentiate into cardiomyocytes expressing chronotropic responses to adrenergic and cholinergic agents and CA2+channel blockers.* Differentiation, 1991. **48**(3): p. 173-182.
356. Millerhance, W.C., et al., *In-vitro chamber specification during embryonic stem-cell cardiogenesis- expression of the ventricular myosin light chain-2 gene is independent of heart tube formation* Journal of Biological Chemistry, 1993. **268**(33): p. 25244-25252.
357. Martin, G.R. and M.J. Evans, *Differentiation of clonal lines of teratocarcinoma cells-formation of embyoid bodies in vitro* Proceedings of the National Academy of Sciences of the United States of America, 1975. **72**(4): p. 1441-1445.
358. Keller, G.M., *In vitro differentiation of embryonic stem cells.* Current Opinion in Cell Biology, 1995. **7**(6): p. 862-869.

359. Serra, M., et al., *Novel culture strategy for human stem cell proliferation and neuronal differentiation.* Journal of Neuroscience Research, 2007. **85**(16): p. 3557-3566.
360. Fassler, R. and M. Meyer, *Consequences of lack of beta-1 integrin gene-expression in mice* Genes & Development, 1995. **9**(15): p. 1896-1908.
361. Stephens, L.E., et al., *Deletion of beta-1 integrins in mice results in inner cell mass failure and periimplantation lethality* Genes & Development, 1995. **9**(15): p. 1883-1895.
362. Weiss, M.J., G. Keller, and S.H. Orkin, *Novel insights into erythroid development revealed through in vitro differentiation of Gata-1 embryonic stem-cells* Genes & Development, 1994. **8**(10): p. 1184-1197.
363. Doetschman, T., et al., *Embryonic stem-cells model systems for vascular morphogenesis and cardiac disorderes.* Hypertension, 1993. **22**(4): p. 618-629.
364. Krah, K., et al., *Induction of vasculogenesis in quail blastodisc-derived embryoid bodies* Developmental Biology, 1994. **164**(1): p. 123-132.
365. Heyward, S.A., et al., *Expression and inducibility of vascular adhesion receptors in development* Faseb Journal, 1995. **9**(10): p. 956-962.
366. Wang, R., R. Clark, and V.L. Bautch, *Embryonic stem cell-derived cystic embryoid bodies from vascular channels- an in vitro model of blood-vessel development DEVELOPMENT.* Development, 1992. **114**(2): p. 303-316.
367. Rohwedel, J., et al., *Muscle-cell differentiation of embryonic stem-cells reflects myogenesis in-vitro developmentally- regulated expression of myogenic determination genes and functional expression of ionic currents* Developmental Biology, 1994. **164**(1): p. 87-101.
368. Wobus, A.M., et al., *Cardiomyocyte-like cells differentiated in-vitro from embryonic carcinoma-cells P19 are characterized by functional expression of adrenoceptors and CA2+ channels* In Vitro Cellular & Developmental Biology-Animal, 1994. **30A**(7): p. 425-434.
369. Wobus, A.M., et al., *Development of cardiomyocytes expressing cardiac-specific genes, action-potentials, and tonic channels during embryonic stem cell-derived cardiogenesis* in *Cardiac Growth and Regeneration*, W.C. Claycomb and P. DiNardo, Editors. 1995. p. 460-469.
370. Mummery, C., et al., *Differentiation of human embryonic stem cells to cardiomyocytes - Role of coculture with visceral endoderm-like cells.* Circulation, 2003. **107**(21): p. 2733-2740.
371. Gassmann, M., et al., *Oxygen supply and oxygen-dependent gene expression in differentiating embryonic stem cells.* Proceedings of the National Academy of Sciences of the United States of America, 1996. **93**(7): p. 2867-2872.
372. Rungarunlert, S., et al., *Embryoid body formation from embryonic and induced pluripotent stem cells: Benefits of bioreactors.* World journal of stem cells, 2009. **1**(1): p. 11-21.
373. He, Z., et al., *Effect of leukemia inhibitory factor on embryonic stem cell differentiation: implications for supporting neuronal differentiation.* Acta Pharmacologica Sinica, 2006. **27**(1): p. 80-90.
374. Takahashi, T., et al., *Ascorbic acid enhances differentiation of embryonic stem cells into cardiac myocytes.* Circulation, 2003. **107**(14): p. 1912-1916.
375. Chen, M., et al., *Enrichment of cardiac differentiation of mouse embryonic stem cells by optimizing the hanging drop method.* Biotechnology Letters, 2011. **33**(4): p. 853-858.
376. Yamada, T., et al., *In vitro functional gut-like organ formation from mouse embryonic stem cells.* Stem Cells, 2002. **20**(1): p. 41-49.
377. Arbatan, T., et al., *Tumor Inside a Pearl Drop.* Advanced Healthcare Materials, 2012. **1**(4): p. 467-469.
378. Kurosawa, H., et al., *A simple method for forming embryoid body from mouse embryonic stem cells.* Journal of Bioscience and Bioengineering, 2003. **96**(4): p. 409-411.
379. Koike, M., H. Kurosawa, and Y. Amano, *A round-bottom 96-well polystyrene plate coated with 2-methacryloyloxyethyl phosphorylcholine as an effective tool for embryoid body formation.* Cytotechnology, 2005. **47**(1-3): p. 3-10.
380. Doetschman, T.C., H. Eistetter, and M. Katz, *The in vitro development of blastocyst-derived embryonic stem cell lines: formation of visceral yolk sac, blood islands and myocardium.* J. Embryol. exp. Morph., 1985. **87**: p. 27-45.

381. Zhang, S.C., et al., *In vitro differentiation of transplantable neural precursors from human embryonic stem cells.* Nature Biotechnology, 2001. **19**(12): p. 1129-1133.
382. Plachta, N., et al., *Developmental potential of defined neural progenitors derived from mouse embryonic stem cells.* Development, 2004. **131**(21): p. 5449-5456.
383. Risau, W., et al., *Vasculogenesis and angiogenesis in embryonic-stem-cell-derived embryoid bodies* Development, 1988. **102**(3): p. 471-478.
384. Jones, E.A., et al., *Hepatic differentiation of murine embryonic stem cells.* Experimental Cell Research, 2002. **272**(1): p. 15-22.
385. Toyooka, Y., et al., *Embryonic stem cells can form germ cells in vitro.* Proceedings of the National Academy of Sciences of the United States of America, 2003. **100**(20): p. 11457-11462.
386. Reubinoff, B.E., et al., *Embryonic stem cell lines from human blastocysts: somatic differentiation in vitro.* Nature Biotechnology, 2000. **18**(4): p. 399-404.
387. Dang, S.M. and P.W. Zandstra, *Scalable production of embryonic stem cell-derived cells.* Methods in molecular biology (Clifton, N.J.), 2005. **290**: p. 353-64.
388. Park, J., et al., *Microfabrication-based modulation of embryonic stem cell differentiation.* Lab on a Chip, 2007. **7**(8): p. 1018-1028.
389. Carpenedo, R.L., C.Y. Sargent, and T.C. McDevitt, *Rotary suspension culture enhances the efficiency, yield, and homogeneity of embryoid body differentiation.* Stem Cells, 2007. **25**(9): p. 2224-2234.
390. Cameron, C.M., W.-S. Hu, and D.S. Kaufman, *Improved development of human embryonic stem cell-derived embryoid bodies by stirred vessel cultivation.* Biotechnology and Bioengineering, 2006. **94**(5): p. 938-948.
391. Bratt-Leal, A.M., R.L. Carpenedo, and T.C. McDevitt, *Engineering the Embryoid Body Microenvironment to Direct Embryonic Stem Cell Differentiation.* Biotechnology Progress, 2009. **25**(1): p. 43-51.
392. Lu, S.H., et al., *Bioreactor cultivation enhances NTEB formation and differentiation of NTES cells into cardiomyocytes.* Cloning and Stem Cells, 2008. **10**(3): p. 363-370.
393. Niebruegge, S., et al., *Cardiomyocyte production in mass suspension culture: embryonic stem cells as a source for great amounts of functional Cardiomyocytes.* Tissue Engineering Part A, 2008. **14**(10): p. 1591-1601.
394. Krawetz, R., et al., *Large-scale expansion of pluripotent human embryonic stem cells in stirred-suspension bioreactors.* Tissue Engineering Part C-Methods, 2010. **16**(4): p. 573-582.
395. Taiani, J.T., et al., *Reduced Differentiation Efficiency of Murine Embryonic Stem Cells in Stirred Suspension Bioreactors.* Stem Cells and Development, 2010. **19**(7): p. 989-998.
396. Sargent, C.Y., G.Y. Berguig, and T.C. McDevitt, *Cardiomyogenic differentiation of embryoid bodies is promoted by rotary Orbital suspension culture.* Tissue Engineering Part A, 2009. **15**(2): p. 331-342.
397. Lu, S., et al., *Bioreactor Cultivation Enhances NTEB Formation and Differentiation of NTES Cells into Cardiomyocytes.* CLONING AND STEM CELLS, 2008. **10**(3): p. 1-8.
398. Doevendans, P.A., et al., *Differentiation of cardiomyocytes in floating embryoid bodies is comparable to fetal cardiomyocytes.* Journal of Molecular and Cellular Cardiology, 2000. **32**(5): p. 839-851.
399. Torisawa, Y.-s., et al., *Efficient formation of uniform-sized embryoid bodies using a compartmentalized microchannel device.* Lab on a Chip, 2007. **7**(6): p. 770-776.
400. Hwang, Y.-S., et al., *Microwell-mediated control of embryoid body size regulates embryonic stem cell fate via differential expression of WNT5a and WNT11.* Proceedings of the National Academy of Sciences of the United States of America, 2009. **106**(40): p. 16978-16983.
401. Peerani, R., et al., *Niche-mediated control of human embryonic stem cell self-renewal and differentiation.* Embo Journal, 2007. **26**(22): p. 4744-4755.
402. Sasaki, D., et al., *Mass preparation of size-controlled mouse embryonic stem cell aggregates and induction of cardiac differentiation by cell patterning method.* Biomaterials, 2009. **30**(26): p. 4384-4389.

403. Mohr, J.C., et al., *The microwell control of embryoid body size in order to regulate cardiac differentiation of human embryonic stem cells.* Biomaterials, 2010. **31**(7): p. 1885-1893.
404. Dahlmann, J., et al., *The use of agarose microwells for scalable embryoid body formation and cardiac differentiation of human and murine pluripotent stem cells.* Biomaterials, 2013. **34**(10): p. 2463-2471.
405. Ungrin, M.D., et al., *Reproducible, ultra high-throughput formation of multicellular organization from single cell suspension-derived human embryonic stem cell aggregates.* Plos One, 2008. **3**(2).
406. Yukawa, H., H. Noguchi, and S. Hayashi, *Embryonic body formation using the tapered soft stencil for cluster culture device.* Biomaterials, 2011. **32**(15): p. 3729-3738.
407. Wartenberg, M., et al., *The embryoid body as a novel in vitro assay system for antiangiogenic agents.* Laboratory Investigation, 1998. **78**(10): p. 1301-1314.
408. Benya, P.D. and J.D. Shaffer, *Dedifferentiated chondrocytes reexpress the differentiated collagen phenotype when cultured in agarose gels* Cell, 1982. **30**(1): p. 215-224.
409. Yu, X.J., G.P. Dillon, and R.V. Bellamkonda, *A laminin and nerve growth factor-laden three-dimensional scaffold for enhanced neurite extension.* Tissue Engineering, 1999. **5**(4): p. 291-304.
410. Levenberg, S., et al., *Differentiation of human embryonic stem cells on three-dimensional polymer scaffolds.* Proceedings of the National Academy of Sciences of the United States of America, 2003. **100**(22): p. 12741-12746.
411. Gerecht, S., et al., *Hyaluronic acid hydrogen for controlled self-renewal and differentiation of human embryonic stem cells.* Proceedings of the National Academy of Sciences of the United States of America, 2007. **104**(27): p. 11298-11303.
412. Liu, H. and K. Roy, *Biomimetic three-dimensional cultures significantly increase hematopoietic differentiation efficacy of embryonic stem cells.* Tissue Engineering, 2005. **11**(1-2): p. 319-330.
413. Liu, H., J. Lin, and K. Roy, *Effect of 3D scaffold and dynamic culture condition on the global gene expression profile of mouse embryonic stem cells.* Biomaterials, 2006. **27**(36): p. 5978-5989.
414. Hwang, N.S., et al., *Effects of three-dimensional culture and growth factors on the chondrogenic differentiation of murine embryonic stem cells.* Stem Cells, 2006. **24**(2): p. 284-291.
415. Hwang, N.S., et al., *Chondrogenic differentiation of human embryonic stem cell-derived cells in arginine-glycine-aspartate modified hydrogels.* Tissue Engineering, 2006. **12**(9): p. 2695-2706.
416. Glicklis, R., et al., *Hepatocyte behavior within three-dimensional porous alginate scaffolds.* Biotechnology and Bioengineering, 2000. **67**(3): p. 344-353.
417. Leor, J., et al., *Bioengineered cardiac grafts - A new approach to repair the infarcted myocardium?* Circulation, 2000. **102**(19): p. 56-61.
418. Jiang, L., et al., *Binary cooperative complementary nanoscale interfacial materials.* Pure and Applied Chemistry, 2000. **72**(1-2): p. 73-81.
419. Barthlott, W. and C. Neinhuis, *Purity of the sacred lotus, or escape from contamination in biological surfaces.* Planta, 1997. **202**(1): p. 1-8.
420. Roach, P., N.J. Shirtcliffe, and M.I. Newton, *Progess in superhydrophobic surface development.* Soft Matter, 2008. **4**(2): p. 224-240.
421. Pike, N., et al., *How aphids lose their marbles.* Proceedings of the Royal Society B-Biological Sciences, 2002. **269**(1497): p. 1211-1215.
422. Zheng, Y., X. Gao, and L. Jiang, *Directional adhesion of superhydrophobic butterfly wings.* Soft Matter, 2007. **3**(2): p. 178-182.
423. Blossey, R., *Self-cleaning surfaces - virtual realities.* Nature Materials, 2003. **2**(5): p. 301-306.
424. McHale, G., M.I. Newton, and N.J. Shirtcliffe, *Immersed superhydrophobic surfaces: Gas exchange, slip and drag reduction properties.* Soft Matter, 2010. **6**(4): p. 714-719.

425. Nosonovsky, M. and B. Bhushan, *Superhydrophobic surfaces and emerging applications: Non-adhesion, energy, green engineering.* Current Opinion in Colloid & Interface Science, 2009. **14**(4): p. 270-280.
426. Nosonovsky, M. and B. Bhushan, *Wetting of rough three-dimensional superhydrophobic surfaces.* Microsystem Technologies-Micro-and Nanosystems-Information Storage and Processing Systems, 2006. **12**(3): p. 273-281.
427. Hong, L. and T. Pan, *Surface microfluidics fabricated by photopatternable superhydrophobic nanocomposite.* Microfluidics and Nanofluidics, 2011. **10**(5): p. 991-997.
428. Ok, J.T., et al., *Fabrication of 3D superhydrophobic micro-ratchets via combined thermal imprint lithography and photolithography* Proceedings of the Asme International Mechanical Engineering Congress and Exposition, Vol 13, Pts a and B2009. 785-790.
429. Kim, T.-I., et al., *Optical lithography with printed metal mask and a simple superhydrophobic surface.* Small, 2008. **4**(2): p. 182-185.
430. Gao, L. and T.J. McCarthy, *"Artificial lotus leaf" prepared using a 1945 patent and a commercial textile.* Langmuir, 2006. **22**(14): p. 5998-6000.
431. Genzer, J. and K. Efimenko, *Recent developments in superhydrophobic surfaces and their relevance to marine fouling: a review.* Biofouling, 2006. **22**(5): p. 339-360.
432. Mahadevan, L. and Y. Pomeau, *Rolling droplets.* Physics of Fluids, 1999. **11**(9): p. 2449-2453.
433. Aussillous, P. and D. Quere, *Liquid marbles.* Nature, 2001. **411**(6840): p. 924-927.
434. Nguyen, T.H., K. Hapgood, and W. Shen, *Observation of the liquid marble morphology using confocal microscopy.* Chemical Engineering Journal, 2010. **162**(1): p. 396-405.
435. Bhosale, P.S. and M.V. Panchagnula, *On synthesizing solid polyelectrolyte microspheres from evaporating liquid marbles.* Langmuir, 2010. **26**(13): p. 10745-10749.
436. Hapgood, K.P., L. Farber, and J.N. Michaels, *Agglomeration of hydrophobic powders via solid spreading nucleation.* Powder Technology, 2009. **188**(3): p. 248-254.
437. Tian, J., et al., *Liquid marble for gas sensing.* Chemical Communications, 2010. **46**(26): p. 4734-4736.
438. Bormashenko, E., et al., *Interfacial and conductive properties of liquid marbles coated with carbon black.* Powder Technology, 2010. **203**(3): p. 529-533.
439. Dandan, M. and H.Y. Erbil, *Evaporation Rate of Graphite Liquid Marbles: Comparison with Water Droplets.* Langmuir, 2009. **25**(14): p. 8362-8367.
440. Bormashenko, E., et al., *New Investigations on Ferrofluidics: Ferrofluidic Marbles and Magnetic-Field-Driven Drops on Superhydrophobic Surfaces.* Langmuir, 2008. **24**(21): p. 12119-12122.
441. Eshtiaghi, N., et al., *Liquid marble formation: Spreading coefficients or kinetic energy?* Powder Technology, 2009. **196**(2): p. 126-132.
442. Bhosale, P.S., M.V. Panchagnula, and H.A. Stretz, *Mechanically robust nanoparticle stabilized transparent liquid marbles.* Applied Physics Letters, 2008. **93**(3).
443. Bormashenko, E., R. Pogreb, and A. Musin, *Stable water and glycerol marbles immersed in organic liquids: From liquid marbles to Pickering-like emulsions.* Journal of Colloid and Interface Science, 2012. **366**(1): p. 196-199.
444. Xue, Y., et al., *Magnetic Liquid Marbles: A "Precise" Miniature Reactor.* Advanced Materials, 2010. **22**(43): p. 4814-+.
445. Gao, L. and T.J. McCarthy, *Ionic liquid marbles.* Langmuir, 2007. **23**(21): p. 10445-10447.
446. Aussillous, P. and D. Quere, *Properties of liquid marbles.* Proceedings of the Royal Society a-Mathematical Physical and Engineering Sciences, 2006. **462**(2067): p. 973-999.
447. Bormashenko, E., et al., *On the Mechanism of Floating and Sliding of Liquid Marbles.* Chemphyschem, 2009. **10**(4): p. 654-656.
448. Zhang, L., et al., *Combination of Bioinspiration: A General Route to Superhydrophobic Particles.* Journal of the American Chemical Society, 2012. **134**(24): p. 9879-9881.
449. Bormashenko, E., *Liquid marbles: Properties and applications.* Current Opinion in Colloid & Interface Science, 2011. **16**(4): p. 266-271.

450. Zhao, Y., et al., *Magnetic Liquid Marbles: Manipulation of Liquid Droplets Using Highly Hydrophobic Fe3O4 Nanoparticles.* Advanced Materials, 2010. **22**(6): p. 707-+.
451. McEleney, P., et al., *Liquid marble formation using hydrophobic powders.* Chemical Engineering Journal, 2009. **147**(2-3): p. 373-382.
452. McHale, G. and M.I. Newton, *Liquid marbles: principles and applications.* Soft Matter, 2011. **7**(12): p. 5473-5481.
453. Tosun, A. and H.Y. Erbil, *Evaporation rate of PTFE liquid marbles.* Applied Surface Science, 2009. **256**(5): p. 1278-1283.
454. Bormashenko, E., et al., *Surface tension of liquid marbles.* Colloids and Surfaces a-Physicochemical and Engineering Aspects, 2009. **351**(1-3): p. 78-82.
455. Tian, J., et al., *Porous liquid marble shell offers possibilities for gas detection and gas reactions.* Chemical Engineering Journal, 2010. **165**(1): p. 347-353.
456. Fujii, S., et al., *pH-Responsive Hairy Particles Synthesized by Dispersion Polymerization with a Macroinitiator as an Inistab and Their Use as a Gas-Sensitive Liquid Marble Stabilizer.* Macromolecules, 2012. **45**(6): p. 2863-2873.
457. Arbatan, T., et al., *Microreactors: Liquid marbles as micro-bioreactors for rapid blood typing (Adv. Healthcare Mater. 1/2012).* Advanced Healthcare Materials, 2012. **1**(1): p. 79-79.
458. Braun, H.-G. and A.Z. Cardoso, *Self-assembly of Fmoc-diphenylalanine inside liquid marbles.* Colloids and Surfaces B-Biointerfaces, 2012. **97**: p. 43-50.
459. Bormashenko, E. and A. Musin, *Revealing of water surface pollution with liquid marbles.* Applied Surface Science, 2009. **255**(12): p. 6429-6431.
460. Forny, L., et al., *Storing water in powder form by self-assembling hydrophobic silica nanoparticles.* Powder Technology, 2007. **171**(1): p. 15-24.
461. Wang, W., et al., *Methane storage in dry water gas hydrates.* Journal of the American Chemical Society, 2008. **130**(35): p. 11608-+.
462. Carter, B.O., et al., *Gas Storage in "Dry Water" and "Dry Gel" Clathrates.* Langmuir, 2010. **26**(5): p. 3186-3193.
463. McHale, G., et al., *Electrowetting of nonwetting liquids and liquid marbles.* Langmuir, 2007. **23**(2): p. 918-924.
464. Zhao, L.H., J. Lee, and P.N. Sen, *Long-term retention of hydrophilic behavior of plasma treated polydimethylsiloxane (PDMS) surfaces stored under water and Luria-Bertani broth.* Sensors and Actuators a-Physical, 2012. **181**: p. 33-42.
465. Hapgood, K.P. and B. Khanmohammadi, *Granulation of hydrophobic powders.* Powder Technology, 2009. **189**(2): p. 253-262.
466. Kawamura, Y., H. Mayama, and Y. Nonomura, *Edible Liquid Marbles and Capsules Covered with Lipid Crystals.* Journal of Oleo Science, 2012. **61**(9): p. 477-482.
467. Dupin, D., S.P. Armes, and S. Fujii, *Stimulus-Responsive Liquid Marbles.* Journal of the American Chemical Society, 2009. **131**(15): p. 5386-+.
468. Tian, J., et al., *Respirable liquid marble for the cultivation of microorganisms.* Colloids and Surfaces B-Biointerfaces, 2013. **106**: p. 187-190.
469. Bormashenko, E., R. Balter, and D. Aurbach, *Micropump based on liquid marbles.* Applied Physics Letters, 2010. **97**(9).
470. Bormashenko, E., R. Balter, and D. Aurbach, *Use of Liquid Marbles as Micro-Reactors.* International Journal of Chemical Reactor Engineering, 2011. **9**.
471. Scadden, D.T., *The stem-cell niche as an entity of action.* Nature, 2006. **441**(7097): p. 1075-1079.
472. Cukierman, E., R. Pankov, and K.M. Yamada, *Cell interactions with three-dimensional matrices.* Current Opinion in Cell Biology, 2002. **14**(5): p. 633-639.
473. Battista, S., et al., *The effect of matrix composition of 3D constructs on embryonic stem cell differentiation.* Biomaterials, 2005. **26**(31): p. 6194-6207.
474. Streuli, C., *Extracellular matrix remodelling and cellular differentiation.* Current Opinion in Cell Biology, 1999. **11**(5): p. 634-640.

475. Tabata, Y., *Biomaterial technology for tissue engineering applications.* Journal of the Royal Society Interface, 2009. **6**: p. S311-S324.
476. Dawson, E., et al., *Biomaterials for stem cell differentiation.* Advanced Drug Delivery Reviews, 2008. **60**(2): p. 215-228.
477. Park, K., K.R. Kamath, and H. Park, *Biodegradable hydrogel for delivery of protein drugs* Abstracts of Papers of the American Chemical Society, 1993. **205**: p. 474-POLY.
478. Salinas, C.N. and K.S. Anseth, *The enhancement of chondrogenic differentiation of human mesenchymal stem cells by enzymatically regulated RGD functionalities.* Biomaterials, 2008. **29**(15): p. 2370-2377.
479. Drury, J.L. and D.J. Mooney, *Hydrogels for tissue engineering: scaffold design variables and applications.* Biomaterials, 2003. **24**(24): p. 4337-4351.
480. Xu, X., et al., *Hyaluronic acid-based hydrogels: from a natural polysaccharide to complex networks.* Soft Matter, 2012. **8**(12): p. 3280-3294.
481. Lee, J., M.J. Cuddihy, and N.A. Kotov, *Three-dimensional cell culture matrices: State of the art.* Tissue Engineering Part B-Reviews, 2008. **14**(1): p. 61-86.
482. Safinia, L., A. Mantalaris, and A. Bismarck, *Nondestructive technique for the characterization of the pore size distribution of soft porous constructs for tissue engineering.* Langmuir, 2006. **22**(7): p. 3235-3242.
483. Stevens, M.M. and J.H. George, *Exploring and engineering the cell surface interface.* Science, 2005. **310**(5751): p. 1135-1138.
484. Gitsov, I. and C. Zhu, *Amphiphilic hydrogels constructed by poly(ethylene glycol) and shape-persistent dendritic fragments.* Macromolecules, 2002. **35**(22): p. 8418-8427.
485. Drumheller, P.D. and J.A. Hubbell, *Densely cross-linked polymer networks of poly(ethylene glycol) in trimethylolpropane triacrylate for cell-adhesion-resistant surfaces* Journal of Biomedical Materials Research, 1995. **29**(2): p. 207-215.
486. Moutos, F.T., L.E. Freed, and F. Guilak, *A biomimetic three-dimensional woven composite scaffold for functional tissue engineering of cartilage.* Nature Materials, 2007. **6**(2): p. 162-167.
487. Kim, S. and K.E. Healy, *Synthesis and characterization of injectable poly(N-isopropylacrylamide-co-acrylic acid) hydrogels with proteolytically degradable cross-links.* Biomacromolecules, 2003. **4**(5): p. 1214-1223.
488. Peppas, N.A., et al., *Physicochemical, foundations and structural design of hydrogels in medicine and biology.* Annual Review of Biomedical Engineering, 2000. **2**: p. 9-29.
489. Kobayashi, M. and M. Oka, *Characterization of a polyvinyl alcohol-hydrogel artificial articular cartilage prepared by injection molding.* Journal of Biomaterials Science-Polymer Edition, 2004. **15**(6): p. 741-751.
490. Burczak, K., E. Gamian, and A. Kochman, *Long-term in vivo performance and biocompatibility of poly(vinyl alcohol) hydrogel macrocapsules for hybrid-type artificial pancreas.* Biomaterials, 1996. **17**(24): p. 2351-2356.
491. Barnes, C.P., et al., *Nanofiber technology: Designing the next generation of tissue engineering scaffolds.* Advanced Drug Delivery Reviews, 2007. **59**(14): p. 1413-1433.
492. Yang, F., et al., *Electrospinning of nano/micro scale poly(L-lactic acid) aligned fibers and their potential in neural tissue engineering.* Biomaterials, 2005. **26**(15): p. 2603-2610.
493. Zarkoob, S., et al., *Structure and morphology of electrospun silk nanofibers.* Polymer, 2004. **45**(11): p. 3973-3977.
494. Vacanti, C.A., *History of tissue engineering and a glimpse into its future.* Tissue Engineering, 2006. **12**(5): p. 1137-1142.
495. Akins, R.E., et al., *Cardiac organogenesis in vitro: Reestablishment of three-dimensional tissue architecture by dissociated neonatal rat ventricular cells.* Tissue Engineering, 1999. **5**(2): p. 103-118.
496. Freed, L.E., et al., *Advanced tools for tissue engineering: Scaffolds, bioreactors, and signaling.* Tissue Engineering, 2006. **12**(12): p. 3285-3305.
497. Zimmermann, W.H., I. Melnychenko, and T. Eschenhagen, *Engineered heart tissue for regeneration of diseased hearts.* Biomaterials, 2004. **25**(9): p. 1639-1647.

498. Sisson, K., et al., *Evaluation of Cross-Linking Methods for Electrospun Gelatin on Cell Growth and Viability.* Biomacromolecules, 2009. **10**(7): p. 1675-1680.
499. Bissell, D.M., et al., *Support of cultured-hepatocytes by a laminin-rich gel- evidence for a functionally significant subendothelial matrix in normal rat-liver* Journal of Clinical Investigation, 1987. **79**(3): p. 801-812.
500. Qi, A., et al., *Hydroxypropyl Cellulose Methacrylate as a Photo-Patternable and Biodegradable Hybrid Paper Substrate for Cell Culture and Other Bioapplications.* Advanced Healthcare Materials, 2013: p. n/a-n/a.
501. Willerth, S.M., et al., *Optimization of fibrin scaffolds for differentiation of murine embryonic stem cells into neural lineage cells.* Biomaterials, 2006. **27**(36): p. 5990-6003.
502. Liu, H., S.F. Collins, and L.J. Suggs, *Three-dimensional culture for expansion and differentiation of mouse embryonic stem cells.* Biomaterials, 2006. **27**(36): p. 6004-6014.
503. Garreta, E., et al., *Fabrication of a three-dimensional nanostructured biomaterial for tissue engineering of bone.* Biomolecular Engineering, 2007. **24**(1): p. 75-80.
504. Perets, A., et al., *Enhancing the vascularization of three-dimensional porous alginate scaffolds by incorporating controlled release basic fibroblast growth factor microspheres.* Journal of Biomedical Materials Research Part A, 2003. **65A**(4): p. 489-497.
505. Magyar, J.P., et al., *Mass production of embryoid bodies in microbeads.* Bioartificial Organs Iii: Tissue Sourcing, Immunoisolation, and Clinical Trials, 2001. **944**: p. 135-143.
506. Martson, M., et al., *Biocompatibility of cellulose sponge with bone.* European Surgical Research, 1998. **30**(6): p. 426-432.
507. Miyamoto, T., et al., *Tissue biocompatibility of cellulose and its derivatives* Journal of Biomedical Materials Research, 1989. **23**(1): p. 125-133.
508. Poustis, J., C. Baquey, and D. Chauveaux, *Mechanical properties of cellulose in orthopaedic devices and related environments.* Clinical materials, 1994. **16**(2): p. 119-24.
509. Tate, M.C., et al., *Biocompatibility of methylcellulose-based constructs designed for intracerebral gelation following experimental traumatic brain injury.* Biomaterials, 2001. **22**(10): p. 1113-1123.
510. Rodriguez, K., S. Renneckar, and P. Gatenholm, *Biomimetic Calcium Phosphate Crystal Mineralization on Electrospun Cellulose-Based Scaffolds.* Acs Applied Materials & Interfaces, 2011. **3**(3): p. 681-689.
511. Entcheva, E., et al., *Functional cardiac cell constructs on cellulose-based scaffolding.* Biomaterials, 2004. **25**(26): p. 5753-5762.
512. Ko, H.-F., C. Sfeir, and P.N. Kumta, *Novel synthesis strategies for natural polymer and composite biomaterials as potential scaffolds for tissue engineering.* Philosophical Transactions of the Royal Society a-Mathematical Physical and Engineering Sciences, 2010. **368**(1917): p. 1981-1997.
513. De Bartolo, L., et al., *Evaluation of cell behaviour related to physico-chemical properties of polymeric membranes to be used in bioartificial organs.* Biomaterials, 2002. **23**(12): p. 2485-2497.
514. Takata, T., H.L. Wang, and M. Miyauchi, *Migration of osteoblastic cells on various guided bone regeneration membranes.* Clinical Oral Implants Research, 2001. **12**(4): p. 332-338.
515. Risbud, M.V. and R.R. Bhonde, *Suitability of cellulose molecular dialysis membrane for bioartificial pancreas: In vitro biocompatibility studies.* Journal of Biomedical Materials Research, 2001. **54**(3): p. 436-444.
516. LaIuppa, J.A., et al., *Culture materials affect ex vivo expansion of hematopoietic progenitor cells.* Journal of Biomedical Materials Research, 1997. **36**(3): p. 347-359.
517. Mastropietro, D.J. and H. Omidian, *Prevalence and trends of cellulosics in pharmaceutical dosage forms.* Drug Development and Industrial Pharmacy, 2013. **39**(2): p. 382-392.
518. Pachence J.M., M.P. Bohrer, and J. Kohn, *Biodegradable polymers.* Principles of Tissue Engineering (Third Edition), 2007: p. 323-339.
519. Chamberlain, G., et al., *Concise review: Mesenchymal stem cells: Their phenotype, differentiation capacity, immunological features, and potential for homing.* Stem Cells, 2007. **25**(11): p. 2739-2749.

520. Canton, I., et al., *Real time detection of stress in 3D tissue engineered constructs using NF-kB activation in transiently transfected human dermal fibroblasts.* Tissue Engineering, 2007. **13**(7): p. 1750-1750.
521. O'Brien, F.J., et al., *Influence of freezing rate on pore structure in freeze-dried collagen-GAG scaffolds.* Biomaterials, 2004. **25**(6): p. 1077-1086.
522. Pampaloni, F., E.G. Reynaud, and E.H.K. Stelzer, *The third dimension bridges the gap between cell culture and live tissue.* Nature Reviews Molecular Cell Biology, 2007. **8**(10): p. 839-845.
523. Mandal, B.B. and S.C. Kundu, *Cell proliferation and migration in silk fibroin 3D scaffolds.* Biomaterials, 2009. **30**(15): p. 2956-2965.
524. Lien, S.-M., L.-Y. Ko, and T.-J. Huang, *Effect of pore size on ECM secretion and cell growth in gelatin scaffold for articular cartilage tissue engineering.* Acta Biomaterialia, 2009. **5**(2): p. 670-679.
525. Chen, G.P., T. Ushida, and T. Tateishi, *Scaffold design for tissue engineering.* Macromolecular Bioscience, 2002. **2**(2): p. 67-77.
526. Levenberg, S., et al., *Engineering vascularized skeletal muscle tissue.* Nature Biotechnology, 2005. **23**(7): p. 879-884.
527. Hollister, S.J., *Porous scaffold design for tissue engineering.* Nature Materials, 2005. **4**(7): p. 518-524.
528. Vihola, H., et al., *Drug Release Characteristics of Physically Cross-Linked Thermosensitive Poly(N-vinylcaprolactam) Hydrogel Particles.* Journal of Pharmaceutical Sciences, 2008. **97**(11): p. 4783-4793.
529. Feil, H., et al., *Effect of comonomer hydrophilicity and ionization on the lower critical solution temperature of N-isopropylacrylamide copolymers* Macromolecules, 1993. **26**(10): p. 2496-2500.
530. Shimizu, K., H. Fujita, and E. Nagamori, *Oxygen Plasma-Treated Thermoresponsive Polymer Surfaces for Cell Sheet Engineering.* Biotechnology and Bioengineering, 2010. **106**(2): p. 303-310.
531. Twaites, B.R., et al., *Thermoresponsive polymers as gene delivery vectors: Cell viability, DNA transport and transfection studies.* Journal of Controlled Release, 2005. **108**(2-3): p. 472-483.
532. Kumashiro, Y., M. Yamato, and T. Okano, *Cell Attachment-Detachment Control on Temperature-Responsive Thin Surfaces for Novel Tissue Engineering.* Annals of Biomedical Engineering, 2010. **38**(6): p. 1977-1988.
533. Varghese, V.M., et al., *In vitro cytocompatibility evaluation of a thermoresponsive NIPAAm-MMA copolymeric surface using L929 cells.* Journal of Materials Science-Materials in Medicine, 2010. **21**(5): p. 1631-1639.
534. Roth, P.J., T.P. Davis, and A.B. Lowe, *Comparison between the LCST and UCST Transitions of Double Thermoresponsive Diblock Copolymers: Insights into the Behavior of POEGMA in Alcohols.* Macromolecules, 2012. **45**(7): p. 3221-3230.
535. Li, Z. and J. Guan, *Thermosensitive hydrogels for drug delivery.* Expert Opinion on Drug Delivery, 2011. **8**(8): p. 991-1007.
536. Jiang, W.-W., et al., *Phagocyte responses to degradable polymers.* Journal of Biomedical Materials Research Part A, 2007. **82A**(2): p. 492-497.
537. Levenberg, S. and R. Langer, *Advances in tissue engineering.* Current Topics in Developmental Biology, Vol. 61, 2004. **61**: p. 113-+.
538. Lanza, R., R. Langer, and J. Vacanti, *Principles of tissue engineering* Principles of Tissue Engineering, 3rd Edition, ed. R. Lanza, R. Langer, and J. Vacanti2007. XXXI-XXXI.
539. Kim, H., et al., *The effect of estrogen compounds on human embryoid bodies.* Reproductive sciences (Thousand Oaks, Calif.), 2013. **20**(6): p. 661-9.
540. Kim, Y.Y., et al., *Use of Long-tenn Cultured Embryoid Bodies May Enhance Cardiomyocyte Differentiation by BMP2.* Yonsei Medical Journal, 2008. **49**(5): p. 819-827.

541. Burridge, P.W., et al., *Improved human embryonic stem cell embryoid body homogeneity and cardiomyocyte differentiation from a novel V-96 plate aggregation system highlights interline variability.* Stem Cells, 2007. **25**(4): p. 929-938.
542. Hammond, T.G. and J.M. Hammond, *Optimized suspension culture: the rotating-wall vessel.* American Journal of Physiology-Renal Physiology, 2001. **281**(1): p. F12-F25.
543. Harrison, J., et al., *Colonization and maintenance of murine embryonic stem cells on poly(alpha-hydroxy esters).* Biomaterials, 2004. **25**(20): p. 4963-4970.
544. Chen, S.S., et al., *Multilineage differentiation of rhesus monkey embryonic stem cells in three-dimensional culture systems.* Stem Cells, 2003. **21**(3): p. 281-295.
545. Noiset, O., Y.J. Schneider, and J. Marchand-Brynaert, *Fibronectin adsorption or and covalent grafting on chemically modified PEEK film surfaces.* Journal of Biomaterials Science-Polymer Edition, 1999. **10**(6): p. 657-677.
546. Ko, I.K. and H. Iwata, *An approach to constructing three-dimensional tissue*, in *Bioartificial Organs Iii: Tissue Sourcing, Immunoisolation, and Clinical Trials*, D. Hunkeler, et al., Editors. 2001. p. 443-455.
547. Yang, M.-J., et al., *Novel method of forming human embryoid bodies in a polystyrene dish surface-coated with a temperature-responsive methylcellulose hydrogel.* Biomacromolecules, 2007. **8**(9): p. 2746-2752.
548. Hoo, S.P., et al., *Preparation of a soft and interconnected macroporous hydroxypropyl cellulose methacrylate scaffold for adipose tissue engineering.* Journal of Materials Chemistry B, 2013. **1**(24): p. 3107-3117.
549. Vinatier, C., et al., *An Injectable Cellulose-Based Hydrogel for the Transfer of Autologous Nasal Chondrocytes in Articular Cartilage Defects.* Biotechnology and Bioengineering, 2009. **102**(4): p. 1259-1267.
550. Chang, C., et al., *Superabsorbent hydrogels based on cellulose for smart swelling and controllable delivery.* European Polymer Journal, 2010. **46**(1): p. 92-100.
551. Ye, S.H., et al., *Antifouling blood purification membrane composed of cellulose acetate and phospholipid polymer.* Biomaterials, 2003. **24**(23): p. 4143-4152.
552. Jiang Huang, Marc A Unger, and Shoujun Xiao, *Polymer surface modification.* 2011.
553. Tang SKY and Whitesides GM, *Basic Microfluidic and Soft Lithographic Techniques, In Optofluidics: Fundamentals, Devices and Applications.*2010
554. Albrecht, W., et al., *Amination of poly(ether imide) membranes using di- and multivalent amines.* Macromolecular Chemistry and Physics, 2003. **204**(3): p. 510-521.
555. Zhang, L., N. Zhao, and J. Xu, *Fabrication and application of superhydrophilic surfaces: a review.* Journal of Adhesion Science and Technology, 2014. **28**(8-9): p. 769-790.
556. Peterson, S.L., et al., *Poly(dimethylsiloxane) thin films as biocompatible coatings for microfluidic devices: Cell culture and flow studies with glial cells.* Journal of Biomedical Materials Research Part A, 2005. **72A**(1): p. 10-18.
557. Smith, P.K., et al., *MEASUREMENT OF PROTEIN USING BICINCHONINIC ACID.* Analytical Biochemistry, 1985. **150**(1): p. 76-85.
558. *Pierce™ BCA Protein Assay Kit.* Available from: http://www.piercenet.com/instructions/2161296.pdf.
559. C-PS, H., *infrared spectroscopy. In: Settle F, (eds), Handbook of instrumental techniques for analytical chemistry.* 1997. **Chapter 15**: p. 247–283.
560. Hass, R. and C. Bertram, *Characterization of human breast cancer epithelial cells (HBCEC) derived from long term cultured biopsies.* Journal of Experimental & Clinical Cancer Research, 2009. **28**.

Chapter 3:Development and Surface Functionalization of PDMS based Micro-bioreactor

3.1 General Overview

Chapter 3 compromises one publication as a full paper.

Cell anchorage is a strict requirement for survival of most cell types. Studies showed that their adhesion to the substrate has a critical role in many cellular functions including migration, proliferation, differentiation, and apoptosis [538, 539]. Many polymer systems promote the physical adsorption of cell adhesion molecules from surrounding fluids due to a thermodynamic driving force, and proteins in solution are extensively deposited onto these hydrophobic surfaces.

In this paper, polydimethylsiloxane (PDMS) was surface functionalized by activation with oxygen plasma and treatment with trimethoxysilylpropyl(polyethyleneimine) followed by grafting with carboxylmethyl cellulose (CMC) to improve its hydrophobic and antifouling properties for further cell and microfluidic applications.

Acid Orange II assay was performed to confirm and quantify the amount of amine groups introduced on the PDMS substrate. It was observed that the amount of amine groups on treated surface was much higher than those on non-treated PDMS. Carboxylmethyl cellulose (CMC) was then grafted covalently onto the aminized surfaces. CMC was conjugated onto the aminized surface via EDC–NHS coupling to form a hydrophilic layer, preventing nonspecific protein adsorption. A protein adsorption assay using bovine serum albumin (BSA) showed that the introduction of CMC could reduce the adsorption of negatively charged BSA. CMC-modified PDMS surfaces showed protein-repelling properties. Confocal imaging also showed only very weak fluorescent signals on a CMC modified surface compared to the native one, indicating that the CMC functionalization was effective in preventing BSA adsorption. The stability of the amino-grafted PDMS (PDMS-NH2) and polysaccharide modified PDMS (PDMS-NH-CMC) surfaces were investigated using water contact measurement after 25 days by exposing to DI water. Both surfaces showed increase in hydrophilicity while polysaccharide modified PDMS remained more hydrophilic compared to aminized and native PDMS ones. Physiochemical properties of functionalized PDMS were also determined using attenuated total reflection Fourier transform infrared (ATR-FTIR) spectra. The results showed the presence of different peaks attributed to the carboxylic acid groups, which confirmed the successful grafting of CMC onto PDMS–NH.

Gelatin type B was conjugated onto the modified polydimethylsiloxane surface to improve cell adhesion ligands, to promote cell anchorage and to advance its cytocompatibility for cancer and

embryonic stem cells applications. Nucleus and cytoskeleton staining revealed that as expected, cancer cells appeared to form aggregates and were not attached to the native PDMS substrate. In contrast, cells adhered well onto PDMS–NH–CMC–GEL and proliferated until they reached confluence. In the case of ESCs, cells on PDMS–NH–CMC led to lower proliferation rates compared to that of the PDMS–NH–CMC–GEL culture, indicating that the cells did not adhere well onto the PDMS–NH–CMC substrate due to the lack of cell adhesion ligands. In contrast, cells grown on PDMS–NH–CMC–GEL appeared to be larger with more spatially dispersed bodies. *In vitro* cultivation of breast cancer cells and mouse embryonic stem cells on the bioactive polydimethylsiloxane showed a significant increase in number of viable cells, while cells retained their proliferation ability and normal morphology during culturing on modified surface.

The potential application of the bio-functionalized polydimethylsiloxane in a microfluidic application was also investigated by fabrication of a micro-bioreactor in the form of a fixed bed bioreactor with a microchannel reactor bed. The PDMS microchannel was fabricated using the photolithographic fabrication method. The inner surface of microchannel was modified with the abovementioned protocol and cells were seeded inside the channels. Live/dead staining was performed using Calcein^{AM} to confirm the viability of cells inside microchannels after 4 days. The results revealed that the majority of cells remained viable (stained in green) inside the microchannel and demonstrated the ability of the present method to support cell cultivation. The results demonstrate a facile method for surface bio-functionalization of PDMS as a micro-bioreactor with CMC towards potential applications in stem cells and microfluidic applications. This work demonstrates the potential of applying polysaccharides in a PDMS microfluidics-based cellular study.

3.2 Surface Functionalization of PDMS for Potential Micro-bioreactor and Embryonic Stem Cell Culture Applications

Journal of
Materials Chemistry B

RSC Publishing

PAPER

Surface-functionalization of PDMS for potential micro-bioreactor and embryonic stem cell culture applications

Cite this: *J. Mater. Chem. B*, 2013, **1**, 987

Fatemeh Sarvi,[a] Zhilian Yue,[bc] Kerry Hourigan,[a] Mark C. Thompson[a] and Peggy P. Y. Chan*[cd]

Received 24th August 2012
Accepted 22nd November 2012

DOI: 10.1039/c2tb00019a

www.rsc.org/MaterialsB

This study presents a novel and inexpensive method to prepare a disposable micro-bioreactor for stem cell expansion. The micro-bioreactor was fabricated in the form of a fixed bed bioreactor with a microchannel reactor bed. The micro-bioreactor was constructed from polydimethylsiloxane (PDMS), and the microchannel was functionalized to enable cell adhesion and resistance to bovine serum albumin protein adsorption. The PDMS reactor bed surface was activated by oxygen plasma, then aminized with trimethoxysilylpropyl(polyethyleneimine), followed by grafting with carboxylmethyl cellulose (CMC) and gelatin in sequence. The functionalized PDMS surface demonstrated improved hydrophilicity and antifouling properties. The grafting of gelatin promoted cell adhesion. The functionalized surface was found to be biocompatible with MDA-MB-231 and Oct4b2 cells and was demonstrated to facilitate cell proliferation. The expanded Oct4b2 cells retained their proliferation potential, undifferentiated phenotype and pluripotency.

Introduction

Embryonic stem cells (ESCs) are pluripotent cells with unlimited self-replicating ability; more importantly, they have the potential to differentiate (pluripotency) into all types of cells with different functions both *in vitro* and *in vivo*.[1] ESCs are excellent choices of an *in vitro* cell model for regenerative medicine, functional genomics, human developmental biology and drug discovery study. However, the use of these cells requires a readily available source of stem cells and/or their differentiated derivatives outside a living body, which is a challenge in their cultivation. Unlike many traditional processes that use a cell's capability to produce a protein, the use of stem cells aims to generate the cells themselves as the product. Some of the applications will benefit from the direct expansion of stem cells (for example, hematopoietic stem cell transplantation),[2] whereas others will require the production of a specific differentiated cell type with defined characteristics. This can be done either by controlling the differentiation in a very specific path or by elimination of undesirable cell types that could arise during the production (differentiation) process. The present day exponentially growing effort of stem cell research is having a major need for convergence of more efficient and appropriate laboratory technologies to sustain the growth. One such technology is the bioreactor system, which can be defined as an industrial form of the contained reaction vessel with well-defined, controlled conditions for specific culture outcomes.[3] Compared with static culture conditions, the use of bioreactors can overcome some limitations of static culture, including the lack of mixing and the need for frequent medium replacement rates.[4] For instance, a recent study has shown that induced pluripotent stem cells can be generated more efficiently in a stirred culture compared to a static culture.[5] However, the success of maximum expansion of stem cells is dependent not only on the bioreactor design but also on several other parameters. It is well known that stem cells can start to differentiate into mature tissue cells and lose their pluripotency when they are exposed to the intrinsic properties of their extracellular matrix (ECM). ECM stimuli, including matrix structure, chemistry, substrate elasticity, and the presence of growth factors, can elicit stem cell differentiation.[6,7] The manipulation of the intrinsic parameters may render these cells unsuitable for various uses, and hence optimization of the extrinsic parameters is a more suitable method for the purpose of getting maximum expansion of stem cells in a bioreactor.

Microfluidic devices expand our ability to control material transport, and material manipulation, at the micro-scale. Microfluidic systems are particularly advantageous for biological and medical applications; these advantages include the ability to create bio-mimetic structures that mimic the *in vivo* cellular microenvironment,[8] allow experimental parallelization under well-controlled conditions, reduce reagent consumption, and require shorter sample analysis time.[9] Micro-bioreactors are the miniaturized versions of conventional bioreactors,

[a]*Department of Mechanical and Aerospace Engineering and Division of Biological Engineering, Monash University, Clayton, Australia*
[b]*Intelligent Polymer Research Institute, University of Wollongong, Australia*
[c]*School of Applied Science, RMIT University, Australia.* [redacted]
[d]*Melbourne Centre for Nanofabrication, Australia*

where high-throughput cell based assays can be carried out at low cost compared with their macro-scale counter-parts. For the development of a micro-bioreactor for stem cell expansion, the micro-bioreactor should mimic the *in vivo* microenvironment of stem cells in order to retain the self-replicating ability and pluripotency of stem cells. The construction materials for the micro-bioreactor should be carefully chosen avoiding stimuli such as growth factors, but yet they should be biocompatible and should be surface functionalized to provide cell adhesion sites, since pluripotent stem cells are anchorage dependent.[1]

Polydimethylsiloxane (PDMS) is a popular material which has been widely used for microfluidic device construction, especially for biological applications due to its attractive properties, including elastomeric properties that are similar to soft biological tissues, biocompatibility, optical transparency, high gas permeability, ease of fabrication (simple fabrication by replica molding), and cost effectiveness.[10–12] Despite the advantages of PDMS, the major drawbacks of using untreated PDMS are its low cell adhesiveness, high hydrophobicity, which restricts fluid flow in microchannels, and surface fouling problems, resulting in substantial sample loss and low device performance.

The properties of micro-bioreactor surfaces have a strong influence on cell analysis. A micro-bioreactor surface should be able to support cell growth, and should be protein resistant in order to prevent undesired adsorption of analyte molecules such as protein and DNA. The native PDMS surface is not suitable for stem cell cultivation; when using a PDMS based micro-bioreactor, the PDMS surface should be functionalized to prevent protein adsorption, to avoid contamination and to minimize the loss of precious samples that are of micro/nano volume.[13] PDMS surfaces can be functionalized by plasma treatment to create silanol groups. The activated surface is then functionalized with amine groups as anchors for further grafting with a hydrophilic polymer to prevent protein adsorption. (3-Aminopropyl)triethoxysilane (APTES) and (3-aminopropyl) trimethoxysilane (APTMS) are organosilanes that are commonly used to introduce amine groups for further protein or biomolecule immobilization on microfluidic devices.[14]

This study presents a novel and inexpensive method to prepare a disposable micro-bioreactor for stem cell expansion. The micro-bioreactor was constructed using PDMS in the form of a fixed bed reactor with a microchannel serving as the reactor bed. A method to functionalize the micro-bioreactor to facilitate stem cell adhesion and propagation was developed. Herein, trimethoxysilylpropyl(polyethyleneimine) was investigated as an alternative organosilane for micro-bioreactor surface aminization. Trimethoxysilylpropyl(polyethyleneimine) has been shown to aminize PDMS surfaces more efficiently compared with APTMS and *N*-(3-trimethoxysilylpropyl)diethylenetriamine,[15] due to the presence of multiple amines per molecule. Carboxymethyl cellulose (CMC) is a derivative of cellulose that is commonly used as a Food and Drug Administration (FDA)-approved disintegrate in pharmaceutical manufacturing.[16] It is water-soluble, biocompatible and available abundantly at low cost, making it an attractive biomaterials candidate. CMC has been employed as a wound dressing material and a co-excipient with drugs.[17] CMC has been demonstrated to inhibit postsurgical and postoperative adhesions.[18–20] This study investigated the potential of using CMC as a low-cost non-fouling material. The aminized PDMS microchannel was further functionalized with CMC, and the resulting protein resistance was examined.

Most mammalian cells are anchorage dependent. Cell adhesion is essential for organogenesis, wound healing, tissue homeostasis and remodelling. Cell attachment to a proper anchoring surface also plays an important role in regulating cell survival, cell cycle progression, and tissue-specific phenotype expression. Abnormal adhesion processes can lead to many pathological conditions such as tumour metastatic invasion and blood clotting defects.[21] PDMS and CMC possess many favourable properties that make them attractive as a material for microfluidic device fabrication, but they both lack ligands that mediate cell adhesion.

Gelatin derived from collagen has widely been used for pharmaceutical and medical applications due to its abundant availability, cost-effectiveness, excellent biodegradability and biocompatibility, and non-immunogenic properties.[22] It is known that gelatin contains arginine–glycine–aspartate (RGD) motifs; RGD peptides provide a high-affinity site for cell binding, and are often incorporated in biomaterials to promote cell adhesion.[23,24] Therefore, the CMC functionalized microchannel was further functionalized with gelatin, which contains RGD peptides to promote cell–substrate adhesion. The performance of the bio-functionalized micro-bioreactor was evaluated for its performance in facilitating cell expansion. The ability of the bio-functionalized surface to maintain stem cell pluripotency was also evaluated.

Experimental

Materials

PDMS substrates were prepared using a silicon elastomer kit (Sylgard 184, Dow Corning, MI) and mixed at a 1 : 10 curing agent to base ratio. Trimethoxysilylpropyl(polyethyleneimine) (50% in isopropanol) (M_w = 2000–4000) was purchased from GelestInc, USA. *N*-Hydroxysuccinimide (NHS), 1-ethyl-3-(3-dimethylaminopropyl)carbodiimide hydrochloride (EDC), carboxymethyl cellulose sodium salt (CMC, M_w ~ 90 kDa), albumin–fluorescein isothiocyanate conjugate (BSA–FITC), bovine serum albumin (BSA), acid orange II, and 2-(*N*-morpholiino)ethane sulfonic acid (MES) were purchased from Sigma-Aldrich, Australia. Calcein AM, 4′,6-diamidino-2-phenylindole, dilactate (DAPI), Texas Red®-X phalloidin, Dulbecco's modified Eagle's medium (DMEM), non-essential amino acids, GlutaMAX™, and penicillin–streptomycin were obtained from Life Technologies, Australia. *n*-Hexane was obtained from Merck. Gelatin (M_w = 80–140 kDa) was obtained from Wako. Unless stated otherwise, all other chemicals were purchased from Sigma-Aldrich, Australia.

Fabrication of PDMS microchannels

The PDMS microchannel was fabricated using the photolithographic fabrication method. A dark field photomask with a

microchannel pattern of 200 μm width, 50 μm height and 3 cm length was designed using AutoCAD. Standard photolithography was employed to fabricate the Si master mold for PDMS replication. In brief, SU8-2050 (Microchem) was spin coated on a wafer at 500 and 1500 rpm for 5 s and 30 s, respectively. The spun coated wafer was placed on a hotplate at 65 °C and 95 °C in sequence for 5 min and 20 min, respectively. The wafer was then allowed to cool to RT. The photomask was lowered over the photoresist coated wafer to form a sandwich assembly, and was irradiated under UV at 240 mJ cm^{-2} in a Contact Aligner (Mask Aligner, EVG 620). After UV-irradiation, the wafer was baked at 65 °C for 5 min followed by 95 °C for 10 min and then cooled down to RT. The wafer was subsequently developed for 15 min followed by rinsing in acetone and isopropyl alcohol (IPA) before drying with dry nitrogen. The patterned master mold was placed in a Petri dish.

The PDMS prepolymer was cast onto the silica master mold. After curing at 85 °C for 4 h, the PDMS microchannel replica was gently peeled off from the master mold and cut into a rectangular plate of dimension 2 × 3 cm^2 to prepare microbioreactor assemblies. Holes for inlet and outlet ports at both ends of the microchannel were punched with a syringe needle. The PDMS substrates were then washed with hexane for 2 days to remove the uncured prepolymer, followed by isopropanol to remove contaminants.

Aminization of PDMS substrates (PDMS–NH_2)

The PDMS substrate containing the microchannel pattern was activated by oxygen plasma treatment at 1000 mTorr for 60 s in a plasma cleaner (Harrick Plasma, PDC-001/002, USA) to generate silanol groups, and then bound to a microscope slide immediately to allow irreversible sealing (Fig. 1). The microchannel was filled with 4% (v/v) trimethoxysilylpropyl(polyethyleneimine) in acetone in a single injection using a syringe, and allowed to react for 2 h at RT. The modified microchannel was rinsed with ethanol and deionized (DI) water to remove any unbound polymer, and dried at 65 °C for 3 h. The microchannel was then equilibrated with MES buffer (50 mM, pH 5.0) for next step modification. The aminized PDMS substrate is denoted as PDMS–NH_2.

Determination of amine content

The amount of surface accessible amine was quantified using an Acid Orange II assay.[25] In brief, PDMS films were cut into 2 × 2 cm^2 samples and aminized according to the above aminization protocol; samples were incubated in 1 ml of Acid Orange II solution in DI water (500 μM, pH 3) overnight at RT. Unbound Acid Orange II was removed by washing the samples with copious water at pH 3 (adjusted by HCl). The samples were then incubated in 1 ml of DI water at pH 12 (adjusted with NaOH) overnight to allow the bound dye to detach. The amount of the bound dye was quantified by measuring the optical density at 492 nm. Unmodified PDMS substrates served as controls. A series of Acid Orange II standard solutions (100–500 μM) were prepared in DI water at pH 12 and used to establish the standard curve. The amount of surface amine groups was calculated based on the assumption that each Acid Orange II molecule complexes with one molecule of the amine.

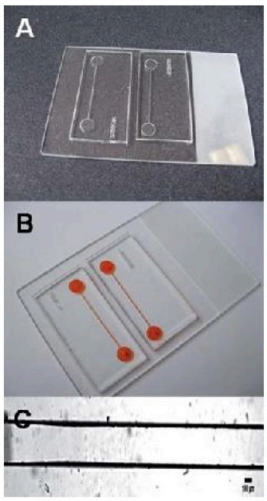

Fig. 1 Photos of (A) a PDMS micro-bioreactor, (B) a food-dye filled micro-bioreactor device showing inlets, outlets and microchannels, (C) an enlarged bright field view of a microchannel, photo taken under an optical microscope (scale bar = 100 μm).

Surface grafting of CMC onto PDMS–NH_2 substrates (PDMS–NH–CMC)

EDC and NHS (1 : 1) were added to 0.6 mg ml^{-1} CMC in MES buffer (50 mM, pH 5.0) to obtain a final concentration of 2.0 mg ml^{-1}, and allowed to react for 30 min at RT. The activated CMC solution prepared according to the above procedures was injected into the PDMS–NH_2 microchannel until the microchannel was fully filled, and was allowed to react at RT overnight. The microchannels were then rinsed by injecting MilliQ water to remove residual reagents followed by injecting 0.1 MES buffer. The samples were dried in an oven at 65 °C for 3 h. The CMC grafted substrate is denoted as PDMS–NH–CMC.

Surface grafting of gelatin onto PDMS–NH–CMC substrates (PDMS–NH–CMC-GEL)

Conjugation of gelatin on PDMS–NH–CMC was performed under aseptic conditions. PDMS–NH–CMC microchannels were first sterilized in 70% ethanol overnight. One ml of EDC (2.0 mg ml^{-1}) and NHS (2.0 mg ml^{-1}) in MES buffer (pH 5) was filter sterilized before injecting into a PDMS–NH–CMC microchannel in a single-injection until the microchannel was fully filled. After reacting for 30 min at RT, sterile gelatin solution (300 μg ml^{-1}) in phosphate buffered saline (PBS) was injected into the activated microchannel in a single-injection until the microchannel was fully filled, and allowed to react overnight at RT. The microchannel was then rinsed by injecting sterile MilliQ water followed by PBS. The gelatin-grafted substrate is denoted as PDMS–NH–CMC-GEL.

Surface characterization of functionalized PDMS substrates

To characterize the functionalized surfaces, PDMS films were cut into 2 × 2 cm^2 samples and functionalized according to the aminization and surface grafting procedures described above. The surface composition analysis of functionalized PDMS was carried out using Fourier Transform Infrared Spectroscopy (FTIR spectrometer, Spectrum 100 series, PerkinElmer, USA). Static water contact angle (WCA) measurements of functionalized PDMS substrates were performed using a sessile drop method (2 μl, MilliQ water) with an optical contact angle measuring instrument (OCA20, Dataphysics Instruments GmbH, Germany). The measurements were performed on at least three different areas on each substrate and the values were averaged. To assess the stability of surface functionalization, the WCAs of PDMS–NH_2 and PDMS–NH–CMC were monitored over a period of 25 days.

Protein adsorption

Protein adsorption of functionalized substrates was investigated using a method modified from Goda *et al.*[26] In brief, after being equilibrated in PBS at RT overnight, samples with a defined size (4.0 cm^2) were immersed in a freshly prepared BSA solution (3 mg ml^{-1}, 1 ml per sample). Adsorptions were allowed to proceed at RT overnight under gentle shaking. The samples were then rinsed with PBS and treated with 1% sodium dodecyl sulphate (SDS) (1 ml per sample) for 20 min to remove the adsorbed protein. The amount of adsorbed protein was quantified using a Micro BCA protein assay kit (Thermo Scientific, Australia). In a separate study, protein adsorption on PDMS and PDMS–NH–CMC was visualized by treating the surface with BSA–FITC using a method modified from Ferrando *et al.*, 2005; Lu *et al.*, 2008; and Wei *et al.*, 2011,[27–29] and the images were acquired using a laser scanning confocal microscope (Nikon A1Rsi MP) with an excitation wavelength of 488 nm and an emission wavelength of 550 nm. The comparison images were obtained using the same confocal microscopy setting.

Cell culture

MDA-MB-231 (human mammary gland adenocarcinoma) and Oct4b2 (murine-derived embryonic stem cell) cell lines obtained from the Monash Institute of Medical Research (Clayton, VIC, Australia) were employed to investigate cell adhesion and proliferation onto the modified PDMS substrates. MDA-MB-231 cells were maintained in high glucose DMEM (11965, Gibco®) supplemented with 10% fetal bovine serum (FBS), and 1% penicillin–streptomycin at 37 °C in a humidified 5% CO_2 incubator. Oct4b2 cells were maintained in high glucose DMEM (11995, Gibco®) supplemented with 10% FBS (JRH Biosciences, Australia), 1% non-essential amino acids, 1% GlutaMAX™, 0.5% penicillin–streptomycin, 0.1 mM β-mercaptoethanol, and 1000 U ml^{-1} ESGRO Leukemia inhibitory factor (LIF, Chemicon, Australia). Prior to cell seeding, all substrates were sterilized in 70% ethanol overnight followed by rinsing with sterile PBS. MDA-MB-231 and Oct4b2 cells were seeded separately onto PDMS or the functionalized PDMS substrate at densities of 80 × 10^3 and 40 × 10^3 cell cm^{-2}, respectively. Pluripotency of Octb2 cells was monitored by examining their GFP expression using X71 Olympus fluorescence microscopes. The cell adhesion and cell growth were examined using optical microscopy and laser scanning confocal microscopy. Cell counting was performed using a hemocytometer after trypsinization. For visualization, the nucleus of cells was stained with DAPI, while the filamentous actin (F-actin) of cells was stained with Texas Red®-X phalloidin. In brief, samples were fixed with 4% formaldehyde for 20 min at RT and washed 3 times with 1× PBS buffer, and then permeabilized with 0.1% Triton X-100-PBS for 2 min, and washed with PBS. The samples were further incubated with 1% bovine serum albumin in PBS (BSA–PBS) for 15 min, followed by Texas Red®-X phalloidin (1/1000 in 1% BSA–PBS) staining for 1 hour. DAPI was then added to the samples and incubated for 5 min. Cell counting was also performed to quantify cell adhesion and cell proliferation.

Statistical analysis

All experiments were performed in at least 3 replicates. The results are presented as average values ± standard deviation. Multiple groups of data were statistically analyzed using ANOVA (analysis of variance); two groups of data were statistically analyzed using the unpaired Student's *t*-test, p values lower than 0.05 were considered statistically significant.

Results and discussion

Surface functionalization

Fig. 2 illustrates the scheme used for microchannel functionalization. Prior to surface functionalization, the PDMS substrates were washed with hexane to remove the uncured monomer, as the migration of low molecular weight species from the bulk to the surface is known as one of the major causes of hydrophobicity recovery of PDMS.[30] Oxygen plasma was employed to treat the PDMS substrate, as plasma treatment has been shown to preferentially remove organic contaminants as well as generate silanol (Si–OH) groups on PDMS.[31] The presence of hydrophilic silanol groups allows microchip sealing and further aminization. It is well known that the effect of plasma treatment is transient as hydrophobic recovery occurs.[31,32] Therefore immediately after plasma treatment, the PDMS substrate was bonded to a microchip to form an irreversible seal, trimethoxysilylpropyl(polyethyleneimine) was then quickly injected into the microchannel to introduce amine groups on the inner surface of the microchannel to form PDMS–NH_2.

CMC was conjugated onto the PDMS–NH_2 surface *via* EDC–NHS coupling to form a hydrophilic layer preventing non-specific protein adsorption. CMC grafting introduces carboxyl groups on the surface of PDMS–NH_2 to form PDMS–NH–CMC and enables further modification with desired biomolecules. An EDC-based coupling technique was employed as the EDC reagent does not remain as a part of the linkage, which eliminates the possibility of releasing cytotoxic agents when the polymer degrades. In addition the by-product produced by the

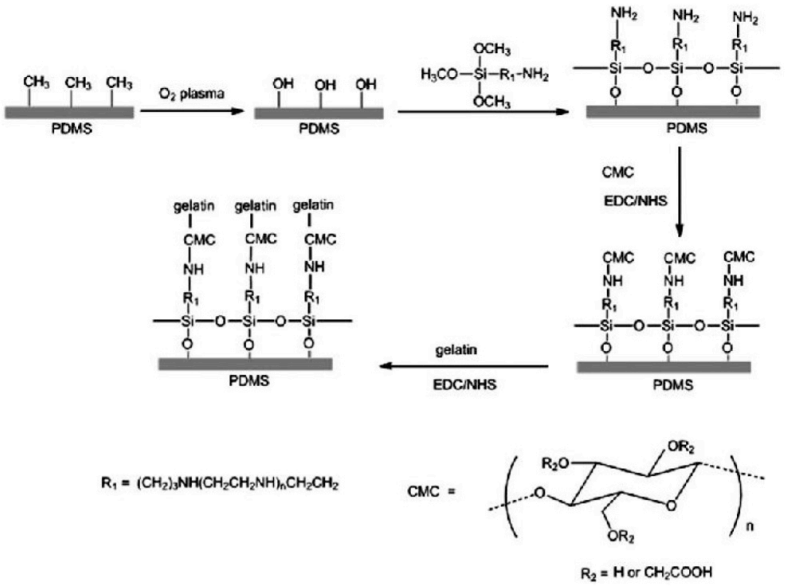

Fig. 2 Schematic illustration of the surface functionalization procedure.

coupling reaction is water-soluble and can be easily removed.[33] Gelatin, as a model biomolecule, was grafted onto PDMS–NH–CMC to form PDMS–NH–CMC-GEL *via* EDC–NHS coupling to promote cell–substrate interactions.

Physiochemical properties of functionalized PDMS

Acid Orange II assay was performed to confirm and quantify the amount of amine groups introduced on the PDMS substrate. Fig. 3 shows that the amount of amine present on PDMS–NH_2 is significantly higher than that on the non-treated PDMS substrate, indicating that the aminization process was successful.

Fig. 4 reveals the FTIR spectra of PDMS (curve A), PDMS–NH_2 (curve B), PDMS–NH–CMC (curve C), and PDMS–NH–CMC-GEL (curve D) substrates, respectively. It has been shown that polyethyleneimine alone has characteristic peaks at 1630 and 1565 cm^{-1}.[34] The PDMS–NH_2 spectrum (curve B) showed new bands at 1520–1720 cm^{-1} and 3360 cm^{-1}, arising from the NH deformation and NH stretching of the amine groups, respectively. The peak at ~1600 cm^{-1} on the PDMS–NH–CMC spectrum (curve C) is attributed to the carboxylic acid groups, which confirmed the successful grafting of CMC onto PDMS–NH_2.

Verification of the existence of successive functionalization of PDMS was obtained through WCA measurements as the functionalization was conducted. Fig. 5A shows the change in wettability of PDMS after each functionalization step. The WCA of native PDMS was found to be 116 ± 0.3°, which is consistent with the inherent hydrophobicity of PDMS. After the PDMS was aminized, the WCA of the resulting PDMS–NH_2 was found to be 55°, and the WCA decreased to 22° after further functionalization with CMC, indicating that the hydrophobic PDMS surface has been converted to a hydrophilic surface. The enhanced

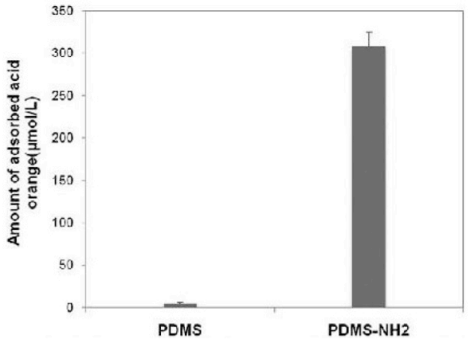

Fig. 3 Quantification of surface amine on native PDMS and PDMS–NH_2 by measuring the amount of adsorbed acid orange.

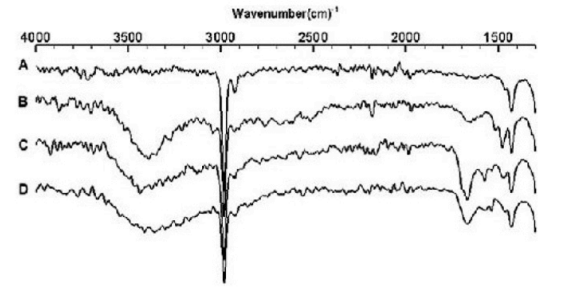

Fig. 4 FTIR spectra of (a) PDMS, (b) PDMS–NH_2, (c) PDMS–NH–CMC, and (d) PDMS–NH–CMC-GEL.

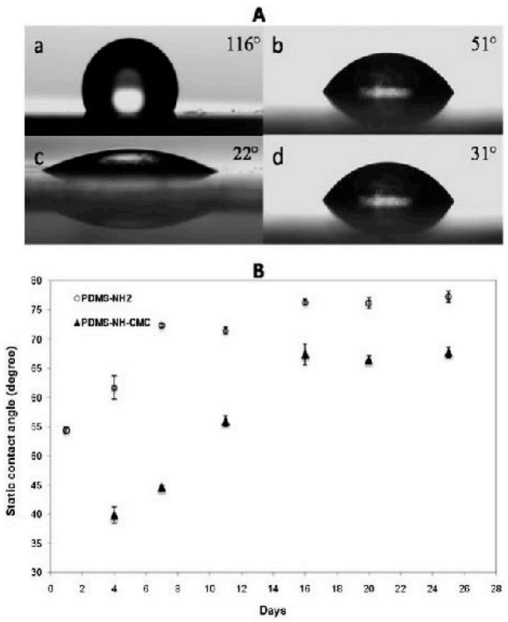

Fig. 5 (A) Static water contact angle of (a) PDMS, (b) PDMS–NH_2, (c) PDMS–NH–CMC, and (d) PDMS–NH–CMC-GEL substrates measured at day 1. (B) shows the variation of static contact angles of PDMS–NH_2 and PDMS–NH– CMC as a function of the storage time in air.

hydrophilicity is attributed to the surface hydroxyl and carboxylic acid groups on PDMS–NH–CMC. Further gelatin conjugation slightly increases the WCA from 22° to 31°, due to the presence of hydrophobic amino acid components on the modified surface. Nevertheless, the final characteristic of functionalized PDMS is still much more hydrophilic than native PDMS.

The WCAs of PDMS–$NH_2$and PDMS–NH–CMC were monitored for another 25 days to assess the stability of the surface functionalization. As shown in Fig. 5B, both PDMS–NH_2 and PDMS–NH–CMC substrates remained hydrophilic over a period of 16 days. After that time, the WCAs of PDMS–NH_2 and PDMS–NH–CMC become stabilized at around 67° and 77°, respectively. Although partial recovery of hydrophobicity was observed after 16 days, both PDMS–NH_2 and PDMS–NH–CMC substrates remain more hydrophilic compared to native PDMS that displayed a WCA of 116° (Fig. 5A). It was observed that the WCA of PDMS–NH–CMC was lower than that of PDMS–NH_2 at each time point, indicating that the grafting of CMC onto the PDMS–NH_2 surface further reduces the hydrophobicity.

It is known that hydrophobicity recovery of PDMS is not solely due to migration of low molecular weight species, but also due to physical surface recovery of PDMS, *i.e.*, reorientation of PDMS.[35] The high molecular weight CMC forms a dense hydrophilic coating on the PDMS surface; this coating minimizes the underlying PDMS from air exposure and subsequent PDMS re-orientation, thereby improving surface hydrophilicity retention. The use of a high molecular weight organosilane, trimethoxysilylpropyl(polyethylene imine), may also contribute to the formation of a dense coating that prevents PDMS surface recovery. In addition, the hydrophobicity recovery of PDMS can also be affected by storage conditions; for example, it is known that storing the samples in a wet environment such as in water and Luria–Bertani broth can retain surface hydrophilicity of PDMS.[36] The storage conditions can be optimized in a future study to maximize the long-term stability of PDMS–NH–CMC hydrophilicity.

Protein adsorption

BSA is a protein produced by the liver and functions as a transport protein *in vivo*. BSA is the most abundant protein component of bovine plasma.[37] BSA–FITC was selected as a model biofouling protein for the study of protein adsorption on the CMC functionalized substrate, because BSA is inexpensive, well characterized and commonly employed in protein adsorption studies.[38–40] The native PDMS substrate served as the control. As shown in Fig. 6A, BSA–FITC was readily adsorbed by the native PDMS substrate. In contrast, only very weak fluorescent signals were observed for the PDMS–NH–CMC substrate, indicating that the CMC functionalization was effective in preventing BSA adsorption.

The amounts of BSA adsorption on PDMS, PDMS–NH_2, and PDMS–NH–CMC substrates were quantified using a BCA protein assay. Fig. 6B shows that the amounts of adsorbed BSA decreased significantly in the sequence of PDMS > PDMS–NH_2 > PDMS–NH–CMC.

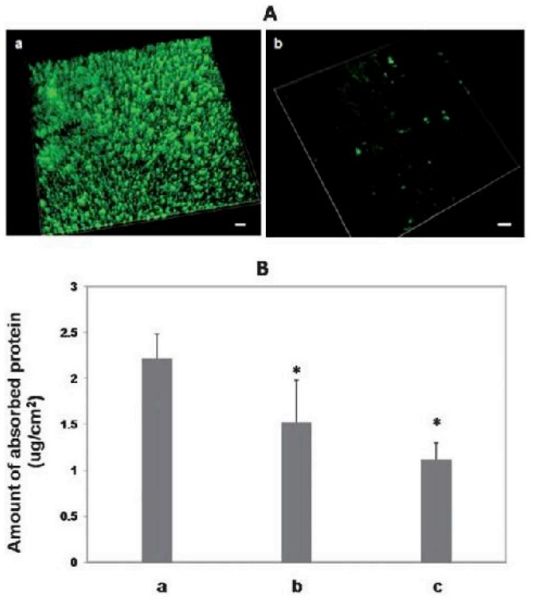

Fig. 6 (A) Confocal microscopy images showing BSA–FITC adsorption on PDMS and PDMS–NH–CMC (scale bar = 100 μm). (B) shows the influence of surface modification on BSA adsorption on (a) PDMS, (b) PDMS–NH_2, and (c) PDMS–NH–CMC substrates. Data are presented as average values ± standard deviation (*$p < 0.05$).

Adsorption of BSA on a hydrophobic surface is driven by non-polar attraction between BSA molecules toward the surface. However, adsorption of BSA on a charged surface is predominantly driven by electrostatic interaction between the charged functional groups on BSA molecules and the oppositely charged surface.[41] It is well known that the hydrophobic interaction is the major driving force of protein adsorption, with protein adsorption tending to be greater on a hydrophobic surface compared to a hydrophilic surface.[42] Compared to the native PDMS substrate, the amount of protein adsorbed onto PDMS–NH_2 and PDMS–NH–CMC substrates decreased by about 1.4 and 2 times, respectively. These results suggested that protein adsorption on PDMS is reduced by rendering its surface hydrophilicity through hydrophilic polysaccharide functionalization. At physiological pH, the carboxylic acid groups of CMC are deprotonated and become anionically charged, which is similar to glycosaminoglycans that play major roles as lubricants in cartilaginous tissues.[16] The high water retention and lubricant nature of CMC[43] make it a favourable anti-fouling coating material for PDMS microchannels.

In contrast to carboxylic acid groups, the majority of amine groups of polyethyleneimine are protonated and become cationically charged at physiological pH.[44] The observations of protein adsorption on a surface functionalized with different functional groups by Chapman *et al.*[45] suggest that a reduction in the hydrogen bond donor moieties in the functional group results in a reduction in protein adsorption. Tangpasuthadol *et al.*[46] studied the adsorption of lysozyme (hydroxyl and amine rich protein) and BSA (carboxylic acid rich protein) on a chitosan surface, and found that the adsorption of BSA was lower on carboxylic acid rich chitosan, possibly due to charge repulsion. BSA as a carboxylic acid rich protein was found to adsorb less onto PDMS–NH–CMC substrates compared to PDMS–NH_2 substrates, possibly due to charge–charge repulsion. The result obtained in this study appears to fit well with the study of interaction of charged proteins on hydrophobic and charged hydrophilic surfaces.[42–45]

It was observed that the difference in the protein adsorption level between PDMS and functionalized PDMS obtained by a confocal microscopy method appeared to be greater than that obtained by the BCA protein assay method. The discrepancy may be due to the fact that the confocal microscopy method measures the local protein adsorption, whereas the BCA protein assay method measures the protein adsorption of the whole sample. For future studies, it is suggested that such difference can be expected to be dependent on the chosen measurement method and other factors such as sample homogeneity.

Cell adhesion

MDA-MB-231 cell adhesion on the PDMS–NH–CMC-GEL substrate was examined and compared to that on PDMS. F-actin was detected using Texas Red®-X phalloidin. F-actin is shown in red while nuclei are shown in blue. As expected, MDA-MB-231 cells appeared to form aggregates and were not attached to the native PDMS substrate. In contrast, cells adhered well onto PDMS–NH–CMC-GEL and proliferated until they reached confluence. Cells adhered onto PDMS–NH–CMC-GEL displayed more well-spread F-actin and normal cell–ECM adhesion (Fig. 7), revealing that the gelatin functionalization process provides appropriate adhesion sites to the cells, thus allowing a normal cytoskeleton formation. For cell growth on the PDMS substrate, the organization of F-actin is more irregular. These results reflect the importance of cell–substrate interaction. They also highlight that cell adhesive ligands can be readily incorporated onto PDMS–NH–CMC to form a PDMS–NH–CMC-GEL based micro-bioreactor while retaining their efficacy for cell adhesion.

Maintenance of pluripotency and proliferation potential of embryonic stem cells

Oct4b2 cells are undifferentiated murine embryonic stem cells that can be cultured on feeder-free culture medium in the presence of LIF. Oct4b2 cell adhesion and proliferation on the

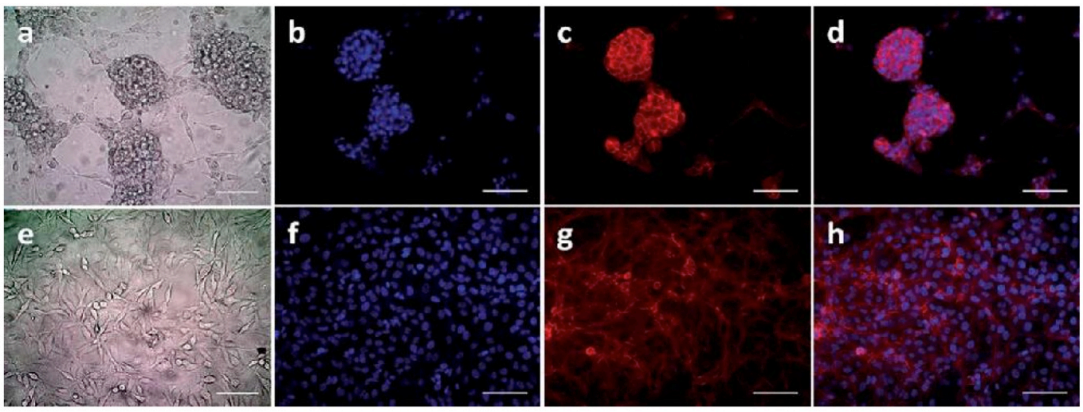

Fig. 7 Bright field and fluorescence microscopy images of MDA-MB-231 cells cultured on (a–d) PDMS, and (e–h) PDMS–NH–CMC-GEL. (a and e) Bright field images. (b and f) Fluorescence microscopy images show cell nuclei stained by DAPI (blue), (c and g) F-actin stained by Red®-X Phalloidin (red), (d and h) overlay of DAPI and Red®-X Phalloidin fluorescence channels (scale bar = 100 μm).

PDMS–NH–CMC-GEL substrate was monitored and compared to that on PDMS, PDMS–CMC, and a TC treated cell culture dish. The morphology of Octo4b2 cells cultured on different substrates is shown in Fig. 8. As expected, cells cultured on the PDMS substrate were round and small after 1 day, and they appeared to form embryoid body (EB) like structures after 4 days, which were floating in the medium instead of attaching to the PDMS substrate, indicating that the PDMS substrate without any functionalization is not suitable for stem cell adhesion. EB formation entails a transition of ESCs to a three-dimensional structure consisting of three embryonic layers: endoderm, mesoderm and ectoderm lineages, similar to embryogenesis.[47] Unlike anchorage dependent stem cells, EB formation takes place on a non-adherent surface. A hydrophobic PDMS surface is known to promote the development of EBs; the results presented here are consistent with the findings of Valamehr *et al.*[48]

Although, some cell adhesion and cell growth were observed on the PDMS–NH–CMC surface, the cells appeared to be small and not well spread after 1 day, and the cells tend to form aggregates as they proliferated. The aggregation of cells on PDMS–NH–CMC led to a decline in the proliferation rate compared to that of the PDMS–NH–CMC-GEL culture, indicating that the cells did not adhere well onto the PDMS–NH–CMC substrate due to the lack of cell adhesion ligands. In contrast, cells grown on PDMS–NH–CMC-GEL appeared to be larger with more spatially dispersed bodies. The cell number increased after 4 days similar to those grown on a TC treated cell culture dish. The cell density of PDMS–NH–CMC-GEL was approximately three times higher than that of PDMS–NH–CMC. This indicates that PDMS–NH–CMC-GEL facilitates cell adhesion *via* the RGD peptide moiety on gelatin. Oct4b2 cells contain the Oct4-green fluorescence protein (Oct4-GFP) reporter.

Oct4 is a pluripotency- and germ-cell-specific marker, and the expression of Oct4-GFP is correlated with pluripotency. The pluripotency of Oct4b2 was monitored by examining the green fluorescence protein (GFP) expression of Oct4b2 cells. The maintenance of pluripotency was illustrated through the fluorescence expressed by Oct4-GFP (depicted in green) in the cytoplasm of Oct4b2 cells observed in the fluorescence microscopy images taken 4 days after cell seeding (Fig. 8). The polysaccharide functionalized PDMS, namely PDMS–NH–CMC-GEL, does not appear to cause undesired differentiation of Oct4b2 cells.

Cell growth in micro-bioreactors

Microfluidic systems have the potential to perform multiple biochemical assays in a single microchip,[9] and provide a

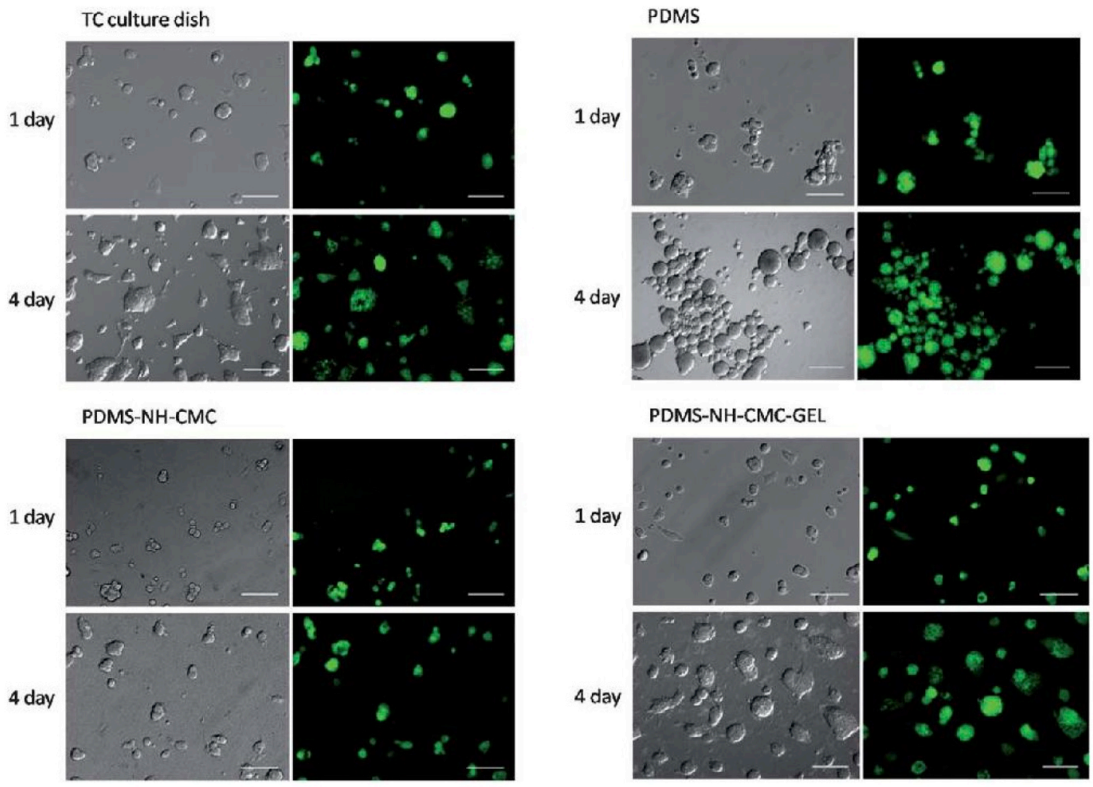

Fig. 8 Phase contrast images of Oct4b2 cells cultured on different substrates. Fluorescence microscopy images show GFP expression of Oct4b2 cells (scale bar for day 1 is 100 μm and for day 4 is 250 μm).

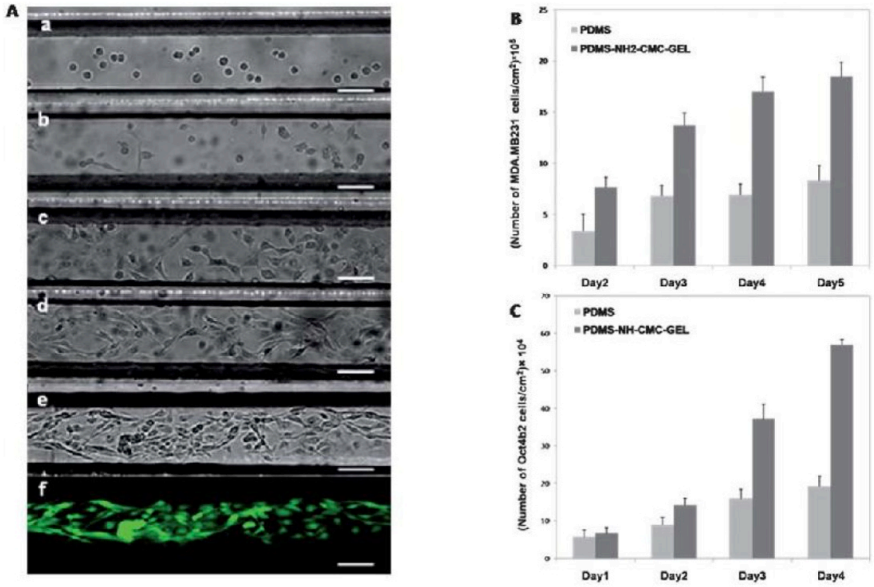

Fig. 9 (A) Phase contrast images of MDA-MB-231 cells cultured in PDMS–NH–CMC-GEL functionalized microchannels after (a) 0 h, (b) 4 h, (c) 1 day, (d) 3 days, and (e) 4 days after cell seeding. (f) Fluorescence microscopy image of live cells stained by Calcein AM (green) after 4 days (scale bar = 100 μm). (B) shows the proliferation of MDA-MB-231 cells, and (C) Oct4b2 cells on PDMS and PDMS–NH–CMC-GEL substrates were monitored over a period of four days.

feasible alternative to the conventional TC cell culture flask by lowering reagent consumption, improving sensitivity and allowing high throughput operation.[49] To show that PDMS–NH–CMC-GEL microchannels can support cell growth, cells were cultured inside the microchannels and monitored over a period of 4 days.

MDA-MB-231 cell attachment and cell morphology were inspected using phase contrast microscopy as shown in Fig. 9A. Four hours after cell seeding, MDA-MB-231 cells appeared to adhere onto the PDMS–NH–CMC-GEL microchannel surface. MDA-MB-231 cells appeared to spread out showing an epithelial-like morphology and proliferating after 1 day. Live/dead staining was performed using Calcein AM to confirm the viability of cells inside microchannels after 4 days. Fig. 9A revealed that the majority of cells remained viable (stained in green) inside the microchannel and demonstrated the ability of the present method to support cell cultivation.

The proliferation of cells on different substrates was quantified and the results are summarized in Fig. 9B and C. The cell growth on the PDMS–NH–CMC-GEL substrate was compared to that on the PDMS control substrate over four consecutive days. The results revealed that the number of cells grown on the PDMS–NH–CMC-GEL substrate was much higher than that cultured on the PDMS substrate, for instance, the number of MDA-MB-231 and Oct4b2 cells on PDMS–NH–CMC-GEL is approximately 2 times and 2.3 times greater than that on PDMS at day three, respectively. The rate of cell proliferation on PDMS–NH–CMC-GEL also appeared to be higher than that on the PDMS substrate. The proliferation of cells implies that the functionalized microchannel surface is biocompatible with cells. It is worth mentioning that the functionalized microchannel system derived in this study can be employed as a perfusion micro-bioreactor when integrated with an appropriate flow control system. The effects of shear stress on stem cells growth and differentiation compared with those in the static culture are currently under investigation.

Conclusions

We have developed a novel method to prepare a micro-bioreactor for stem cell expansion. This method is cost effective, and allows functionalization to be carried out by needle injection of reagents into the micro-bioreactor surface, and is thereby compatible with standard microfabrication processes. Enhanced and extended surface hydrophilicity were permitted by the proposed functionalization method. The cytocompatibility has also been demonstrated by cultivating MDA-MB-231 on a functionalized micro-bioreactor surface. We also demonstrated that the functionalized surface facilitates Oct4b2 cell propagation, as well as retaining the undifferentiated phenotype and pluripotency of the cells. The results demonstrate the potential use of the micro-bioreactor as a stem cell study tool.

Acknowledgements

We acknowledge the funding provided by the Department of Mechanical and Aerospace Engineering at Monash University. Funding for this research was also partly provided through an Australia Research Council Discovery Project Grant ARC DP 120102570 and through the Australia–India Strategic Research Fund BF050038. We also thank Dr Paul Verma from Monash Institute of Medical Research (MIMR) for supplying Oct4b2

cells. We would like to thank Dr Ricky Tjeung for his assistance with microchannel fabrication and Ms Karla Contreras for her assistance with cell culturing. This work was performed in part at the Melbourne Centre for Nanofabrication, an initiative partly funded by the Commonwealth of Australia and the Victorian Government.

Notes and references

1 N. Xu, T. Papagiannakopoulos, G. Pan, J. A. Thomson and K. S. Kosik, *Cell*, 2009, **137**, 647–658.
2 Z. Du, H. Cai, Z. Ye and W.-S. Tan, *J. Biotechnol.*, 2012, **164**, 211–219.
3 C. A. V. Rodrigues, T. G. Fernandes, M. M. Diogo, C. L. da Silva and J. M. S. Cabral, *Biotechnol. Adv.*, 2011, **29**, 815–829.
4 T. Liu, *Comprehensive Biotechnology*, 2nd edn, 2011, vol. 5, pp. 389–396.
5 J. Chen and D. Pei, *Nat. Methods*, 2012, **9**, 449–451.
6 G. C. Reilly and A. J. Engler, *J. Biomech.*, 2010, **43**, 55–62.
7 A. J. Engler, S. Sen, H. L. Sweeney and D. E. Discher, *Cell*, 2006, **126**, 677–689.
8 E. Cimetta, E. Figallo, C. Cannizzaro, N. Elvassore and G. Vunjak-Novakovic, *Methods*, 2009, **47**, 81–89.
9 L. Y. Yeo, H.-C. Chang, P. P. Y. Chan and J. R. Friend, *Small*, 2011, **7**, 12–48.
10 V. Compan, A. Lopez-Alemany, E. Riande and M. F. Refojo, *Biomaterials*, 2004, **25**, 359–365.
11 F. Abbasi, H. Mirzadeh and A. A. Katbab, *Polym. Int.*, 2001, **50**, 1279–1287.
12 M. L. van Poll, F. Zhou, M. Ramstedt, L. Hu and W. T. S. Huck, *Angew. Chem., Int. Ed.*, 2007, **46**, 6634–6637.
13 H. Yan, B. Zhang and H. Wu, *Electrophoresis*, 2008, **29**, 1775–1786.
14 N. R. Glass, R. Tjeung, P. Chan, L. Y. Yeo and J. R. Friend, *Biomicrofluidics*, 2011, **5**, 36501–365017.
15 Z. Yue, X. Liu, P. J. Molino and G. G. Wallace, *Biomaterials*, 2011, **32**, 4714–4724.
16 A. T. Reza and S. B. Nicoll, *Acta Biomater.*, 2010, **6**, 179–186.
17 N. A. Ramli and T. W. Wong, *Int. J. Pharm.*, 2011, **403**, 73–82.
18 C. K. Ryan and H. C. Sax, *Am. J. Surg.*, 1995, **169**, 154–160.
19 J. Ma, Y. Xu, B. Fan and B. Liang, *Eur. Polym. J.*, 2007, **43**, 2221–2228.
20 M. A. Lalountas, K. D. Ballas, C. Skouras, C. Asteriou, T. Kontoulis, D. Pissas, A. Triantafyllou and A. K. Sakantamis, *Am. J. Surg.*, 2010, **200**, 118–123.
21 A. J. García and D. Boettiger, *Biomaterials*, 1999, **20**, 2427–2433.
22 S. Young, M. Wong, Y. Tabata and A. G. Mikos, *J. Control. Release*, 2005, **109**, 256–274.
23 H. Shin, S. Jo and A. G. Mikos, *Biomaterials*, 2003, **24**, 4353–4364.
24 L. S. Wang, J. E. Chung, P. P. Y. Chan and M. Kurisawa, *Biomaterials*, 2010, **31**, 1148–1157.
25 W. Albrecht, B. Seifert, T. Weigel, M. Schossig, A. Hollander, T. Groth and R. Hilke, *Macromol. Chem. Phys.*, 2003, **204**, 510–521.
26 T. Goda, T. Konno, M. Takai, T. Moro and K. Ishihara, *Biomaterials*, 2006, **27**, 5151–5160.
27 M. Ferrando, A. Rozek, M. Zator, F. Lopez and C. Guell, *J. Membr. Sci.*, 2005, **250**, 283–293.
28 T. Lu, X. Chen, Q. Shi, Y. Wang, P. Zhang and X. Jing, *Acta Biomater.*, 2008, **4**, 1770–1777.
29 J. Wei, L. Yan, X. Hu, X. Chen, Y. Huang and X. Jing, *Colloids Surf., B*, 2011, **83**, 220–228.
30 S. Hemmilä, J. V. Cauich-Rodríguez, J. Kreutzer and P. Kallio, *Appl. Surf. Sci.*, 2012, **258**, 9864–9875.
31 M. Farrell and S. Beaudoin, *Colloids Surf., B*, 2010, **81**, 468–475.
32 H. T. Kim and O. C. Jeong, *Microelectron. Eng.*, 2011, **88**, 2281–2285.
33 P. F. Gratzer and J. M. Lee, *J. Biomed. Mater. Res.*, 2001, **58**, 172–179.
34 L. Bertilsson, H. Elwing, B. Liedberg, O. Larm, J. Risenfeld and E. Scholander, *Macromol. Eng.*, 1991, **1**, 49–57.
35 D. Bodas and C. Khan-Malek, *Sens. Actuators, B*, 2007, **123**, 368–373.
36 L. H. Zhao, J. Lee and P. N. Sen, *Sens. Actuators, A*, 2012, **181**, 33–42.
37 T. Mogues, J. Z. Li, J. Coburn and D. J. Kuter, *J. Immunol. Methods*, 2005, **300**, 1–11.
38 S. M. Moghimi, *Biochim. Biophys. Acta, Mol. Cell Res.*, 2002, **1590**, 131–139.
39 J. Hu, S. J. Li and B. L. Liu, *Biochem. Eng. J.*, 2005, **23**, 259–263.
40 Y. L. Jeyachandran, J. A. Mielczarski, E. Mielczarski and B. Rai, *J. Colloid Interface Sci.*, 2010, **341**, 136–142.
41 Y. L. Jeyachandran, E. Mielezarski, B. Rai and J. A. Mielczarski, *Langmuir*, 2009, **25**, 11614–11620.
42 J. Y. Yoon, H. Y. Park, J. H. Kim and W. S. Kim, *J. Colloid Interface Sci.*, 1996, **177**, 613–620.
43 C. Chang and L. Zhang, *Carbohydr. Polym.*, 2011, **84**, 40–53.
44 J. D. Ziebarth and Y. Wang, *Biomacromolecules*, 2010, **11**, 29–38.
45 R. G. Chapman, E. Ostuni, S. Takayama, R. E. Holmlin, L. Yan and G. M. Whitesides, *J. Am. Chem. Soc.*, 2000, **122**, 8303–8304.
46 V. Tangpasuthadol, N. Pongchaisirikul and V. P. Hoven, *Carbohydr. Res.*, 2003, **338**, 937–942.
47 H. Kurosawa, *J. Biosci. Bioeng.*, 2007, **103**, 389–398.
48 B. Valamehr, S. J. Jonas, J. Polleux, R. Qiao, S. Guo, E. H. Gschweng, B. Stiles, K. Kam, T.-J. M. Luo, O. N. Witte, X. Liu, B. Dunn and H. Wu, *Proc. Natl. Acad. Sci. U. S. A.*, 2008, **105**, 14459–14464.
49 I. Meyvantsson and D. J. Beebe, *Annu. Rev. Anal. Chem.*, 2008, 423–449.

Chapter 4: Tumor inside a Pearl Drop

4.1 General Overview

This chapter comprises one published communication paper.

For more than a century, the comprehensive understanding of cancer processes and development has come from precise scientific research of the histopathology of tumours. The formation of tumour cells as multicellular tumour spheroids (MTS) is a useful tool in anticancer drug evaluations, which can lead to better understanding in the design and development of drug delivery systems. Spheroids have been employed for a diverse range of studies in cancer biology and in radiobiological investigations, due to the fact that they can reasonably mimick the radio resistant hypoxic cell population that is commonly found in tumours *in vitro*[1].

In this chapter, we proposed a novel approach for *in vitro* formation of cancer cell spheroids. Micro-bioreactors made of liquid marbles were explored in this chapter as a powerful means for forming 3D cancer cell spheroid culture. The difficulties associated with the common methods (e.g., hanging drop and suspension, using non-adhesive dishes and conventional bioreactors), including generating spheroids with low yield, low viability and irregular structures, have raised the demand in developing novel approaches capable of overcoming these limitations. Cancer cells were cultured inside the liquid marbles, a miniature, yet efficient bioreactor, made of cell growth medium and polytetrafluoroethylene powder particles. *In vitro* formation of 3D cancer cell spheroids, a tumour-like structure, is proven to be not only possible but more efficient in the liquid marble bioreactor. After innoculation, successful cell aggregation was observed after one day in the liquid marbles. In addition, the resulting cell aggregates remain viable in the liquid marble. Liquid marble bioreactors were used to facilitate stem cell aggregate formation and subsequent differentiation, and will be described in the next two chapters. A publication was derived from the results obtained during liquid marble bioreactor development, and is attached below.

4.2 Tumor inside a Pearl Drop

Tumor Inside a Pearl Drop

*Tina Arbatan, Aswan Al-Abboodi, Fatemeh Sarvi, Peggy Pui Yik Chan, and Wei Shen**

Liquid marbles are exploited in this study as efficient miniature bioreactors inoculated with Hep G2 (hepatocellular carcinoma) cells to culture cell spheroids in vitro. This method successfully yields numerous cell spheroids, via a facile and straight-forward route, thanks to the constrained internal structure of liquid marbles, along with their non-adhesive shell. Since in vitro cultured cancer cell spheroids are of paramount importance in biomedical science and applications, this novel approach may open new avenues in the field of cancer research.

Cancer cell spheroids (CCSs) cultured in vitro are believed to be capable of reflecting the in vivo physiology of tumors more realistically than two dimensional cell cultures.[1] Therefore, in vitro cultured CCSs are frequently exploited as models[2] to study the physiology of tumors, and several methods have been hitherto developed to culture them.[3] Among all the available methods in the literature,[3] the hanging drop method[4] used by Kelm et al.[5] is the most common method over others, yielding a single homogeneous multicellular CCS in each drop, with similar architecture alike in vivo tumors. In a typical hanging-drop spheroid-culture experiment,[5] 20–50 µL cell suspensions is dispensed into each of the 60 wells of a MicroWell MiniTray, followed by inversion of the tray which leads to 60 hanging drops. The first inherent experimental challenge of the method, however, appears right here; since in order to form a sufficiently stable hanging drop for easy experimental handling, the volume of the drop must be carefully controlled, because the stability of a hanging drop is governed by the balance of the liquid surface tension force, that holds the drop around the opening of each well, and the gravitational force of the drop, that pulls it off the well. Although efficient in yielding spheroids, the hanging drop technique is well known to be laborious, and requires a great deal of manipulation.

Herein a novel approach is reported for in vitro CCSs formation; to culture cancer cell spheroid inside liquid marbles, also known as pearl drops.[6] Liquid marbles[7] were first introduced in 2001 by Aussillous and Quéré,[7a] as liquid drops covered with hydrophobic powder particles. A liquid marble can be simply made by gently rolling a drop of liquid, placed on a hydrophobic powder bed, so the hydrophobic powder particles cover the liquid surface. The as prepared liquid marble can then be regarded as a non-wetting drop of liquid that can be transferred, manipulated, or even collapsed when needed.

One of the main applications suggested for liquid marbles is to use them as miniature reactors, capable of containing chemical and biological reactions.[8–11] In this study, we show for the first time that liquid marbles can be used to contain living cells, and present how liquid marbles can be effectively exploited in in vitro CCS formation. Liquid marbles of varied size can be easily formed using a variety of readily available hydrophobic powders. In this study,chemically inert polytetrafluoroethylene (PTFE) powder was chosen as the non-adhesive material utilized in the liquid marble shell. Our recent study shows that the inert PTFE particles do not significantly change important interfacial properties of liquid marbles, such as their surface tension.

Hypothetically, there are three major factors which make liquid marbles convenient for cells to live in: 1) A porous shell allow O_2 and CO_2 exchange between cell culture medium and surrounding environment; 2) hydrophobic powder particles that forms the shell and provides a non-adhesive surface, which encourages the cells to suspend in the medium and, 3) a confined liquid core volume that promotes effective contact between cells, hence leads to better aggregation. To support the above-mentioned hypothesis, liquid marbles of varied sizes were formed.

A schematic comparison of liquid marble bioreactor versus the hanging drop method can be seen in (**Figure 1**, note that the powder particles on the liquid marble shell are not drawn). The dimensions of PTFE powder particles are shown in the micrograph (**Figure 2**); the observed PTFE powder particles sizes are in reasonable agreement with the material specification from the supplier (100 µm). The selection of this particle size is based on our previous study,[10] which showed that liquid marbles made of 100 µm PTFE particles were more stable than those made of smaller particles. In case of Hep G2 cells, cell aggregation could be clearly observed after 24 hours, while formation of numerous three dimensional cell aggregates were observed using confocal microscopy by the end of day 10, as shown in **Figure 3**.

The successful cell aggregation observed after one day and 10 days inside liquid marbles proves that our hypothesis was right - liquid marbles can indeed conveniently accommodate cells to survive and form aggregates. As was hypothesized, the confined volume of a liquid marble promotes the intimate intercellular interaction, resulting in aggregation. On the other hand, the cell-PTFE particle interactions at the liquid marble shell is biochemically discouraged by the low surface tension and anti-adhesion nature of PTFE particles.

T. Arbatan, A. Al-Abboodi, Prof. W. Shen
Department of Chemical Engineering
Monash University
VIC 3800, Australia
[redacted]
F. Sarvi
Department of Mechanical Engineering
Biological Division
Monash University
Clayton, VIC 3800, Australia
Dr. P. P. Y. Yik Chan
School of Applied Science
RMIT University, VIC, Australia

DOI: 10.1002/adhm.201200050

ADVANCED HEALTHCARE MATERIALS
www.advhealthmat.de

Materials Views
www.MaterialsViews.com

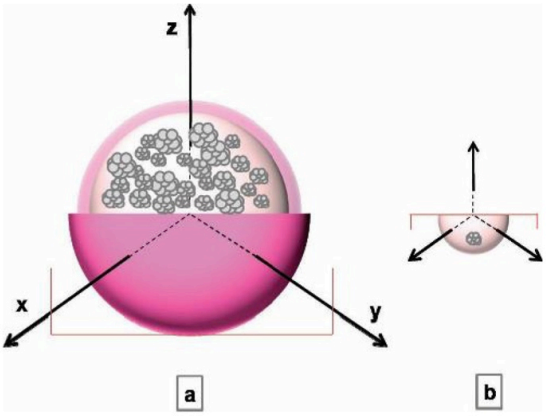

Figure 1. Schematic comparison of cancer cell spheroid (CCS) formation in; a) a liquid marble (the powder particles are not drawn), b) a hanging drop. Unlike hanging method which has a stringent droplet size limitation, liquid marbles can accommodate a larger quantity of liquid, therefore allowing formation of a large number of cell aggregates. Besides, liquid marble size can be varied by aspirating or dispensing fluid held within the marble using a micropipette, where nutrient and waste exchange is permissible. Liquid marble also allows cell aggregates to be incubated inside the marble for a long period time until spheroids are formed.

To use liquid marble for CCSs formation has several advantages: 1) Quick cell aggregates formation, as CCSs are formed in time similar to the hanging drop method. 2) The yield of CCSs formation is high, since a single liquid marble micro bio-reactor produces numerous spheroids. 3) the liquid marble method is simple and easy to operate; it does not require instrumentation other than customary cell culture equipment. 4) Human intervention is kept to a minimum; once the liquid marbles are prepared, they can be placed in an incubator until the spheroids are formed. 5) The flexible structure of liquid marbles enables the extraction, replenishment, or change of the liquid core of the liquid marble to be carried out easily, should they be needed. This significantly increases the flexibility for the manipulation of the medium in cell culture experiments. 6) The liquid marble bioreactors are cost-effective; they are much cheaper than some of the conventional bioreactors.

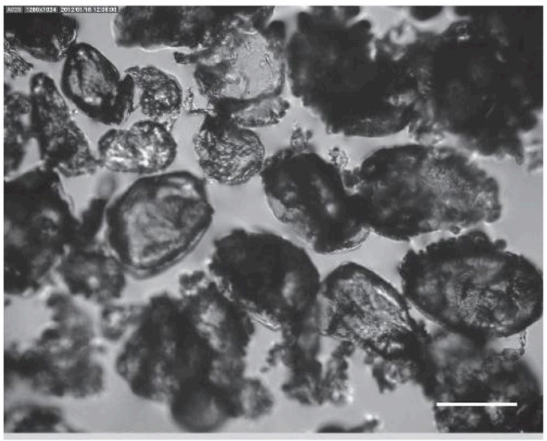

Figure 2. Optical microscopy image of PTFE powder particles on the surface of a liquid marble. (Scale bar = 100 μm).

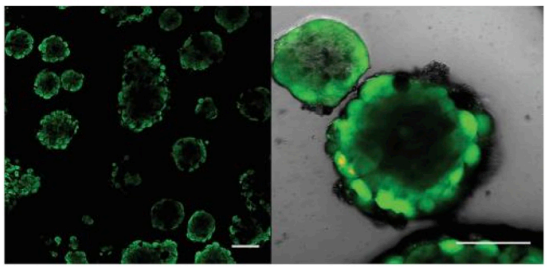

Figure 3. Hep G2 cells inside a liquid marble on day 10; viable cell aggregates stained by Calcein AM (green) can be observed. (Scale bar = 50 um). Note the formation of dark lining around the cell aggregates indicated the transition of cell aggregates into tumor spheroid. (Scale bar = 50 μm).

In this application, liquid marble micro bio-reactors also present two difficulties: 1) It is more difficult to perform an entire medium exchange and, 2) the liquid core of the marble must be evacuated to enable the microscopic monitoring of the cell growth. To overcome the first difficulty, a different medium control method was used. We added fresh medium into the liquid marbles during the 10-day experiment, instead of performing an entire medium exchange of the liquid marbles. This method worked very well; the CCSs formation did not seem to have been suppressed. To overcome the second difficulty, we think it possible to design magnetic hydrophobic powder to form the marble shell,[8d] which enables opening and closing of the north pole of the liquid marble by means of magnetic force. In situ microscopic observation would then be enabled using an upright microscopy; the liquid marble could then be closed after the observation.

The method outlined in this paper can certainly be tailored to also culture aggregates of other cell types. For instance, as embryonic cells in suspension tend to form cell aggregates similar to cancer cells. Hence, this method can be potentially used in embryonic body formations with obvious implications in tissue engineering. Overall, this study shows that liquid marbles made of inert PTFE particles can serve not only as novel platforms for formation of CCSs, but also as potential means to understand the mechanisms through which cells interact with one another, leading to the formation of cell aggregation. Encapsulation of living cells in a liquid marble can open new avenues in biomedical science and tissue engineering.

Experimental Section

In a typical CCSs formation experiment, 100–400 μL drops of medium containing Hep G2 cells (~10^4 per 100 μL) were placed in a Petri dish containing a PTFE powder bed (particle size = 100 μm, see Figure 2). The liquid drops were then gently rolled on the powder bed until they were covered completely with powder particles to form liquid marbles. This Petri dish containing the

liquid marble on powder bed was then placed in a larger Petri dish, half filled with water, to provide an atmosphere saturated with water vapour to suppress the evaporation of the medium from the liquid marble. This experimental setup eliminates the problem of water core evaporation from water marbles reported in the literature.[11] The Petri dish was then capped and placed inside an incubator, to provide the cells with suitable growth conditions. In order to monitor cell aggregation, the liquid core of a marble was extracted out of the marble using a micropipette for confocal imaging.

Acknowledgements

The authors would like to thank Mr. Matthew O'Connor for proof reading the manuscript.

Received: February 21, 2012
Revised: April 12, 2012
Published online: May 31, 2012

[1] W. Mueller-Klieser, *Am. J. Physiol.- Cell Physiol.* **1997**, *273*, C1109.
[2] G. Hamilton, *Cancer let.* **1998**, *131*, 29.
[3] M. T. Santini, G. Rainaldi, *Pathobiology* **1999**, *67*, 148.
[4] K. Gordon M, *Curr. Opin. Cell Biol.* **1995**, *7*, 862.
[5] J. M. Kelm, N. E. Timmins, C. J. Brown, M. Fussenegger, L. K. Nielsen, *Biotechnol. Bioeng.* **2003**, *83*, 173.
[6] J. Bico, C. Marzolin, D. Quéré, *EPL (Europhy. Let.)* **1999**, *47*, 220.
[7] a) P. Aussillous, D. Quéré, *Nature* **2001**, *411*, 924; b) P. Aussillous, D. Quéré, *Proc. Royal Soc. A: Math., Phys. Eng. Sci.* **2006**, *462*, 973; c) G. McHale, M. I. Newton, *Soft Matter* **2011**, *7*, 5473; d) B. Edward, *Curr. Opin. Colloid Interface Sci.* **2011**, *16*, 266.
[8] a) J. Tian, T. Arbatan, X. Li, W. Shen, *Chem. Commun.* **2010**, *46*, 4734; b) J. Tian, T. Arbatan, X. Li, W. Shen, *Chem. Eng. J.* **2010**, *165*, 347; c) T. Arbatan, L. Li, J. Tian, W. Shen, *Adv. Healthcare Mater.* **2012**, *1*, 80; d) Y. Xue, H. Wang, Y. Zhao, L. Dai, L. Feng, X. Wang, T. Lin, *Adv. Mater.* **2010**, *22*, 4814.
[9] E. Bormashenko, R. Balter, D. Aurbach, *Int. J. Chem. Reactor Eng.* **2011**, *9*, 10.
[10] T. Arbatan, W. Shen, *Langmuir* **2011**, *27*, 12923.
[11] a) A. Tosun, H. Y. Erbil, *Appl. Surf. Sci.* **2009**, *256*, 1278; b) M. Dandan, H. Y. Erbil, *Langmuir* **2009**, *25*, 8362.

Chapter 5: Formation of Embryoid Bodies inside Liquid Marble Bioreactor

5.1 General Overview

This chapter comprises one published journal paper. The capability of a liquid marble bioreactor for formation of embryoid bodies from stem cells was investigated in this publication (section 5.2).

Understanding the factors that regulate stem cell fate will lead to better control of their differentiation in potential clinical applications. In addition to responding to growth factors, retinoic acid, and other soluble regulators [2, 3], stem cells can be stimulated to differentiate by physical means. Stem cells self assemble into embryoid bodies that mimic the inner cell mass of embryos. EB formation has been widely used as a trigger to induce *in vitro* differentiation in ESCs and iPSCs into 3 germ layers, the formation of 3 germ layers is a critical intermediate step in the induction of lineage specific differentiation [4]. The differentiation into the specific lineage within EBs closely simulates lineage differentiation in the developing embryo, which is of great importance in morphogenesis study [5].

In this chapter, we report the use of liquid marbles as low cost, high-yield and easy-to-control micro bioreactors for the formation of EBs. The effect of different factors - including liquid marble shell properties, liquid marble size and the cell seeding density on the size, uniformity and quality of the EBs formed - were investigated. Cell seeding density (CSD) and liquid marble size (LMS) are shown to have an influence on the efficiency of the method; the greater the CSD and LMS, the higher is the efficiency of the EB formation inside liquid marbles.

The EB formation efficiency inside a liquid marble (LM technique) was compared with the liquid suspension culture method (LS technique), which is a common technique used for EB formation. It was found that there is a significant difference in the viability of cells obtained from the LM and LS methods. Viability of cells formed inside LM was observed to be higher than those formed in low adhesion plates. The morphology of EBs formed via both methods also confirmed that the LM technique in comparison produces more homogeneous EBs in terms of size distributions. Markers of all three germ layers were observed in the EBs formed inside liquid marbles, which confirmed the *in vitro* differentiation potential of EBs formed using the liquid marble technique. Our initial study also confirmed that LM may have the potential to differentiate EBs to beating cardiomyocyte-like cells.

The liquid marble micro bioreactor provides a facile new method for highly efficient production of EBs. Herein, we optimize the condition used for EB formation, and show that the liquid marble bioreactor is capable of producing EBs of more homogeneous size and shape compared to the liquid suspension method. Miniaturization of bioreactors using the liquid marble concept also has a clear

economical advantage over the existing methods. A publication was derived from the results obtained in this study, and is attached below.

5.2 A novel technique for Formation of Embryoid Bodies inside Liquid Marbles

RSC Advances

RSC Publishing

PAPER

A novel technique for the formation of embryoid bodies inside liquid marbles†

Cite this: *RSC Advances*, 2013, **3**, 14501

Fatemeh Sarvi,‡[a] Tina Arbatan,‡[b] Peggy Pui Yik Chan[cd] and Wei Shen*[b]

Received 23rd January 2013,
Accepted 3rd June 2013

DOI: 10.1039/c3ra40364e

www.rsc.org/advances

The significant and inherent limitations associated with commonly used methods of *in vitro* embryoid body (EB) formation motivate the development of novel, facile, efficient and reproducible techniques. In this study we report the possibility of using ''liquid marbles'' as facile and efficient micro bioreactors for *in vitro* EB formation. To exploit liquid marbles as micro biological reactors, embryonic stem cells (ES cells) were inoculated into liquid marbles containing embryonic cell growth medium. Herein we show how the confined internal space of a liquid marble, along with the porous and non-adhesive properties of the highly hydrophobic liquid marble shell, can provide the necessary conditions for the formation of uniform EBs inside liquid marbles. Factors such as the powder particle size, the liquid marble volume and the cell seeding density inside each liquid marble were also investigated to evaluate the effects of varying experimental conditions on the efficiency of EB formation within a liquid marble.

Introduction

The term ''liquid marble'' was first introduced to describe an interfacial phenomenon whereby upon the contact of a small drop of liquid with hydrophobic powder particles, the drop becomes covered by a multilayer of powder particles of micro- to nano-sizes.[1,2] The powder particles encase the liquid drop, forming a powder shell which prevents the liquid drop from coming into contact with the supporting substrate, while allowing gases to freely transport across the shell. Liquid marbles also have the flexibility of a liquid drop; when small enough, they stably retain a near-spherical shape on the supporting liquid or solid surface. Whilst many studies have investigated the fundamental interfacial properties of liquid marbles,[3–6] several studies have also focused on the exploitation of liquid marbles as miniature reactors.[7–10] Tian *et al.* investigated the possibility of using liquid marbles for gas sensing applications.[7,8] Lin's group also reported some novel powder materials for making liquid marbles into controllable miniature reactors.[9,10] Recently, Arbatan *et al.* explored the use of liquid marbles to perform immunohaemotological assays[11] and to culture cancer spheroids.[12] These works clearly demonstrate the promising potential of liquid marbles for biological and biomedical applications. The current report aims to demonstrate yet another particularly important biological application of liquid marbles – their use as platforms for the culturing of embryoid bodies (EBs) from embryonic stem cells (ES cells).

Embryonic stem cells are pluripotent cells that are directly derived from the inner cell mass of preimplantation embryos, and have the unique potential to continuously proliferate *in vitro*.[13] Thanks to their unique capability of long-term self-renewal and their ability to differentiate into a variety of specific cell lineages, stem cells are of paramount importance in regenerative tissue studies and cell-based therapies.[14] ES cells can form EBs with all three somatic germ layers (mesoderm, ectoderm and endoderm) under well defined *in vitro* conditions, and have the potential to differentiate into different types of tissues including hematopoietic,[15,16] endothelial,[17] cardiac,[18,19] and neuronal[20] tissues. An existing biological challenge is to find efficient methods to yield EBs from ES cells. In this endeavour, liquid marbles are introduced as micro bioreactors to explore the efficient production of EBs from ES cells.

ES cells can differentiate into a variety of cell lineages, but only after they aggregate and form 3D cell structures known as EBs.[21] EB formation facilitates subsequent multicellular interactions and the formed EBs have the potential to differentiate into derivatives of all three germ layers. Structurally, EBs consist of ectodermal, mesodermal and endodermal tissues, mimicking the structure of a developing embryo. Hence, EB formation is of paramount importance for the *in vitro* investigation of embryonic development, and differentiation between mouse and human ES cells.[22,23]

[a]*Department of Mechanical & Aerospace Engineering & Division of Biological Engineering, Monash University, Clayton, Australia*
[b]*Department of Chemical Engineering, Monash University, VIC 3800, Australia.* [redacted]
[c]*School of Applied Science, RMIT University, Australia*
[d]*Melbourne Centre for Nanofabrication, Australia*

† Electronic supplementary information (ESI) available. See DOI: 10.1039/c3ra40364e

‡ FS and TA contributed equally to the preparation of this paper and hence are the co-first authors of this report.

Several methods are currently being used for *in vitro* EB formation.[24–26] These methods are mostly based on preventing the adhesion of ES cells to the surface of the culturing dish, hence maintaining the cells in suspension so that they can adhere to one another and form EBs. In these methods, EB formation is generally initiated either by removing the Leukemia Inhibitory Factor (LIF) from the medium, or by culturing ES cells in the absence of MEF (Mouse Embryonic Feeder) layer. The most common methods of inducing EB formation are the suspension culture method (*e.g.* culturing cells in anti-adhesive bacterial-grade dishes) and the hanging drop method.[27,28] Furthermore, forced aggregation methods have been reported; these methods include the use of a round-bottomed 96-well plate, the use of methylcellulose semisolid media and the use of bioreactors.[28–30]

The EB formation methods currently in use have some disadvantages, preventing them from producing EBs in high yield and also inhibiting quality. For instance, although the suspension technique has been successfully used to generate EBs that can differentiate into various cell types, it only provides limited control over EB size, shape and uniformity, as it relies on the accidental aggregation of ES cells. Consequently, considerable heterogeneity in size and shape will be observed. Moreover, the possibility of EB attachment to the dish, mainly arising due to defects in the surface chemistry of the culture dish, causes greater heterogeneity and may result in the loss of EBs from the suspension culture.[28–31] In contrast, culturing EBs in methylcellulose semisolid media, in which single cells tend to remain separated and isolated by the matrix of methylcellulose, enables the reproducible formation of EBs from single ES cells. The main drawbacks of this method are that the methylcellulose matrix may slow down the mass transfer of factors added during the EB formation experiment, and the handling of a semi-solid solution by pipette is also challenging. The obtained yield is often low because of the inherent instability of the prolonged single cell culture of the pluripotent stem cells. Further complication may also be encountered when isolating EBs from the hydrogel for further use.[28–32]

The hanging drop technique is the most commonly used small scale technique for EB formation. The method is based on dispensing equal numbers of ES cells into physically separated droplets of media suspended from the lid of a Petri dish, which leads to gravity induced EB formation.[23] Under normal conditions, the hanging drop method only yields a single EB from each hanging drop. Furthermore, medium exchange of the hanging drops is laborious and may disturb the conditions necessary for EB formation. The reproducibility of the size and quality of EBs formed by the hanging drop method is heavily dependent on the operator's level of skill and experience.[33]

The development of bioreactors has made EB formation more facile and controllable compared with the methods discussed above. The use of bioreactors such as the spinner flask offers the possibility for large scale production of EBs, thanks to their simple design, scalable configuration and ability to produce homogeneous culture conditions. Bioreactors also facilitate the measurement of different environmental factors such as oxygen tension, pH and medium exchange.[25] However, a significant drawback of this method is the shear stress induced by the rotation of the impellers which may damage the cells, disrupt cell–cell signalling, damage the fragile cellular components and affect the subsequent cell differentiation.[34]

The same drawbacks apply to the rotating suspension technique, in which cell suspensions are rotated on a horizontal rotating device equipped with a membrane for gas exchange, and ports for media exchange and sampling at different speeds.[35] Although the rotation culture system improves oxygen supply and enables the production of high density cultures, the method may not be suitable for assessing multiple experimental samples in parallel. Also this system requires specialized culture equipment and larger volume bioreactors, which makes this system very costly.

In this study, we report the use of liquid marbles as low-cost, high-yield and easy-to-control micro bioreactors for the formation of EBs. Factors including liquid marble shell properties, liquid marble size and the cell seeding density are investigated in order to understand their effects on the size, uniformity and quality of the embryoid bodies formed.

Experimental

Murine-derived embryonic stem cell lines (Oct4b2) which possess an Oct4-green fluorescent protein (Oct4-GFP) reporter were used, the expression of Oct4-GFP being correlated to the stem cell pluripotency. Oct4b2 cells were maintained in knockout medium (Gibco, Australia) supplemented with 20% knockout serum replacement (Gibco), 1% nonessential amino acids (Gibco), 0.1 mM 2-mercaptoethanol (Gibco), 1% Glutamax (Gibco), 1% penicillin–streptomycin (Gibco) and 1000 U ml^{-1} murine leukemia inhibitory factor (mLIF, Chemicon, Australia). Cells were seeded on a 0.1% gelatin-coated dish at 37 °C in humidified air with 5% CO_2. Cells were passaged every 2–3 days after 70–80% of confluency. In order to induce EB formation, ES cells were dissociated with Tryple™ express and suspended in a medium that did not contain LIF (EB medium).

Polytetrafluoroethylene (PTFE) powder with particle sizes of 35 and 100 μm were acquired from Sigma-Aldrich. To create the liquid marbles, a powder bed was prepared inside a Petri dish and a spatula was used to gently make a curved gully at the centre of the powder bed (Fig. 5). A micropipette was then used to dispense the required volume of EB medium containing a predetermined number of cells on the powder bed. The Petri dish was then gently shaken in a circular motion so the powder particles covered the surface of the liquid drop. The Petri dish was then placed in a larger Petri dish containing sterile water and both Petri dishes were capped. The use of the second Petri dish was necessary to prevent liquid marble evaporation. The liquid marble content was then monitored

Table 1 PCR primer sequences

Primer	Primer sequences (forward-reverse) 5′→3′	NCBI accession no.	PCR product size bp
Nestin	TCTGGAAGTCAACAGAGGTGG/ACGGAGTCTTGTTCACCTGC	NM_016701.3	350
Brachyury	CATGTACTCTTTCTTGCTGG/GGTCTCGGGAAAGCAGTGGC	NM_009309.2	313
Foxa2	TGGTCACTGGGGACAAGGGAA/GCAACAACAGCAATAGAGAAC	NM_010446.2	289
β-Actin	CACCACACCTTCTACAATGAGC/TCGTAGATGGGCACAGTGTGGG	NM_007393.3	242

on days 3 and 7 of incubation, using an optical–fluorescent microscope (Nikon, Eclipse Ti), to examine the cell growth and EB formation. To prepare the samples, a micropipette was adjusted to the required volume, equal to that of the liquid marble. Once the liquid core was drawn from the liquid marble, it was gently placed inside a small Petri dish and the cells were examined using the microscope.

The EB formation efficiency inside a liquid marble (LM technique) was further evaluated and compared with the suspension culture method (LS technique) as a common traditional technique used for EB formation. In order to do this, the total number of viable cells was counted and the variation in EB size and morphology alterations were estimated during cultivation. Throughout this set of experiments, the initial cell seeding density was kept constant at 20 000 cells ml^{-1}. One set of cells were seeded onto a low attachment well-plate (cat# 351178, BD, suspension method), while another set of cells were seeded inside liquid marbles and were allowed to form EBs for 3, 7 and 10 days. In order to count single cells, EBs were dissociated by the addition of Tryple (Life Technologies Pty Ltd, Australia) for 10–15 min. Cell counting was then performed for each of the above mentioned culture techniques at different time intervals using trypan blue dye and a haemocytometer.

RNA isolation and cDNA synthesis were also carried out in another set of experiments. As for the quantitative reverse-transcription (RT) polymerase chain reaction (PCR), EBs were allowed to form inside the liquid marbles and were then harvested for RNA isolation using a RNeasy kit (QIAGEN Inc.) at days 3 and 7. They were subsequently treated with Turbo DNase (Ambion), according to the manufacturer's instructions, in order to remove any remaining genomic DNA contamination. The PCR amplification consisted of a total of 35 cycles of denaturation at 95 °C for 2 min, followed by annealing at an appropriate temperature for 30 s and extension at 72 °C for 30 s, with a first denaturation step at 95 °C for 4 min and a final extension step at 74 °C for 10 min. The names of the primers of the three germ layers, annealing temperatures and product sizes are presented in Table 1; undifferentiated ES cells were employed as negative control. The house keeping β-actin was used as an internal control.

Results and discussion

Multiple liquid marbles containing mouse embryonic cells were formed and incubated for ten days, using the liquid marble method reported previously.[12] The effect of powder particle size, liquid marble size and the cell seeding density inside the liquid marbles was investigated. The liquid cores of the liquid marbles were drawn on day 3 and day 7 in order to monitor the cell growth, cell aggregation and EB formation, using optical and fluorescent microscopy. In all cases, embryoid body formation was clearly observable on day 3. However, the shape, uniformity and number of the acquired EBs were significantly affected by altering the experimental conditions. To optimize the experimental conditions, the following experiments were carried out:

1. Monitoring the effect of powder particle size: two different particle sizes of the polytetrafluoroethylene (PTFE) powders (35 μm and 100 μm) were used to investigate the effect of powder particle size on EB formation inside liquid marbles, while the cell seeding density and the liquid marble size were kept constant. EB formation was observed on day 3 in liquid marbles made from both 35 and 100 μm PTFE powders. However, it was observed, through repeated experiments, that liquid marbles formed from 35 μm PTFE powder promoted EB formation more efficiently compared with liquid marbles made from 100 μm particles, in terms of shape and uniformity of the EBs, number of EBs formed and their surface compactness (Fig. 1). The corresponding microscopic images show a layer of aggregated but less compact cells on the surfaces of the EBs formed within liquid marbles made from 100 μm PTFE particles. The aggregated cell layer was uneven and as thick as few individual cells combined. The reason for the significant influence of the liquid marble shell particle size on EB quality is unclear and requires further study. A possible explanation, however, could be the different mechanical properties of the shell of liquid marble formed from powder particles of different particle size. Arbatan and Shen previously reported that the force required to pierce a glass slide through a layer of PTFE powder of different particle sizes over water is different.[36] This force is smaller when the particle size of the powder is smaller. It may be possible that a mechanically weaker PTFE powder layer on water could further reduce the cell adhesion, despite the fact that the powder particles all have the same chemical structure regardless of the powder particle size. On the other hand, it is well known that the focal adhesion of cells on soft substrates is irregular and unstable compared to those attached on a hard substrate.[37] From our observations, the marble shells consisting of 35 μm powder particles provided a liquid marble shell that was less adhesive to cells than the marble shells consisting of 100 μm powder

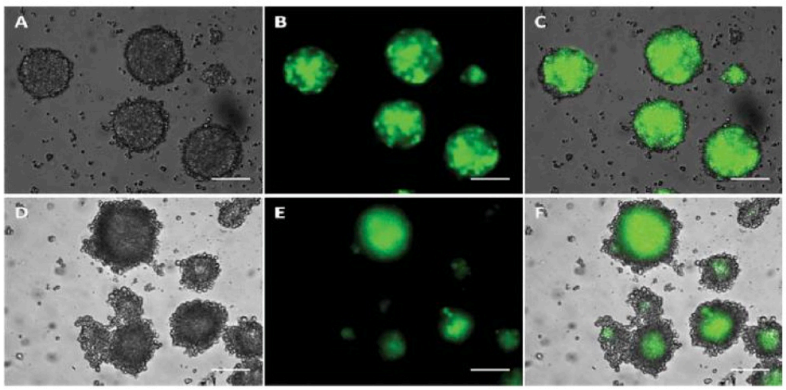

Fig. 1 The difference in morphology and shape in EBs formed in liquid marbles made using (1A–C) 35 μm PTFE powder and (1D–F) 100 μm PTFE powder, scale bar = 100 μm. 1A and 1D are bright field images, while 1B and 1E are fluorescent microscopy images. 1C and 1F are obtained by overlaying the bright field and fluorescent images.

particles. This lower cell adhesion encourages stronger cell aggregation and the formation of EBs.

2. The effect of liquid marble size (volume): two different liquid marble sizes were investigated to monitor the effect of liquid marble size on EB formation and properties: either 50 μL or 300 μL of cell culture medium were used to form the liquid marbles. The liquid marble size seems to have a clear influence on the shape and number of EBs formed inside liquid marble micro bioreactors. When keeping the number of cells and the powder particle size constant, liquid marbles of 300 μL yielded a higher number of EBs that were more uniform than those harvested from the 50 μL liquid marbles. These results are in complete accordance with expectations, since a larger liquid marble contains a greater quantity of growth medium (6 times greater in this set of experiments), so it can provide a more nutrient-rich cell growth medium than a smaller liquid marble (Fig. 2). It should be noted that, unlike conventional methods such as the hanging drop method which requires daily exchange of growth medium, in our EB formation approach we did not perform growth medium exchange. Therefore it is important in our approach to provide the cells and EBs with enough necessary nutrients for the duration of the experiment (generally from 3 to 7 days). Based on our observations, the quantity of nutrients of a 300 μL liquid marble is sufficient to keep the ES cells alive and active inside the liquid marble, throughout the experiment's time frame.

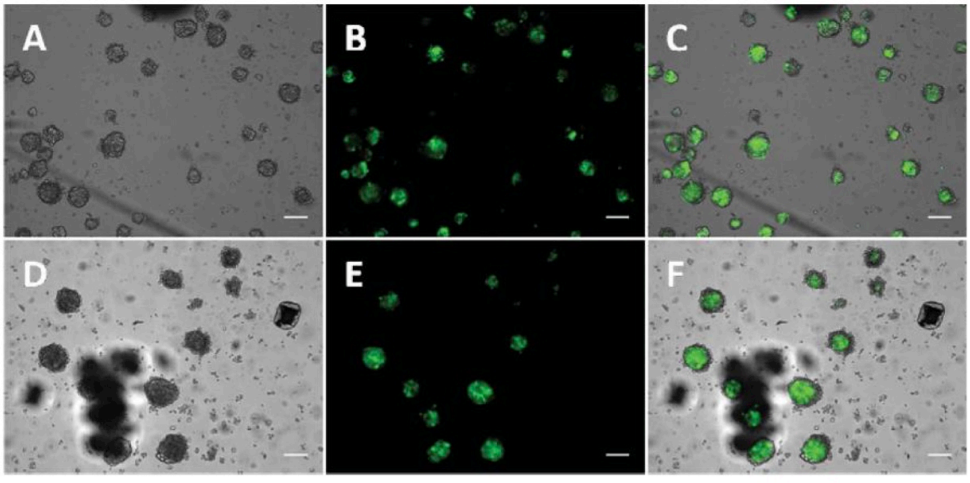

Fig. 2 Higher number of EBs formed in a 300 μl liquid marble (2A–C) compared with a 50 μl liquid marble (2D–F). Both liquid marbles were made from 100 μm PTFE powder and initially inoculated with 10 000 cells. 2A and 2D are optical microscopy images, while 2B and 2E are fluorescent microscopy images. 2C and 2F are obtained by overlaying the corresponding optical and fluorescent images.

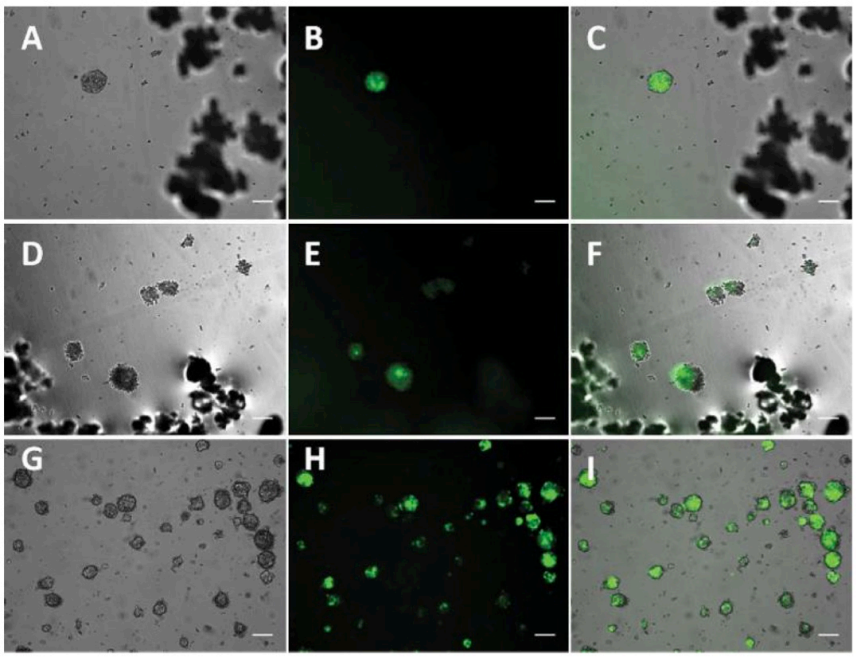

Fig. 3 Comparison of the number of the EBs formed in liquid marbles inoculated with ES cells, with various cell seeding densities: 1000 (3A–C), 5000 (3D–F) and 10 000 (3G–I) cells, (scale bar = 100 μm). 3A, 3D, and 3G are bright field images, while 3B, 3E, 3H are fluorescent microscopy images. 3C, 3F, and 3I are obtained by overlaying the bright field and fluorescent images.

3. The effect of cell seeding density: the cell seeding density inside liquid marbles also plays an important role in the yield and uniformity of the formed EBs. Liquid marbles of the same size, containing four different cell seeding densities (1000, 5000, 10 000 and 20 000 cells per liquid marble), were made and investigated. EB formation in marbles containing 1000, 5000, and 10 000 ES cells are shown in Fig. 3, while the best result which was obtained when using 20 000 cells can be seen in Fig. 4. As can be seen in these figures, although EB formation was observed in all cases, liquid marbles having a higher cell seeding density led to the formation of a greater number of EBs compared with liquid marbles containing lower cell seeding densities. A liquid marble provides a confined space in which cells are free to interact effectively with one another, while having minimal contact with the powder particles thanks to the anti-adhesive property of the hydrophobic powder shell. On the other hand, EB formation partly depends on the accidental impact of ES cells with one another. It is therefore expected that a higher density of cells will provide a higher chance of impact, hence a higher number of EBs.

4. EB formation efficiency inside liquid marbles was compared with the liquid suspension technique as the chosen control method for (a) examining the morphology of the EBs, (b) counting the number of viable cells in the EBs and (c) measuring the size variation in the EBs formed by these two

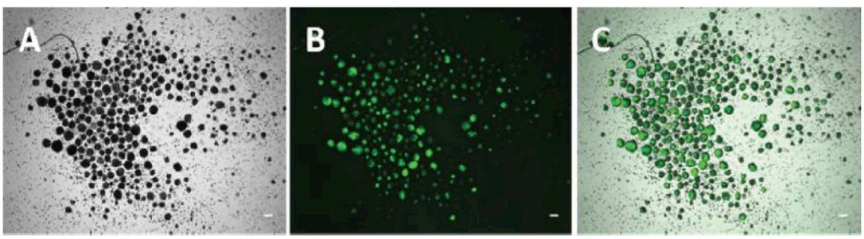

Fig. 4 The high number of EBs formed inside a liquid marble micro bioreactor under optimized conditions on day 3. The liquid marble was 300 μL in volume and was formed using 35 μm PTFE powder, with a cell density of 20 000 ES cells. A is a bright field image, B is a fluorescent microscopy image and C is composed of overlaid corresponding bright field and fluorescent images. Note that the EBs are located in intimate proximity to one another. Bar = 100 μm.

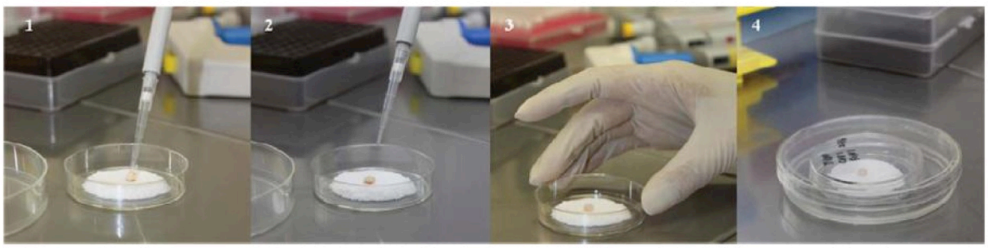

Fig. 5 Steps towards the formation of liquid marbles containing stem cells. The liquid containing the suspended stem cells in the growth medium are placed on the hydrophobic powder bed where the liquid beads up, due to the high hydrophobicity of the powder. The drop is then rolled on the powder bed to cover it with the hydrophobic powder. The Petri dish containing the resulting liquid marble is then placed inside a second Petri dish that is half filled with sterile water, and it is placed in the incubator.

methods. The morphology of EBs formed *via* both methods (LM and LS) after 3, 7 and 10 days of being in culture can be seen in Fig. 6. Our observations suggest that the efficiency of EB formation is significantly affected by the culture method. For instance, the formation of a large number of EBs in both LM and LS methods on day 3 is observed as shown in Fig. 6 and 7. Yet it is clear that the EBs obtained by the LM method are morphologically more uniform and of a narrower size distribution compared to those formed in LS. As for the LS technique, EBs with a wider size distribution and non-uniform morphologies were observed over time (Fig. 6B and D). With continuous growth of EBs in both LM and LS methods, EBs with necrotic cores are observed (darker EBs) as the diameter of EBs increases (Fig. 7). Moreover, as can be seen in Fig. 8, when the average diameter of EBs formed by LM and LS methods are compared at different times, the obtained standard deviation confirms that there is broad size distribution among EBs formed by the LS method. Furthermore, the size variation was found to be much smaller for EBs formed by the LM method. To conclude, although EBs can be generated using the low adhesion suspension culture method, the LM technique in comparison produces more homogeneous EBs, while the former technique suffers from a large variation in size and morphology of the obtained EBs, limiting its yield.

5. The viability of cells inside EBs was also quantified by counting the number of viable cells from cells dissociated from EBs. It was found that there is a significant difference in the viability of cells obtained from the LM and LS methods. In addition, the number of cells increased by factors of 29 and 24 in LM compared to 13 and 11 in LS after 5 and 10 days of being in culture respectively, as shown in (Fig. 9) (initial number of cells was 20 000). The number of viable cells decreased over time for both the LM and LS methods, most probably because nutrient diffusion becomes the limiting factor as the size of EBs increases, as nutrients cannot reach the cores of the EBs.

6. Isolation of RNA was also carried out in another set of experiments using a RNeasy kit (QIAGEN Inc.) on days 3 and 7 of EB culturing. The brachyury expression is known as a mesoderm marker associated with gastrulation, the FOXA2 expression is also known as an endoderm marker, whereas the

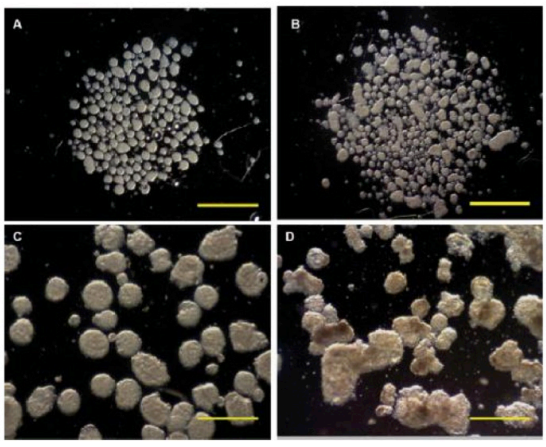

Fig. 6 Bright field images of EBs formed using liquid marble (A, C) and a suspension culture well plate (B, D) for 3 and 7 days in culture, scale bar: 500 μm.

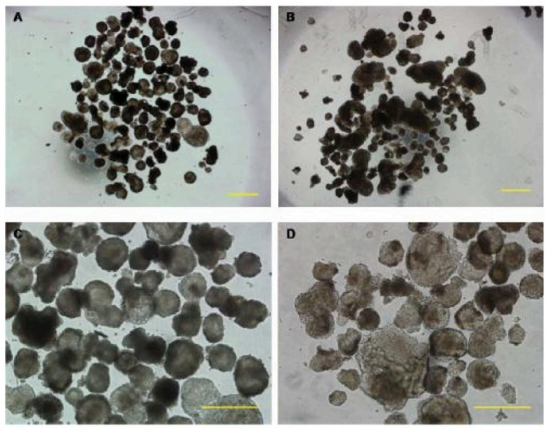

Fig. 7 Bright field images of EBs formed using liquid marble (A, C) and a low adhesion culture plate (B, D) after 10 days in culture, scale bar: 500 μm.

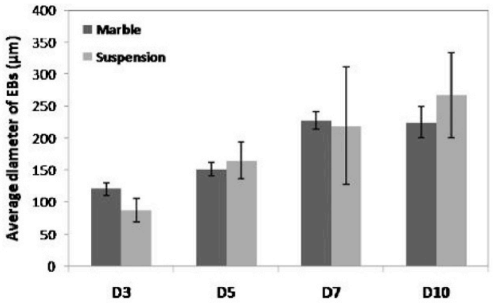

Fig. 8 Average diameter of EBs formed by LM and LS methods. Error bars represent the standard deviation.

nestin expression is an ectoderm marker.[38,39] Fig. 10 shows the RT-PCR of EBs collected at days 3 and 7. Markers of all three germ layers were observed in the EBs which confirms the *in vitro* differentiation potential of EBs that are formed using the liquid marble technique. The presence of these three germ layers demonstrates the potential of these EBs to differentiate into multipotent stem cells (progenitors), which will eventually progress into terminally differentiated cells. Further research into the differentiation of EBs inside liquid marbles is beyond the scope of this paper, but is currently underway in our group and will be reported in another paper.

In summary, when seeded with 2×10^4 ES cells, 300 μL liquid marbles made from PTFE powder with a 35 μm particle size resulted in the formation of hundreds of uniform EBs (Fig. 4). Large liquid marbles made from smaller PTFE powder particles were also found to be easier to handle and manipulate; it was easier to pierce the liquid marble shell of such marbles, to draw the liquid core for microscopy studies. After inoculation of ES cells into a liquid marble, green fluorescence protein expression from the EBs was observed for the first 3 days, indicating that these cells were able to maintain their pluripotency in liquid marbles prior to their differentiation. Some preliminary study on the feasibility of EB differentiation inside liquid marbles was also carried out. Once left in the incubator for 7 days, some EBs were naturally

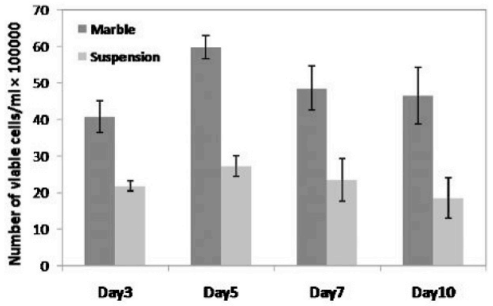

Fig. 9 Number of viable cells in EBs after 3, 5, 7 and 10 days in liquid marble and in suspension culture.

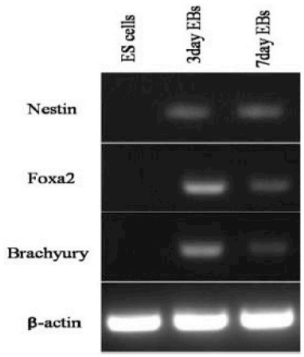

Fig. 10 RT-PCR for the expression of 3 germ layers for 3-day and 7-day old EBs formed inside the liquid marble.

differentiated to beating cardiomyocyte-like cells inside liquid marbles (see ESI†). This is a promising observation, which encourages future studies on the one-pot formation and differentiation of EBs inside liquid marbles as bioreactors. Therefore, we speculate that the addition of appropriate differentiation factors to the liquid marbles upon formation of EBs on day 3 could result in the formation of differentiated cells of desired cell types. The influence of the physical properties of liquid marble on EB differentiation and beating EB characteristics is currently under investigation.

Conclusion

The formation of EBs inside liquid marbles made from hydrophobic PTFE particles was investigated in this study. Liquid marbles are introduced as a novel and efficient means for *in vitro* preparation of EBs that could subsequently be differentiated into different cell lineages, such as cardiovascular cells. Although further studies are required to fully comprehend the biochemical aspects of the interactions between ES cells as well as EBs, and the hydrophobic powder particles, smaller powder particles generally resulted in more efficient liquid marble micro bioreactors for the formation of EBs. The cell seeding density (CSD) and liquid marble size (LMS) can also affect the efficiency of the method; the greater the CSD and LMS, the higher the efficiency of EB formation inside the liquid marbles. Liquid marble micro bioreactors provide a facile new method for the highly efficient production of EBs. Optimization of this method shows that it is capable of producing EBs of more homogeneous size and shape compared to EBs produced by the liquid suspension method. Miniaturization of bioreactors using the liquid marble concept also has a clear economical advantage over the existing methods.

Acknowledgements

FS is grateful for the scholarship provided by the Department of Mechanical and Aerospace Engineering at Monash University. FS also appreciates guidance from Prof. Kerry Hourigan and Prof. Mark C. Thompson from Monash University. Funding for this research was also partly provided through an Australia Research Council Discovery Project Grants ARC DP 120102570 and ARC LP0989823. We also thank Professor Paul Verma from Monash Institute of Medical Research (MIMR) for supplying Oct4b2 cells, PCR equipment and kind intellectual cooperation. PPYC is grateful for a RMIT University Senior Research Fellowship and an MCN Technology Fellowship that supported this work. This work was performed in part at the Melbourne Centre for Nanofabrication.

Notes and references

1 P. Aussillous and D. Quere, *Nature*, 2001, **411**, 924–927.
2 P. Aussillous and D. Quere, *Proc. R. Soc. London, Ser. A*, 2006, **462**, 973–999.
3 E. Bormashenko, *Curr. Opin. Colloid Interface Sci.*, 2011, **16**, 266–271.
4 G. McHale and M. I. Newton, *Soft Matter*, 2011, **7**, 5473–5481.
5 T. H. Nguyen, K. Hapgood and W. Shen, *Chem. Eng. J.*, 2010, **162**, 396–405.
6 E. Bormashenko, Y. Bormashenko, A. Musin and Z. Barkay, *ChemPhysChem*, 2009, **10**, 654–656.
7 J. Tian, T. Arbatan, X. Li and W. Shen, *Chem. Commun.*, 2010, **46**, 4734–4736.
8 J. Tian, T. Arbatan, X. Li and W. Shen, *Chem. Eng. J.*, 2010, **165**, 347–353.
9 Y. Xue, H. Wang, Y. Zhao, L. Dai, L. Feng, X. Wang and T. Lin, *Adv. Mater.*, 2010, **22**, 4814.
10 Y. Zhao, J. Fang, H. Wang, X. Wang and T. Lin, *Adv. Mater.*, 2010, **22**, 707.
11 T. Arbatan, L. Li, J. Tian and W. Shen, *Adv. Healthcare Mater.*, 2012, **1**, 79–79.
12 T. Arbatan, A. Al-Abboodi, F. Sarvi, P. P. Y. Chan and W. Shen, *Adv. Healthcare Mater.*, 2012, **1**, 467–469.
13 M. J. Evans and M. H. Kaufman, *Nature*, 1981, **292**, 154–156.
14 A. G. Smith, *Annu. Rev. Cell Dev. Biol.*, 2001, **17**, 435–462.
15 R. Palacios, E. Golunski and J. Samaridis, *Proc. Natl. Acad. Sci. U. S. A.*, 1995, **92**, 7530–7534.
16 M. V. Wiles and G. Keller, *Development*, 1991, **111**, 259.
17 R. Wang, R. Clark and V. L. Bautch, *Development*, 1992, **114**, 303–316.
18 C. Mummery, D. Ward, C. E. van den Brink, S. D. Bird, P. A. Doevendans, T. Opthof, A. B. de la Riviere, L. Tertoolen, M. van der Heyden and M. Pera, *J. Anat.*, 2002, **200**, 233–242.
19 V. A. Maltsev, A. M. Wobus, J. Rohwedel, M. Bader and J. Hescheler, *Circ. Res.*, 1994, **75**, 233–244.
20 G. Bain, D. Kitchens, M. Yao, J. E. Huettner and D. I. Gottlieb, *Dev. Biol.*, 1995, **168**, 342–357.
21 A. G. Smith, J. K. Heath, D. D. Donaldson, G. G. Wong, J. Moreau, M. Stahl and D. Rogers, *Nature*, 1988, **336**, 688–690.
22 I. Desbaillets, U. Ziegler, P. Groscurth and M. Gassmann, *Exp. Physiol.*, 2000, **85**, 645–651.
23 G. M. Keller, *Curr. Opin. Cell Biol.*, 1995, **7**, 862–869.
24 S. M. Dang, S. Gerecht-Nir, J. Chen, J. Itskovitz-Eldor and P. W. Zandstra, *Stem Cells*, 2004, **22**, 275–282.
25 P. W. Zandstra, C. Bauwens, T. Yin, Q. Liu, H. Schiller, R. Zweigerdt, K. B. S. Pasumarthi and L. J. Field, *Tissue Eng.*, 2003, **9**, 767–778.
26 F. UIIoa-Montoya, C. M. Verfaillie and W.-s. Hu, *J. Biosci. Bioeng.*, 2005, **100**, 12–27.
27 J. M. Kelm and M. Fussenegger, *Trends Biotechnol.*, 2004, **22**, 195–202.
28 S. M. Dang, M. Kyba, R. Perlingeiro, G. Q. Daley and P. W. Zandstra, *Biotechnol. Bioeng.*, 2002, **78**, 442–453.
29 M. Koike, S. Sakaki, Y. Amano and H. Kurosawa, *J. Biosci. Bioeng.*, 2007, **104**, 294–299.
30 S. Niebruegge, C. L. Bauwens, R. Peerani, N. Thavandiran, S. Masse, E. Sevaptisidis, K. Nanthakumar, K. Woodhouse, M. Husain, E. Kumacheva and P. W. Zandstra, *Biotechnol. Bioeng.*, 2009, **102**, 493–507.
31 M. Wartenberg, J. Gunther, J. Hescheler and H. Sauer, *Lab. Invest.*, 1998, **78**, 1301–1314.
32 M. V. Wiles, *Methods Enzymol.*, 1993, **225**, 900.
33 D. E. Kehoe, D. Jing, L. T. Lock and E. S. Tzanakakis, *Tissue Eng. A*, 2010, **16**, 405–421.
34 Y. Chisti, *Crit. Rev. Biotechnol.*, 2001, **21**, 67–110.
35 C. M. Begley and S. J. Kleis, *Biotechnol. Bioeng.*, 2000, **70**, 32–40.
36 T. Arbatan and W. Shen, *Langmuir*, 2011, **27**, 12923–12929.
37 R. J. Pelham and Y. L. Wang, *Biol. Bull.*, 1998, **194**, 348–349.
38 2A. Mogi, H. Ichikawa, C. Matsumoto, T. Hieda, D. Tomotsune, S. Sakaki, S. Yamada and K. Sasaki, *Tissue Cell*, 2009, **41**, 79–84.
39 M. Nishikawa, N. Yanagawa, N. Kojima, S. Yuri, P. V. Hauser, O. D. Jo and N. Yanagawa, *Biochem. Biophys. Res. Commun.*, 2012, **417**, 897–902.

5.3 Appendix

5.3.1 Effect of different parameters including powder particle size, liquid marble volume and cell seeding density on EB formation

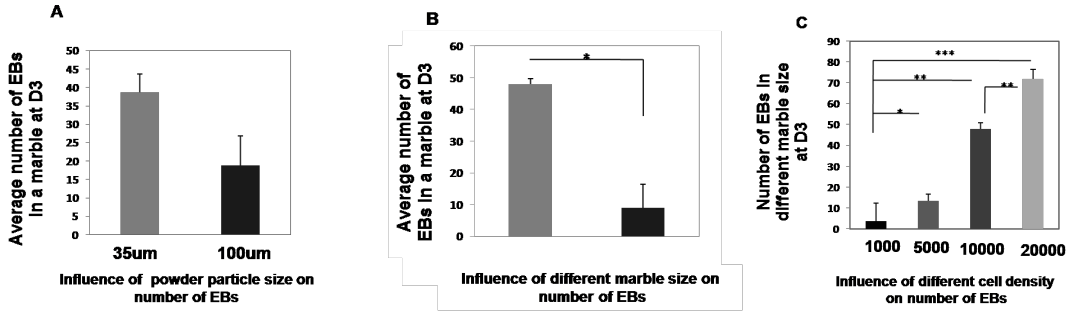

Figure (A-1): the effect of (A) powder particle size, (B) liquid marble volume and (C) cell seeding density at day three of EB formation in liquid marble; the results are presented as mean value ± standard deviation. Then, the means of each group of data were compared by using analysis of variance (ANOVA), where p values lower than 0.05 were considered statistically significant.

It was observed, through repeated quantitative and qualitative experiments, that liquid marbles formed from smaller PTFE powder promoted EB formation more efficiently compared with liquid marbles made from larger particles, in terms of shape and uniformity of the EBs, number of EBs formed and their surface compactness (A-1A).

When keeping the number of cells and the powder particle size constant, liquid marbles of 300 mL yielded a higher number of EBs that were more uniform than those harvested from the 50 mL liquid marbles. These results are in complete accordance with expectations, since a larger liquid marble contains a greater quantity of growth medium (6 times greater in this set of experiments), so it can provide a cell growth medium more nutrient-rich than a smaller liquid marble (A-1B).

Liquid marbles of the same size, containing four different cell seeding densities (1000, 5000, 10000 and 20000 cells per liquid marble), were made and investigated. As can be seen in these figures, although EB formation was observed in all cases, liquid marbles having a higher cell seeding density led to the formation of a greater number of EBs compared with liquid marbles containing lower cell seeding densities. (A-1C)

Chapter 6: Stem cell Differentiation through Liquid Marble Technique

6.1 General Overview

Cardiovascular disease is one of the leading causes of death worldwide. On the other hand, adult cardiomyocytes are unable to replace the damaged myocardium in any clinically significant manner [6]. The regeneration of the injured or diseased myocardium to prevent or treat heart failure has proven to be a difficult challenge that has attracted many investigators over the past two decades.

Differentiation of ESCs via EB formation remains the most promising, convenient and economical approach; however, there remain several drawbacks with the common methods using for EB formation.

This chapter includes a comprehensive study on the capability of liquid marble in terms of forming EBs and subsequently inducing cardiomyocytes differentiation for future transplantation and clinical application.

To achieve this aim, a 5-day-old EB formed via the liquid marble method was attached onto a gelatin-coated plate and cultured for further differentiation. Quantitative gene expression studies demonstrated that the cells inside the EB expressed cardiac specific structural genes including the Myosin light chain-2v (MLC2v), the myosin light chain 2a (MLC2a), α-actinin as cardiac sarcomeric protein and cardiac transcription factors GATA4, Nkx2.5. Upon differentiation, spontaneous beating cells were observed after plating down the EBs for 3-4 days, the number of beating EBs increased over time, and retained contractility for over 18 days. Cells in the contracting areas were stained positively for cardiac marker (cardiac troponinT (cTnT)).

Altogether, these results demonstrated that mES cells could differentiate into myocytes cells using the liquid marble technique as a simple, cost effective and straightforward method. Liquid marbles is a promising tool that facilitates cardiac differentiation, and can be used in various biology and genetic studies.

This chapter compromises one submitted article as a full paper to the Journal of Advanced Healthcare Materials.

6.2 Cardiogenesis of Embryonic Stem Cells with Liquid Marble Micro-bioreactor

Fatemeh Sarvi, Kanika Jain, Tina Arbatan, Paul J. Verma, Kerry Hourigan, Mark C. Thompson, Wei Shen, Peggy P.Y. Chan**

F.Sarvi, Prof. K. Hourigan, Prof. M.C. Thompson
Department of Mechanical & Aerospace Engineering & Division of Biological Engineering, Monash University, VIC 3800, Australia
K. Jain, Dr. T. Arbatan, Prof. W. Shen
Department of Chemical Engineering, Monash University, VIC 3800, Australia
[redacted]
Prof. P.J. Verma
South Australia Research and Development Institute (SARDI), Rosedale SA 5350, Australia
Division of Biological Engineering, Monash University, VIC 3800, Australia
Dr. P.Y. Chan
Micro/Nanophysics Research Laboratory, School of Applied Science, RMIT University, Melbourne, VIC 3000, Australia, Melbourne Centre for Nanofabrication, Australia National Fabrication Facility, Clayton, VIC 3168, Australia
[redacted]
* Corresponding authors contributed equally to this work

Keywords: Liquid marble, Embryonic stem cells, Cardiomyocytes, Embryoid Bodies, Micro-bioreactor

6.2.1 Abstract

A liquid marble micro-bioreactor is prepared by placing a drop of murine ESC (Oct4B2-ESC) suspension onto a polytetrafluoroethylene (PTFE) particle bed. The Oct4B2-ESC aggregate to form EBs with relatively uniform size and shape in a liquid marble within 3 days. For the first time, the feasibility of differentiating ESC into cardiac lineages within liquid marbles is being investigated. Without the addition of growth factors, suspended EBs from liquid marbles express various pre-cardiac mesoderm markers including Flk-1, Gata4 and Nkx2.5. Some of the suspended EBs exhibit spontaneous contraction. These results indicate that the liquid marble provides a suitable microenvironment to induce EB formation and spontaneous cardiac mesoderm differentiation. Some of the EBs are subsequently plated onto gelatin-coated tissue culture dishes. Plated EBs express mature cardiac markers MLC2a and MLC2v, and the cardiac structural marker α-actinin. More than 60% of the plated EBs exhibit spontaneous contraction and express mature cardiomyocyte marker cardiac troponinT (cTnT), indicating that these EBs have differentiated into functional cardiomyocytes. Together, these results demonstrate that the liquid marble technique is an easily

employed, cost effective, and efficient approach to generate EBs and facilitating their cardiogenesis. The cardiomyocytes generated using this liquid marble approach could be useful for transplantation.

6.2.2 Introduction

Adult hearts have a very limited capacity for self-regeneration after myocardial infarction (MI; heart attack). Transplanted stem cells or progenitor cells have the capacity to repair infarcted myocardium [7, 8]. Pluripotent ESC, isolated from the inner cell mass of a developing blastocyst [9] possess the ability to self-renew, and have the potential to differentiate into various cell lineages, including all three germ layers [10] and cardiomyocytes [11]. The ability to engineer these ESC genetically, together with their ability to differentiate into cardiomyocytes in vitro, make them valuable and promising cell sources for cell therapy, tissue engineering and regenerative medicine [12]. Forming three-dimensional (3D) embryo-like cell aggregates, known as embryoid bodies (EBs), is a key step for the in-vitro differentiation of ESC [4]. Indeed, an embryoid body consists of three germ layers (ectodermal, mesodermal, and endodermal tissues) that emulate the features of a developing embryo [10, 13], thereby providing a valuable tool for various embryogenesis studies [14, 15].

Several methods have been employed to form EBs from ESC and to subsequently differentiate them into cardiomyocytes. These include: hanging-drop culture, [14] spinner flask, [16] centrifuge-forced aggregation, [17] and suspension culture in a low-adherence vessel. [4, 10] The hanging-drop method is the most commonly used technique for EB formation, in which an ESC suspension was placed on the inner surface of a petri dish lid. EBs can be formed after inverting the lid due to the balance of gravitational and surface tension forces. Changing the droplet volume and seeding density can tune the size of the EBs. However, the hanging drop method is labour intensive and time consuming. It is also practically impossible to perform medium exchange using this method. In addition, the drop volume is limited to less than 50 μl, thereby making it incapable of supporting large-scale production. [13] Rotation-based methods, such as the spinner flask and centrifuge-forced aggregation methods, can facilitate large-scale production. However, these methods require costly equipment; moreover, the shear stress induced by the rotation may reduce cell viability, and disrupt cell-cell signalling and the subsequent cell differentiation. The method based on suspension culturing using conventional low-adherence vessels has limited control over size, shape and uniformity of EBs [18].

The liquid marble was first described by [19] and consists of a drop of liquid encapsulated by hydrophobic powder particles. These particles adhere to the surface of the liquid drop, isolating the liquid core from the supporting surface, while allowing gas exchange between the interior liquid and the surrounding environment [20]. A liquid marble can be rolled around similar to a droplet of mercury [21]. As the shells of liquid marbles are made from discrete particles, the shells can be

opened, allowing materials such as reagents and products to be introduced into or extracted from the liquid marble; this unique property therefore facilitates chemical and biochemical reactions to be controlled within liquid marbles.

In addition, reagent consumption can be reduced due to the small size of a liquid marble. The chance of contamination is low as a result of the indirect contact between the liquid core and the supporting surface, thus providing an advantage for a variety of applications [20, 22-24]. The use of liquid marbles as miniaturized bioreactors is particularly attractive because of the capability to contain chemical and biological reactions [23, 25-27]. Our previous studies reported the production of 3D cancer-cell spheroids using liquid marble micro-bioreactors [26]. This liquid marble method is advantageous for spheroid production, as it allows the production of spheroids with homogeneous size and shape at a larger scale compared with the hanging drop method, as well as facilitating medium exchange. Unlike rotation-based methods, the liquid-marble method does not induce shear stress on the spheroids, thereby producing viable spheroids [18].

Herein, we report the use of the liquid marble as a micro-bioreactor to produce EBs from ESC and, for the first time, we study the feasibility to further differentiate the EBs into lineage-specific cells. The in-vitro cardiac differentiation ability of the resulting EBs was assessed by examining gene expression, protein expression and contraction characteristics. We demonstrate that liquid marbles provide a promising platform to facilitate EB differentiation into cardiac lineages.

6.2.3 Experimental Section

6.2.3.1 Tissue Culture

Feeder free murine Oct4B2-ESC (129/Sv) containing the Oct4-GFP-IRES-puromycin and hygromycin resistance cassettes were used for this work. For expansion, ESC were cultured in Dulbecco's modified eagle medium (cat#11995, Gibco) supplemented with 10% FBS (JRH Biosciences, Australia), 1% non-essential amino acids (NEAA) (cat#11140-050, Invitrogen), 1% GlutaMAX™ (cat#35050061, Invitrogen), 0.5% penicillin-streptomycin (cat#15070-063, Invitrogen), 0.1 mMβ-mercaptoethanol (cat#21985-023, Invitrogen), and 1,000 U/ml ESGRO leukemia inhibitory factor (mLIF, Chemicon, Australia). The medium was filtered through a 0.22um filter for sterilization and was stored at 4°C for up to a fortnight. Cells were cultured on 0.1% gelatin-coated 6-wellplates (BD Falcon) at 37°C in a humidified 5% CO2 incubator and were passaged every 2-3 days. The GFP expression of the cells was monitored using an IX71 Olympus epifluorescence microscope.

6.2.3.2 Preparation of cell containing liquid marble micro-bioreactor

ESC were cultured to 70-80% confluency; cells were then washed with Dulbecco's phosphate buffered saline (DPBS, Sigma) and dispersed into single cells using TrypleTm express (Gibco, Life Technologies, Australia). To form liquid marbles, 2×104 ESCs were suspended in 300µl of differentiation medium. The differentiation medium consisted of high glucose DMEM (Gibco, Life Technologies, Australia) supplemented with 10% FBS (JRH Biosciences, Australia), 1% non-essential amino acids, 1% GlutaMAX™ (Gibco, Life Technologies, Australia), 0.5% penicillin-streptomycin (Gibco, Life Technologies, Australia), 0.1 mMβ- mercaptoethanol (Gibco, Life Technologies, Australia) and without mLIF. This drop of cell suspension was placed onto a polytetrafluoroethylene (PTFE, 35µm particle size, Sigma, Australia) powder bed inside a petri dish (60 mm diameter) using a micropipette. When the drop of cell suspension was rolled on the hydrophobic powder bed, the powder particles wrapped the surface of the drop, thus leading to the formation of a liquid marble. The petri dish was then placed inside a larger petri dish (100 mm diameter) containing sterile water to minimise evaporation from the liquid marbles, following which the set of dishes was covered and kept inside a humidified incubator. The ESCs were allowed to aggregate to form EBs within the liquid marble over a period of 5 days. Figure 6.1 illustrates the process of forming the liquid marbles.

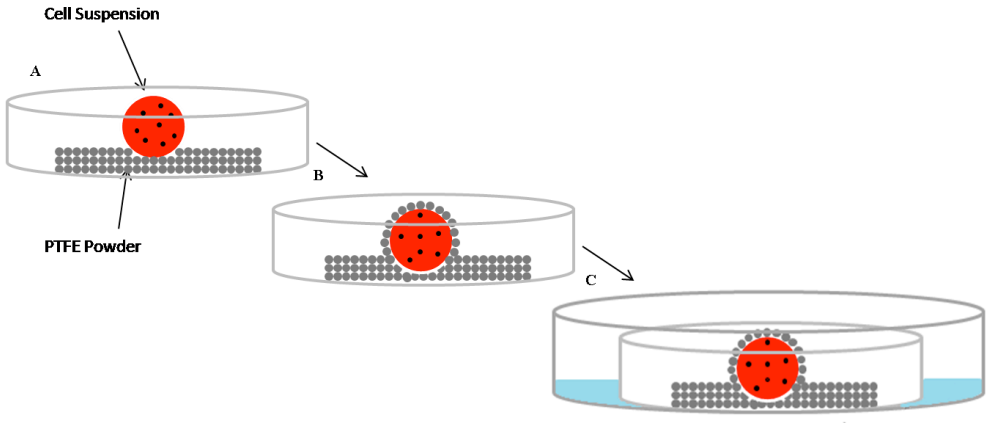

Figure (6.1): Schematic illustration of the steps involved in preparing a liquid marble bioreactor. (A) 300 microlitre of cell suspension is placed onto a hydrophobic PTFE powder bed, (B) The Petri dish was then rolled gently to allow the PTFE particles to cover the cell suspension to form the liquid marble. (C) Placing the marble dish inside a bigger petri dish with sterilized water to prevent evaporation.

6.2.3.3 *EB morphology and pluripotency characterization*

ESC-containing liquid marbles were prepared and allowed to incubate for a period of 10 days. EB samples were taken from the liquid marbles at day 3, 7 and 10. The morphology and GFP expression of EBs were monitored using optical and epifluorescence microscopy (Olympus 1X70 microscope). Both phase-contrast and epifluorescent images were captured. The collected EBs were further dissociated into single cells using TrypleTm express; the GFP expression of these cells was quantified using fluorescence-activated cell sorting (FACS) at different time points during EB formation.

6.2.3.4 *In Vitro cardiac differentiation*

For cardiac differentiation, 5 day old EBs were removed from the marbles and transferred to 0.1% gelatin-coated 24-well plates and cultured in differentiation medium for further analysis. The plated EBs were examined daily for contractile activity based on videos captured at 15 fps using a camera through an optical microscope. The detailed description of the protocol is illustrated in Figure 6.2.

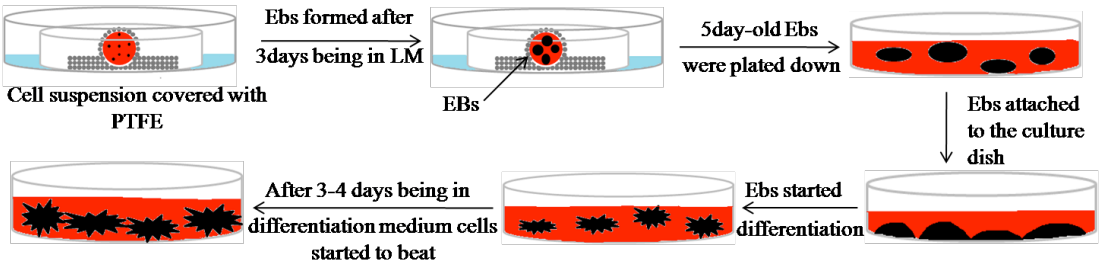

Figure (6.2): Schematic steps for cardiac differentiation

6.2.3.5 *Reverse-Transcription and Real-Time Polymerase Chain Reaction*

The gene expression analysis of the EBs and the cells undergoing differentiation was carried out quantitatively using the reverse-transcription (RT) polymerase chain reaction (PCR). Liquid-marble suspended EBs and plated-down EBs were both subjected to RT-PCR analysis using various differentiation markers.

EBs were allowed to form inside the liquid marbles for 3, 7 and 10 days, and were then retrieved from the LM for RT-PCR. To allow further differentiation, some EBs were retrieved from liquid marble

after 5 days and plated down on gelatin-coated wells for another 15 days. The plated EBs were analysed for differentiation markers at time points D6, 8, 10, 12 and 15 days. Cells were harvested with TrypleTM express, the resulting cell pellets were snap chilled at -80°C prior to analysis. For RT-PCR, ribonucleic acid (RNA) was isolated from cells using the RNeasy kit (Qiagen, Australia) according to the manufacturer's instructions. RNA quality and concentration were measured using a NanoDrop ND-1000 (NanoDrop Technologies, Australia). The isolated RNA was subjected to RQ1 DNase (Ambion, Australia) treatment to remove any contaminating genomic deoxyribonucleic acid (DNA). Complementary DNA (cDNA) was generated using the Superscript III enzyme (Life Technologies, Australia) according to the manufacturer's protocols. The cDNA samples were subjected to PCR amplification with mouse cardiac specific primers. β-actin was used as an internal control. The primer sequences were obtained from the online NCBI Primer-Blast databank and are listed in Table 6.1. The PCR products were size fractionated using 1% agarose gel electrophoresis at 110V for 1 h. For quantification, real-time PCR was performed. Real-time PCR analysis was performed using a 7900HT Fast Real-Time PCR system (Applied Biosystems, Australia) at standard reaction conditions using the Power SYBR Green PCR Master Mix (Applied Biosystems, Australia). Briefly, after 2 min denaturation at 95°C, 35 PCR cycles were carried out at 95°C for 15s, 58°C for 30s and 72°C for 30s, followed by a dissociation stage. Relative mRNA levels were calculated using the ΔΔCT method [28] and were analysed using SDS Version 2.4.1 software. The experiment was replicated three times.

Table (6.1): PCR primers sequences and the NCBI accession numbers for the corresponding genes

Gene name	Forward/ Reverse (5'→3')	NCBI accession no.
Flk-1	GGCGGTGGTGACAGTATCTT/CTCGGTGATGTACACGATGC	NM_010612.2
Nkx2.5	ACACCCACGCCTTTCTCAGTCAAA/CGACAGGTACCGCTGTTGCTTGAA	NM_008700.2
Gata4	TCTCACTATGGGCACAGCAG/GCGATGTCTGAGTGACAGGA	NM_008092
MLC2a	TCAGCTGCATTGACCAGAAC/AAGACGGTGAAGTTGATGGG	NM_022879.2
MLC2v	AAAGAGGCTCCAGGTCCAAT/CCTCTCTGCTTGTGTGGTCA	NM_010861.3
α-actinin	ATGAGGATTGGCTGCTTT/ TGTTCCACCCGGTCTTG	NM_013456
β-actin	CACCACACCTTCTACAATGAGC/TCGTAGATGGGCACAGTGTGGG	NM_007393.3
Oct4	GTTCAGCCAGACCACCATCT/CCAGGGTCTCCGATTTGCAT	NM_013633

6.2.3.6 Immunocytochemistry

The protein markers on the cells were characterized using immunostaining. Incubated cells were first fixed in 4% paraformaldehyde for 30 minutes and washed three times with 1% bovine serum albumin

(BSA) in +/+DPBS. Fixed cells were incubated with blocking solution (5% goat serum, 1% BSA in +/+DPBS) for 1 hour at room temperature. Cells were then incubated overnight with NKx2.5 primary antibody (Santa Cruz, ThermoFisher Scientific, Australia) and cTnT primary antibody (Abcam, Sapphire Bioscience, Australia) diluted (1:500) in blocking solution at 4°C. Next, the cells were washed three times with 1% BSA in +/+DPBS and then incubated at room temperature for 1 hour with Alexa 594 labelled secondary antibodies (Molecular Probes, Life technologies, Australia) at a concentration of 1:400 in blocking solution. Cells were washed three times with 1% BSA in DPBS for 10 minutes. Nuclei were counterstained with Hoechst (1µg/ml, Sigma, Australia) dye. Cells were analysed by epifluorescence microscopy (IX71 Olympus microscope, Australia).

6.2.3.7 Image analysis

After plating 5-day-old EBs for another 4 days in gelatin-coated wells, beating foci appeared in the outgrowing EBs. Videos of the beating foci were captured using the microscope camera system; these videos were converted into image sequences using NIS viewer elements software (Nikon, USA). The images were converted to gray scale. The contraction rhythm of the EBs was evaluated using a modified image processing method described in Arshi et al. [29]. As the EB underwent rhythmic beating, the cell cluster colour changed from dark to light. Ten different areas were selected from each video, the contracting motion through changes in gray scale intensity in each area was analysed using ImageJ software (NIH, USA), and the resulting mean intensity was plotted against time.

6.2.4 Result and Discussion

6.2.4.1 Pluripotency and propagation of EB

Formation of three-dimensional aggregates called EBs is an important step that precedes the initiation of in vitro differentiation of ESC into various cell types [30]. Under the in vitro conditions, an EB is known to simulate the events of a developing embryo. In a previous study, we reported the possibility of using LMs as a facile and efficient micro-bioreactor for in-vitro EB formation [18]. In that study, ESC were cultivated inside liquid marbles and cell aggregates were obtained from day 3. All three germ layers developed spontaneously within the cell aggregates, indicating that the ESC formed EBs successfully inside the liquid marbles [18]. In our present study, we use liquid marbles as micro-bioreactors to generate EBs from Oct4B2-ESC and investigate, for the first time, the capability of liquid marble to facilitate cardiac differentiation. The morphology of cells harvested from the liquid

marbles was assessed using optical microscopy. The Oct4B2-ESC contain a pluripotency marker that drives the expression of GFP, hence GFP expression is a direct indicator of cell pluripotency [31].

The pluripotency of cells forming the EBs was monitored by examining their GFP expression. Representative images in Figure 6.3 show that after cultivating Oct4B2-ESC in liquid marbles for 3 days, these cells aggregated to form EBs, and that these EBs exhibited a compact and round shape with relatively uniform size.

As evident from Figure 6.3A,B, the ES cells, while aggregating to form clusters destined to form EBs, retained their GFP expression, indicating that the cells do not lose their pluripotency. The Day 10 analysis of the EBs revealed an increase in size suggesting the proliferation of cells within the LM. There was a decrease in the GFP flourescence observed, stipulating the loss of pluripotency and that there was an initiation of differentiation of ES cells within the LM (Figure 6.3D).

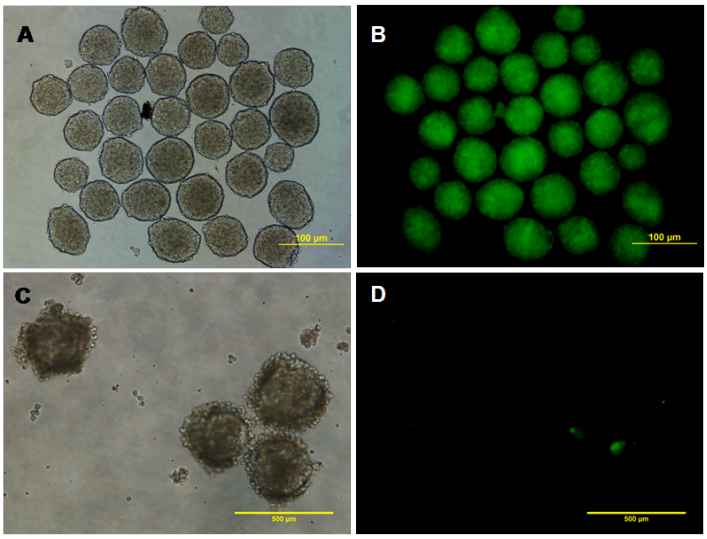

Figure (6.3): Representative phase-contrast and fluorescence microscopy images showing the morphology of EBs. These EBs were formed by allowing Oct4B2-ESC to aggregate inside liquid marbles for (A,B) 3 days (scale bars represent 100 µm) and (C,D) 10 days (scale bars represent 500 µm). Fluorescence microscopy images (B,D) show the expression of GFP under the control of Oct4.

Oct4B2 cells were allowed to form EBs in liquid marbles for 10 days; samples were collected from the liquid marbles at day 0 (control), 3, 7 and 10. FACS analysis was performed on the dissociated cells to quantify the number of GFP+ cells in an EB in order to examine their pluripotency. Representative FACS analysis profiles in Figure 6.4 show that 98.8% and 92.4% of cells expressed GFP at day 0 and 3, respectively. The GFP expression gradually reduced to 20% and 9.4% at day 7 and 10, respectively. Thus, the loss of GFP expression as suggested from the FACS analysis and the flourescence data implies the ability of LM to allow proliferation and differentiation of Oct4B2 cells.

This novel system is thus capable of providing a suitable microenvironment for the growth and differentiation of ESCs.

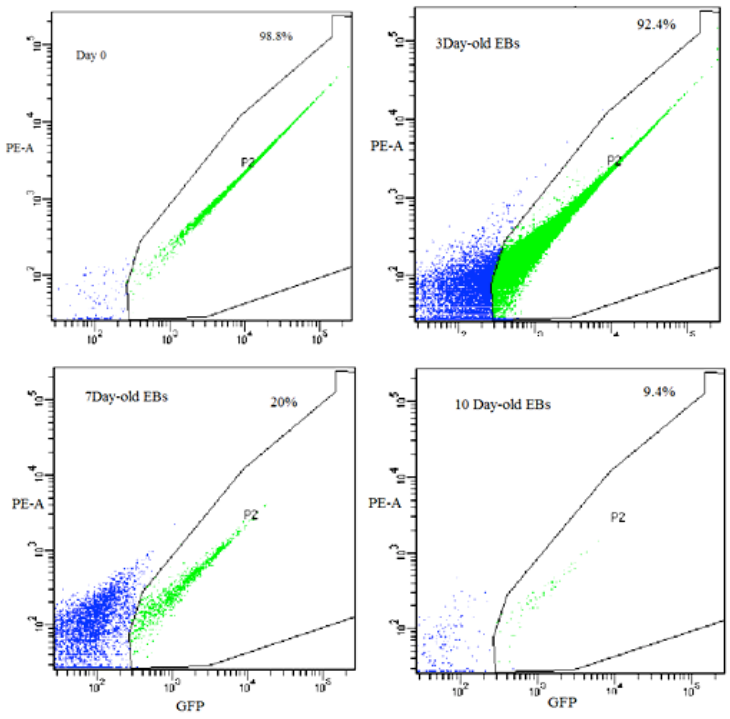

Figure (6.4): FACS analysis: GFP expression of LM induced EBs of Oct4B2 at day 0 (control), 3, 7 and 10. Numbers indicate the percentage of GFP^+ cells. GFP is indicated on *x*-axis, and autofluorescence on *y*-axis. GFP^- population is represented by blue dots, while GFP^+ events are represented by green dots.

It has been well documented that during the development of contractile cardiomyocytes, progenitor cells need to first anchor to a substrate followed by cell spreading, withdrawal from the cell cycle, and fusion with nascent myotubes before their ultimate differentiation into cardiomyocytes [32]. In order to promote cardiogenesis of our LM induced EBs, 5-day old EBs were plated onto gelatin-coated 6-wells and allowed to differentiate further. Upon EB adhesion, the cells began to migrate and grew outwards from the periphery of the EB to form a monolayer, as shown in the representative images in Figure 6.5A and 5B. In the outgrown areas shown in Figure 6.5C, it was observed that cells exhibited heterogeneous cell morphology. At the start of cardiac differentiation, cells were small and rounded, which upon further differentiation changed to elongated, spindle shaped cells. This observation was in-line with the results of the electrophysiological measurements conducted by Hescheler, et al. 1997 [33] wherein the heterogeneous population of cardiomyocytes undergoes a shift from early stage cardiomyocytes (small and rounded with rarely developed sarcomeres) to terminally differentiated atrial-/ventricular- like (elongated with high content of organized myofibrils) cells.

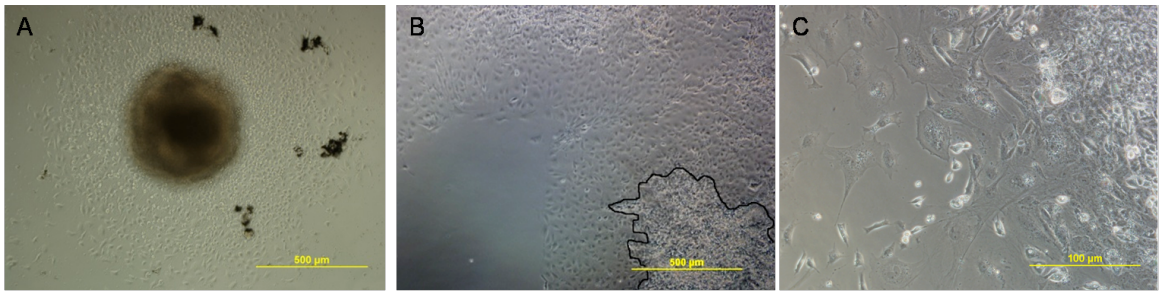

Figure (6.5): Phase-contrast images of a cardiac explants outgrowth. (A) Representative image showing a plated EB attached to a gelatin-coated plate after 1 day, (B) representative image of plated EB outgrowth at day 4, scale bars represent 500 µm. The black line shows the border of flattened EBs after plating down. (C) Representative image of the plated EB depicting the heterogeneous cell morphology (small and round, spindle shaped cells), at day 8, scale bar represent 100 µm.

6.2.4.2 Reverse Transcription PCR analysis of cardiac marker expression during cardiogenesis

To characterize the differentiation pathway of EBs generated from a liquid marble, the gene expression of EB-derived cells was qualitatively determined using RT-PCR. Cells from a suspended EB obtained from a liquid marble and plated EBs were collected at different time points and were characterized using a series of cardiac markers. Flk-1 expression is found in mesodermal progenitor cells that have the ability to further differentiate into cardiac muscles [34, 35]. Gata4 is a regulator of early cardiogenesis [36], it expresses in pre-cardiac mesoderm and subsequently expresses in the endocardial and myocardial tissues of developing heart and heart tube; overexpression of Gata4 is known to up-regulate the expression of transcription factors Nkx2.5 [37]. The cardiac specific transcription factor Nkx-2.5 is the key regulator of cardiac-specific transcription involved in cardiogenesis which is generally observed in the pluripotent stem cell-derived cardiomyocytes [38]. Therefore, Flk-1, Gata4 and Nkx2.5 were all employed as pre-cardiac mesoderm markers in this study. β-actin was used as housekeeping marker gene. Atrial myosin light chain 2a (MLC2a) and ventricular myosin light chain (MLC2v) are both cardiac structural proteins, and are often employed as mature cardiac cell markers[39, 40]. Sarcomeric protein α-actinin is a cardiac structural protein that crosslinks actin filaments within the Z-disc of cardiac muscle [39, 41]. MLC2a, MLC2v and α-actinin were thereby used as mature cardiomyocyte markers in this study. Figure 6.6A shows that cells from suspended EBs expressed Gata4 from day 3 to day 10. Flk1 and Nkx2.5 expressions could also be detected in suspended EBs from day 3 to day 10. The positive expression of Flk1, Gata4 and Nkx2.5 suggests that liquid marbles provide a suitable environment to induce cardiac mesoderm differentiation in ESC. Figure 6.6B shows the RT-PCR analysis of the plated-down EBs. Nkx2.5, Gata4, MLC2a, MLC2v, and α-actinin expressions were detected from day 6 to 15, revealing that these cells had differentiated into pre-cardiac mesoderm and mature cardiomyocytes after plating-

down. Similar to the ESC differentiation seen in a hanging drop [42], removing LIF from the medium in our culture system, signs of ESC differentiation were detected in suspended EBs inside liquid marbles as well as in outgrown cells in plated-down culture. The use of the liquid marble allows the formation of EBs, which in turn enables cell-to-cell interactions. This cell-to-cell interaction is known to stimulate the expression of early cardiac lineage markers [39], Nevertheless, the liquid marble method permits the use of larger drop volumes compared to the hanging drop method, and is therefore more advantageous for larger scale studies.

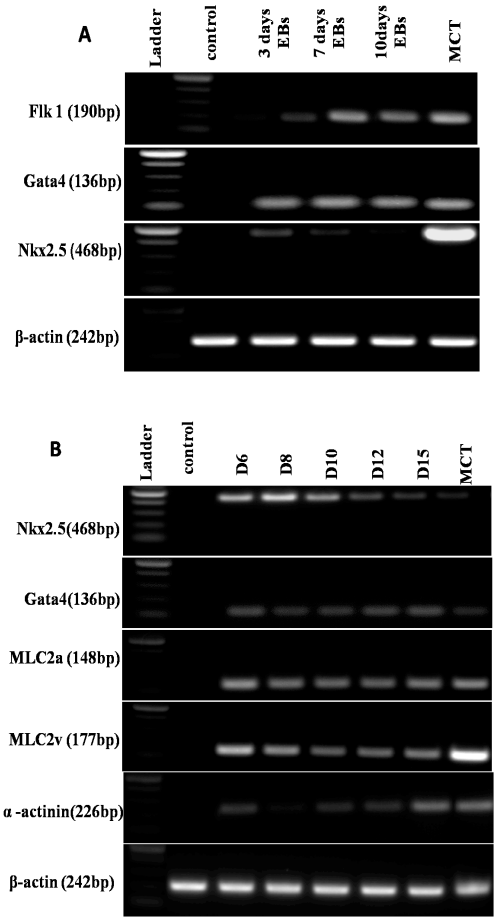

Figure (6.6): (A) Representative RT-PCR analysis for pre-cardiac mesoderm markers expression in cells from EB suspensions obtained from liquid marbles after 3, 7 and 10 days of culture. (B) Representative RT-PCR analysis for pre-cardiac mesoderm and mature cardiomyocytes markers expression from EBs after plating down for 6, 8, 10, 12 and 15 days. β-actin was used as a housekeeping gene. Cells obtained from murine cardiac tissue (MCT) were used as a positive control. Undifferentiated ES cells were used as a negative control.

6.2.4.3 Quantitative Real-time PCR analysis of cardiac markers expression during cardiogenesis

EBs were allowed to form inside liquid marbles for 5 days, and were plated in gelatin-coated plates with differentiation medium that contained no growth factors. The gene expression of these cells was quantitatively determined using real-time PCR by harvesting cells at days 6, 8, 10, 12. The time dependent expressions of various lineage and cardiac markers during the course of differentiation is shown in Figure 6.7. β-actin was used as a constitutive housekeeping gene for real time PCR and used to normalize changes in specific gene expressions. Octamer-binding transcription factor 4 (Oct4) was used as a marker of undifferentiated cells. Oct4 expression was down regulated from day 6, which suggested that the ESC had lost their pluripotency. The expression of pre-cardiac mesoderm markers Flk-1, Gata4 and Nkx2.5 were up regulated after plating down the EBs for 6 days compared with undifferentiated ES cells. The expression of Flk-1 decreased from day 8 onward, while the expression of Gata4 and Nkx2.5 decreased from day 10 onward. These results together suggested that the ESC had differentiated into cardiac mesoderm and subsequently differentiate into other cell types. The formation of cardiac mesoderm is a prerequisite intermediate step for cardiomyocytes differentiation from pluripotent stem cells. Expressions of MLC2a, MLC2v and α–actinin were first detected at day 6. The MLC2a expression increased at day 10, and decreased gradually from day 12. The MLC2v expression increased at day 8, and decreased gradually from day 10. The α–actinin expression remained constant from day 6 to day 12, and increased sharply at day 15, thus suggesting that stable sarcomeric structural protein was formed within the cell culture. The expression of MLC2a, MLC2v and α–actinin, together indicated that plated EBs had differentiated into cardiomyocytes spontaneously. It is noted that spontaneous beating was observed in EBs after plating down for 4 days. The results are consistent with those reported in other studies, where Nkx2.5, MLC2v and MLC2a are expressed in beating cardiomyocytes that had differentiated from ES cells [37]. Altogether, the results indicate that EBs derived from liquid marbles had differentiated into mesoderm and subsequently into mature cardiomyocytes.

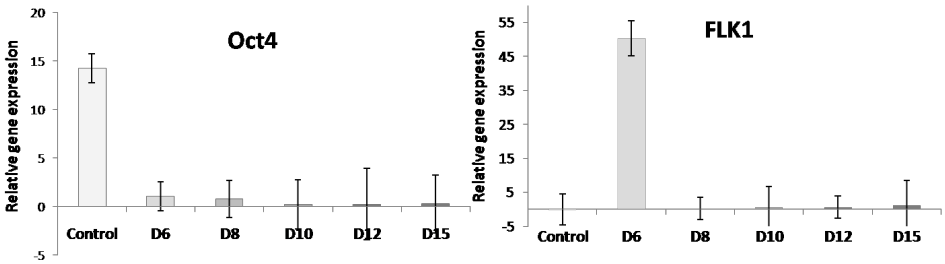

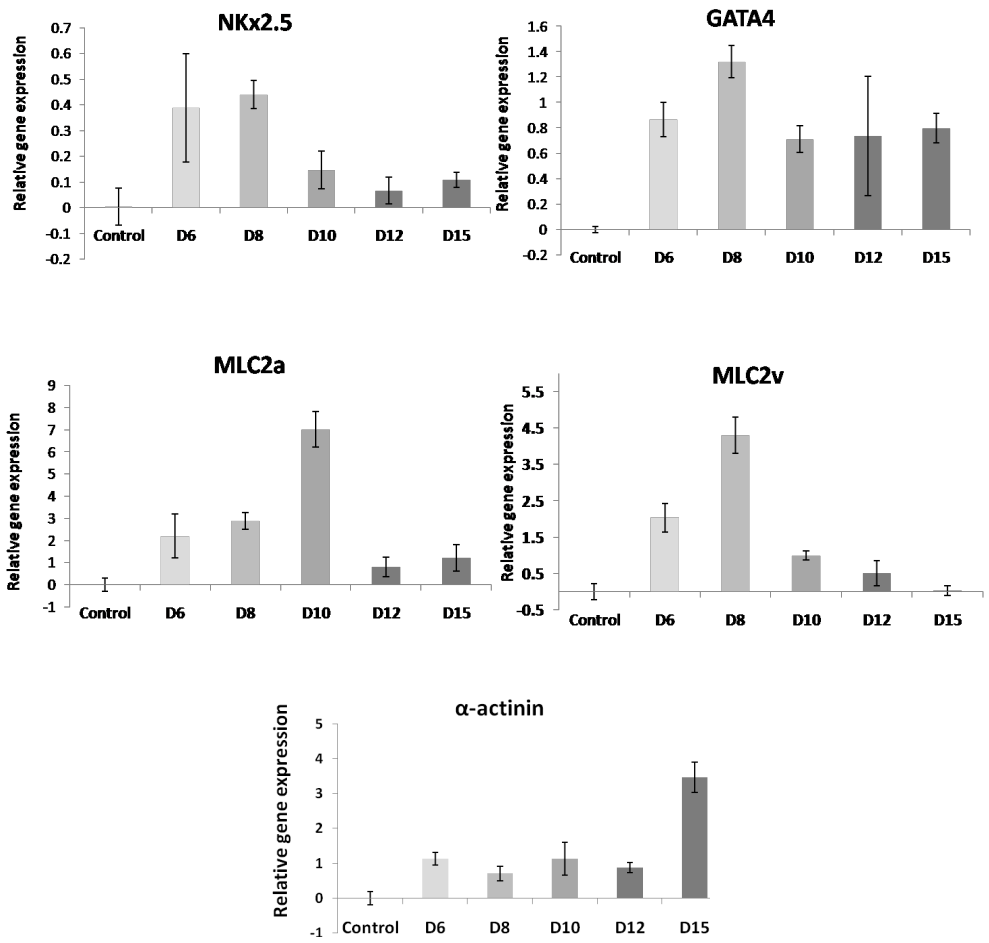

Figure (6.7): Real-time PCR analysis of gene expression over 15 days of cardiomyogenesis after plating down 5-days old EBs derived from liquid marbles. Cardiomyogenesis was characterized by a continuous decrease in pluripotency marker (Oct4) expression over the course of differentiation, followed by an initial increase in the expression of the pre-cardiac mesoderm markers (Flk1, Nkx2.5 and Gata4) expression, which eventually decreased. The increase in the expression of mature cardiomyocytes markers (MLC2v, MLC2a and α-actinin) expression as seen resulted in the formation of mature cardiomyocytes.

6.2.4.4 Immunocytochemistry

Five day-old EBs were collected from liquid marbles and plated down. Immunostaining was performed on EBs that exhibited spontaneous contraction to detect the presence of the cardiac specific proteins. As shown in representative images in Figure 6.8 (top panel), the expression of the cardiac transcription factor Nkx2.5 (AlexaFlour594, stained red) was detected after plating down the EB for 7 days. Nkx2.5 is a transcription factor that is expressed in myocardiogenic progenitor cells during myocardial development [38, 43]; Nkx2.5 is the earliest known marker for cardiogenesis in the veterbrate embryo [44-46]. Representative images in Figure 6.8 (bottom panel) show that cells expressed cTnT markers (AlexaFlour594, stained red) after plating down for 12 days. Cardiac

troponin T (cTnT) is a marker for mature cardiomyocytes [39], EB derived cells expressed cardiac specific protein markers, thus further confirming that this liquid marble method can generate functional EBs that can further differentiate into mature cardiomyocytes.

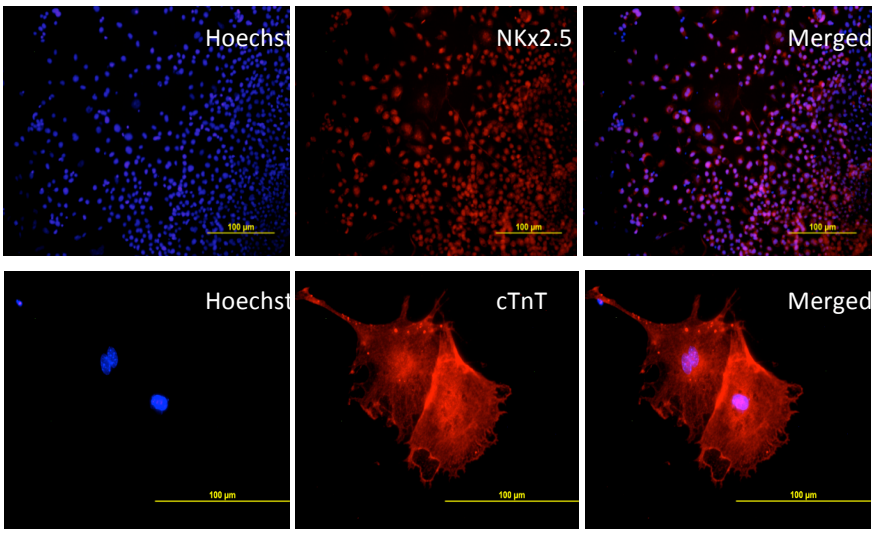

Figure (6.8): Immunostaining for Nkx2.5 (after 7 days) and cTNT (after 12 days) of plated down cells, Nuclei were counterstained with Hoechst (blue). Scale bars represent 100 μm.

6.2.4.5 Beating cardiac cells

In order to observe contractile, EBs were kept inside liquid marbles for 7 days. At day 7, EBs were retrieved and suspended in a low-adhesion dish. After 8 hours, it was observed that only ~4.5% of EBs exhibited spontaneous contraction (Supporting information 1), the contraction only lasted for a few hours, probably because once the ESC had differentiated into lineage-specific progenitor cells, they needed to anchor onto a substrate for optimal differentiation, as reported by Engler et al.[32] Nevertheless, this observation confirmed the differentiation potential of EBs into generate cardiomyocyte-like cells inside liquid marbles. To examine if EBs generated from liquid marbles can further differentiate into beating cardiac cells, 5 days old EBs were removed from the liquid marble and plated down in a gelatin-coated wells and the activities of the EBs were monitored. These EBs adhered and proliferated well on the substrate. Spontaneous rhythmic beating was detected in the outgrown EBs after plating down for 4 days. Supporting information 2, 3 show the videos of beating cells derived from EBs after plating down for 4 and 7 days, respectively. The rhythmic beating was considered as a functional cardiac marker [47]. For brevity, EBs that differentiated into beating cells are denoted as *beating* EBs. Figure 6.9A and 9B show the mean intensity of beating obtained from representative areas of beating foci after plating down the EBs for 4 and 7 days, respectively. At day

4, the beating was relatively regular with minor arrhythmia. At day 7, the beating became more regular. The beating frequency was calculated by measuring the time interval between two consecutive peaks in the mean intensity patterns. The frequency increased from 0.76 s^{-1} at day 4, to 1.29 s^{-1} at day 7, as shown in Figure 6.9C. This was probably because the cells were initially beating asynchronously after migrating out from the EB; these cells became more synchronized given the longer culture time.

After plating the EBs for 4 days, approximately 16% of the EBs underwent differentiation into rhythmic beating cells (Figure 6.9D). The percentage of beating EBs increased to 48% after 7 days. The percentage of beating EBs continued to increase over time reaching a maximum of 64% after 9 days. After 10 days, the rhythmic beating activity declined, possibly due to the overgrowth of cells causing peeling of cells from the plate, although approximately 35% of the EBs still exhibited rhythmic beating activity from day 12 to day 16. Approximately 8% of EBs still exhibited rhythmic beating at day 25. As expected, a larger number of EBs exhibited spontaneous contraction in plated culture compared to suspension culture. This observation is consistent with other studies that found that EBs differentiate extensively after attaching to a substrate [48, 49]. The observation of spontaneous rhythmic beating again confirmed that liquid marble derived EBs differentiated into functional cardiac cells. Taken together, these results indicate that the liquid marble is a promising platform for EB generation, and for facilitating further differentiation into cells with a cardiac lineage.

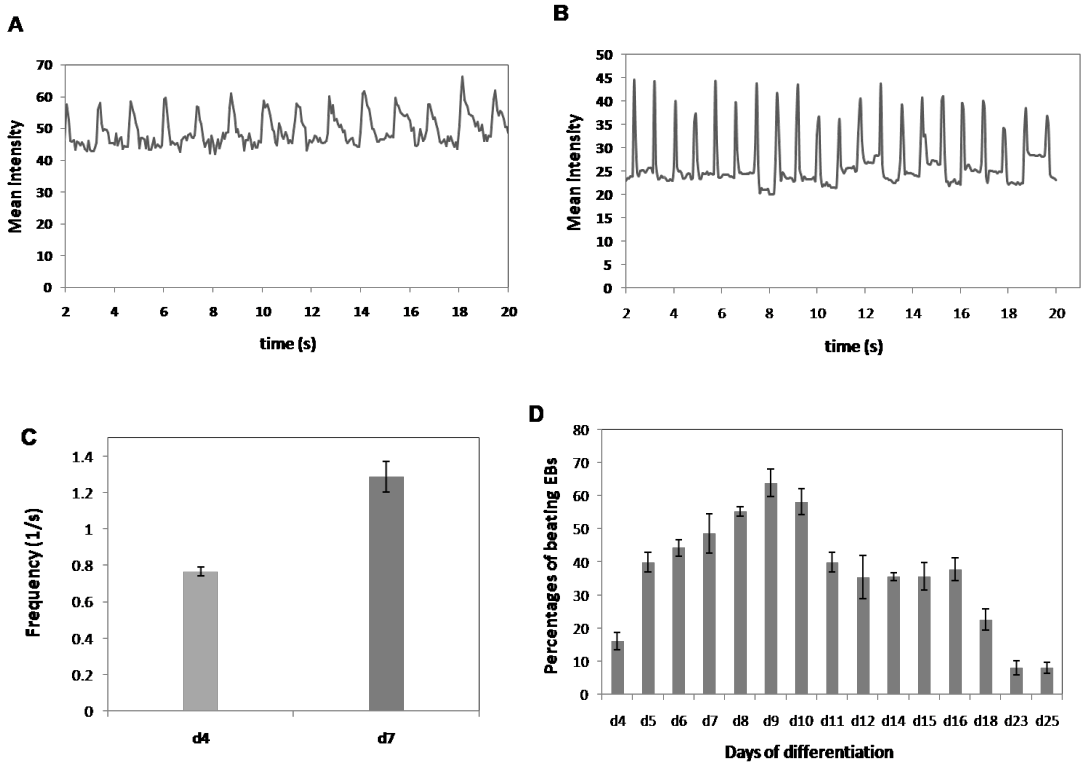

Figure (6.9): Mean intensity patterns obtained from representative areas in contractile EBs after plating for (A) 4 and (B) 7 days. (C) The beating frequency of EBs at day 4 and 7. (D) The percentages of contractile EBs at different time points.

6.2.5 Conclusion

In this study, we investigated the capability of liquid marbles to induce EB formation and subsequent differentiation into cardiomyocytes. Liquid marbles were prepared by inoculating ESC onto a bed of hydrophobic PTFE particles. ESC aggregated to form uniform EBs after inoculation, and subsequently differentiated into cardiac mesoderm cells without the use of growth factors. Further on plating, these EBs further differentiated into contractile cardiomyocytes. The contraction of cardiomyocytes was synchronized with longer time in culture. The liquid marble method was found to be advantageous for EB formation as it is cost effective and simple; it also allows larger-scale EB production compared with the hanging drop method. Overall, this study shows that liquid marbles can serve not only as a novel platform to induce the formation of EBs, but also to facilitate cardiogenesis. The cardiomyocytes generated via this liquid marble strategy could provide a continuous source of donor cardiomyocytes for cell replacement therapy in damaged hearts. Furthermore, this technology would be highly beneficial to provide cardiomyocytes for use in cardiac drug discovery programs and safety testing. Since the quantity of cells required for the above mentioned applications is very high, it becomes imperative to develop defined and efficient in vitro protocols, which would then provide the stringent levels of safety and quality control making stem cell transplantation therapy realizable. Our study provides a step up this ladder and gives a new promise and hope in cardiovascular research.

6.2.6 Acknowledgment

Funding for this research was partly provided through an Australia Research Council Discovery Project Grants ARC DP 1094179 and ARC DP 120102570 and through the Australia-India Strategic Research Fund BF050038. We would like to thank Ms Karla Contreras for her assistance with cell culturing. F.S also would like to thank Mr. Amir Taheri for his assistance in performing real time PCR, Dr. Camden Lo for assistance in image processing, and Mr. Luis Fernando Malaver for assistance in FACS analysis. This work was performed in part at Melbourne Centre for Nanofabrication (MCN), which comprises the Victorian Node of the Australian National Fabrication Facility (ANFF). PPYC is grateful for an MCN Technology Fellowship and an RMIT University Senior Research Fellowship that supported this work. F.Sarvi and K.Jain contributed equally to this work.

Supplementary video 1: Beating EB derived from liquid marble. Oct4b2 cells were allowed to aggregate inside liquid marble to form EB for 7 days. The EB was transferred to a low adhesion dish, when beating activity was observed 8 hours later.

Supplementary material 2: Contracting foci in plated down EB. Oct4b2 cells were allowed to form EB inside liquid marble for 5 days, beating activity was observed in EB that was plate down after another 4 days.

Supplementary material 3: Contracting foci in plated down EB. Oct4b2 cells were allowed to form EB inside liquid for 5 days, beating activity was observed in EB that was plate down after another 7 days.

6.3 Reference

1. Khaitan, D., et al., *Establishment and characterization of multicellular spheroids from a human glioma cell line; Implications for tumor therapy*. Journal of Translational Medicine, 2006. **4**.
2. Chen, S.S., et al., *Multilineage differentiation of rhesus monkey embryonic stem cells in three-dimensional culture systems*. Stem Cells, 2003. **21**(3): p. 281-295.
3. Griffith, L.G. and M.A. Swartz, *Capturing complex 3D tissue physiology in vitro.* Nature Reviews Molecular Cell Biology, 2006. **7**(3): p. 211-224.
4. Doetschman, T.C., H. Eistetter, and M. Katz, *The in vitro development of blastocyst-derived embryonic stem cell lines: formation of visceral yolk sac, blood islands and myocardium*. J. Embryol. exp. Morph., 1985. **87**: p. 27-45.
5. Lumelsky, N., et al., *Differentiation of embryonic stem cells to insulin-secreting structures similar to pancreatic islets*. Science, 2001. **292**(5520): p. 1389-1394.
6. Sdek, P., et al., *Rb and p130 control cell cycle gene silencing to maintain the postmitotic phenotype in cardiac myocytes*. Journal of Cell Biology, 2011. **194**(3): p. 407-423.
7. Taylor, D.A., et al., *Regenerating functional myocardium: Improved performance after skeletal myoblast transplantation*. Nature Medicine, 1998. **4**(8): p. 929-933.
8. Orlic, D., et al., T*ransplanted adult bone marrow cells repair myocardial infarcts in mice, in Hematopoietic Stem Cells* 2000 Basic and Clinical Sciences, D. Orlic, et al., Editors. 2001. p. 221-230.
9. Evans, M.J. and M.H. Kaufman, E*stablishment in culture of pluripotential cells from mouse embryos.* Nature, 1981. **292**(5819): p. 154-156.
10. Koike, M., et al., *Characterization of embryoid bodies of mouse embryonic stem cells formed under various culture conditions and estimation of differentiation status of such bodies*. Journal of Bioscience and Bioengineering, 2007. **104**(4): p. 294-299.
11. Maltsev, V.A., et al., *Embryonic stem-cell differentiate in vitro into cardiomyocytes representing sinusnodal, atrial and ventricular cell types*. Mechanisms of Development, 1993. **44**(1): p. 41-50.
12. Ungrin, M.D., et al., *Reproducible, Ultra High-Throughput Formation of Multicellular Organization from Single Cell Suspension-Derived Human Embryonic Stem Cell Aggregates.* PLoS One, 2008. **3**(2).
13. Kurosawa, H., *Methods for inducing embryoid body formation: In vitro differentiation system of embryonic stem cells.* Journal of Bioscience and Bioengineering, 2007. **103**(5): p. 389-398.
14. Keller, G.M., In vitro differentiation of embryonic stem cells. Current Opinion in Cell Biology, 1995. **7**(6): p. 862-869.
15. Smith, A.G., *Embryo-derived stem cells: Of mice and men.* Annual Review of Cell and Developmental Biology, 2001. **17**: p. 435-462.
16. Niebruegge, S., et al., *Cardiomyocyte production in mass suspension culture: embryonic stem cells as a source for great amounts of functional Cardiomyocytes*. Tissue Engineering Part A, 2008. **14**(10): p. 1591-1601.
17. Burridge, P.W., et al., *Improved human embryonic stem cell embryoid body homogeneity and cardiomyocyte differentiation from a novel V-96 plate aggregation system highlights interline variability.* Stem Cells, 2007. **25**(4): p. 929-938.
18. Sarvi, F., et al., *A novel technique for the formation of embryoid bodies inside liquid marbles.* Rsc Advances, 2013. **3**(34): p. 14501-14508.
19. Aussillous, P. and D. Quere, *Liquid marbles*. Nature, 2001. **411**(6840): p. 924-927.
20. Bormashenko, E., R. Balter, and D. Aurbach, *Micropump based on liquid marbles*. Applied Physics Letters, 2010. **97**(9).
21. Mahadevan, L. and Y. Pomeau, *Rolling droplets*. Physics of Fluids, 1999. **11**(9): p. 2449-2453.
22. Bormashenko, E., et al., *On the Mechanism of Floating and Sliding of Liquid Marbles*. Chemphyschem, 2009. **10**(4): p. 654-656.

23. Tian, J., et al., *Liquid marble for gas sensing.* Chemical Communications, 2010. **46**(26): p. 4734-4736.
24. Xue, Y., et al., *Magnetic Liquid Marbles: A "Precise" Miniature Reactor.* Advanced Materials, 2010. **22**(43): p. 4814-+.
25. McHale, G. and M.I. *Newton, Liquid marbles: principles and applications.* Soft Matter, 2011. **7**(12): p. 5473-5481.
26. Arbatan, T., et al., *Tumor Inside a Pearl Drop.* Advanced Healthcare Materials, 2012. **1**(4): p. 467-469.
27. Arbatan, T., et al., *Microreactors: Liquid marbles as micro-bioreactors for rapid blood typing* (Adv. Healthcare Mater. 1/2012). Advanced Healthcare Materials, 2012. **1**(1): p. 79-79.
28. Livak, K.J. and T.D. Schmittgen, *Analysis of relative gene expression data using real-time quantitative PCR and the 2(T)(-Delta Delta C) method*. Methods, 2001. **25**(4): p. 402-408.
29. Arshi, A., et al., *Rigid microenvironments promote cardiac differentiation of mouse and human embryonic stem cells.* Science and Technology of Advanced Materials, 2013. **14**(2).
30. O'Shea, K.S., Self-renewal vs. d*ifferentiation of mouse embryonic stem cells*. Biology of Reproduction, 2004. **71**(6): p. 1755-1765.
31. Sarvi, F., et al., S*urface-functionalization of PDMS for potential micro-bioreactor and embryonic stem cell culture applications*. Journal of Materials Chemistry B, 2013. **1**(7): p. 987-996.
32. Engler, A.J., et al., *Myotubes differentiate optimally on substrates with tissue-like stiffness: pathological implications for soft or stiff microenvironments*. Journal of Cell Biology, 2004. **166**(6): p. 877-887.
33. Hescheler, J., et al., *Embryonic stem cells: a model to study structural and functional properties in cardiomyogenesis.* Cardiovasc Res, 1997. **36**(2): p. 149-62.
34. Ema, M., S. Takahashi, and J. Rossant, *Deletion of the selection cassette, but not cis-acting elements, in targeted Flk1-lacZ allele reveals Flk1 expression in multipotent mesodermal progenitors*. Blood, 2006. **107**(1): p. 111.
35. Motoike, T., et al., *Evidence for novel fate of Flk1(+) progenitor: Contribution to muscle lineage*. Genesis, 2003. **35**(3): p. 153-159.
36. Svensson, E.C., et al., *Molecular cloning of FOG-2: A modulator of transcription factor GATA-4 in cardiomyocytes.* Proceedings of the National Academy of Sciences of the United States of America, 1999. **96**(3): p. 956-961.
37. Boheler, K.R., et al., D*ifferentiation of Pluripotent Embryonic Stem Cells Into Cardiomyocytes*. Circulation Research 2002. **91**: p. 189-201.
38. Lints, T.J., et al., *NKX-2.5 - A novel murine homeobox gene expressed in early progenitor cells and their myogenic descendants.* Development, 1993. **119**(2): p. 419-431.
39. Rajala, K., M. Pekkanen-Mattila, and K. Aalto-Setala, C*ardiac Differentiation of Pluripotent Stem Cells.* Stem Cells International, 2011: p. 1-12.
40. Baba, S., et al., *Generation of cardiac and endothelial cells from neonatal mouse testis-derived multipotent germline stem cells*. Stem Cells, 2007. **25**(6): p. 1375-1383.
41. Samarel, A.M., *Costameres, focal adhesions, and cardiomyocyte mechanotransduction*. Am J Physiol-Heart C, 2005. **289**(6): p. H2291-H2301.
42. O'Shea, K.S., *Embryonic stem cell models of development.* Anatomical Record, 1999. **257**(1): p. 32-41.
43. Mauritz, C., et al., *Generation of functional murine cardiac myocytes from induced pluripotent stem cells*. Circulation, 2008. **118**(5): p. 507-517.
44. Biben, C. and R.P. Harvey, *Homeodomain factor Nkx2-5 controls left/right asymmetric expression of bHLH gene eHand during murine heart development*. Genes & Development, 1997. **11**(11): p. 1357-1369.
45. Lyons, I., et al., *Myogenic and morphonenetic deffects in the heart of murine embryos lacking the homeo box gene Nkx2.5*. Genes & Development, 1995. **9**(13): p. 1654-1666.
46. Azpiazu, N. and M. Frasch, *Tinman and bagpipe 2 homeo box genes that determine cell fates in the dorsal mesoderm of drosophila.* Genes & Development, 1993. **7**(7B): p. 1325-1340.

47. Zhu, M.-X., J.-Y. Zhao, and G.-A. Chen, *Mesoderm is committed to hemato-endothelial and cardiac lineages in human embryoid bodies by sequential exposure to cytokines*. Experimental Cell Research, 2013. **319**(1): p. 21-34.
48. Martin, G.R. and M.J. Evans, *Differentiation of clonal lines of teratocarcinoma cells-formation of embyoid bodies in vitro*. Proceedings of the National Academy of Sciences of the United States of America, 1975. **72**(4): p. 1441-1445.
49. Gajovic, S. and P. Gruss, *Differentiation of the mouse embryoid bodies grafted on the chorioallantoic membrane of the chick embryo*. International Journal of Developmental Biology, 1998. **42**(2): p. 225-228.

Chapter 7: Development of Cellulosic Hydrogel based Bioreactor for Embryoid Body Formation

7.1 General Overview

Embryoid bodies (EBs) are three dimensional (3D) aggregates of cells derived from embryonic stem (ES) cells, which provide an excellent model for studying the molecular and cellular interactions in the very first stages of embryo development. Indeed, formation of stem cell 3D structures (EBs) is a prerequisite for further ESC differentiation.

Currently, most of the current techniques for generating EBs are based on employment of hanging drops or suspensions in non-tissue culture treated plates, microwells, and spinner flasks. The practical application of these methods is limited in terms of scalability, size uniformity, labour-intensively, production process complicacy and economical impracticality. However, more importantly, all these methods suffer from not providing proper 3D environments to cells that behave more like ECMs [1]. Hydrogels made of natural and synthetic polymer network are promising candidates for 3D tissue engineering scaffolds [2]. Macroporous hydrogels as scaffolds have been shown to be advantageous in supporting cell proliferation, migration, cell aggregation and tissue regeneration compared to non-porous ones [3-5].

In this regard, applying a new biodegradable, biocompatible scaffold with interconnecting pores and appropriate mechanical strength, capable of EB formation and further differentiation is the main aim of this part of study.

There have been extensive studies on the efficacy of biocompatible polymeric material hydrogels as 3D tissue scaffolds, ranging from natural to synthetic polymers with the ability to degrade and function as “smart” hydrogels, as well as in the microfluidics field. However, the use of modified cellulose as a 3D tissue scaffold for embryonic body formation has yet to be fully exploited.

This chapter concerns the feasibility of formation of embryonic body formation and subsequent differentiation through a novel porous hydrogel, which acts as a 3D culture scaffold. To meet this aim, mouse embryonic stem cells were seeded into the biocompatible cellulose scaffold with defined pore sizes. Formation of EBs were observed via fluorescent, confocal and SEM microscopy. The images clearly showed the ability of cells to attach, grow and successfully form 3D aggregates inside the hydrogel. Size distribution of EBs compared to that for the liquid suspension method with the same conditions also showed the formation of more uniform EBs. The results also confirmed higher cell viability in EBs formed inside scaffolds than those formed in liquid suspension during the period of culturing. Expression of germ markers via quantitative PCR and immunostaining confirmed that the hydrogel-born EBs have the *in vitro* differentiation potential. RT-PCR also demonstrated that all

cardiac markers tested, such as Flk1, Nkx2.5, and Gata4, have been expressed in EBs in hydrogel. Positive immunostaining of cardiac marker (cTnT) and observation of beating EBs showed the further potential of EBs to differentiate into cardiac cells lineage.

7.2 Porous Hydroxypropyl Cellulose hydrogel for Embryoid Body Engineering

Fatemeh Sarvi[a], Siew P Hoo[b], Kerry Hourigan[a], Mark C.Thompson[a], and Peggy P.Y. Chan*[c,e]

[a]*Department of Mechanical & Aerospace Engineering & Division of Biological Engineering, Monash University, Clayton, Vic 3800, Australia.*
[b]*Department of Chemical Engineering, Monash University, Clayton, Vic 3800, Australia.*
[c] *School of Applied Science, RMIT University, Melbourne, VIC 3000, Australia.*
[e] *Melbourne Centre for Nanofabrication, Clayton, VIC 3168, Australia*

7.2.1 Abstract

Differentiation of embryonic stem cells (ESCs) can be prompted through the formation of embryo-like aggregates in suspension, known as embryoid bodies (EBs). ESCs are promising for tissue engineering primarily because of their ability to differentiate into multiple tissue lineages and their capacity to exhibit pluripotent differentiation. The combination of stem cells with biomaterials scaffold provides a promising strategy for engineering tissues and cellular delivery, since scaffolding materials can mimic the microenvironment of the extracellular matrix in a human body.

In this study, a porous hydrogel scaffold prepared from bifunctional methacrylates (MA) modified Hydroxypropylcellulose (HPC) was used for formation of spherically symmetric EBs. When single ES cells were seeded in three dimensional cellulose scaffolds, they grew into aggregates gradually and formed EBs with circular structures that would eventually differentiate into the three embryonic germ layers. The ES cells seeded scaffolds were characterized using scanning electron, confocal and fluorescence microscopy. It was observed that the stem cells attached to the scaffold, followed by penetration into the pores and proliferation within, and consequently formation of uniform EBs. Evaluation of the EBs in terms of morphology and potential to differentiate indicated that they exhibited the typical structure of EB and could generate three germ layers (mesoderm, endoderm, and ectoderm). Moreover, the results demonstrated that culturing ES cells inside the HPC-MA porous hydrogel with controlled porosity could eventually allow ES cells to differentiate towards cardiogenic lineage; the resulting cells expressed cardiac markers and showed spontaneous contraction after culturing in the scaffold for 13 days.

Keywords:
Embryonic stem cell, Embryoid body, Porous Hydrogel, three germ layer makers, cardiogenesis

7.2.2 Introduction

In the body, cells are surrounded by a complex molecular framework known as the extracellular matrix (ECM). ECM has several functions such as supporting and isolating tissues from one another, and regulating intercellular communication. The rapidly increasing demand for organ and tissue transplantation has promoted tissue engineering as a promising alternative, in particular the use of stem cells seeded tissue scaffolds. Artificial three dimensional (3D) scaffolds are structures that mimic native ECM for attachment, growth and organization of cells. It has been shown that along with ECM's structural role, it plays a physiological role by affecting the immediate microenvironment of the cardiomyocytes. Biocompatible and biodegradable three dimensional (3D) polymeric scaffolds have received much attention due to their ability to provide structural support similarity to the ECM, while as well as providing newly secreted tissues with the appropriate 3D architecture for *in vivo* tissue regeneration[6].

Embryonic stem cells (ESCs) are pluripotent cells with the ability to organize into multi-cell-type structures during embryonic like differentiation, which make them powerful sources for therapeutic, drug discovery and cell replace applications [7-11]. The formation of the three-dimensional structure of ES aggregation known as embryoid bodies (EBs) is a key step to induce ES cells differentiation [12, 13]. In fact, utilizing EB as a reliable *in vitro* model is widely proposed for *in vitro* mouse embryogenesis studies since the study of embryos imposes certain restrictions [14].

EB compromises 3 germ layers known as the ectodermal, mesodermal, and endodermal tissues, which resemble the construction of the developing embryo, and are often used as *in vitro* model for morphogenesis study [15, 16]. So far, different methods have been employed to aggregate ES cells in order to produce EBs, including forced aggregation, bioreactor-based methods, hanging drop, suspension culture and spinner flask cultures [12, 17-23]. Most of these methods for producing EBs are based on preventing cell attachment to the surfaces of the dish and keep cells in suspension culture [24, 25]. However, each method is limited by at least one of the drawbacks such as laborious procedure, tedious manipulation, time consuming, production of hydrodynamic shear stress, complication and difficult manageability and requirement for large amount of medium [20, 25-27].

It is worth noting that the common limitation of all these techniques is the lack of extra-cellular matrix support, which represents an important role in cell growth and development. From the material science and biomedical engineering view, biodegradable porous scaffolds provide significant advantages to facilitate repairing or regenerating damaged organs, because they can be customized to modulate cell attachment, grow and differentiation.

Embryonic stem cells have been employed for cardiac repair; however, dissociated ESCs displayed poor viability in the scaffold and do not form the embryoid body (EB)-like structures [28]. Using a

porous scaffold on the other hand can provides 3D environment that is essential for the formation of tissue-like structures, as a structural support provide a better cell interactions and more physiologically relevant environment for the cultivated cells [4, 5]. In addition, porous gels improve cells functions by providing proper 3D structure [29, 30].

Typically both natural and synthetic polymers have been widely used as biomaterials for the fabrication of medical device and 3D architectures scaffolds for cell seeding and cultivation [31]. However, natural materials have advantages compared to synthetic materials in tissue engineering due to similarity to materials in the body and therefore support tissue development by directing cell adhesion and function[32].

More recently, there is an increasing demand for using environmentally friendly materials and renewable resources such as cellulosic materials in polymer composites [33]. Cellulose, consisting of glucose-based repeating units, is the most abundant naturally occurring polysaccharide found in nature. It can be chemically modified by esterification or etherification of their hydroxyl groups. Cellulose and its derivatives are eco- friendly, as it is biodegradable in nature by microbial or fungal enzymes. The biocompatibility of cellulose and its derivatives is well established [34, 35]. These interesting features of cellulose have encouraged the use of cellulose-based devices in biomedical applications such as tissue regeneration [36, 37], and controlled release of drugs [38].

Hydroxypropyl-cellulose (HPC) is the commercial derivative of cellulose which is water-soluble, non-toxic and inexpensive component. Recently, it has been reported that biodegradable 3D hydrogel constructed from hydroxypropyl cellulose (HPC), modified with bio-functional methacrylic anhydride (MA), is hydrolytically degradable and biocompatible to human adipose-derived stem cells (ASCs). The successful adipocytes differentiation in HPC-MA scaffolds demonstrated the usefulness of this scaffolds in tissue engineering [39]. In addition, it has been demonstrated that the cellulose-based materials provide better adhesion properties due to a their resulting surface tension, an indicator of material hydrophilicity/hydrophobicity, compared with other polymers such as polysulfone (PSf), polypropylene (PP) and perfluoropolymer (PF), which was confirmed with study using liver cells [40].

To the best of our knowledge, there have been few studies into the application of cellulose scaffolds for cell culturing, direct formation of EBs inside cellulose-derived scaffolds and the cardiac differentiation potential of hydrogel-born EBs have not been reported. To test the feasibility, a modified macro-porous hydrogel prepared from bifunctional methacrylic anhydride (MA) modified HPC is used to study the capability of a 3D porous scaffold to support stem cell growth and, more importantly, the feasibility of embryoid body formation. The potential of the EBs formed in hydrogel to differentiate into cardiac lineage cells will also be investigated. The cells in EBs were shown to express protein markers specific for the three embryonic germ layers. Finally, the feasibility to further differentiate these EB to cardiac cells will be evaluated.

7.2.3 Material and methods:

7.2.3.1 Synthesis of HPC derivatives

Hydroxypropyl cellulose methacrylate (HPC-MA) was synthesized by a two-step reaction and the synthesis route is shown schematically in Scheme 1. Briefly Hydroxypropyl cellulose (HPC, Sigma-Aldrich, M_W=10, 000 g/mol) was dehydrated by azeotropic distillation at 50^oC in toluene to remove the moisture prior to use. The typical procedure for the activation of HPC by methylacrylic anhydride is as follows. Briefly dehydrated HPC (4.0 g) was first dissolved in 150 mL of chloroform and then 4.17 mmole of methylacrylic anhydride (MA) and 4.17 mmole of N'N-dicyclohexylcarbodiimide (DCC) were added drop by drop in chloroform. 0.4 g of 4-dimethylaminopyridine (DMAP) was added as catalyst and the reaction mixture was stirred for 48 h. The resultant product (HPC-MA) was then purified by precipitation in anhydrous diethyl ether. Better purification of HPC-MA was achieved by frequent dissolution in chloroform and precipitation into diethyl ether. The purified HPC-MA was dissolved in water, filtered, and then dialyzed in deionised water for 72 h and finally lyophilized.

7.2.3.2 Preparation of HPC scaffolds

The solution of HPC-MA in deionised water (20%w/v) was prepared, 2-hydroxy-1-[4-(2-hydroxyethoxy)phenyl]-2-methyl-1-propanone (Irgacure 2959, Sigma-Aldric, Australia) was added as photo-initiator to a final concentration of 3-5%. The solution was placed in a water bath at 45^oC for 10 minutes to induce phase separation. The resultant solution was then cross linked in a ultra-violet ray (UV) cross-linker (Honle UV Technology, UV-F 400, Germany) for approximately 6 minutes. The cross-linked gels were then washed with deionised water to remove any uncross-linked HPC-MA conjugate and photo-initiator before used. The samples were kept at -20^oC before lyophilisation. The samples were then sterilized by washing twice with PBS and soaking in pure ethanol for 12h followed by washing with PBS and soaking in PBS for 12h. Samples were then dried and incubated in 0.1% gelatin 48h prior to cell seeding.

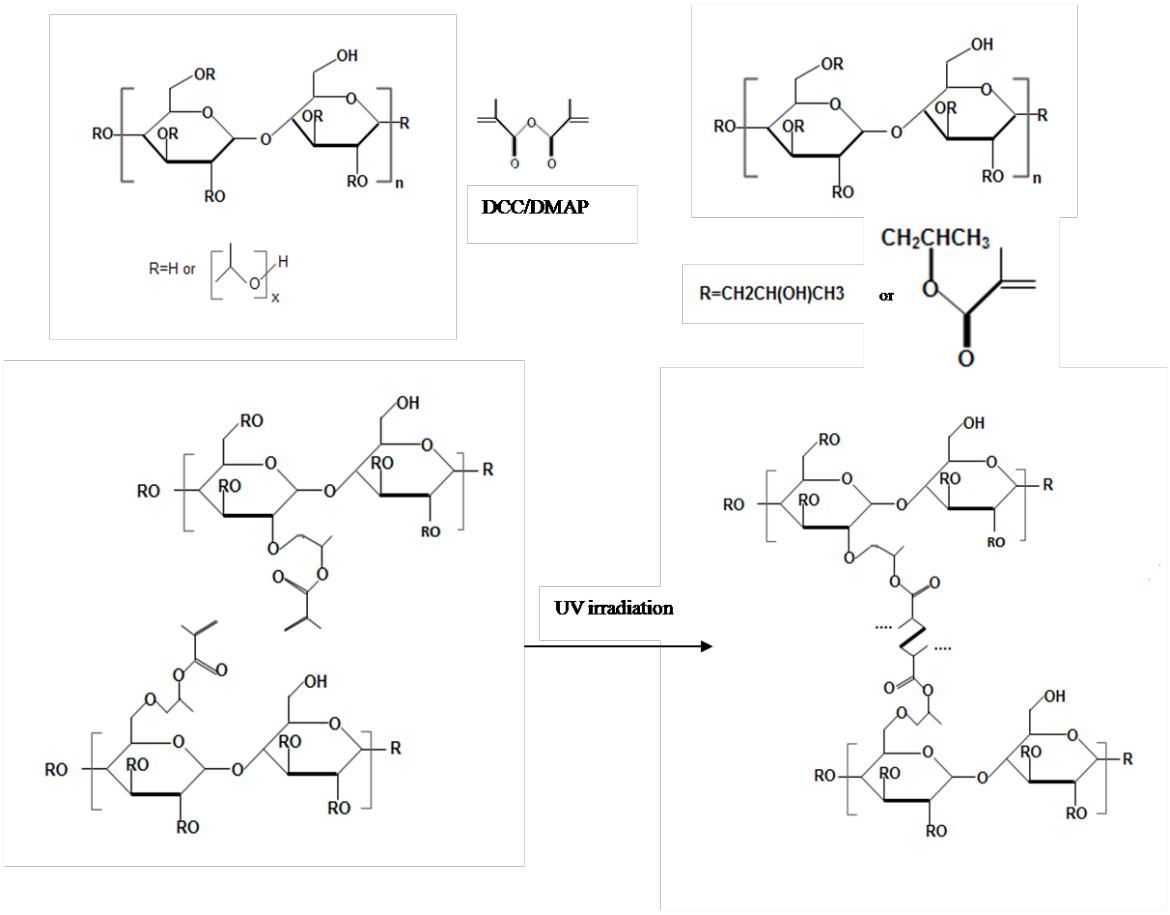

Figure (7.1): Schematic of the synthesis of HPC-MA and sketch of the cross-linking reaction between photo-initiator and HPC-MA

7.2.3.3 Swelling ratio and mechanical properties of HPC-MA

The lyophilized HPC-MA scaffolds were submerged in water at 4°C, room temperature and 42°C for 48 h. The weight of the swollen sample was obtained after blot drying with a moist filter paper and the dry weight of the sample was measured after drying the sample under vacuum at 25°C for 48 h. The swelling ratio, SR, of scaffold was calculated according to the equation 1 below,

$$SR = (W_h - W_d) / W_d \qquad (1)$$

where W_h is the weight of the scaffold in the swollen equilibrium and W_d is the weight of the dried scaffold. Each sample was measured three times from the four replicate specimens and the average value of the measurement was taken. The mechanical properties of the hydrated scaffolds were carried out using a dynamic mechanical analyzer (TA Instruments, Q800) at a frequency of 1 Hz and at 0.01 N. The testing was performed under atmospheric condition and 310 K. The compression testing was performed in quadruplicate.

7.2.3.4 Culture of murine ES Cells

Feeder free Oct4B2 ES cells contained Oct4-GFP-IRES-puromycin and hygromycin resistance cassettes were used for this work. This cell line possesses a green fluorescent protein (GFP) under control of the Oct4 promoter (Oct4-GFP) [41]. Cells were maintained in Dulbecco's modified eagle medium [DMEM, cat# 1995, Gibco] supplemented with 10% FBS (JRH Biosciences, Australia), 1% nonessential amino acids (NEAA,cat#11140-050, Invitrogen), 0.1mM 2-mercaptoethanol (cat# 21985-023, Invitrogen), 1% GlutaMAX™ (cat#35050061, Invitrogen), 1% penicillin-streptomycin (cat# 15070-063, Invitrogen), and 1000U/ml murine leukemia inhibitory factor (mLIF, Chemicon, Australia) on 0.1% gelatin-coated dish (cat#9391, Sigma) at 37°C in humidified air with 5% CO_2. Cells were passaged every 2-3 days after 70-80% of confluency. After aspiration of the medium and washing with DPBS (cat#D8662, Sigma), Tryple^{tm} express (cat#12605, Gibco) was added and the dish was kept inside the incubator for 5min. Tryple was inactivated by addition of ES media. The cell suspension was centrifuged for 3min at 1600rpm. The supernatant was aspirated and the cell pellet was resuspended in appropriate amount of ES medium.

7.2.3.5 Embryoid Body formation inside porous gel

For EB formation the dissociated ES cells were resuspended in DMEM medium supplemented with 10% FBS, 1% NEAA, 1% mM L-glutamine, 1% penicillin-streptomycin (EB formation medium). It is worth mentioning that EB-forming medium does not contain any Leukemia inhibitory factor LIF. Prior to cell seeding, the scaffolds were first soaked in PBS overnight and then sterilized with 70% ethanol for 5hr by changing ethanol three times. Scaffold was then rinsed with PBS for 5hr. PBS was then removed from the scaffold, and the well plate kept inside the hood overnight. For EB formation 2.5×10^5 cells in approximately 40µl of EB medium was then added drop-wise on top of the hydrogel surface in each 48-well plate. The cell-seeded scaffolds were then pre-incubated in 5% CO_2 incubator at 37°C for 15-20min to allow cells to penetrate into hydrogel pores. Fresh medium was then added to cover the scaffolds. The next day 0.1% gelatin was added and incubated for 24hr for better cell attachment before cell seeding. EB formation and the microstructure of the hydrogel without and with cells were investigated using a laser scanning confocal microscope (Nikon A1Rsi MP) with an excitation wavelength of 488 nm and an emission wavelength of 550 nm and fluorescent microscope (Nikon, Eclipse Ti) on different days. EB diameters were measured using Imagej software.

7.2.3.6 Immunocytochemistry

Cells were fixed in 4% paraformaldehyde for 10 min and washed three times with 1% BSA in DPBS. For determining the expression of three germ layers, Nestin (MAB 353, Ectoderm marker), Brachyury (ab20680, Mesoderm marker) and Foxa2 (SC-6554, Endoderm marker) were selected as primary antibodies. Fixed cells were incubated for 1 h at room temperature with blocking solution [(5% goat serum (for Nestin and Brychury), 1% BSA in DPBS and 5% donkey serum (for Foxa2), 1% BSA in DPBS)]. Cells were then incubated overnight with the primary antibodies diluted (1:1000) in blocking solution at 4°C. Next, cells were washed three times with 1% BSA in DPBS and then incubated at room temperature for 1h with appropriate secondary antibodies (for Nestin goat anti-mouse, goat anti-rabbit for Brachyury and for Foxa2 donkey anti-goat IgG Alexa-Fluor 594, Invitrogen Australia) at a concentration of (1:400) in appropriate blocking solution. Cells were washed three times with 1% BSA in DPBS for 10min each. Negative controls for staining were performed using only the secondary antibody. The protocol for NKx2.5 (Sc-14033, Santa Cruz) and cTnT immunostaining (ab10214, abcam) was similar to the above mentioned, with the primary antibodies diluted (1:500) in blocking solution at 4°C and secondary antibodies (goat PAb to RbIgG Alexa 594, goat anti-mouse Alexa 594, Invitrogen Australia) at a concentration of 1:400 in blocking solution.

7.2.3.7 Scanning electron microscopy (SEM)

For observation of EBs inside scaffolds, gels were fixed for 30min in 4% paraformaldehyde. The samples were then quickly soaked in liquid nitrogen and keep in -80 overnight. Sample was then freeze dried for 72hr. The freeze-dried samples were sputter coated with platinum-gold alloy and examined using JEOL JSM-7001F FEG SEM (Japan).

7.2.3.8 RNA isolation, cDNA synthesis and qRT-PCR

For quantitative RT-PCR analysis, the EBs inside hydrogel were lysed, and total RNA was isolated by using the RNeasy kit (QIAGEN Inc.) and subsequently cleaned up for removing any remaining genomic DNA contamination by treating with Turbo DNase (Ambion) according to the manufacturer's instructions. Reverse transcription reaction carried out by using Superscript III First Strand Synthesis System (Invitrogen) according to the manufacturer's instructions. Real-time PCR analysis was performed on the 7900HT Fast Real-Time PCR system (Applied Biosystems) at standard

reaction conditions using Power SYBR Green PCR Master Mix (Applied Biosystems) in triplicate for each sample and each gene. Briefly, after a 2 min denaturation at 95°C, 35 cycles were carried out at 95°C for 15s, 58°C for 30s and 72°C for 30s following by a dissociation stage. Relative mRNA levels calculated with the ΔΔCT method [42] were analysed using SDS Version 2.4.1 software. Primer sequences used for SYBR Green PCRs are listed in Table (7.1). The house keeping β-actin was used as an internal control.

Table (7.1): PCR primers name and details

Primer	**Primer sequences (Forward-Reverse)** **5'→3'**	**PCR Product size**	**NCBI Accession No.**
Nestin	TCTGGAAGTCAACAGAGGTGG/ACGGAGTCTTGTTCACCTGC	350	NM_016701.3
Brachyury	CATGTACTCTTTCTTGCTGG/GGTCTCGGGAAAGCAGTGGC	313	NM_009309.2
Foxa2	TGGTCACTGGGGACAAGGGAA/GCAACAACAGCAATAGAGAAC	289	NM_010446.2
Flk-1	GGCGGTGGTGACAGTATCTT/CTCGGTGATGTACACGATGC	203	NM_010612.2
Nkx2.5	ACACCCACGCCTTTCTCAGTCAAA/CGACAGGTACCGCTGT TGCTTGAA	468	NM_008700.2
Gata4	TCTCACTATGGGCACAGCAG/GCGATGTCTGAGTGACAGGA	136	NM_008092
β-actin	CACCACACCTTCTACAATGAGC/TCGTAGATGGGCACAGTGTGGG	242	NM_007393.3

7.2.3.9 Cell viability assay

CellTitre-Glu^{R} Luminescent cell viability assay (Promega) was conducted according to the manufacturer's instructions. Cells (including EBs) were collected from inside the hydrogel or low suspension well plates. A volume of CellTitre-Glu^{R} equal to the volume of cell culture medium was added. The contents were manually mixed for 2mins to induce cell lysis. After 5 min incubation time at RT to stabilize the luminescent signal, the cell solutions were seeded in a white opaque-walled 96-multiwell assay plate. Control wells readout contained medium without cells for background luminescence. The plate was analysed at the appropriate time points by a stable glow-type luminescent signal on a Fluostar Optima (BMG Labtech, Australia).

7.2.4 Results and Discussion

7.2.4.1 Synthesis and preparation of HPC-MA

To create a 3D supportive environment to organize mES cells into embryoid bodies and direct differentiation, we used a biodegradable cellulosic scaffolds. HPC-MA hydrogel was prepared as illustrated in Figure 7.2. Briefly, HPC-MA conjugates with 0.35 degree of substitution (DS) is water-soluble and formed single-phase solution when dissolved in aqueous solution. The aqueous solution, upon heating at 45^{o}C underwent phase transition from isotropic solution to colloidal solution owing to the low critical solution temperature (LCST) transition properties of HPC at around 42°C. The fixation of colloidal structure of HPC-MA was achieved by UV polymerizing the HPC-MA conjugate and produced an opaque hydrogel. UV-irradiation was selected to induce photopolymerization due to its many advantages including ease of hydrogel shaping and fast polymerization rate at low temperature[43]. Irgacure 2959 has demonstrated to cause minimal toxicity to a wide range of mammalian cells [44], and was employed as photoinitiator in this study. HPC-MA-20 % hydrogel samples were prepared, lyophilized and subjected to characterization, and will be described in later sections.

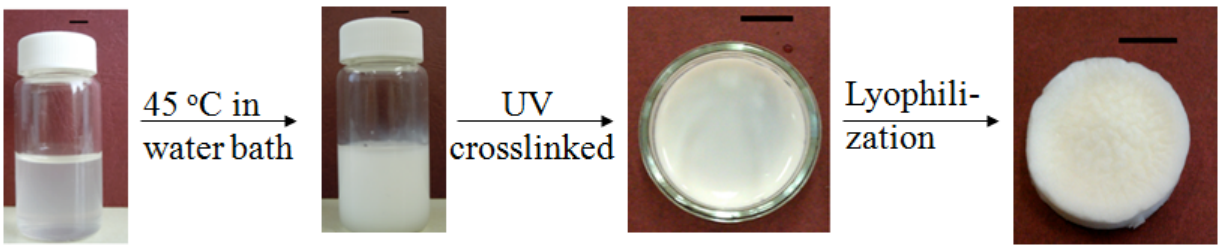

Figure (7.2): Preparation of HPC-MA scaffold (scale bar 1.0 cm)

7.2.4.2 Swelling ratio and mechanical properties of HPC-MA

The swelling behaviour of HPC-MA- 20 wt% is shown in Figure 7.3 and was carried out at 4^{o}C, room temperature and 42^{o}C. The SR was found to be decreasing with increasing temperature ($p < 0.05$). At 4^{o}C and room temperature, the hydrogel exhibited a SR of 13.44 g/g and 12.94 g/g, while the swelling ratio decreases from 12.94 g/g to 8 g/g at 37^{o}C. As the temperature drops further, the swelling ratio was reported to be 6.4 g/g. The swelling ratio is a measure of hygroscopic behaviour, its swelling attributed to the presence of hydroxyl groups on the HPC chain that participate in hydrogen bonding with surrounding water molecules; further, the presence of pores also result in water retention. Hydrogels with high swelling ratio are highly permeable, which facilitates oxygen, nutrient and metabolites exchange, and are considered as promising material for tissue scaffolding [45].

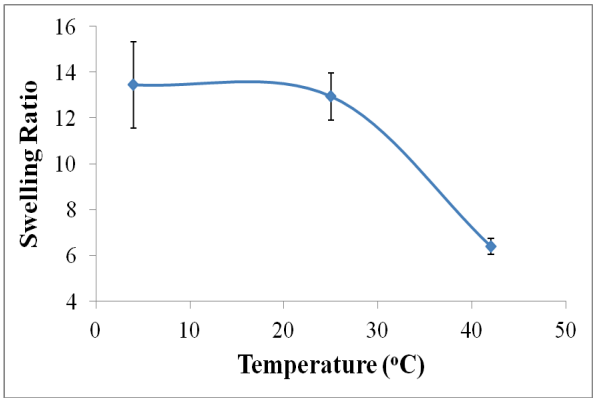

Figure (7.3): Swelling behaviour of HPC-MA–20 wt%.

A hydrogel should provide sufficient mechanical support necessary for a given application. The stiffness of the substrate is an important parameter that regulates stem cell behaviour. For example, a soft substrate is known to stimulate neurogenesis of stem cell cultures, whereas stiffer substrates have been reported to stimulate myogenesis [46]. For tissue regeneration to be successful, it is believed that the mechanical properties of scaffold should match roughly the mechanical properties of tissue growth in order to provide cells with instructive microenvironment. The storage modulus of HPC-MA-20 wt% was found to be 4.19±0.56 KPa at 37^{o}C. This storage modulus is comparable to those of soft tissues such as organs such as breast tumour, brain, lymph node, mammary gland, liver, fat and kidney[47] and neonatal rat heart tissue[48]. The result reported by Rodriguez et al.[49] also indicated that culturing cardiomyocytes on stiffer substrates led to a myofibril structure that helped to improve cardiac contractility which suggests that HPC-MA hydrogels can be used as tissues scaffolds for the formation of embryoid body.

7.2.4.3 EB formation

Culturing ESCs *in vitro* as EBs provides possibilities to mechanistically investigate early differentiation functions of 3D constructions of pluripotent cells. For instance, gene mutation or knockouts, which have been proven to be lethal during normal embryonic development, could be studied through *in vitro* differentiation studies of ESCs. EB formation has already been regarded to be an important step to induce lineage differentiation, which recapitulates various aspects of early embryonic development [50, 51]. EB differentiation begins with the formation of the ESCs aggregates, the size of which varies based on the initial number of cells which self assembled via cell-cell adhesion receptors [12, 52]. Since EB formation is similar to embryonic gastrulation process, it has been widely used to promote spontaneous differentiation of ESCs [53]. It is known that ESCs can

be induced to form 3D multicellular aggregates (EBs) when cultivating in suspension without anti-differentiation factors, which yields aggregates with highly irregular geometry [54-56].

In this study, we examined the capability of the 3D novel porous cellulose based scaffolds (HPC-MA) to efficiently entrap the seeded mESCs and support the formation of EBs.

Toward this end, undifferentiated mESCs were dissociated and resuspended in EB formation medium. Cells were seeded onto the scaffold coated with gelatin to initiate cell adhesion. Cells were then seeded into the porous gel with pore diameter of ranging from 30 to 300um with median pore diameter of approximately (42.4 μm) and controlled porosity of ((~96 ± 0.9%) as measured by mercury porosimetry, which is believe to be suitable for inducing cell aggregation into EB [39].

The Oct4b2 mouse ES cells express green fluorescent protein (GFP) under the Oct4 promoter and thus enable cell visualization with a fluorescence microscope without the need to further stain these cells. Figure 7.4 shows the bright field and fluorescent images of the ES cells seeded into the gel and the formation of EBs after 1hr, 3 and 14 days of culturing. As shown, seeding ES cells into the gel resulted in formation of relatively uniform EBs with the size variation of 100-200 micron, which matched the size of the scaffold pores. The seeded cells aggregated to form rounded discrete EBs after 3 days, while the GFP expression decreases over time, likely because EBs are maturing over time, when cystic structures of EBs were observed at day 14 (darker parts), revealing the presence of various type of differentiated cells from the EBs. It was observed that EBs retained their original spherical structures with almost no outgrowths around in cellulose scaffolds, even after culturing for 14 days, which indicates that cellulose could provide the physical confinement for EBs formation, provision of physical confinement has been used widely in *in vitro* model for mouse embryogenesis [14]. Decrease in GFP intensity is an indicator showing ES cells are losing their pluripotency over time (Figure 7.4E,F). The arrows show the formation of EBs at different layers of hydrogel.

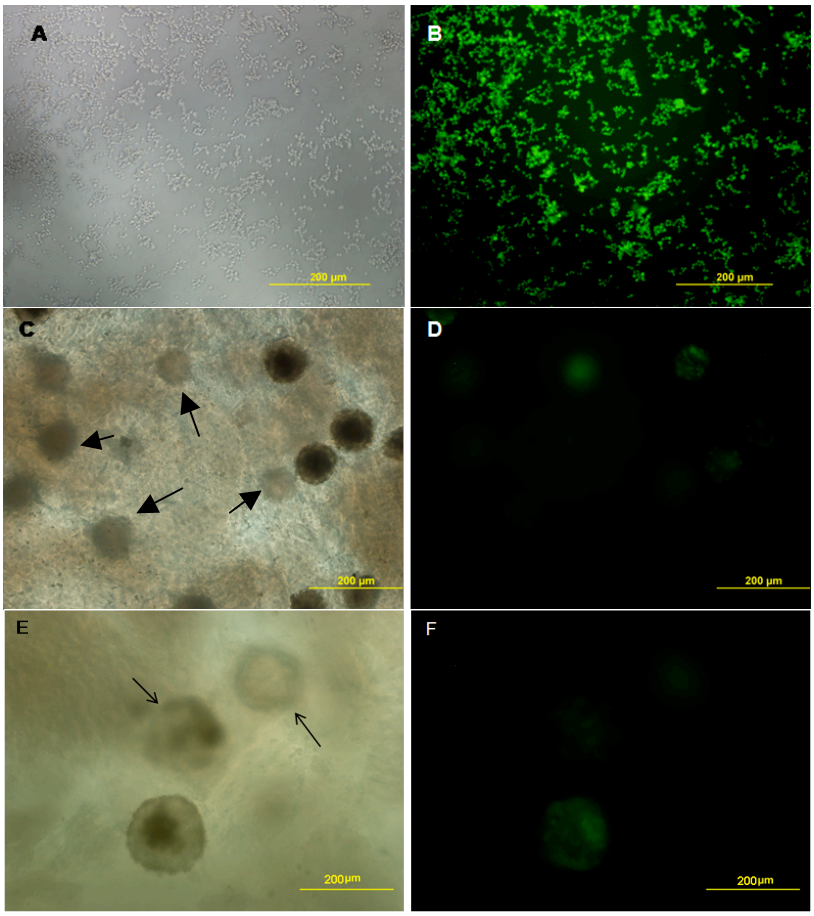

Figure (7.4): The morphology of EBs formed in porous gel after 1hr of seeding (A,B), 3days (C,D) and 14days (E,F) , A,B,E are bright field images while B,D,F are GFP expression, Scale bar=200µm

We compared the size distribution of EBs inside porous hydrogel to those produced in low adhesion suspension method (a common method for EB formation [54]) at different point times by measuring EBs diameter using Imagej software.

For this purpose, cells with defined density were seeded (2.5×10^5cells/well) into 48 well-plates containing hydrogel and were compared to those seeded onto low adhesion 48 well-plates. Size of EBs is an important parameter, not only to improve the reproducibility of ESC differentiation experiments, but also to regulate cell type-specific differentiation lineages [53].

As shown in Figure 7.5, the average diameters of EBs cultivated in both scaffold and suspension increases with continuous growth. There is no significant increase in the size of EBs formed in gel during day 6 to 14. When compared with the EBs formed in liquid suspension, the scaffold-EBs, were more uniform with smaller size distribution after 14 days of culturing. As for the suspension technique, EBs with a wider size distribution and non-uniform morphologies were observed over time.

Moreover, as can be seen in Figure 7.5, when the average diameter of EBs formed inside scaffold and liquid suspension are compared at different times, the obtained standard deviation confirms that there

is a broad size distribution among EBs formed by suspension method while the size variation was found to be much smaller for EBs formed by the scaffold method. Although EBs can be generated using the low adhesion suspension culture method, EBs formed inside scaffold are more homogeneous, while the former technique suffers from a large variation in size and morphology of the obtained EBs, limiting its yield. A study by Valamehr [57] showed that EBs formed with 100-300 micron size hold the greatest differentiation potential, and have the lowest rate of cell death compared with smaller or larger than these range. The diameter of EBs formed inside hydrogel were in the range of 100–300 µm.

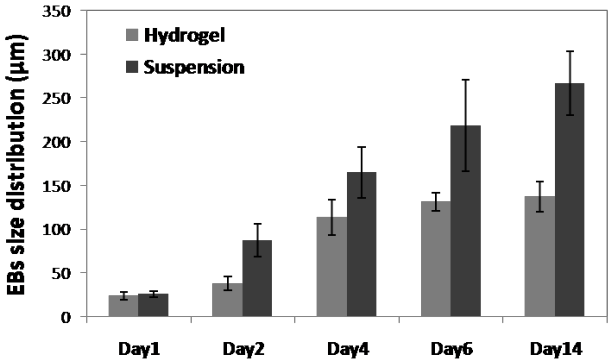

Figure (7.5): Size distribution of EBs formed inside HPC gel and in suspension low adhesion dish over 14 days of culturing, results are shown as mean± the standard error (SEM).

The viability of cells inside EBs formed via scaffold and liquid suspension methods was also quantified by measuring ATP activity of cells. The results revealed that at each time point hydrogel method gives more viable cells compared to suspension method. For example, the viability of cells increased by about 1.4 and 1.8 fold in hydrogel method after 5 and 14 days, respectively (Figure 7.6).

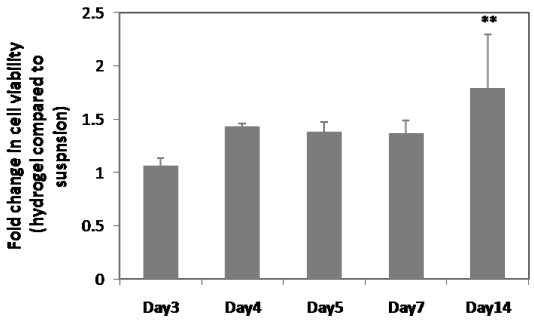

Figure (7.6): Cell viability measured by CellTitre-GluR Luminescent cell viability assay in scaffold-borne EBs compared with EBs formed in liquid suspension method. Data are expressed as mean± the standard error of the mean (SEM). Statistical significance was determined by analysis of variance (One-way ANOVA) with $p < 0.05$.

Distribution of ES cells and EB formation in a scaffold over time is an indication of cellular compatibility and appropriateness for tissue engineering applications which is known to be dependent whether the scaffold can facilitate cell migration and proliferation within [58]. GFP expression and proliferation of cell and distribution on 3D scaffolds were observed using confocal microscopy. As cells seeded into pores gel hydrogel, they were observed to penetrate into the pores and fill the pores. Figure 7.7 shows the distribution of cells after seeding into the porous hydrogel. Cells were closely associated with each other (Figure 7.7 A,B) and began to self-assemble, formed cell clumps (Figure 7.7 D) and formed a single cell aggregate (EB) within 36h (dashed circles show the boundaries of pores in hydrogel) and subsequently forming round and compact EB after 3 days (Figure7.7E). *In vitro* aggregation of murine ES cells are known to trigger the formation of embryo and facilitates spontaneous, unguided differentiation analogous to that seen in developing mouse embryos [59].

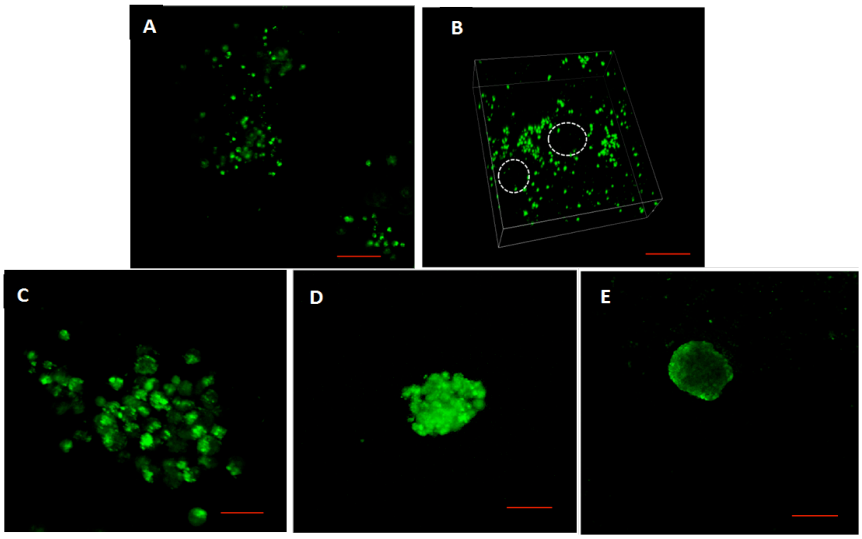

Figure (7.7): Dispersion of single stem cells in porous hydrogel 3 hours after seeding (A,B), dashed lines in (B) illustrate the boundaries of pores in porous. Cell start accumulation in gel at 8hours (C) and form cell aggregation after 36hr (D) and consequently compact EBs after 3 days (E), Scale bar=50micron

The microstructures of the lyophilized HPC hydrogel before and after cell seeding were investigated using scanning electron microscopy (SEM). From the SEM observation of the cross-sectioned hydrogel before seeding cells showed a highly porous structure with submicron size interconnected pores as shown in Figure (7.8A). This highly porous structure should allow cell penetration, growth, differentiation and proliferation. A few hours after seeding ES cells into the scaffold, they started to cover the pores (Figure 7.8B,C). The images clearly show the attachment of ES cells to the inner walls of hydrogel and covering pores over time. After 36hr, ES cells started to grow and were able to form bigger aggregates and colonised into the 3D structure (Figure 7.8D). Figure (7.8E) also clearly

shows the attachment of the round and compact EB to the base of hydrogel at day 3. The attachment of a number of EBs on the surface of scaffolds clearly demonstrates the potential of HPC-MA scaffold to support cell-cell interaction for further *in vivo* studies.

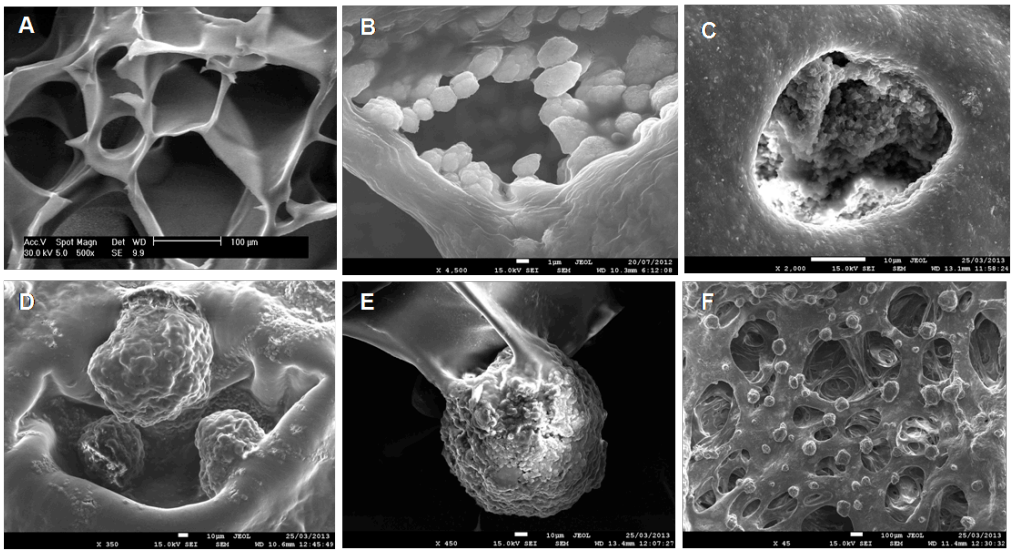

Figure (7.8): Cross-sectional SEM images of a 3D HPC hydrogel showing a porous structure of gel before cell seeding (A) 3 and 8 hours after seeding (B,C) and three days (D,E,F) after seeding cells.

7.2.4.4 Reverse Transcription PCR analysis of three germ layer markers and cardiac marker expression in embryoid bodies

To assess the potential of mESCs to form derivatives of all three embryonic germ layers in scaffolds, cells in scaffold were characterized for their (Brachyury (mesoderm), Foxa2 (endoderm) and Nestin (ectoderm)) gene expression. Cells were cultured in HPC-MA and allowed to from EB inside the hydrogel. At day 3, 6, 8, and 10, EBs were collected for RT-PCR analysis. All EBs collected at different points expressed all these differentiation markers, confirming the *in vitro* differentiation of EBs, while three germ layers markers were not detectable in the ES cells (control) (Figure 7.9A).

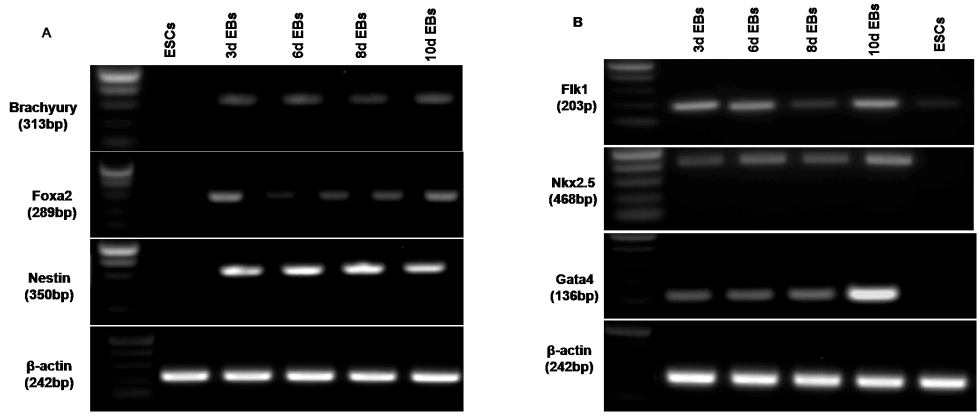

Figure (7.9): The differentiation status of EBs at different time points, using three different germ layer markers (A). The expression of cardiac lineage and progenitor markers at different time points of EB formation (B). β-actin was used as a housekeeping gene. Undifferentiated cells were used as negative control.

Quantitative real-time PCR analyses were performed to characterize the differentiation markers for the 3 germ layers (endoderm: mesoderm, and ectoderm). The markers expression of EBs generated and collected from scaffold were compared to those collected from liquid suspension method. Octamer-binding transcription factor 4 (Oct4) was used as a marker of undifferentiated cells. Oct4 expression was down regulated from day 3 of EB formation, which suggested that the ES cells had lost their pluripotency when EBs are becoming mature.

The expression of Foxa2 as endoderm marker increased in a time-dependent manner in both methods and reached its peak at day12 in hydrogel method. However, this Foxa2 level decreased in suspension techniques from day 8.

The expression of ectodermal marker (Nestin), gradually increased in hydrogel and suspension method over time except a slight decrease at day 8 for suspension. Although higher endodermal expression was observed in suspension-EBs at day 8, endoderm marker reached its highest level at day 12 in hydrogel-born EBs.

The result also showed that although there is a slight decrease in the expression of Brachyury from day 3 to 6, this gene started to increase and reach its maximum level 12 days after EB formation. Overall, higher Brachyury expression was observed in scaffold-born EB compared to that formed in suspension at day 6 and day 8.

Expression of 3germ layers showed the level of Fox2a, Brachyury and Nestin increased over time in EBs formed inside scaffold which confirms the *in vitro* differentiation potential of EBs which are formed using the scaffold technique. The successful potential of hydrogel to further induce differentiation of EBs confirms that hydrogel could be a reliable substitute for liquid suspension method.

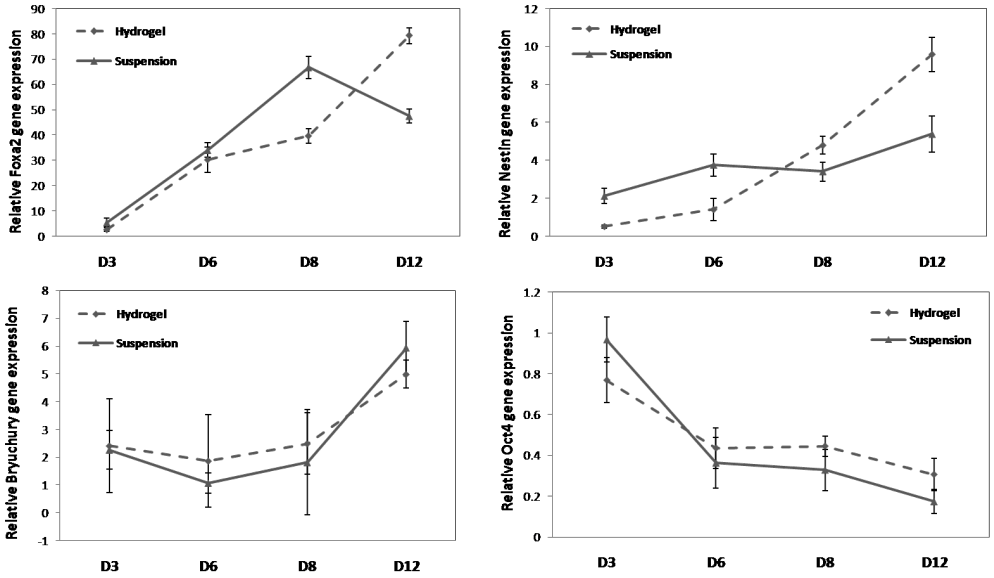

Figure (7.10): The results shown are mean values (± SD).

We have also investigated the protein expression of three germ layers for EBs formed inside HPC-MA scaffold. For this purpose, 5-day-old EBs were collected from hydrogel and were stained. We examined the expression of these markers by plating down some 5-day-old EBs for another 5 days in gelatinized dish. The results (Figure 7.11, and 7.12) confirmed the presence of ectoderm (Nestin), mesoderm (Brachyury) and endoderm (Fox2a) in EBs and also in plated EBs. All secondary antibodies were selected red because ES cells were already GFP positive.

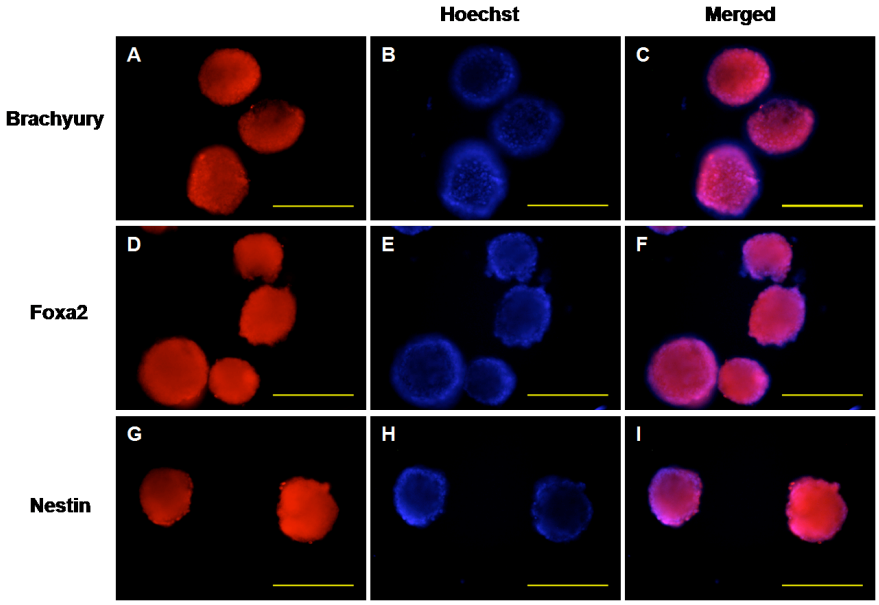

Figure (7.11): Immunostaining 5-day- old EBs for three germ layers mesoderm (Brychyury,A) endoderm (Foxa2, B) and ectoderm (Nestin,C), the blue staining is Hoechst for nuclei, Scale bar=250micron.

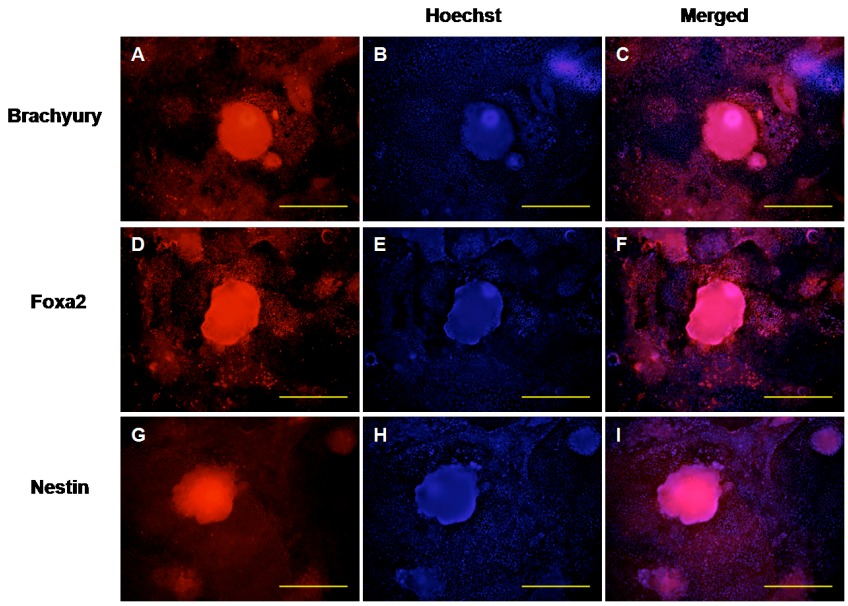

Figure (7.12): Immunostaining of plated down EBs for three germ layers Brychury, Foxa2 and Nestin, the blue staining is Hoechst for nuclei, Scale bar=500micron.

These results suggest that a porous HPC-MA scaffold can preferentially induce the formation of 3D stem cells structure with the potential to differentiate into all 3 germ layers.

One of the first types of differentiated cells derived from pluripotent stem cells in embryoid bodies is cardiomyocytes, in which cell to cell interactions stimulate the expression of markers for mesodermal and early cardiac cell lineages [60]. To characterize the cardiac differentiation potential of EBs

generated from a hydrogel, the gene expression of EB-derived cells was qualitatively determined using RT-PCR (Figure 7.9B).

Flk1 is quite promiscuous with the lineage derived from mesoderm, and since the cardiomyocytes are derived from the mesodermal lineages, it serves as a lineage marker to detect the initiation of mesoderm during differentiation.

The study of post implantation development pointed out that Flk1 is the factor first detected during gastrulation in mesoderm cells in a region that further developed into heart. This gene is then expressed in endothelial cell precursors and developing endothelial cells of the heart and embryonic and extraembryonic vasculature [61]. Thus, Flk1 is found to be the initial molecular marker of endothelial cell precursors [62, 63]. For this purpose, Flk1 was chosen as an early cardiovascular progenitor which usually expresses in the early stage of mouse cardiac development.

We also chose two markers, Gata4 and Nkx2.5, that are key regulators of cardiac-specific transcription associated with cardiogenesis; these markers are usually detected in the pluripotent stem cell-derived cardiomyocytes [64, 65].

Nkx2.5 is one of the cardiac specific transcription factors that plays an important role in the specification of myocardial progenitors in heart looping in mice [66] . It has been shown that Nkx2.5 plays an important role in the process of heart development and a considerable amount of Nkx2.5 is expressed in the heart during the initiating of cardiac differentiation [67].

Gata4 is another transcriptional factor that plays an important role in promoting cardiac muscle development. This factor was also detected in cardiac progenitors cells [65, 68]. Studies suggest that differentiation of cardiomyocytes from non-cardiac cells (e.g., bone marrow stem cells) or in the ES-EB cell system is associated with increased expression of well-characterized transcriptional factors including Csx/Nkx2.5, and Gata4 [69, 70], suggesting a role for these transcriptional factors in cardiac development. Gata4 regulation occurs by Nkx2.5 transcription factor as the coactivator and corepressor during differentiation of heart, for regulating the transcription and expression of downstream structural and regulatory genes [71]. Positive expression of this gene indicates that cells at the mesodermal stage were committing to cardiac differentiation.

Semi-quantitative RT-PCR demonstrated that all cardiac markers tested, including Flk1, Nkx2.5, Gata4, were expressed in 3, 6, 8 and 10-day old EBs, indicating that cells in EB became precardiac mesoderm. These findings demonstrate the cardiac potential of EBs formed inside cellulosic scaffold, and showed the fact that the mouse ES cells are able to differentiate to a cardiac lineage.

To promote cardiac differentiation, 5 day-old EBs were collected from scaffold and plated down on gelatinized plate. Cardiac immunostaining using specific cardiac markers, including Nkx2.5 and cTnT, was then conducted. The expression of two cardiac-specific proteins, Nkx2.5 and cardiac troponin T (cTnT), were examined by immunofluorescence.

Representative images show the positive protein expressions of the cardiac markers (cTnT) (appeared in red) after 12 days of cultivation, which revealed the successful formation of organized sarcomeric myofilaments in differentiated cell population (Figure 7.13). As shown in Figure 7.13A-B, cells in plated down EB have differentiate toward cardiomyocytes, as indicated by their early cardiac markers Nkx2.5 (appeared in red) and cardiac-specific markers expression. The nuclei were counterstained by Hoechst (appeared in blue).

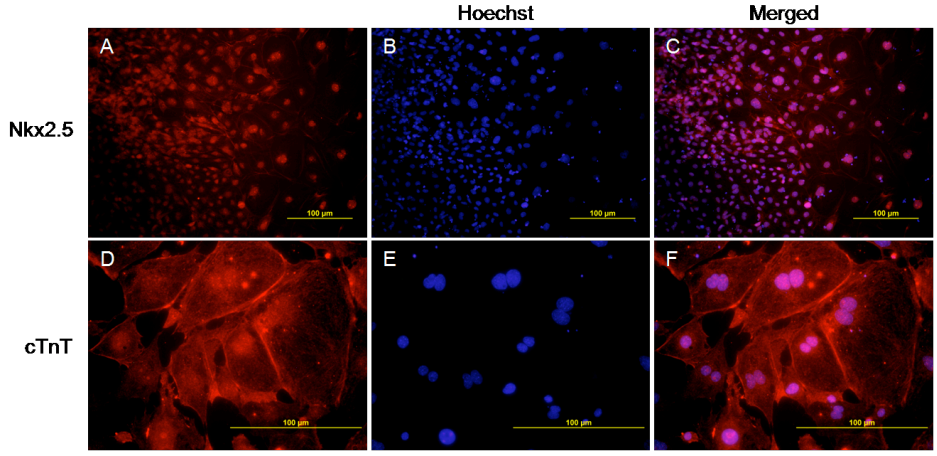

Figure (7.13): Immunostaining for expression of Nkx2.5 (on day 7) and cTNT(cardiac troponin) (on day 12), Nuclei were stained with Hoechst (blue).

7.2.4.5 Spontaneous beating foci

We tested the differentiation potential of hydrogel-born EBs into cardiomyocytes by routinely examining the presence of spontaneous beating. Interestingly, after around 13 days of being in hydrogel, some of the EBs contained beating cardiomyocyte foci (supplementary video). It is worth mentioning that although the results confirm the potential of cellulose scaffold to induce beating EBs, the efficiency of beating should be optimised.

7.2.5 Conclusion

The production of large numbers of homogeneous cell populations for use in regenerative cellular therapies and diagnostic cell-based technologies could be facilitated by engineering the EB microenvironment through engineered biomaterials to enhance the directed differentiation of ESCs.
In this study, a new model for EB formation and ES cell differentiation was successfully established. Cardiac differentiation is accomplished in a three dimensional extra-cellular matrix composed of a degradable and highly hydrated porous cellulose-based hydrogel, which more closely mimics the *in vivo* environment. We also showed that porous hydrogel with controlled porosity (between ~96 ±

0.9%) can result in formation of uniform EBs that can be further used in directing the differentiation of ESCs for different clinical applications.

7.2.6 Acknowledgment

We acknowledge the funding provided by the Department of Mechanical and Aerospace Engineering at Monash University. Funding for this research was also partly provided through an Australia Research Council Discovery Project Grant ARC DP 120102570 and through the Australia-India Strategic Research Fund BF050038. This work was performed in part at the Melbourne Centre for Nanofabrication, an initiative partly funded by the Commonwealth of Australia and the Victorian Government.

Appendix 7.3: Use of Cellulosic Hydrogel for Cell-releasing

A 7.3.1 General Overview

This section compromises one published paper.

In this publication, the application of a thermo-responsive hydrogel (hydroxypropyl cellulose (HPC)) with cell releasing behaviour was carried out. The thermoresponsive membrane applied for cell grafting took advantage of the temperature responsive property of HPC. The thermo-responsive properties (such as turbidity, water contact angle, swelling ratio, dynamic mechanical analysis and thermal analysis) of these HPC-MA hydrogels were evaluated. Temperature-modulated cell-releasing characteristics were studied using African green monkey kidney cells (COS-7 cells) and murine-derived embryonic stem (mES) cells. The results showed that embryonic stem cells adhered and proliferated well on the hydrogel surfaces under normal cell-culture conditions, and spontaneously detached from the hydrogels without trypsinization when the temperature was reduced to 4 degree. These unique properties make our HPC-MA hydrogels potential substrates for cell sheet engineering.

A 7.3.2 Thermoresponsive Cellulosic Hydrogels with Cell-Releasing Behavior

ACS APPLIED MATERIALS & INTERFACES

Research Article

www.acsami.org

Thermoresponsive Cellulosic Hydrogels with Cell-Releasing Behavior

Siew P. Hoo,[†,‡] Fatemeh Sarvi,[§] Wai Ho Li,[∥] Peggy P.Y. Chan,*[,‡,⊥] and Zhilian Yue*[,‡,#]

[†]Department of Chemical Engineering, Monash University, Australia

[‡]MicroNanophysics Research Laboratory, School of Applied Science, RMIT University, Australia

[§]Department of Mechanical and Aerospace Engineering, Monash University, Australia

[∥]Monash Vision group, Monash University, Australia

[⊥]Melbourne Centre for Nanofabrication, Clayton, Australia

[#]ARC Centre of Excellence for Electromaterials Science, Intelligent Polymer Research Institute, University of Wollongong, Australia

ABSTRACT: Here we report the preparation and characterization of thermoresponsive cellulosic hydrogels with cell-releasing behavior. Hydroxypropyl cellulose (HPC) was modified with methacrylic anhydride (MA). The resultant macromonomer, HPC-MA, retains the characteristic thermoresponsive phase behavior of HPC, with an onset temperature of 36 °C and a lower critical solution temperature (LCST) of 37−38 °C, as determined by turbidity measurement. Homogenous HPC-MA hydrogels were prepared by UV-cross-linking the aqueous solutions of the macromonomer at room temperature, and characterized by water contact angle and swelling ratio measurements, and dynamic mechanical analysis. These hydrogels exhibit temperature-dependent surface hydrophilicity and hydrophobicity, equilibrium water content as well as mechanical properties. Cell-releasing characteristics were demonstrated using African green monkey kidney cell line (COS-7 cells) and murine-derived embryonic stem cell line (Oct4b2). By reducing temperature to 4 °C, the cultivated cells spontaneously detached from the hydrogels without the need of trypsin treatment. These unique properties make our HPC-MA hydrogels potential substrates for cell sheet engineering.

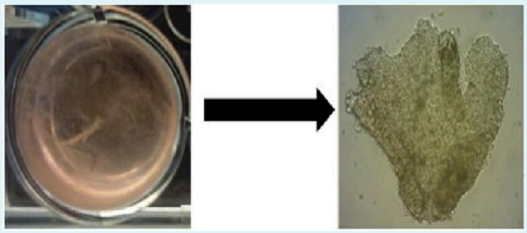

KEYWORDS: *thermoresponsive hydrogels, cellulose, lower critical solution temperature, murine-derived embryonic stem cells, cell sheet engineering*

INTRODUCTION

There has been extensive research into intelligent substrates that allow for spontaneous cell harvesting in response to an environmental stimulus.[1−3] A typical example is the thermoresponsive culture dishes prepared by grafting nanometer-sized poly(*N*-isopropylacrylamide) (PNIPAAm), or its copolymers, onto commercial tissue culture polystyrene dishes.[4] PNIPAAm undergoes a distinct phase transition from a dehydrated, collapsed structure to a highly hydrated, extended structure across a lower critical solution temperature (LCST) of 32 °C.[5,6] Such thermosensitive nature allows controlled alteration of surface hydrophobicity and hydrophilicity of the PNIPAAm-grafted dishes and, consequently, cell adhesion and detachment, by a small change in temperature. When temperature is below the LCST, cells cultivated on the substrate spontaneously detach as intact cell sheets with retained cell-to-cell junctions and extracellular matrix proteins, without the use of traditional methods involving enzymatic digestion or mechanical treatment.[7,8] Cell sheet engineering represents a novel scaffold-free approach suited for the regeneration of cell-dense tissues such as skin,[9] corneal,[10] cardiac,[11,12] esophageal, and hepatic[13] tissues.

Efforts have been made into extending the thermoresponsive culture surfaces with thermoresponsive hydrogels for cell sheet engineering. The highly hydrated structures and soft-tissue-like biomechanical properties of hydrogels and, more importantly, their capability for sustained delivery of bioactive molecules can provide a more physiologically relevant environment for the cultivated cells. For example, interpenetrating nanocomposite hydrogels have been prepared from hectorite clay nanoparticles, PNIPAAm and alginate. The presence of alginate has shown to significantly accelerate cell detachment, as a result of improved water penetration in the resulting hydrogels.[14] Although NIPAAm have been demonstrated to be a promising substrate for cell sheet engineering, NIPAAm is not derived from renewable resources, and NIPAAm does induce cellular cytotoxicity at physiological temperature.[15]

A number of studies have attempted to developed new thermoresponsive substrates to engineer cell sheets. For example, hydroxybutyl chitosan,[16] poly(*N*-isopropylacrylamide)/clay nanocomposite hydrogel,[17] methylcellulose/collagen hydrogel,[18] poly(*N*-isopropylacrylamide-*co*-acrylic acid)-*b*-poly(L-lactic acid),[19] and elastic protein-based polymer.[20] Some studies have attempted to engineer cell sheets using non-

Received: March 13, 2013
Accepted: June 4, 2013
Published: June 4, 2013

thermoresponsive substrate; for example, Guillaume-Gentil et al.[21] developed a RGD-modified poly(L-lysine)-*graft*-poly(ethylene glycol) substrate that can release cell sheet upon electrochemical polarization; Edahiro et al.[22] developed a photoresponsive NIPAAm-nitrospiropyran substrate that releases cells after UV irradiation and low temperature washing; Nagai et al.[23] developed a salmon atelocollagen fibrillar gel that releases cell sheet when subjected to collagenase digestion. Table 1 listed the substrates that have been studied for cell sheet engineering.

Table 1. Summary of Different Substrates Used for Cell Sheet Engineering

substrate material	release mechanism	ref
poly(*N*-isopropylacrylamide) (PIPAAm)	thermoresponsive	48
hydroxybutyl chitosan	thermoresponsive	16
poly(*N*-isopropylacrylamide)/clay nanocomposite hydrogel	thermoresponsive	17
methylcellulose/PBS/collagen hydrogel	thermoresponsive	18
elastic protein based polymer	thermoresponsive	20
poly(*N*-isopropylacrylamide-*co*-acrylic acid)-*b*-poly(L-lactic acid)	thermoresponsive	19
RGD-modified poly(L-lysine)-*graft*-poly(ethylene glycol)	electrochemical polarization	21
poly(*N*-isopropylacrylamide)-nitrospiropyran	photoresponsive	22
salmon atelocollagen fibrillar gel	collagenase digestion	23

Due to the many promising applications of thermoresponsive polymer, new thermoresponsive polymer systems with new biochemical properties, new physiochemical properties, lower cytotoxicities, and preferably derived from renewable resources, are still needed to provide multifunctional platforms. Herein, we report the preparation of a thermoresponsive hydrogel based on hydroxypropyl cellulose (HPC). HPC is a commercial derivative of cellulose, the most abundant renewable polysaccharide resource; it shows no cytotoxicity and has been approved by the Food and Drug Administration (FDA) as an agent for drug delivery applications. Also, HPC is soluble in water and many organic solvents. This has partly contributed to its use in biomedical and pharmaceutical applications. More importantly, for this study, HPC exhibits a phase transition from isotropic aqueous solution to metastable biphasic system above its LCST.[24−28] In this work, HPC was modified with bifunctional methacrylic anhydride (MA). The resulting polymer contains photocross-linkable methacrylate pendant group, namely HPC-MA. The thermoresponsive properties such as turbidity, water contact angle, swelling ratio, and dynamic mechanical analysis of these HPC-MA hydrogel were evaluated. Temperature-modulated cell-releasing characteristics were studied using COS-7 (African green monkey kidney) cell line and Oct4b2 (murine-derived embryonic stem cell) cell line.

MATERIALS AND METHODS

Synthesis. All chemicals used were purchased from Sigma-Aldrich, Australia, unless otherwise stated. Hydroxypropyl cellulose (HPC, M_n = 10 000 g/mol, degree of etherification ∼ 3.4, as determined previously by ^{1}H NMR[24]) was dehydrated by azeotropic distillation in toluene. The HPC hydrogel precursor was prepared by modifying HPC with methacrylic anhydride (MA). Briefly, the dehydrated HPC (4.0 g) was dissolved in chloroform (150 mL). MA (4.17 mmol) followed by *N*,*N*-dicyclohexylcardodiimide (DCC, 4.17 mmol) was added dropwise in chloroform, respectively. The solution was then stirred for 48 h in the presence of 4-dimethylaminopyrinde (DMAP, 0.4 g) as catalyst. The solution was concentrated and precipitated into diethyl ether. The polymer was then collected, redissolved in chloroform and precipitated into diethyl ether. Finally, the product was dissolved in water, filtered to remove any insoluble impurities, and dialyzed against deionized water for 72 h before lyophilization in a freeze-dryer (HETO PowerDry PL6000, Thermo Scientific, Australia). It was denoted as HPC-MA and characterized by ^{1}H NMR spectroscopy in $CDCl_3$. ^{1}H NMR ($CDCl_3$, δppm): 0.5−1.5 ($-CH_3-CH-$), 1.8−2.0 ($CH_3-C=CH_2$), 5.5−6.2 ($-C=CH_2$), 2.5−5.3 (other protons). The degree of modification of HPC-MA is defined as the number of MA groups per repeating unit, and determined by ^{1}H NMR spectroscopy.

Turbidimetry Measurement of HPC-MA in Deionized Water. The turbidity of HPC-MA was investigated by dissolving the lyophilize HPC-MA in deionized water to form a 15% (w/v) aqueous solution. The transmittance of the sample was monitored as a function of temperature at a fixed wavelength of 500 nm, using a UV−vis spectrophotometer (Agilent Technologies Cary 60 UVVIS, Australia) with the sample cell temperature controlled with a circulating water bath. The onset temperature was defined as the temperature at which signs of opaqueness were first observed. The transmittance was measured four times and the average value of the measurement was taken.

Preparation of HPC-MA Hydrogels. HPC-MA was dissolved in deionized water at 15% or 20% (w/v), to which a photoinitiator 2-hydroxy-1-[4-(2-hydroxyethoxy)phenyl]-2-methyl-1-propanone was added to a concentration of 4% (w/w) of the polymer weight, equivalent to a final concentration of 0.6% for HPC-MA-15% and 0.8% (w/v) for HPC-MA-20%. The solution was first warmed to 40−45 °C to allow the photonitiator to dissolve, the solution was then allowed to cool down to room temperature before cross-linking. The solution was cross-linked with UV light (320−405 nm, 200 mW cm^{-2}) at a distance of approximately 200 mm using an UV cross-linker (Honle UV Technology, UV-F 400, Germany) for approximately 6 min. The cross-linked gels were then washed with deionized water to remove any uncross-linked HPC-MA and the photoinitiator to minimize possible cytotoxicity effect from residual photoinitiator. The hydrogel prepared from 15% and 20% (w/v) of HPC-MA are denoted as HPC-MA-15% and HPC-MA-20%, respectively.

Water Contact Angle Measurement. Static contact angles were measured using the static sessile drop method by employing water contact angle equipment (OCA 20, DataPhysics Instrument, GmbH, Germany) equipped with automatic dispenser. In this experiment, a 10 μL deionized water droplet was dropped on the surface of the gel and the angle is measured by using the circle fit. To examine the dependence of contact angle on temperature, 25, 37, and 42 °C were selected as the testing temperatures.

Equilibrium Swelling Measurement. The as-prepared hydrogels were submerged in water at 4, 25, 37, and 42 °C for 48 h. The weight of the swollen sample (W_h) was measured after wiping off the excess water with a piece of filter paper. The weight of the dried sample (W_d) was measured after drying the swollen sample in an vacuum oven at 40 °C for 48 h. The weight of samples dehydrated using vacuum oven at 40 °C for 48 h were compared to the weight of samples prepared with the same formulation but dehydrated by lyophilization for 5 days; no significant weight difference was noted. The swelling ratio, SR, of the hydrogel was calculated according to eq 1. Each sample was measured three times from the four parallel specimens, and the average value of the measurement was taken.

$$SR = \frac{W_h - W_d}{W_d} \quad (1)$$

Dynamic Mechanical Analysis. The storage moduli of HPC-MA-15% and HPC-MA-20% were tested on a dynamic mechanical analyzer (DMA) add in software (TA Instruments, Q800) at a frequency of 1 Hz and a preload of 0.01 N over a temperature range of 25−45 °C under compression mode. The testing was performed under atmospheric condition with a heating rate of 1 °C min^{-1}.

Cell Culture. All culture mediums used were obtained from Gibco, Australia, unless stated otherwise. The Oct4b2 cell lines that possess a

Scheme 1. Synthesis Scheme of HPC-MA

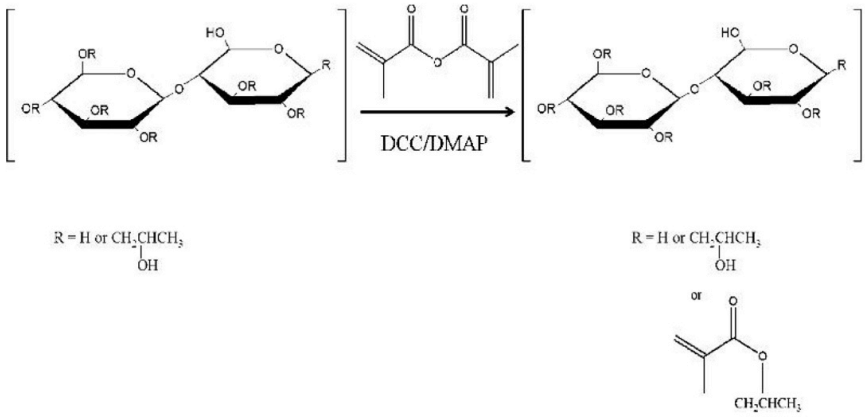

green fluorescent protein (GFP) under the control of the Oct4 promoter (Oct4-GFP)[29] were cultured according to the procedure reported in Sarvi et al.[30] Prior to cell seeding, Oct4b2 cells were cultured on 0.1% gelatin-coated dish with knockout medium supplemented with 20% knockout serum replacement, 1% nonessential amino acids, 0.1 mM 2-mercaptoethanol, 2 mM Glutamax, 1% penicillin-streptomycin (P/S), and 1000 U/mL murine leukemia inhibitory factor (mLIF, Chemicon, Australia). COS-7 cells were grown and maintained in Dulbecco's modified Eagle's medium (DMEM) supplemented with 10% fetal bovine serum (FBS), 2 mM L-glutamine, and 50 units/mL penicillin-streptomycin (P/S). Both COS-7 and Oct4b2 cells were cultured in a 37 °C, humidified 5% CO_2 incubator.

Temperature-Dependent Cell Release. HPC-MA-20% scaffolds with dimensions of 1.6 cm diameter by 0.5 cm thickness were sterilized by soaking in 70% ethanol overnight followed by washing with sterile phosphate buffered saline (PBS) before cell seeding. COS-7 and Oct4b2 cells were seeded with a cell density of 2×10^4 cells per scaffold. 10% (v/v) of gelatin was added to the culture media to improve cell adhesion. The plate was incubated at 37 °C in a humidified 5% CO_2 incubator for 3 h for cell attachment, and then 1 mL of fresh culture medium was added and the cells were allowed to cultivate on the hydrogel. COS-7 and Oct4b2 cells detachment was carried out at selected time point by incubating the culture plates at 4 °C for 30 and 10 min, respectively. Culture medium containing the detached cells was transferred to a new well-plate for reculturing to determine the regrowth ability of the retrieved cells. Images of cells at each stage of the process were visualized using fluorescent microscopy (Nikon, Eclipse Ti).

Cell Proliferation Assay. The viability of the recultured COS-7 cells was analyzed using the alamarBlue assay on days 1 to day 4. At each time point, 200 μL of 10% alamarBlue dye (diluted with complete medium) was added to each well containing cold treated cells and each well containing control cells (cells cultured on well-plate without cold treatment). The well-plate was then incubated at 37 °C for 4 h in a humidified 5% CO_2 incubator. Fluorescence analysis using an excitation wavelength of 570 nm and emission wavelength of 600 nm was carried out with a microplate reader (SynergyTM Mx, Biotek). The viability of cells was expressed as the percentage of alamarBlue reduction. Cells that have not been cultured on hydrogel and have not subjected to cold treatment were cultured on a well-plate and used as control.

The number of cells proliferating on the hydrogel was determined by quantifying the DNA content using PicoGreen assay kit (Quanti-iT PicoGreen dsDNA Reagent, Life Technologies, Australia) according to the manufacturer protocol. In brief, the cells were trypsinized from substrate and centrifuge for 5 min at 1200 rpm. The cell pellet was rinsed by cold PBS twice each followed by centrifugation for 5 min at 1200 rpm. The resultant cell pellet was collected by discarding the supernatant. The cells were lysed using 100 μL of NP40 cell lysis buffer (Life Technologies, Australia) for 30 min on ice and vortexed at 10 min intervals. The extract was transferred to microcentrifuge tubes and centrifuge at 13 000 rpm for 10 min at 4 °C. The clear lysate was aliquoted to clean microcentrifuge tube where 100 μL of PicoGreen reagent was added and allowed to incubate for 5 min at room temperature in the dark. The final solution was transferred into a 96-well plate, and the fluorescence was read using a microplate reader at excitation wavelength 480 nm and emission wavelength 520 nm. The number of cells in the sample was determined by correlating the DNA content with a DNA standard curve. The DNA standard curve was determined using cell lysates with known number of cells. In a separate experiment, the COS-7 cells were cultured on hydrogel followed by cold treatment on day 4, the harvested cells were readhered on culture dish and allowed to proliferate for 5 days. To examine the proliferation of the cold treated cells, COS-7 cells were first cultured on the hydrogels for 4 days followed by 4 °C cold treatment, the harvested cells were transferred to culture dish without further trypsinization, these cells were allowed to culture for another 5 days, and the DNA contents were quantified using the PicoGreen assay as described above.

Statistical Analysis. All experiments were performed in at least three replicates. Results were reported as average value ± standard deviation. One-way analysis of variance (ANOVA) was used to compare multiple groups of data statically; p values lower than 0.05 were considered statistically significant.

RESULTS AND DISCUSSION

Preparation of HPC-MA Macromonomer. HPC-MA was synthesized using a scheme illustrated in Scheme 1. DCC has been used for activation of carboxylic acids for coupling of cellulose derivatives with DMAP as catalyst.[31,32] DCC is known as a condensation reagent for producing anhydrides from corresponding acids with the formation of urea byproduct. The limitation of using anhydride is that only half the acid is stoichiometrically coupled and the other half is wasted[33] (i.e., released in the form of less reactive acid form). The use of DCC here is to react with these acids to regenerate anhydrides therefore improving the reaction efficacy. The degree of substitution (DS) was determined to be ~0.4 by ^{1}H NMR spectroscopy. HPC-MA with 0.4 DS was selected as an example for scaffold preparation as the higher degree of substitution polymer tend to lose its solubility in water and lower degree of substitution fails to provide adequate mechanical properties. Aqueous HPC exhibits low critical solution temperature

(LCST) transition, from isotropic solutions at room temperature to metastable colloidal systems upon heating.[24,26] This thermal-induced phase separation is due to dehydration of HPC and consequently increased hydrophobic associations among HPC molecules with increasing temperature. HPC-MA retains the phase behavior characteristic of HPC, as demonstrated in the turbidity measurement shown in Figure 1 ($p < 0.05$, $n = 4$). The first sign of turbidity was observed at approximately 36 °C. The LCST of HPC-MA was determined to be approximately 37 to 38 °C, after which the transmittance decreases drastically with increasing temperature until reaching a plateau at ~45 °C.

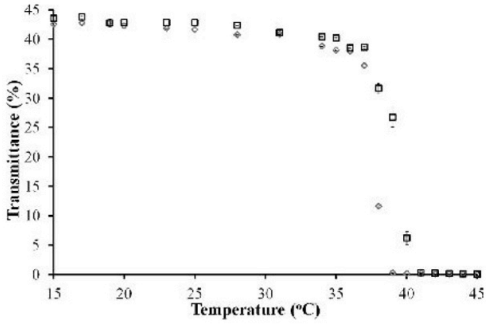

Figure 1. Turbidimetry measurement for HPC-MA-15% (black □) and HPC-MA-20% (gray ◇).The percent transmittance decreases as the temperature increases ($p < 0.05$, $n = 4$). Data are shown as mean values with standard deviation as error bars in the form of mean value ± standard deviation.

Physiochemical Characterization of HPC-MA Hydrogels. UV-irradiation was selected to induce cross-linking of aqueous HPC-MA due to its many advantages, including fast polymerization rate at low temperature and ease of hydrogel shaping.[34] The photoinitiator, 2-hydroxy-1-[4-(2-hydroxyethoxy)phenyl]-2-methyl-1-propanone (Irgacure 2959), has shown to cause minimal toxicity to a wide range of mammalian cells[35] and, therefore, was employed for the preparation of HPC-MA-15% and HPC-MA-20% hydrogel samples. Figure 2 shows the representative photos of the water contact angles on HPC-MA-20% at 25, 37, and 42 °C, as the testing temperature is increased from 25 to 37 °C; the water contact angle of the HPC-MA gel increased from 35.1° to 52.1°, reflecting an increase in surface hydrophobicity. This finding revealed that the thermoresponsive behavior of HPC-MA conjugates was retained after cross-linking, resulting in chemically cross-linked thermoresponsive hydrogels that underwent phase transition at an onset temperature of 37 °C. A further increased in temperature above the HPC-MA gel LCST results in a contact angle of 61°.

Equilibrium swelling of HPC-MA hydrogels was measured gravimetrically at 4, 25, 37, and 42 °C. Figure 3 shows that as the temperature increases, the equilibrium swelling ratio decreases ($p < 0.05$, $n = 5$), indicating that the hydrogels undergo a temperature-triggered deswelling process. The magnitude of change in equilibrium swelling ratio of the hydrogels, from a swollen to deswollen state, decreases as the polymer concentration in the hydrogels increases from 15% to 20% (w/v). Concurrently, the hydrogels also change their appearances from transparent to opaque as the temperatures rises above 42 °C (Figure 4).

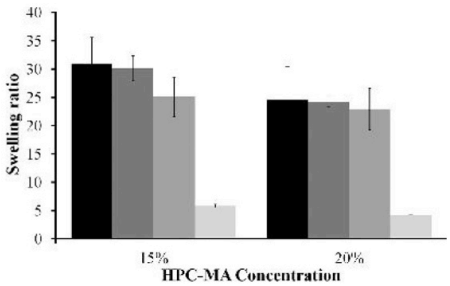

Figure 3. Swelling ratio for HPC-MA-15% and HPC-MA-20% at 4 °C (black bar), 25 °C (dark gray bar), 37 °C (medium gray bar), and 42 °C (light gray bar). The swelling ratio decreases as the temperature increases ($p < 0.05$, $n = 5$). Data are shown as mean values with standard deviation as error bars in the form of mean value ± standard deviation.

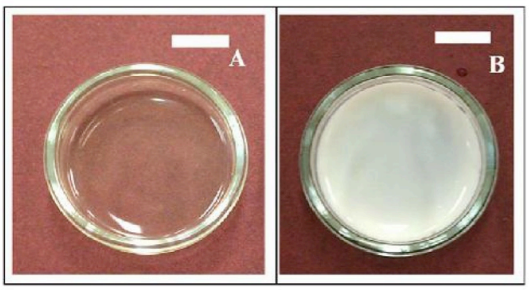

Figure 4. Thermal sensitivity of HPC-MA gel (scale bar of 1 cm) at 25 °C (A) and 42 °C (B).

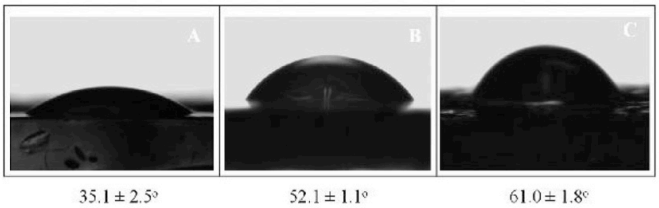

Figure 2. Contact angle of HPC-MA-20% gel at room temperature (A), 37 °C (B), and 42 °C (C). Data are shown as mean values with standard deviation as error bars in the form of mean value ± standard deviation.

HPC-MA contains both hydrophilic and hydrophobic groups. At temperature below the lower critical solution temperature, the hydrophilic groups of the HPC-MA in the hydrogels bond to water molecules through hydrogen bonds to form a stable shell around the hydrophobic groups, hence giving rise to a high equilibrium swelling ratio and low water contact angle. As seen from Figure 3, the equilibrium swelling ratio starts to decrease at approximately 37 °C. This is due to breaking of the hydrogen bonds between the water molecules and/surrounding the polymer at elevated temperature, and consequently the interactions among the hydrophobic groups become dominant. As a result, the water molecules are released out, and the polymer networks in the hydrogels collapse with increased hydrophobicity, similar behavior has been observed for other types of thermo-responsive hydrogel systems.[36,37]

Storage moduli of HPC-MA-15% and HPC-MA-20% are shown in Figure 5 as a function of temperature. It is well-known that cross-linking density in hydrogel increases with increasing polymer concentration due to the formation of longer attached chain,[4,38] and a densely cross-linked network exhibits higher mechanical strength compared to loosely cross-linked network. As expected, the storage modulus of the hydrogels increases with increasing the polymer concentration from 15% to 20% (w/v). As temperature increases from 25 to 45 °C, the storage modulus increases from 0.7 to 0.9 kPa for HPC-MA-15%, and from 1.9 to 2.5 kPa from HPC-MA-20%, respectively. The HPC-MA hydrogels exhibit temperature dependent storage modulus; a similar trend has also been reported for other types of thermoresponsive hydrogels, such as a hydrogel composed of PNIPAAm and methylcellulose.[39] As the temperature rises above the LCST, the polymer chains within hydrogel undergo coil−globule transition, leading to a more densely packed network, thereby exhibiting higher storage modulus. The mechanical property of a hydrogel is an important factor for promoting tissue repair and regeneration.[40,41] Different targeted tissue types require the use of hydrogels with matching mechanical properties for cell cultivation. The range of storage modulus exhibited by the HPC-MA hydrogels is comparable to that of soft tissues and organs such as brain, lymph node, mammary gland, liver, breast tumor, and kidney,[42] which suggests that they can be used as biomimicry culture substrates to simulate these soft tissues. Further fine-tuning of the mechanical properties of HPC-MA hydrogels can be achieved by varying the concentration and degree of substitution of HPC-MA.

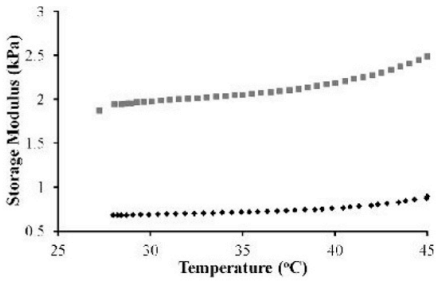

Figure 5. Storage modulus for HPC-MA-15% (black ◆) and HPC-MA-20% (gray ■).

Cell Proliferation on HPC-MA Hydrogels. To assess the cytocompatibility of the HPC-MA hydrogels, COS-7 cells were seeded onto the surface of HPC-MA-20% hydrogel as shown in Figure 6A and cultured at 37 °C in a humidified 5% CO_2 incubator. Figure 6B−E shows that COS-7 cells exhibited spindle morphology and reached confluency after 5 days, indicating that these cells adhered well on the hydrogel. The number of cells proliferated on the hydrogel was quantified by determining the DNA content, because DNA is the cellular component that reflects the cell number most accurately.[43] Figure 7 shows that the DNA content, and hence the number of cells, on the hydrogel increased over the 5 day period ($p < 0.05$, $n = 4$), indicating that the HPC-MA hydrogel is biocompatible to COS-7 cells and facilitate cell proliferation.

Temperature-Dependent Cell-Release Behavior. Traditionally, to detach cells that adhere to culture surfaces, enzymatic digestion such as trypsin or Dispase is utilized. Such

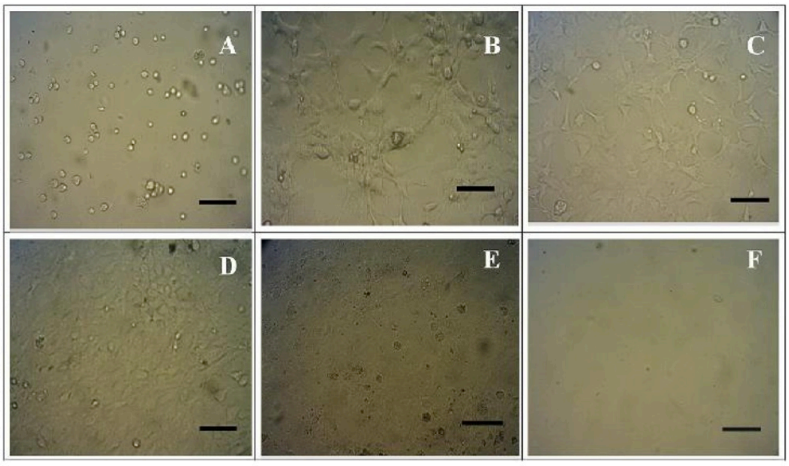

Figure 6. COS 7 cell growth (scale bar of 100 μm): day 0 (A), day 2 (B), day 3 (C), day 4 (D), day 5 (E) on hydrogel, and the surface of hydrogel after cold treatment (F).

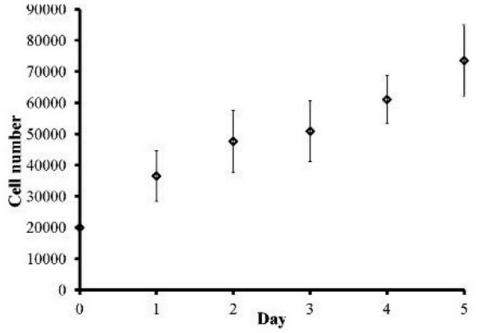

Figure 7. Proliferation of COS-7 cells on HPC-MA-20% hydrogel. Cell growth on hydrogel increased gradually over a period of 5 days ($p < 0.05$, $n = 4$). Data are shown as mean values with standard deviation as error bars in the form of mean value ± standard deviation.

detachment of cells caused the destruction of extracellular matrix, growth factor receptors, and cellular junctions.[1,5,6] In this study, COS-7 cells are employed for monitoring cell attachment on and detachment from the HPC-MA hydrogel surfaces, because of their rapid division and growth.[44] Cells were seeded onto the surface of HPC-MA-20% hydrogel. At day 4, the hydrogel was subjected to cold treatment at 4 °C for 30 min. It was found that approximately 80 to 90% of the attached cells were detached from the hydrogel by this cold treatment (Figure 6F). At the onset LCST, cells adhere on the hydrogel surface passively due to hydrophobic interaction between the cells and the gel surface. During cold treatment, the hydrogel undergoes phase transition and becomes hydrophilic which is less favorable to cell adhesion, thus causing the cells to detach from the hydrogel surface. The detachment of cells is accelerated probably due to water penetration as the hydrogel underwent low temperature induced swelling. In another set of experiment, COS-7 cells were allowed to cultivate for 10 day (Figure 8A) followed by cold treatment.

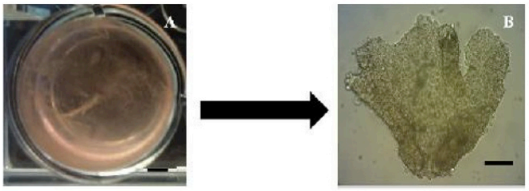

Figure 8. (A) COS 7 cells grown on hydrogel (scale bar 0.2 cm) at day 10. The hydrogel was subjected to cold treatment; the cell sheet was then transferred to a culture dish. (B) Representative image showing a cell sheet retrieved after cold treatment (scale bar 100 μm).

Figure 8B shows that a detached COS-7 cell sheet was transferred and readhered on a culture dish after cold treatment without trypsin treatment. It was observed that cell−cell connections were maintained after cold detachment, which is important for tissue regeneration.

Similar process involving cell seeding, attachment and detachment was carried out using Oct4b2 cells. Figure 9A−D shows the cells seeded on hydrogel at day 0 and cell growth on hydrogel at day 3. At day 3, the cultured Oct4b2 cells were detached from the hydrogel followed by incubation at 4 °C for 10 min. Reculturing of the detached Oct4b2 cells onto a new

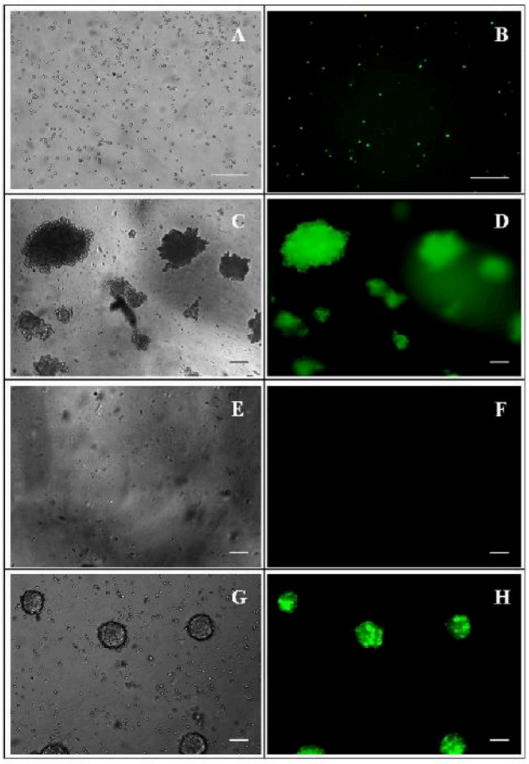

Figure 9. Representative images showing bright field and GFP expression of Oct4b2 cells growth (scale bar of 100 μm) at day 0 (A, B), and day 3 on hydrogel (C, D). Oct4b2 cells were cultured on a hydrogel for a period of 3 days, the hydrogel was then subjected to cold treatment, and the detached cells were transfer to a culture dish for readhesion. Representative images show the (E) bright field and (F) GFP filter view of the surface of hydrogel after cold treatment; apart from debris, very little cells and GFP signal can be detected, indicating that the cold treatment can detach most of the cells from the hydrogel. Representative images show the (G) bright field and (H) GFP filter view of cells retrieved after cold treatment; images were taken on day 3 after the retrieved cells were transferred to a culture dish.

tissue-culture plate was undertaken to preliminarily access the viability of the detached cells. Oct4b2 cells carry the Oct4-green fluorescence protein (Oct4-GFP) reporter, and the Oct4-GFP expression is directly correlated with the pluripotency of these cells. During the course of the experiment, the GFP expression of Oct4b2 cells was monitored using a fluorescence microscope. Figure 9E and F shows that the detached Oct4b2 cells demonstrated good viability and healthy morphology of the Oct4b2 cells as compared to Oct4b2 cells cultured on T-flask without cold treatment (control) in Figure 10. The Oct4-GFP expression observed in Oct4b2 cells at day 3 in Figure 9G and H revealed that the pluripotency of Oct4b2 cells were maintained after the cold treatment of the hydrogel, indicating that these cells can be further proliferated for tissue engineering applications.

Cell Viability after Cold Treatment. COS-7 cells were cultured on the hydrogel as described above. At day 4, the hydrogel was subjected to cold treatment at 4 °C for 30 min.

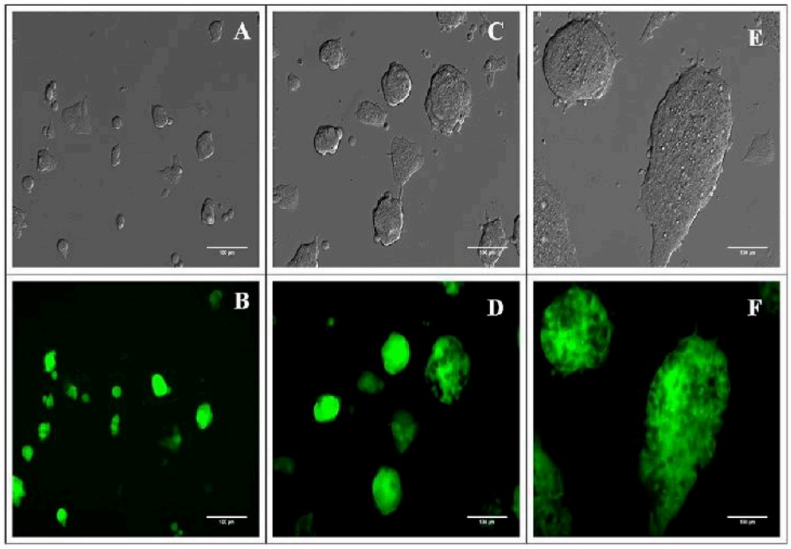

Figure 10. Bright field and GFP expression of Oct4b2 cells growth on culture dish (scale bar of 100 μm): day 1 (A, B), day 2 (C, D), and day 3 (E, F).

The readhesion and proliferation of the detached COS-7 cells were assessed preliminarily by reculturing them onto a well-plate and measured using alamarBlue assay. Figure 11A shows a

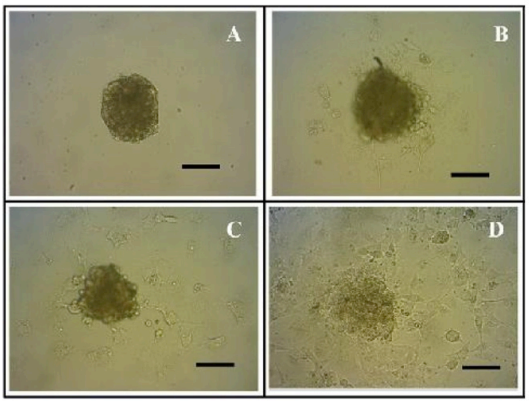

Figure 11. COS 7 cells were cultured on hydrogel for 4 days followed by cold treatment. The detached cells were allowed to readhere and proliferate on culture dish for (a) 0 day, (B) 1 day, (C) 3 days, and (D) 4 days (scale bar of 100 μm).

photo of the detached cell sheet from the hydrogel after cold treatment. The harvested cell sheet shrunk due to the inherent contractile force within cells and their connectivity to the sheet, similar phenomena was observed by other study that retrieve cell sheet from poly(NIPAAm) substrate.[45] Hirose et al.[46] demonstrated that the use of a hydrophilically modified polyvinylidenefluoride membrane as a supporter can prevent the cell sheet from shrinkage and wrinkling when transferring the cell sheet to another surface, such support membrane can be used in future study to prevent the shrinkage of the harvested cell sheet. Nevertheless, once the cell sheet from HPC-MA hydrogel was allowed to readhere on a culture dish, the cell sheet started to spread out as the cells started to adhere and migrate along the culture dish (Figure 11B–D). It was shown that these cells adhered well to the new surface and resumed normal growth (Figures 11 and 12). Figure 12 shows

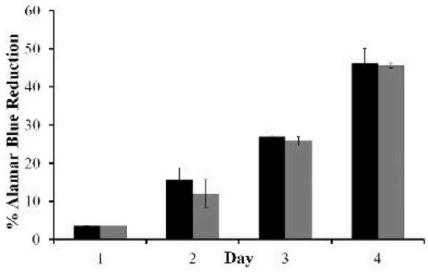

Figure 12. Cell viability of COS-7 cells with cold treatment (gray bar) compared to cells without hydrogel and cold treatment (black bar) (control) in terms of percent reduction in alamarBlue. No significant difference in viability of cold treated cells and control cells was observed ($p < 0.05$, $n = 3$). Data are shown as mean values with standard deviation as error bars in the form of mean value ± standard deviation.

the viability of cells after undergoing cold treatment as compared to cells that have not been cultured on hydrogel and have not been subjected to cold treatment (control). The metabolic activity of cells causes a chemical reduction of the alamarBlue reagent and leads to color change in this redox indicator. In another word, the increase in metabolic activity increases the amount of reduced alamarBlue.[47] The result shows that there is no significant difference in percentage of alamarBlue reduction in both the cold treated cells and control cells ($p < 0.05$, $n = 3$). The increase in percentage of alamarBlue reduction from ~3.5% to ~46% indicates that the cells are not

only viable but also proliferate continuously, thus revealing that the cells were not affected by undergoing cold treatment as compared to control cells. This indicates that the cells retrieved from the hydrogel can be further proliferated for tissue engineering applications. After cold treatment, the number of cells was quantified by measuring the DNA content. Figure 13

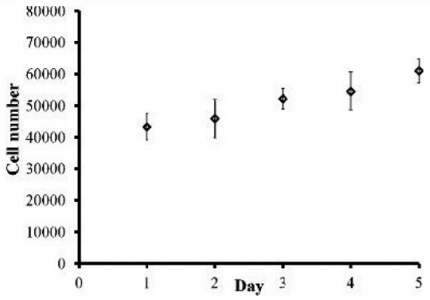

Figure 13. Proliferation of COS-7 cells that were harvested from hydrogel using cold treatment. COS 7 cells were firsts cultured on hydrogel for 4 days followed by cold treatment; the detached cells were allowed to readhere and proliferate on culture dish. The number of cells increased gradually over a period of 5 days ($p < 0.05$, $n = 6$). The data are shown as mean values with standard deviation as error bars in the form of mean value ± standard deviation.

shows that the cell number increases over a period of 5 days ($p < 0.05$, $n = 6$). The growth of cold-treated cells was observed to be slower compared to those grew on hydrogel before cold treatment. This is probably due to uneven cell seeding, as the cold-treated cells were readhered on a culture plate as cell sheet without further trypsinization, the proliferation of cells at the center of a cell sheet is restricted due to the lack of space. As shown in Figure 11, those cells at the center of the cell sheet need to migrate out first before proceeding to proliferation. Nonetheless, the increase in cell number confirmed that cells retained their proliferation ability after cold treatment.

The findings from this study suggest that the HPC-MA hydrogel possess thermoresponsive properties and exhibit temperature dependent cell-release behavior. It is worthwhile to mention that the LCST of HPC-MA can be further modulated by engineering the side chain chemistry. The influence of introduced side groups on the thermal-responsive properties of HPC-MA hydrogel is currently under investigation.

■ CONCLUSION

Serving as a proof of concept study, thermoresponsive cellulosic hydrogels were prepared by UV cross-linking aqueous HPC-MA at room temperature. The hydrogels exhibit temperature-modulated characteristics including surface hydrophilicity and hydrophobicity, equilibrium swelling and deswelling, as well as mechanical properties. A LCST of HPC-MA conjugate was found to be ~37−38 °C as determined by turbidity measurement. Cell-releasing characteristics were demonstrated using COS-7 cells and Oct4b2 cells. Both COS-7 and Oct4b2 cells adhere and proliferate well on the hydrogel surfaces under normal cell-culture conditions. By reducing the temperature to 4 °C, the cultivated cells spontaneously detach from the hydrogels without trypsin treatment. These unique properties of HPC-MA hydrogels would make them potential culture substrates for cell sheet engineering.

■ AUTHOR INFORMATION

Corresponding Author

[redacted]

Notes

The authors declare no competing financial interest.

■ ACKNOWLEDGMENTS

Funding for this research was partly provided through an Australia Research Council Discovery Project Grant ARC DP 120102570. We also thank Dr. Paul Verma from Monash Institute of Medical Research (MIMR) for supplying Oct4b2 cells. We would like to thank Prof. Robert Shanks and Izan Roshawaty Mustapa for their assistance with DMA measurements. This work was performed in part at the Melbourne Centre for Nanofabrication, an initiative partly funded by the Commonwealth of Australia and the Victoria Government. P.P.Y.C. is grateful for a MCN Technology Fellowship and a RMIT University Senior Research Fellowship that supported this work.

■ REFERENCES

(1) Shimizu, T.; Yamato, M.; Kikuchi, A.; Okano, T. *Biomaterials* **2003**, *24* (13), 2309−2316.
(2) Iwata, T.; Yamato, M.; Okano, T. Intelligent Surfaces for Cell-Sheet Engineering. In *Principles of Regenerative Medicine*, second ed.; Atala, A., Lanza, R., Thomson, J., Nerem, R., Eds.; Academic Press: San Diego, 2011; Chapter 29, pp 517−527.
(3) Zahn, R.; Thomasson, E.; Guillaume-Gentil, O.; Voros, J.; Zambelli, T. *Biomater* **2012**, *33* (12), 3421−7.
(4) Lee, F.; Chung, J. E.; Kurisawa, M. *J. Controlled Release* **2009**, *134* (3), 186−193.
(5) Biazar, E.; Montazeri, N.; Pourshamsian, K.; Asadifard, F.; Ghorbanalinezhad, E.; Keshel, S. H.; Hashemi, M.; F.H, S. R.; Majdi, A. *J. Paramed. Sci.* **2010**, *1* (3), 27−33.
(6) Yamato, M.; Akiyama, Y.; Kobayashi, J.; Yang, J.; Kikuchi, A.; Okano, T. *Prog. Polym. Sci.* **2007**, *32* (8−9), 1123−1133.
(7) da Silva, R. M. P.; Mano, J. F.; Reis, R. L. *Trends Biotechnol.* **2007**, *25* (12), 577−583.
(8) Wu, J.-Y.; Liu, S.-Q.; Heng, P. W.-S.; Yang, Y.-Y. *J. Controlled Release* **2005**, *102* (2), 361−372.
(9) Okano, T. *Rinsho Shinkeigaku* **2006**, *46* (11), 795−798.
(10) Biazar, E.; Pourshamsian, K. *Orient. J. Chem.* **2011**, *27* (4), 1443−1449.
(11) Haraguchi, Y.; Shimizu, T.; Yamato, M.; Okano, T. *Cardiol. Res. Practice* **2011**, *2011*, 1−8.
(12) Masuda, S.; Shimizu, T.; Yamato, M.; Okano, T. *Adv. Drug Delivery Rev.* **2008**, *60* (2), 277−285.
(13) Sakaguchi, K.; Shimizu, T.; Horaguchi, S.; Sekine, H.; Yamato, M.; Umezu, M.; Okano, T. *Sci. Rep.* **2013**, *3*, 1316.
(14) Wang, T.; Liu, D.; Lian, C.; Zheng, S.; Liu, X.; Wang, C.; Tong, Z. *React. Funct. Polym.* **2011**, *71* (4), 447−454.
(15) Vihola, H.; Laukkanen, A.; Valtola, L.; Tenhu, H.; Hirvonen, J. *Biomater* **2005**, *26* (16), 3055−3064.
(16) Chen, B.; Dang, J.; Tan, T. L.; Fang, N.; Chen, W. N.; Leong, K. W.; Chan, V. *Biomater* **2007**, *28* (8), 1503−1514.
(17) Haraguchi, K.; Takehisa, T.; Ebato, M. *Biomacromolecules* **2006**, *7* (11), 3267−3275.
(18) Chen, C.-H.; Tsai, C.-C.; Chen, W.; Mi, F.-L.; Liang, H.-F.; Chen, S.-C.; Sung, H.-W. *Biomacromolecules* **2006**, *7* (3), 736−743.
(19) Kim, Y. S.; Lim, J. Y.; Donahue, H. J.; Lowe, T. L. *Tissue Eng* **2005**, *11* (1−2), 30−40.

(20) Zhang, H.; Iwama, M.; Akaike, T.; Urry, D. W.; Pattanaik, A.; Parker, T. M.; Konishi, I.; Nikaido, T. *Tissue Eng.* **2006**, *12* (2), 391–401.
(21) Guillaume-Gentil, O.; Akiyama, Y.; Schuler, M.; Tang, C.; Textor, M.; Yamato, M.; Okano, T.; Vörös, J. *Adv. Mater.* **2008**, *20* (3), 560–565.
(22) Edahiro, J.-i.; Sumaru, K.; Tada, Y.; Ohi, K.; Takagi, T.; Kameda, M.; Shinbo, T.; Kanamori, T.; Yoshimi, Y. *Biomacromolecules* **2005**, *6* (2), 970–974.
(23) Nagai, N.; Yunoki, S.; Satoh, Y.; Tajima, K.; Munekata, M. *J. Biosci. Bioeng.* **2004**, *98* (6), 493–496.
(24) Yue, Z.; Wen, F.; Gao, S.; Ang, M. Y.; Pallathadka, P. K.; Liu, L.; Yu, H. *Biomaterials* **2010**, *31* (32), 8141–521.
(25) Hussain, M. A. *J. Polym. Sci., Part A: Polym. Chem.* **2008**, *46* (2), 747–752.
(26) Hirsch, S. G.; Spontak, R. J. *Polymer* **2002**, *43* (1), 123–129.
(27) Francis, M. F.; Piredda, M.; Winnik, F. M. *J. Controlled Release* **2003**, *93* (1), 59–68.
(28) Hoo, S. P.; Loh, Q. L.; Yue, Z.; Fu, J.; Tan, T. T. Y.; Choong, C.; Chan, P. P. Y. *J. Mater. Chem. B* **2013**, *1* (24), 3107–3117.
(29) Yeom, Y. I.; Fuhrmann, G.; Ovitt, C. E.; Brehm, A.; Ohbo, K.; Gross, M.; Hubner, K.; Scholer, H. R. *Development* **1996**, *122* (3), 881–894.
(30) Sarvi, F.; Yue, Z.; Hourigan, K.; Thompson, M. C.; Chan, P. P. Y. *J. Mater. Chem. B* **2013**, *1* (7), 987–996.
(31) Yue, Z.; Cowie, J. M. G. *Polymer* **2002**, *43* (16), 4453–4460.
(32) Zhang, Z. B.; McCormick, C. L. *J. Appl. Polym. Sci.* **1997**, *66* (2), 293–305.
(33) Montalbetti, C. A. G. N.; Falque, V. *Tetrahedron* **2005**, *61* (46), 10827–10852.
(34) Benson, R. S. *Nucl. Instrum. Methods Phys. Res., Sect. B* **2002**, *191* (1–4), 752–757.
(35) Nair, L. S.; Laurencin, C. T.; Tandon, M. Injectable Hydrogels as Biomaterials. In *Advanced Biomaterials*; Basu, B., Kati, D. S., Kumar, K., Eds.; John Wiley & Sons, Inc.: Hoboken, NJ, 2010; pp 179–203.
(36) Cole, M. A.; Voelcker, N. H.; Thissen, H.; Griesser, H. J. *Biomaterials* **2009**, *30* (9), 1827–1850.
(37) Temtem, M.; Casimiro, T.; Mano, J. F.; Aguiar-Ricardo, A. *Green Chem.* **2007**, *9* (1), 75–79.
(38) Wang, L. S.; Chow, P. Y.; Phan, T. T.; Lim, I. J.; Yang, Y. Y. *Adv. Funct. Mater.* **2006**, *16* (9), 1171–1178.
(39) Liu, W.; Zhang, B.; Lu, W. W.; Li, X.; Zhu, D.; De Yao, K.; Wang, Q.; Zhao, C.; Wang, C. *Biomaterials* **2004**, *25* (15), 3005–3012.
(40) Nicodemus, G. D.; Bryant, S. J. *Tissue Eng., Part B* **2008**, *14* (2), 149–65.
(41) Straley, K. S.; Foo, C. W.; Heilshorn, S. C. *J. Neurotrauma* **2010**, *27* (1), 1–19.
(42) Levental, I.; Georges, P. C.; Janmey, P. A. *Soft Matter* **2007**, *3* (3), 299–306.
(43) Rage, R.; Mitchen, J.; Wilding, G. *Anal. Biochem.* **1990**, *191* (1), 31–34.
(44) Knapek, K.; Frondorf, K.; Post, J.; Short, S.; Cox, D.; Gomez-Cambronero, J. *Mol. Cell. Biol.* **2010**, *30* (18), 4492–506.
(45) Mizutani, A.; Kikuchi, A.; Yamato, M.; Kanazawa, H.; Okano, T. *Biomaterials* **2008**, *29* (13), 2073–2081.
(46) Hirose, M.; Kwon, O. H.; Yamato, M.; Kikuchi, A.; Okano, T. *Biomacromolecules* **2000**, *1* (3), 377–381.
(47) Das, G. K.; Chan, P. P. Y.; Teo, A.; Loo, J. S. C.; Anderson, J. M.; Tan, T. T. Y. *J. Biomed. Mater. Res., Part A* **2010**, *93A* (1), 337–346.
(48) Kushida, A.; Yamato, M.; Konno, C.; Kikuchi, A.; Sakurai, Y.; Okano, T. *J. Biomed. Mater. Res.* **2000**, *51* (2), 216–223.

A 7.3.3 Reference

1. Zhang, Y. and Y. Xia, *Formation of Embryoid Bodies with Controlled Sizes and Maintained Pluripotency in Three-Dimensional Inverse Opal Scaffolds.* Advanced Functional Materials, 2012. **22**(1): p. 121-129.
2. da Silva, J., et al., *The cavity-to-cavity migration of leukaemic cells through 3D honey-combed hydrogels with adjustable internal dimension and stiffness.* Biomaterials, 2010. **31**(8): p. 2201-2208.
3. Ford, M.C., et al., *A macroporous hydrogel for the coculture of neural progenitor and endothelial cells to form functional vascular networks in vivo.* Proceedings of the National Academy of Sciences of the United States of America, 2006. **103**(8): p. 2512-2517.
4. Hollister, S.J., *Porous scaffold design for tissue engineering.* Nature Materials, 2005. **4**(7): p. 518-524.
5. Slaughter, B.V., et al., *Hydrogels in Regenerative Medicine.* Advanced Materials, 2009. **21**(32-33): p. 3307-3329.
6. Dhandayuthapani, B., et al., *Polymeric Scaffolds in Tissue Engineering Application: A Review.* International Journal of Polymer Science, 2011.
7. Evans, M.J. and M.H. Kaufman, *Establishment in culture of pluripotential cells from mouse embryos* Nature, 1981. **292**(5819): p. 154-156.
8. Martin, G.R., *Isolation of a pluripotent cell-line from early mouse embryos cultured in medium conditioned by teratocarcinoma stem-cells* Proceedings of the National Academy of Sciences of the United States of America-Biological Sciences, 1981. **78**(12): p. 7634-7638.
9. Ungrin, M.D., et al., *Reproducible, ultra high-throughput formation of multicellular organization from single cell suspension-derived human embryonic stem cell aggregates.* Plos One, 2008. **3**(2).
10. Palacios, R., E. Golunski, and J. Samaridis, *In vitro generation of hematopoietic stem cells from an embryonic stem cell line.* Proceedings of the National Academy of Sciences of the United States of America, 1995. **92**(16): p. 7530-7534.
11. Kehat, I., et al., *Human embryonic stem cells can differentiate into myocytes with structural and functional properties of cardiomyocytes.* The Journal of Clinical Investigation, 2001. **108**(3): p. 407-414.
12. Dang, S.M., et al., *Controlled, scalable embryonic stem cell differentiation culture.* Stem Cells, 2004. **22**(3): p. 275-282.
13. Koike, M., et al., *Characterization of embryoid bodies of mouse embryonic stem cells formed under various culture conditions and estimation of differentiation status of such bodies.* Journal of Bioscience and Bioengineering, 2007. **104**(4): p. 294-299.
14. Messana, J.M., et al., *Size of the embryoid body influences chondrogenesis of mouse embryonic stem cells.* Journal of Tissue Engineering and Regenerative Medicine, 2008. **2**(8): p. 499-506.
15. Itskovitz-Eldor, J., et al., *Differentiation of human embryonic stem cells into embryoid bodies comprising the three embryonic germ layers.* Molecular Medicine, 2000. **6**(2): p. 88-95.
16. Nsiah, B.A., et al., *Fluid Shear Stress Pre-Conditioning Promotes Endothelial Morphogenesis of Embryonic Stem Cells Within Embryoid Bodies.* Tissue Engineering Part A, 2014. **20**(5-6): p. 954-65.
17. Serra, M., et al., *Integrating human stem cell expansion and neuronal differentiation in bioreactors.* BMC Biotechnology, 2009. **9**: p. 82.
18. UIIoa-Montoya, F., C.M. Verfaillie, and W.-s. Hu, *Culture system for Pluripotent stem cells.* Journal of Bioscience and Bioengineering, 2005. **100**(1): p. 12-27.
19. Ng, E.S., et al., *Forced aggregation of defined numbers of human embryonic stem cells into embryoid bodies fosters robust, reproducible hematopoietic differentiation.* Blood, 2005. **106**(5): p. 1601-1603.

20. Niebruegge, S., et al., *Generation of Human Embryonic Stem Cell-Derived Mesoderm and Cardiac Cells Using Size-Specified Aggregates in an Oxygen-Controlled Bioreactor.* Biotechnology and Bioengineering, 2009. **102**(2): p. 493-507.
21. Niebruegge, S., et al., *Cardiomyocyte production in mass suspension culture: embryonic stem cells as a source for great amounts of functional Cardiomyocytes.* Tissue Engineering Part A, 2008. **14**(10): p. 1591-1601.
22. Keller, G.M., *In vitro differentiation of embryonic stem cells.* Current Opinion in Cell Biology, 1995. **7**(6): p. 862-869.
23. Martin, G.R. and M.J. Evans, *Differentiation of clonal lines of teratocarcinoma cells-fromation of embryoid bodies in vitro.* Proceedings of the National Academy of Sciences of the United States of America, 1975. **72**(4): p. 1441-1445.
24. Kelm, J.M. and M. Fussenegger, *Microscale tissue engineering using gravity-enforced cell assembly.* Trends in Biotechnology, 2004. **22**(4): p. 195-202.
25. Dang, S.M., et al., *Efficiency of embryoid body formation and hematopoietic development from embryonic stem cells in different culture systems.* Biotechnology and Bioengineering, 2002. **78**(4): p. 442-453.
26. Thomson, J.A., et al., *Embryonic stem cell lines derived from human blastocysts.* Science, 1998. **282**(5391): p. 1145-1147.
27. zur Nieden, N.I., et al., *Embryonic stem cells remain highly pluripotent following long term expansion as aggregates in suspension bioreactors.* Journal of Biotechnology, 2007. **129**(3): p. 421-432.
28. Willerth, S.M., et al., *Optimization of fibrin scaffolds for differentiation of murine embryonic stem cells into neural lineage cells.* Biomaterials, 2006. **27**(36): p. 5990-6003.
29. Yeh, J., et al., *Micromolding of shape-controlled, harvestable cell-laden hydrogels.* Biomaterials, 2006. **27**(31): p. 5391-5398.
30. Nguyen, K.T. and J.L. West, *Photopolymerizable hydrogels for tissue engineering applications.* Biomaterials, 2002. **23**(22): p. 4307-4314.
31. Chen, G.P., T. Ushida, and T. Tateishi, *Scaffold design for tissue engineering.* Macromolecular Bioscience, 2002. **2**(2): p. 67-77.
32. Lee, K.Y. and D.J. Mooney, *Hydrogels for tissue engineering.* Chemical Reviews, 2001. **101**(7): p. 1869-1879.
33. Soykeabkaew, N., et al., *All-cellulose nanocomposites by surface selective dissolution of bacterial cellulose.* Cellulose, 2009. **16**(3): p. 435-444.
34. Martson, M., et al., *Biocompatibility of cellulose sponge with bone.* European Surgical Research, 1998. **30**(6): p. 426-432.
35. Miyamoto, T., et al., *TISSUE BIOCOMPATIBILITY OF CELLULOSE AND ITS DERIVATIVES.* Journal of Biomedical Materials Research, 1989. **23**(1): p. 125-133.
36. Entcheva, E., et al., *Functional cardiac cell constructs on cellulose-based scaffolding.* Biomaterials, 2004. **25**(26): p. 5753-5762.
37. Rodriguez, K., S. Renneckar, and P. Gatenholm, *Biomimetic Calcium Phosphate Crystal Mineralization on Electrospun Cellulose-Based Scaffolds.* Acs Applied Materials & Interfaces, 2011. **3**(3): p. 681-689.
38. Ko, H.-F., C. Sfeir, and P.N. Kumta, *Novel synthesis strategies for natural polymer and composite biomaterials as potential scaffolds for tissue engineering.* Philosophical Transactions of the Royal Society a-Mathematical Physical and Engineering Sciences, 2010. **368**(1917): p. 1981-1997.
39. Hoo, S.P., et al., *Preparation of a soft and interconnected macroporous hydroxypropyl cellulose methacrylate scaffold for adipose tissue engineering.* Journal of Materials Chemistry B, 2013. **1**(24): p. 3107-3117.
40. De Bartolo, L., et al., *Evaluation of cell behaviour related to physico-chemical properties of polymeric membranes to be used in bioartificial organs.* Biomaterials, 2002. **23**(12): p. 2485-2497.
41. Yeom, Y.I., et al., *Germline regulatory element of Oct-4 specific for the totipotent cycle of embryonal cells.* Development, 1996. **122**(3): p. 881-894.

42. Livak, K.J. and T.D. Schmittgen, *Analysis of relative gene expression data using real-time quantitative PCR and the 2(T)(-Delta Delta C) method.* Methods, 2001. **25**(4): p. 402-408.
43. Benson, R.S., *Use of radiation in biomaterials science.* Nuclear Instruments and Methods in Physics Research Section B: Beam Interactions with Materials and Atoms, 2002. **191**(1–4): p. 752-757.
44. Nair, L.S., C.T. Laurencin, and M. Tandon, *Injectable Hydrogels as Biomaterials*, in *Advanced Biomaterials*2010, John Wiley & Sons, Inc. p. 179-203.
45. Wang, L.-S., et al., *Injectable biodegradable hydrogels with tunable mechanical properties for the stimulation of neurogenesic differentiation of human mesenchymal stem cells in 3D culture.* Biomaterials, 2010. **31**(6): p. 1148-1157.
46. Wang, L.-S., et al., *The role of stiffness of gelatin–hydroxyphenylpropionic acid hydrogels formed by enzyme-mediated crosslinking on the differentiation of human mesenchymal stem cell.* Biomaterials, 2010. **31**(33): p. 8608-8616.
47. Levental, I., P.C. Georges, and P.A. Janmey, *Soft biological materials and their impact on cell function.* Soft Matter, 2007. **3**(3): p. 299-306.
48. Bhana, B., et al., *Influence of Substrate Stiffness on the Phenotype of Heart Cells.* Biotechnology and Bioengineering, 2010. **105**(6): p. 1148-1160.
49. Rodriguez, A.G., et al., *Substrate Stiffness Increases Twitch Power of Neonatal Cardiomyocytes in Correlation with Changes in Myofibril Structure and Intracellular Calcium.* Biophysical Journal, 2011. **101**(10): p. 2455-2464.
50. Li, X.F., et al., *Fibroblast growth factor signaling and basement membrane assembly are connected during epithelial morphogenesis of the embryoid body.* Journal of Cell Biology, 2001. **153**(4): p. 811-822.
51. Komura, H., et al., *Establishment of cell polarity by afadin during the formation of embryoid bodies.* Genes to Cells, 2008. **13**(1): p. 79-90.
52. Dasgupta, A., et al., *E-cadherin synergistically induces hepatospecific phenotype and maturation of embryonic stem cells in conjunction with hepatotrophic factors.* Biotechnology and Bioengineering, 2005. **92**(3): p. 257-266.
53. Hwang, Y.-S., et al., *Microwell-mediated control of embryoid body size regulates embryonic stem cell fate via differential expression of WNT5a and WNT11.* Proceedings of the National Academy of Sciences of the United States of America, 2009. **106**(40): p. 16978-16983.
54. Kurosawa, H., *Methods for inducing embryoid body formation: In vitro differentiation system of embryonic stem cells.* Journal of Bioscience and Bioengineering, 2007. **103**(5): p. 389-398.
55. Yang, M.-J., et al., *Novel method of forming human embryoid bodies in a polystyrene dish surface-coated with a temperature-responsive methylcellulose hydrogel.* Biomacromolecules, 2007. **8**(9): p. 2746-2752.
56. Sarvi, F., et al., *A novel technique for the formation of embryoid bodies inside liquid marbles.* Rsc Advances, 2013. **3**(34): p. 14501-14508.
57. Valamehr, B., et al., *Hydrophobic surfaces for enhanced differentiation of embryonic stem cell-derived embryoid bodies.* Proceedings of the National Academy of Sciences of the United States of America, 2008. **105**(38): p. 14459-14464.
58. Hwang, C.M., et al., *Fabrication of three-dimensional porous cell-laden hydrogel for tissue engineering.* Biofabrication, 2010. **2**(3).
59. Novik, E.I., et al., *Embryoid body-mediated differentiation of mouse embryonic stem cells along a hepatocyte lineage: Insights from gene expression profiles.* Tissue Engineering, 2006. **12**(6): p. 1515-1525.
60. Rajala, K., et al., *Cardiac Differentiation of Pluripotent Stem Cells.* Stem Cells International, 2011. **2011**.
61. Yamaguchi, T.P., et al., *FLK-1, an FLT-related receptor tyrosine kinase an early marker for endothelial cell precursors.* Development, 1993. **118**(2): p. 489-498.
62. Ema, M., S. Takahashi, and J. Rossant, *Deletion of the selection cassette, but not cis-acting elements, in targeted Flk1-lacZ allele reveals Flk1 expression in multipotent mesodermal progenitors.* Blood, 2006. **107**(1): p. 111.

63. Motoike, T., et al., *Evidence for novel fate of Flk1(+) progenitor: Contribution to muscle lineage.* Genesis, 2003. **35**(3): p. 153-159.
64. Lints, T.J., et al., *NKX-2.5 - A novel murine homeobox gene expressed in early progenitor cells and their myogenic descendants* Development, 1993. **119**(2): p. 419-431.
65. Heikinheimo, M., J.M. Scandrett, and D.B. Wilson, *Localization of transcription factor Gata-4 to regions the mouse embryo involved in cardiac development.* Developmental Biology, 1994. **164**(2): p. 361-373.
66. Biben, C. and R.P. Harvey, *Homeodomain factor Nkx2-5 controls left/right asymmetric expression of bHLH gene eHand during murine heart development.* Genes & Development, 1997. **11**(11): p. 1357-1369.
67. Lyons, I., et al., *Myogenic and morphonenetic deffects in the heart of murine embryos lacking the homeo box gene Nkx2.5.* Genes & Development, 1995. **9**(13): p. 1654-1666.
68. Wang, G.F., et al., *A positive GATA element and a negative vitamin D receptor-like element control atrial chamber-specific expression of a slow myosin heavy-chain gene during cardiac morphogenesis.* Molecular and Cellular Biology, 1998. **18**(10): p. 6023-6034.
69. Bruneau, B.G., *Transcriptional regulation of vertebrate cardiac morphogenesis.* Circulation Research, 2002. **90**(5): p. 509-519.
70. Orlic, D., J.M. Hill, and A.E. Arai, *Stem cells for myocardial regeneration.* Circulation Research, 2002. **91**(12): p. 1092-1102.
71. Akazawa, H. and I. Komuro, *Roles of cardiac transcription factors in cardiac hypertrophy.* Circulation Research, 2003. **92**(10): p. 1079-1088.

Chapter 8

8.1 Concluding remarks

A summary of what has been discussed in this thesis will be presented in this chapter, in addition to some suggestions for the future work on each part (PDMS modification, liquid marble bioreactor and porous scaffold bioreactor).

This thesis consists of three major parts: The first part (chapter 3) focused on providing a useful method for improving the ability of stem cells to attach and grow on the surface of the substrate. For this purpose, we presented a novel, facile and cost effective method that surface bio-functionalizes PDMS with silane, CMC polysaccharide and gelatin to render it bioadhesive.

Native PDMS inhibits protein and encourages cell attachment. Modification of a PDMS surface is therefore needed to render it hydrophilic; such modification can be carried out with a physiochemical method, which provides more hydrophilic coatings for improving biocompatibility of PDMS. In our method, PDMS was first activated with oxygen plasma, followed by treatment with trimethoxysilylpropyl(polyethylene imine) as one of the most efficient silane solutions in surface amination of PDMS. The aminized surface was subsequently conjugated with CMC followed by gelatin using EC/NHS coupling. Verification of the existence of successive functionalization of PDMS was obtained through FTIR measurements, which showed the presence of carboxylic acid groups on the surface of the modified PDMS and confirmed the successful grafting of CMC. Contact angle measurements showed that the introduction of the CMC greatly improved the hydrophilicity of native PDMS substrates. Water contact measurement showed that the modified surfaces keep their hydrophilicity for a long time, which confirmed the long-lasting stability of the surfaces. Quantitative and qualitative protein adsorption assays showed that that CMC modified PDMS surfaces can reduce the adsorption of negatively charged BSA albumin, and exhibited protein-repelling properties. The ease of PDMS modified surface for further modification with bioactive molecules (gelatin) to promote interfacing with different cells was demonstrated.

Compared with the native PDMS substrates, the introduction of the polysaccharides on the PDMS surfaces greatly improved the viability of the cells. The proliferation of cells on different substrates was quantified and the results revealed that the number of cells grown on the modified substrate was much higher than that cultured on the unmodified PDMS substrate. It was demonstrated that the functionalized surface facilitates stem cell propagation, as well as retaining the undifferentiated phenotype and pluripotency of the cells. The proliferation of cells implies that the functionalized microchannel surface is biocompatible with the cells. As a whole, this study provides a simple approach for the treatment of PDMS substrates to prevent protein adsorption while enhancing cell

adhesion and growth. This work also demonstrated the potential of applying polysaccharide in a PDMS microfluidics-based cellular study.

Research on liquid marbles has been the core subject of the second part of this thesis (Chapter 4,5,6). Liquid marbles (LMs) are known as non-wetting droplets of liquid that can slide and float on solid or liquid supporting surfaces, thanks to their non-adhesive hydrophobic powdery shell. Having unique interfacial properties, liquid marbles offer immense possibilities in many fields. The unique properties of liquid marbles make it possible to utilize these LMs as microreactors and bio microreactors. In a proof of concept study demonstrated in this thesis, liquid marbles made of liquid growth medium and non-adhesive powder particles were introduced as efficient bio microreactors capable of supplying a non adhesive environment for cells to grow and aggregate. Cancer cell growth and aggregation inside liquid marbles were studied to demonstrate the capacity of liquid marble bio microreactors to facilitate these cells to form cell aggregates known as spheroids.

The feasibility of using liquid marble microreactors for formation of embryonic stem cell aggregates called embryoid bodies (EBs) was also investigated. The results revealed that many EBs can be formed inside a single liquid marble with more uniform morphology compared to the suspension culture method. The results showed that liquid marbles formed from smaller powder particles promoted EB formation more efficiently compared with liquid marbles made from larger particles, in terms of shape and uniformity of the EBs, number of EBs formed and EB surface compactness. Liquid marble made of different volumes of medium showed different influences on the shape and number of EBs formed inside liquid marble micro bioreactors. Larger liquid marbles yielded a higher number of EBs that were more uniform than those harvested from the smaller ones, which is in complete accordance with expectations. This is because a larger liquid marble contains a greater quantity of medium and, therefore, can provide a cell growth medium more nutrient-rich than a smaller liquid marble. It was also shown that increasing the cell density allows the formation of a greater number of EBs.

The efficiency of liquid marble-born-EBs compared to the conventional liquid suspension (LS) technique as the chosen control method in terms of cell viability and EB uniformity revealed that cells in liquid marble are more viable compared to those in suspension. Measuring EB size distribution as an indicator of uniformity also confirmed that EBs obtained by the LM method are morphologically more uniform and of a narrower size distribution compared to those formed in LS.

The gene expression of LM generated from EBs were studied. The expression of markers of all three germ layers was quantified using the RT-PCR and qPCR method in EBs, which confirmed the *in vitro* differentiation potential of EBs formed using the liquid marble technique. The presence of three germ layers demonstrates the potential of these EBs to differentiate into multipotent stem cells (progenitors), which will eventually progress into terminally differentiated cells. This part of the study used liquid marble micro bioreactors as a facile new method for the highly efficient production of

EBs. Optimization of this method showed that LM is capable of producing EBs of more homogeneous size and shape compared to EBs produced by the liquid suspension method. The preliminary study on the feasibility of EB differentiation inside liquid marbles also showed that the LM technique can support specific lineage differentiation.

In the next study, we proposed for the first time that liquid marbles could greatly contribute to ES cardiac differentiation. The work on small scale bioreactors made of liquid marbles successfully proved that liquid marbles can provide a powerful means for biological and biomedical studies, because of the unique interfacial properties and structure of liquid marbles. Simply consisting of a non-adhesive shell and a confined liquid core, liquid marbles have all that is required for cells to reside; the porous shell allows oxygen and carbon dioxide exchange, while the liquid core provides all the nutrients needed for the cells' metabolism and growth. Moreover, flexibility of the structure of a liquid marble allows easy control and manipulation of the bioreactors made of liquid marbles. A comprehensive study was then conducted to determine the feasibility of cardiomyocyte differentiation of mouse ES cells after formation of EBs inside the liquid marble micro-bioreactor. Gene expression studies demonstrated that the cardiomyocyte differentiation of the ES cells occurred, and was characterized by expression of mesoderm and cardiomesoderm markers, followed by expression of cardiac specific transcription factors, and finally by cardiac-specific structural genes. Spontaneous beating was observed 4 days after plating down the EBs and lasted for at least another 25 days. Cells in the contracting areas were stained positively for cardiac markers (cardiac troponinT (cTnT)). These results demonstrated that ES cells could differentiate into myocyte cells through the liquid marble technique.

The third section of this thesis (chapter 7) concentrated on the feasibility of formation of embryoid bodies using a novel biodegradable and macroporous 3D hydrogel made from modified cellulose as bioreactor embedding material. EB formation inside hydrogel was observed using scanning electron, confocal and fluorescence microscopy; this observation implied that the stem cells attached to and penetrated into the hydrogel pores, and proliferated well, while forming uniform EBs. Uniformity of EBs formed inside hydrogel compared to the EBs formed in the suspension method showed that hydrogel-born EBs are more homogeneous. Quantitative expression of differentiation markers (mesoderm, endoderm and ectoderm) using RT-PCR confirmed the *in vitro* potential of EBs grown in scaffolds to form derivatives of all three embryonic germ layers. EBs were stained positive for the presence of three germ layers markers [mesoderm (Brachyury) endoderm (Foxa2) and ectoderm (Nestin)]. Quantitative PCR (real time) analysis of differentiation markers for the 3 germ layers for EBs formed inside hydrogel and in the suspension method was also performed, with the results showing an increase in level of Fox2a, Brachyury and Nestin over the time in EBs formed inside hydrogel. The positive cardiac markers immunostaining and observation of spontaneous contracting in hydrogel-born EBs showed the inherent potential of this scaffold for different clinical applications.

Overall, we investigated the capability of the formation of EBs inside a biodegradable porous 3D tissue scaffold, derived from porous cellulose (HPC). In this part, we showed that culturing ES cells inside the porous hydrogel with controlled porosity induces the formation of uniform EBs inside the pores with the preferential spontaneous differentiation towards cardiogenic lineage.

8.2 Future work

There are many opportunities to follow up on aspects of the work reported here. Some prospects for future work are identified below:

- In the PDMS functionalization work, we chose a feeder independent type of stem cell; it would be interesting to use a feeder dependent cell line and compare the efficiency of the functionalization method for both cell lines.
- Another area of future work is to investigate the potential of the modified surface to direct differentiation of stem cells with combination of different growth factors.

- In the marble section, further study is required to find out why different liquid marble shell particle sizes affect the uniformity and quality of EBs differently.
- There is also need to improve the efficiency and purity of differentiated cardiac cells using different growth factors.

- For the hydrogel part, it would be interesting to study the effect of hydrogel with different stiffness on cardiomyocyte behaviour (e.g., beating frequency).
- Improving the efficiency of cardiac differentiation inside the hydrogel by introduction of different growth factors would be another important area of future study.